PHYSIOLOGICAL AND PHARMACOLOGICAL MODELS FOR CONTROL OF ANAESTHESIA

A DISSERTATION

SUBMITTED TO THE FACULTY OF ENGINEERING

OF GLASGOW UNIVERSITY

IN PARTIAL FULFILMENT OF THE REQUIREMENTS

FOR THE DEGREE OF

DOCTOR OF PHILOSOPHY

By

George Robin Worship

September 1992

ProQuest LLC.
789 East Eisenhower Parkway
P.O. Box 1346
Ann Arbor, MI 48106 – 1346

Dedication

I dedicate this thesis to my Mother and Father, Fiona and Ronald Worship, in recognition of the love, encouragement and support they have given me and also in recognition of the many things they have given up for me.

I further acknowledge my Mother for ensuring that I pursued my first degree after my Father's death. Without her sacrifices then, and since then, I would have been unable to carry out this work.

Abstract

This thesis describes the development of physiological and pharmacological models for the control of anaesthesia. These models form the basis of techniques intended to support the automatic control of anaesthesia. Each technique has been implemented and has performed successfully in the operating theatre.

In more detail, the thesis describes the development and use of an estimation scheme, based upon a pharmacological model, to estimate a patient's cardiac output and tissue anaesthetic tensions during anaesthesia. The scheme employs a physiologically–based model of inhaled anaesthetic pharmacokinetics. The thesis describes the representation of physiologically–based pharmacokinetic models, the parameterisation of a physiologically–based model of isoflurane pharmacokinetics, a scheme to match such a model to individuals, and the simulated and actual performance of the estimation scheme.

A physiological model forms the basis of a scheme developed to diagnose inappropriate physiological and pharmacological conditions in the patient's state during anaesthesia. This scheme is based upon a model of homeostasis and the stress response. The thesis describes the development of this model, the performance of a prototype implementation, its development to allow the diagnosis of inappropriate conditions and its diagnostic performance both using stored data and in the operating theatre.

Acknowledgements

The work described in this thesis was carried out as part of a project funded by the U.K. Science and Engineering Research Council. I am grateful to S.E.R.C. for the support and to the grant holders, Prof. P.J. Gawthrop, Dr. A.J. Asbury and Dr. W.M. Gray for giving me the chance to work with them in this area.

In particular, I wish to thank John Asbury for his consistent enthusiasm, encouragement and contribution from the early stages of the work in introducting me to anaesthesia to the latter stages in suggesting improvements to the thesis. I thank Peter Gawthrop for sharing his perception, direction and understanding and for supporting my incorporation of physiology and pharmacology. I thank Bill Gray for his patience and experience in the refinement and development of hardware components, for freely sharing many of the software developments which he has produced and for his painstaking effort in the preparation of written material.

I also wish to thank Drs. M.J. Higgins and D.P. Gilmore for giving of their time to discuss issues of physiology, pharmacology and anaesthesia with me. Thanks are also due to Sister J. Gibson and her staff of G6 Theatre in the Western Infirmary for their support during the practical work described in the thesis.

Personally, I also wish to thank my colleagues in the Control Group for contributing to an exciting working atmosphere with special thanks to Yasmine Mather and Dr. Donald Ballance for their support in the last few months.

Specifically, I wish to thank Alasdair Thin and Lorna Murray for their

assistance. Alasdair has contributed to the structure and presentation of the thesis and helped put many issues in perspective. Lorna has helped me to relax and renew my enthusiasm, partly by allowing me to paint some rooms in her flat.

Perspective

The author graduated in Electrical and Electronic Engineering and had experience of control engineering and artificial intelligence techniques prior to beginning the work described in this thesis.

The work described in the thesis was supported by the SERC through a reseach project involving collaboration between the Department of Anaesthesia and Department of Mechanical Engineering at the University of Glasgow and the West of Scotland Health Boards' Department of Clinical Physics and Bio–Engineering. At an early stage in the project, the author was able to observe the practice of anaesthesia in the operating theatre. This provided practical motivation for research and also opportunities to observe and further enquire about the activities of the anaesthetist.

The combination of the desire to understand the 'system' rooted in engineering and the ability to witness and further investigate practical anaesthetics has led to the pursuit of physiology and pharmacology as sources of scientific explanation of events in anaesthesia. The use of engineering skills has allowed the development of the physiological and pharmacological models described in this thesis.

The thesis therefore describes the relevant aspects of anaesthesia in terms of physiology and pharmacology, models these aspects using a combination of physiological and pharmcological understanding and the application of engineering skills and develops techniques to support the control of anaesthesia from these models using engineering skills.

It can be conceived that the thesis could be written to suit an engineering readership, to suit an anaesthesia readership or a combination of both. This thesis has been written so as to be suited to both an engineering and anaesthesia readership. However, because the techniques described have used engineering to provide beneficial effects for anaesthesia, the thesis is biased slightly towards an anaesthesia readership. It is believed that the advantages of making the thesis more palatable in its area of application far outweigh any slight inconvenience which may be experienced by a pure engineering reader.

Contents

List of Tables

List of Figures

Chapter 1

Introduction

SUMMARY

This chapter summarises the application of automatic control in anaesthesia and describes the structure of this thesis. Consideration of automatic control activity includes both the control of depth of anaesthesia and the control of purely physiologic quantities such as blood pressure. Three themes are drawn from current approaches to the control of depth of anaesthesia and these are assessed. The approaches adopted and contributions made by work described in this thesis are introduced and the structure of the thesis is outlined.

1.1 Anaesthesia

Anaesthesia is the "absence of sensation" but in a clinical context, involves both the absence of sensation for the patient and the existence of suitable operating conditions for the surgeon. The anaesthetist is responsible for the provision of anaesthesia and the maintenance of the patient's physiological state. This process can involve the administration of both inhaled and intravenous anaesthetic

drugs, injected analgesic drugs [1], neuromuscular blockers (to produce reversible muscle paralysis during surgery) and others according to the surgical requirements. The nature of surgery also dictates that the anaesthetist manages blood loss using blood or fluid replacement and, where muscle relaxation is involved, the anaesthetist also manages the ventilation of the patient.

Patients of wide–ranging age, health and fitness undergo surgery. The anaesthetist relies upon education, training and experience in order to provide suitable anaesthetic conditions for each patient.

1.1.1 The Maintenance of Anaesthesia

While surgery is in progress, the anaesthetist aims to maintain anaesthesia and manage any physiological problems of the patient which may arise. In qualitative terms, the anaesthetist performs tasks which are analogous to feedback control: The suitability of the anaesthetic and the patient's physiologic condition are assessed, and drugs, fluids and gases are administered according to the requirements perceived by the anaesthetist. This analogy has encouraged the application of control engineering to anaesthesia. Control Engineering has been accompanied by other related approaches, in particular, those which have grown out of artificial intelligence.

1.2 Control Engineering in Anaesthesia

To the control engineer, superficially at least, anaesthesia is a rich and extensive area of application: The anaesthetist routinely makes many measurements, some quantitative and automatically recorded, some qualitative and relying upon observation. Based upon interpretation of those measurements, the anaesthetist decides upon drug delivery, fluid delivery and sometimes ventilation requirements.

[1] analgesic drugs alter the perception of pain

In collaboration with the anaesthetist, schemes which deliver drugs according to the value of one measurement, or the combination of several measurements can be envisaged.

Control systems have been developed for the automatic control of drug delivery in many areas of medicine. Some of these specifically allow the anaesthetist to provide and maintain conditions appropriate for surgery, and others aim to control the 'depth of anaesthesia' of the patient. Systems for the automatic control of drug administration have been reviewed by Linkens and Hacisalihzade [1], Summers [2], Packer [3], Carson [4] and Linkens [5]. The automatic control of anaesthesia has been reviewed by Chilcoat [6]. These reviews include applications which are not directly related to anaesthesia and should be consulted for such information. Within the confines of anaesthesia, the following are relevant

1. The control of muscle relaxation.
2. The control of arterial blood pressure.
3. The control of depth of anaesthesia.

1.3 Automatic Control Related to Anaesthesia

1.3.1 Automatic Control of Muscle Relaxation

General anaesthetic agents produce a reduction in the resting tone of skeletal muscle in a dose–related manner. A reduction in skeletal muscle tone makes it easier for the surgeon to manipulate organs and structures which lie beneath skeletal muscle. While it is possible to produce sufficient reduction in muscle tone with anaesthetic agents, the doses required are in excess of those which are reasonable. Neuromuscular blocking drugs are therefore administered so as to provide a practically useful level of muscle relaxation. The anaesthetist is responsible for the administration of the neuromuscular blocking drugs.

In controlling the administration of muscle relaxants, the anaesthetist may choose to deliver a continuous infusion of the drug but more commonly administers repeated boluses of it. The extent of muscle relaxation can be assessed using a Relaxograph [7]. This measurement allows the dynamics between drug administration and the relaxant effect to be modelled and supports control design using a model. Workers have observed and described a wide range of individual responses to muscle relaxant drug administration and the response to a repeated dose may change even within the duration of an anaesthetic. Fixed controllers have been developed to perform PI and PID control [8] [9] with reasonable performance. Adaptive controllers have included self–tuning pole placement and Smith predictor structures [10] and self–tuning PID [7]. The controller described by Jaklitsch and Westenkow [11] operates in two phases. One controller achieves the initial establishment of muscle relaxation at the desired level and another is an adaptive controller which regulates the muscle–relaxation afterwards. Recently, approaches have included the application of fuzzy logic [12] to the control of muscle relaxation, and some effort has been made to integrate the measurement of muscle relaxation, the administration of muscle relaxation and the control of the administration in one device [13].

1.3.2 Automatic Control of Blood Pressure

The control of arterial blood pressure is desirable during some surgical procedures and following others. In some operations carried out on the ear, nose or throat, blood pressure is deliberately reduced so as to cut down or eliminate bleeding around the operation site [14]. Similar procedures are necessary during eye surgery and often in intensive care units after major surgery.

In simple terms, blood pressure results from the flow of blood through the resistance presented by blood vessels. If the flow increases, due to an increase in the rate at which the heart pumps blood (the cardiac output) but the resistance

of the blood vessels (the peripheral vascular resistance) remains constant, then the blood pressure will increase. Similarly, if flow remains constant, a reduction in the resistance of the blood vessels will cause a reduction in blood pressure.

These mechanisms, although simplified for clarity, offer two distinct routes to the regulation of blood pressure: the manipulation of cardiac output and peripheral resistance. Practically, however, it is not appropriate to reduce blood flow in order to reduce cardiac output because this compromises nutrient delivery to, and waste product removal, from tissues.

The automatic control of blood pressure has been reviewed by Linkens and Hacisalihzade [1], Linkens [5], Carson [4] and Packer [3]. Schemes for control of blood pressure have relied upon drugs which cause vasodilation[2] and affect the heart. The most extensively used vasodilator in the control development performed has been sodium nitroprusside.

Automatic Control of Blood Pressure using Sodium Nitroprusside

Sodium nitroprusside acts on blood vessels causing vasodilatation. The infusion of sodium nitroprusside therefore allows control of blood pressure. Early work using sodium nitroprusside, described by Sheppard [15], used a table of gain values to parameterise a PID controller. The model described by Slate et al. [16] was used in an adaptive scheme as described by Slate and Sheppard [17]. Many adaptive approaches have been pursued including self-tuning minimum-variance control [18], model reference adaptive control [19] and an extension of a minimum variance controller called the Control Advance Moving Average Controller (CAMAC) [20]. Martin et al. [21] describe a multiple-model adaptive controller for sodium nitroprusside infusion which employs Slate's model. More recent work by Behbehani and Cross [22] has employed an integrating self-tuning control strategy. Martin et al. [23] [24] have focussed on maintaining control

[2] vasodilation is the widening of blood vessels

performance in the regulation of blood pressure but preventing the controller from responding to physiologic or pharmacologic disturbances or measurement artifacts. This scheme involves the development of a supervisor to prevent unnecessary controller action. The TITRATOR system is a commercially available device, developed by the IVAC Corporation and described by Voss [25]. TITRATOR infuses sodium nitroprusside so as to control blood pressure. Voss suggested that early results of product evaluation indicated that the automatic controller not only produced better control during the period of control but also that the patient's requirement for blood products and for emergency surgery were reduced as was the overall time spent in the recovery areas. This may imply that automatic control can improve patient outcome in those areas [25].

Automatic Control of Blood Pressure using Isoflurane

Isoflurane is an inhaled anaesthetic and is routinely used in general anaesthesia. Isoflurane has many desirable properties in terms of its effects upon the organ systems of the body [26]. Isoflurane appears to cause very little change in cardiac output over a range of concentrations [27] but causes a dose–dependent decrease in peripheral vascular resistance. This enables isoflurane to be used in the control of blood pressure.

This approach has been adopted by Millard et al. [14] and Monk et al. [28]. These workers used a self–tuning controller to maintain a model of the patient's response to isoflurane and to maintain control performance. The authors identify the need for supervisory software to ensure that the self–tuner can operate properly without user interaction.

1.4 Automatic Control of Anaesthesia

Anaesthesia can be produced by a combination of drugs. Inhaled anaesthetics can be delivered to the patient in the inspired gas stream and injected anaesthetics can be delivered by infusion. The delivery of insufficient anaesthetic may result in the patient responding to surgical stimulation. The delivery of excessive anaesthetic may result in unwanted effects upon the respiration and circulation of the patient and will prolong the patient's recovery from surgery. The concept of 'depth of anaesthesia' is used by anaesthetists to describe the suitability of the anaesthetic state of the patient. A 'light' anaesthetic is inadequate and is likely to be accompanied by characteristic changes in cardiovascular and respiratory variables and specific clinical signs. A 'deep' anaesthetic is excessive and and is also likely to be accompanied by characteristic changes in cardiovascular and respiratory variables and other clinical signs. Unfortunately, there is no single measurement, or combination of measurements which can be used to indicate 'depth' for all patients and all drug combinations. The depth of anaesthesia cannot be measured directly and is perceived by the anaesthetist.

In the absence of a measurement of depth of anaesthesia, it is not possible to model the relationship between drug inputs and the resulting depth. This process is further hindered by the inability to measure or otherwise quantify the extent of surgical stimulation. In the absence of either a model or a measurement, a controller which directly manipulates depth of anaesthesia cannot be developed. Despite this, the depth of anaesthesia has been controlled automatically using indirect means. The indirect methods developed can be grouped as shown in Figure 1.1.

The motivations for these approaches and work of relevance are summarised as follows:

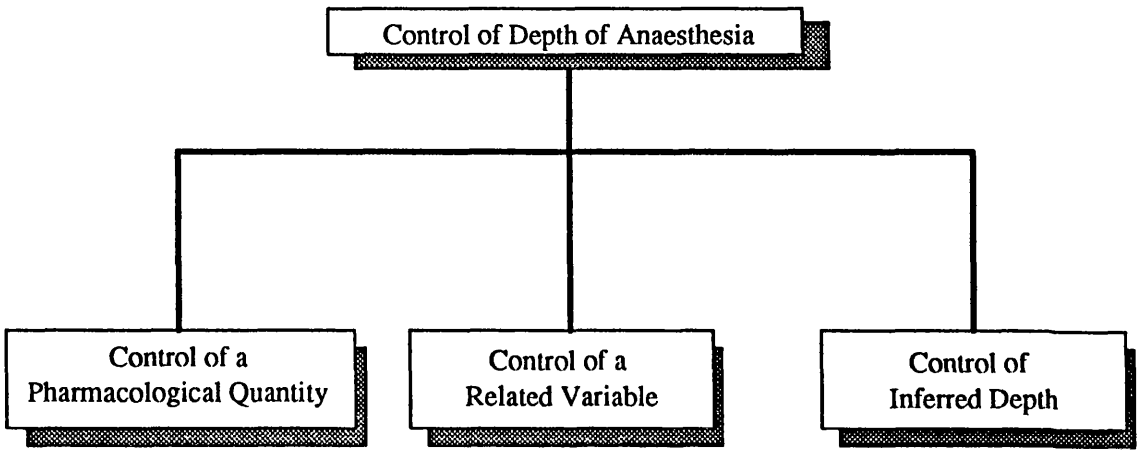

Figure 1.1: Summary of Approaches to the Control of Anaesthesia

1.4.1 The Control of Depth of Anaesthesia using a Pharmacological Quantity

General anaesthetic agents act in the central nervous system (spinal column and brain). The effect of the anaesthetic is related to its concentration in these tissues although the precise relationship is not known [27] [29]. The concentration in the central nervous system is related to the dose of the drug administered and its administration timecourse. Pharmacology describes the relationships between drug dose and effect. Within pharmacology, pharmacokinetics describe the relationship between the drug dose and the drug concentration at the site of action; pharmacodynamics describes the relationship between the concentration at the sites of effect and the effects produced. Although pharmacodynamic relationships for general anaesthetics are not adequately understood, general anaesthetic pharmacokinetics are reasonably well described.

General anaesthetic pharmacokinetics have formed the basis of several controllers for anaesthesia. These are all 'open–loop' controllers in that they aim to produce a drug concentration in the central nervous system but because this cannot be measured, no feedback can be applied.

Control of Propofol Anaesthesia

Propofol is an intravenous anaesthetic agent which has advantageous pharmacokinetic properties allowing rapid induction of anaesthesia and rapid recovery afterwards. A scheme for the manual administration of propofol [30] was subsequently implemented using a computer–controlled infusion [31]. Schuttler et al. [32] used the method described by Schwilden [33] to implement controlled infusions of both propofol and alfentanil during anaesthesia. White and Kenny [34] using a three–compartment model for propofol, developed a controller to achieve concentrations of propofol in the blood. This system adopted the three compartment model derived by Gepts et al. [35]. Marsh et al. [36] developed the scheme described by White and Kenny for use in paediatric surgery. This process involved the generation of a propofol pharmacokinetic model for children.

Control of Inhaled Agent Delivery using a Pharmacological Model

Physiologically–based pharmacological models for inhaled agents have been developed by Mapleson [37] [38] [39] [40] and other authors [41] [42] [43] [44] [45] [46]. Mapleson's models use physiologically accurate tissue groups, volumes and perfusions and use experimentally derived physicochemical parameters for each drug. The full structure of the Mapleson models is described in Chapter 3. Relevant parameters of the physiological components of the model are; tissue volumes, tissue perfusions, cardiac output and alveolar ventilation. The technique of Mapleson et al. [47] uses estimates of alveolar ventilation and cardiac output to fully parameterise a physiologically–based model of a dog. The model was then used to

determine the inspired concentration of halothane to be delivered to the dog in order to maintain the arterial tension of anaesthetic at a setpoint.

A later development [48] used a physiologically–based model for a dog to determine the necessary inspired halothane concentration required to achieve a desired brain anaesthetic tension. Again this approach proved successful.

A more extensive description of the control scheme is given by Chilcoat et al. [79]. In these experiments, impedance cardiography was used to estimate changes in the cardiac output of the dog. Alveolar ventilation was measured using a respirometer and the model was matched to the patient. During the experiments, arterial blood samples were taken every 10 minutes and, every 30 minutes, the anaesthetic tension in the sample was used to 'correct' that predicted by the model. The correction of the model involved changing the model's cardiac output so as to match the measured and predicted arterial tensions. Despite some unreliability in measurements, these experiments suggested that such an approach to the control of brain tension and hence control of depth of anaesthesia is valid.

The method of Tatnall, Morris and West [49] controlled the alveolar (end–tidal) halothane tension. This approach identified two constants during the first 8 to 10 breaths of halothane mixture and used these to parameterise a simple model relating inspired tension, alveolar tension and mixed–venous tension. Initially, this approach was applied to off–line data from 20 cases and demonstrated encouraging performance. Further work [50] applied the same scheme to 80 patients and demonstrated its ability to cope with a wide range of patients and to be robust to measurement disturbances.

Tatnall [51] describes further enhancement of the control scheme to incorporate a PI controller following 60 to 90 breaths. This change allows any error between the actual and desired alveolar tensions to be eliminated by the integral action of the controller. The enhanced system was involved in 120 trials in patients ranging in age from 7 months to 62 years and is reported to have performed reliably in all

cases.

Control of Inhaled Agent Delivery without a Pharmacological Model

The use of a pharmacological model allows control performance to be matched to the individual patient. In the absence of a model, more simple control algorithms can be used.

Ross et al. [52] describe a simple proportional controller for the control of end–tidal halothane. Not surprisingly, this controller produced a steady–state error. O'Callaghan et al. [53] describe the use of the same scheme to administer isoflurane. Smith et al. [54] describe the modification of a PI type controller [55] for use in controlling end–tidal halothane concentration. Their main aim was however to compare the performance of the controller with that of the anaesthetist and so detailed description of the control performance was not given. Ritchie et al. [56] [57] [58] describe an integrated set of controllers for ventilation, oxygen, nitrous oxide and anaesthetic delivery. The controllers are fixed PI controllers and no account for patient variability in uptake is taken. Hayes et al. [59] used PID controllers to control the concentrations of oxygen, nitrous oxide and enflurane in an anaesthesia delivery system.

More recently, adaptive controllers for oxygen and halothane concentrations have been developed [60]. These controllers have achieved more reliable performance than fixed controllers.

1.4.2 Control of Anaesthesia using a Physiological Measurement

To date, no combination of measurements has proved generally applicable to the assessment of anaesthetic depth and the best indication seems to be provided by the clinical signs routinely used by the anaesthetist [61]. In some circumstances, however, some measured quantities can provide a reasonable indication of depth of

anaesthesia in the presence of specific drugs or drug combinations. An extensive review of some suggested measurements and combinations of measurements is given by Robb [61]. Robb concluded that "no single clinical sign can be used as an indicator of anaesthetic depth in all cases" but that the combination of several signs is clinically useful. In consideration of some other suggested indicators of anaesthetic depth, Robb concluded that: The raw encephalogram (EEG) cannot be usefully applied to the assessment of depth of anaesthesia. The processed EEG which includes frequency domain measures such as the spectral edge frequency (SEF), zero–crossing frequency (ZXF) and the median frequency (MF) provides useful information although it is not clear whether the changes in these measures genuinely reflect the anaesthetic state. Sensory evoked potentials such as the auditory evoked potential (AEP) also undergo changes related to the anaesthetic dose but again, it is unclear whether these reflect a change in the anaesthetic state. Overall, the use of the EEG measures is hampered by agent specific EEG changes and the influence of other physiological variables such as arterial carbon dioxide. Further effects on the EEG include the actions of narcotics as discussed by Hug [62].

Robb also appraised the electromyogram (EMG) and both the spontaneous and provoked lower osophageal contractility (LOC) as measures of depth of anaesthesia. The use of the EMG, he concluded, is hampered by large inter–individual variability, the use of opiates and the presence of muscle relaxants. LOC is similarly affected by inter–individual variability and indeed, in some people, activity in the lower osophagus may be absent even during inadequate anaesthesia.

Although no particular sign, measurement or combination thereof appears to offer a reliable route to the assessment in all cases, for a wide range of drugs, of the anaesthetic depth, the automatic control of the depth of anaesthesia based upon such measures has been successful in some circumstances.

Control of Anaesthesia using the Processed EEG

Because EEG changes are agent specific, it has proved necessary to evaluate the changes in EEG resulting from varying doses of different drugs and combinations of drugs. The effects of inhaled agents on the EEG are summarised by Stoelting [27]. The effects upon the EEG of isoflurane in nitrous oxide have been investigated by Schwilden and Stoeckel [63]. The effects upon the EEG of fentanyl and alfentanil have been investigated by Scott et al. [64].

The work of Thomsen et al. [65] [66] has produced a scheme for the assessment of depth of anaesthesia during isoflurane anaesthesia [65] and for isoflurane, halothane and etomidate/fentanyl anaesthesia [66]. This approach classified the EEG waveform components in order to produce a measure of anaesthetic depth.

Schwilden et al. [67] used a simple bi-exponential model to represent the pharmacokinetics of methohexitone, and a simple sigmoid relationship to represent its effect upon the EEG median frequency. This model was used within a controller for median frequency which delivered methohexitone. The pharmacodynamic relationship between drug concentration and the median frequency was assumed constant and the pharmacokinetic model was adjusted to match the patient's median frequency with that predicted by the model. The pharmacokinetic model was then used to determine the propofol infusion rate. In a later scheme [68], the authors developed an EEG-based propofol infusion scheme.

The scheme described by Schils et al. [69] uses the spectral edge frequency and mean arterial pressure as input variables to control the administration of halothane. At any time, the controller manipulates only one variable: either the mean arterial pressure or the spectral edge frequency. A 'coordinator' was developed to select the variable to be controlled and this was integrated into the control scheme.

Control of Anaesthesia using the EMG

Recent work by Chang et al. [70] tested the use of an EMG monitor during surgery. Although not involved in closed–loop control, the usefulness of the EMG trace was investigated by either allowing or denying the anaesthetist access to it. The authors concluded that the EMG was not a useful indicator of depth of anaesthesia due to individual variabi lity and that the availability of the measurement did not improve the resulting control of anaesthesia.

Control of Anaesthesia using Cardiovascular and Respiratory Variables

Cardiovascular signs such as heart rate, blood pressures and the peripheral pulse are important components in the clinical signs used by the anaesthetist to assess anaesthetic depth. The results of Savege et al. [71] suggest that the cardiovascular response to noxious stimulus may be more sensitive than any of the changes in the processed EEG. The control of anaesthesia based upon the values of the cardiovascular variables may therefore provide a suitable anaesthetic state.

Suppan advocated the use of pulse rate, systolic arterial pressure, respiration rate and tidal volume to control the delivery of halothane, injected analgesics and fluids during anaesthesia. He described the results of clinical studies using the pulse rate [72], respiratory patterns [73] and arterial pressure [74] as the controlled variable. In his scheme, measurements were passed to 'integrators' which had 'low' and 'high' limits. The movement of an integrator output below the low limit or above the high limit caused a drug change. Given the simplicity of the proposed schemes, the performance achieved was surprisingly good.

The controller of Lampard et al. [75] manipulated ventilation, the delivery of anaesthetic (halothane) and the provision of muscle relaxation. The anaesthetic was delivered so as to control blood pressure.

Robb [61] developed and trialled PI type controllers for the delivery of enflurane and isoflurane in order to maintain systolic arterial pressure at a target

value. An additional rule was added so as to deliver a morphine bolus if the volatile agent concentration had exceeded certain limits over the last 5 minutes.

The control of systolic arterial pressure achieved a satisfactory anaesthetic state in the majority of patients. This also produced a satisfactory physiological state during surgery and a good recovery afterwards.

One case described by Robb, and in which the controller was used, involved significant blood loss by the patient. The blood pressure dropped as a result and this caused the controller to deliver no anaesthetic until the provision of fluids by the anaesthetist had restored the blood volume and hence the blood pressure had recovered. This apparently did not result in a period of anaesthetic inadequacy. It does however illustrate that because blood pressure results from the complex interaction of physiologic and pharmacologic effects, interpretation of blood pressure solely as an indicator of depth of anaesthesia may result in inappropriate interpretations and subsequent inappropriate anaesthetic states.

1.4.3 Control of Anaesthesia using an Inferred Depth of Anaesthesia

An alternative approach to the automatic control of anaesthesia involves the inference of depth of anaesthesia and the subsequent delivery of drugs in order to manipulate the inferred depth.

The RESAC system described by Linkens, Greenhow and Asbury [76] and Greenhow [77] employs a rule-based backward chaining Bayesian inference engine with fuzzy logic. The aims of RESAC were to provide both an assessment of the depth of anaesthesia and to suggest appropriate concentrations of anaesthetic agent which should be administered in order to control the depth of anaesthesia. RESAC includes a sophisticated user-interface for the input of qualitative and quantitative information on both clinical sign values and drug delivery. A further feature is the interfacing of RESAC to a monitor so as to periodically receive

arterial pressure and heart rate measurements. RESAC was developed to interpret the values of and changes in systolic arterial pressure, heart rate, movement, pupil size, pupil divergence, pupil movement, sweating and respiration rate. Three goals were tested in assessing the depth of anaesthesia. These were 'anaesthesia too light', 'anaesthesia OK' and 'anaesthesia too deep'. This assessment incorporated drug effects through the concept of 'relevance'. For example, the administration of muscle relaxant caused respiration rate cease to be relevant as an indicator of depth of anaesthesia. A fourth goal of RESAC was used to determine the necessary action in order to control anaesthesia. Evaluation of this goal, as described by Greenhow [77] takes account of reductions in anaesthetic requirement caused by the concomitant administration of muscle relaxants or analgesics. As explicit examples, RESAC took account of the effects of morphine, fentanyl, atracurium and vecuronium when determining the concentration of anaesthetic to be administered.

A detailed and informative account of the iterative refinements of RESAC following clinical trials is given by Greenhow [77]. Later versions of RESAC have clearly demonstrated very effective results.

1.5 Appraisal of the Current Directions in Control of Anaesthesia

1.5.1 Drug Delivery based upon Pharmacological Models and Measurements

Considering work of this type developed to control depth of anaesthesia and also related work in the control of muscle relaxation and control of blood pressure, several themes emerge with respect to modelling and control. These are:

1. The use of a pharmacokinetically–related variable as feedback in a simple controller.

2. The use of population pharmacokinetic models to determine the infusion rate for a drug in an individual.

3. The use of simple transfer function models in adaptive schemes to match the model to the patient and then control drug delivery based upon the model.

4. The use of sophisticated physiologically–based models matched to the individual to determine the rate of drug delivery in the individual.

Schemes of type 1 cannot provide consistent control performance over a range of patients because they cannot adapt. Schemes of type 2 are also weakened by the differences between the response of the individual and the response of the population. In using their control scheme to control propofol infusion in children, Marsh et al. [36] actually developed new models to represent the pharmacokinetics of propofol in children thereby moving the response of the model much closer to that of the individual with associated improvement in control performance. Maitre et al. [78] illustrated that significant errors resulted from the use of a population pharmacokinetic model to predict plasma concentrations. Similar errors are therefore possible if a population model is used in control. Adaptive control schemes involving the identification of a simple model (type 3) are largely justified in order to accommodate both the wide range of individual responses and the apparent time–varying response even within an individual. These schemes have proved capable of good performance in a wide range of patients.

The presence of inter–individual and intra–individual variation in drug response has prompted the development of adaptive controllers. Chapter 4 analyses the effects of different body composition on the pharmacokinetics of isoflurane. Although the pharmacodynamics of inhaled agents are not adequately understood,

it becomes apparent that a significant component of the inter–individual variability can be attributed to pharmacokinetic differences alone. Similarly, during anaesthesia, changes in respiration and circulation occur in response to changes in anaesthetic dose. As analysed in Chapter 4, the alteration of alveolar ventilation and cardiac output cause changes in the apparent dynamics of the pharmacokinetic response. The need for adaptive control schemes may therefore be partly due to the ineffective modelling of the physical systems involved. Intuitively, it can be expected that an obese individual would have a different anaesthetic requirement to that of an athlete and it is equally apparent that the apparent time–varying dynamics in the individual cannot be due to changes in body mass or composition during the anaesthetic but instead is due to fundamental physiological changes caused by drugs.

The use of physiologically–based models to control drug delivery (type 4) allows explicit representation of both inter–individual body composition changes and intra–individual physiological changes. In consideration of previous approaches to the control of depth of anaesthesia, Chilcoat, Lunn and Mapleson [79] concluded that most control systems involved "the feedback control of some variable used as an indirect measure of anaesthetic depth, such as some aspect of the EEG, the arterial pressure, or the end–tidal anaesthetic concentration". They further stated that "We consider that, in any one individual, a closer correlate of depth of anaesthesia is brain tension". Although brain tension cannot be measured, it seems that the direct relationship between the brain tension and the anaesthetic effect is more straightforward than the relationships between depth of anaesthesia and the other variables.

In the belief that the use of physiologically–based models and the control of brain tension (or brain concentration) of anaesthetic represent the most realistic means of approaching the modelling and control of anaesthesia pharmacokinetics, this approach has been adopted in the work described in this thesis.

1.5.2 Control of Anaesthesia by Controlling a Related Variable

Without exception, this approach involves the indirect monitoring of a pharmacologic effect using a physiological variable. Such effects, however, have significant interactions with other physiologic and pharmacologic processes. For example, changes occur in the EEG with changes in arterial carbon dioxide tension; blood pressure changes can occur in response to stressful stimuli and blood volume changes as well as in response to anaesthetic agents and other drugs. In using a related variable as an indicator of depth of anaesthesia, it is therefore essential to ensure that none of the additional physiological or pharmacological factors which also affect the variable are present. In consideration of the unreliability of most routinely available measurements as indicators of depth of anaesthesia, this approach has not been pursued in the work described in this thesis.

1.5.3 Inferring Depth of Anaesthesia

The RESAC system of Linkens et al. [76] and Greenhow [77] interprets an extensive range of quantitative and qualitative clinical signs, in the context of the drugs being given to the patient, to infer depth of anaesthesia. A further step is the determination of volatile agent concentration to be administered to the patient in order to control the depth of anaesthesia. This system has been developed following discussion with anaesthetists and aims to replicate their performance.

This approach is itself a significant contribution to the reliable inference and subsequent control of anaesthesia. In recognition of this, work in this thesis adopts a similar direction so as to interpret clinical signs in consideration of anaesthetic and other drugs. As a further step, the interpretation of clinical signs in terms of both pharmacologic events (drug administration) and physiologic changes is pursued. This direction is consistent with that of RESAC although the actual

approach, as described in Chapter 7, is different.

1.6 Contributions of this Thesis

As described above, this thesis adopts the direction of some previous work in the area and in so doing introduces some new approaches to both the assessment and control of anaesthesia. In summary, the thesis contributes the following:

- An unambiguous graphical representation for the physiologically–based models of pharmacokinetics such as those of Mapleson [40] and Davis and Mapleson [45].
- A physiological and physicochemical parameterisation of such a model to represent the pharmacokinetics of isoflurane.
- A scheme to allow matching of a physiologically–based model to an individual patient using only measurements of body mass and an estimate of body fat.
- A scheme for the estimation of cardiac output and tissue anaesthetic tensions in the individual undergoing surgery.
- A physiologically–based qualitative model of the homeostasis processes involved in the control of respiration, blood pressure and blood volume, the response to an extreme stressor and the effects of depressant drugs (anaesthetics).
- A qualitising filter for description of the trends of physiological and pharmacological variables.
- A scheme for the differential diagnosis of physiological and pharmacological imbalances in the patient's anaesthetic state.

- An architecture for the overall control of the anaesthetic state
- CLASS: The Closed-Loop Anaesthesia Support System — An object-oriented software library allowing interrupt driven communication handling and virtual devices for anaesthetic monitors, an infusion pump and a servo-vaporiser.
- GAEL: The Glasgow Anaesthesia Estimation Library — An object-oriented software library providing facilities to match a physiologically-based model to the individual patient, load individual inhaled drug physicochemical properties and estimate the patient tissue tensions and cardiac output.
- MASIE: Model-based Anaesthetic State Imbalance Evaluation — An object-oriented software library allowing the creation of variable threshold qualitising filters and the evaluation of possible anaesthetic state imbalances in the current patient anaesthetic state.

1.7 Summary of Contribution and Direction

In summary, work in this thesis involves;

1. The development and use of physiologically-based pharmacokinetic models with the intent of controlling drug delivery so as to achieve desired brain anaesthetic tensions.
2. The development and use of physiologically-based models to support the interpretation of clinical signs in the context of physiologic and pharmacologic events.

Figure 1.1 gave an overview of previous approaches to the control of anaesthesia. Figure 1.2 includes the contributions of this thesis in that context.

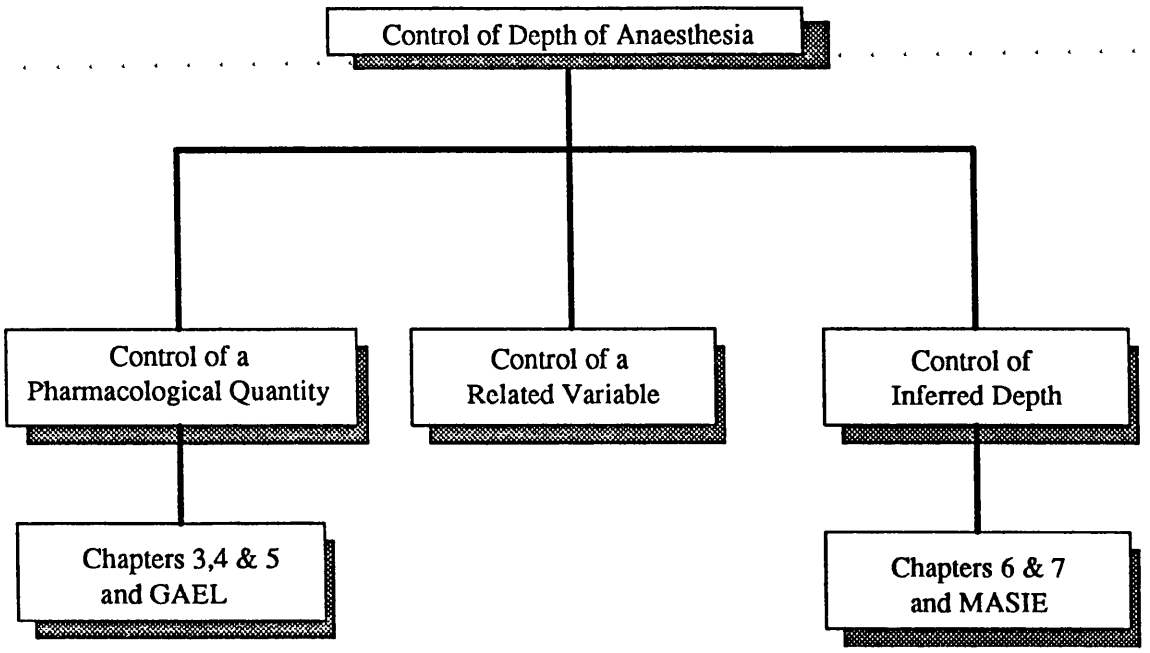

Figure 1.2: The Approaches Presented in this Thesis

1.8 The Structure of this Thesis

This thesis has been organised in three areas. The first consists of Chapter 2 and acts as an overview of anaesthesia. The second area consists of Chapter 3, Chapter 4 and Chapter 5. These chapters cover the use of pharmacology and physiology to develop models which can be used in the delivery of anaesthetic and related drugs, and in the estimation of inhaled anaesthetic tensions in the body. The third area consists of Chapter 6 and Chapter 7 and describes the use of physiology to develop a model of the homeostasis loops and stress response of the body which can be used to assess the anaesthetic state of a patient undergoing surgery. Each chapter is described in more detail below:

Chapter 2 of this thesis considers the processes and components of anaesthesia. A brief historical note is presented before the effects of local anaesthetic, analgesic and general anaesthetic drugs are described in terms of their physiological effects.

General anaesthesia is summarised and the activities important in monitoring anaesthesia are introduced. The chapter concludes with the description of conventional drug delivery and monitoring equipment used in anaesthesia and specialised software and hardware made available and developed for use in the work described in this thesis.

Chapter 3 introduces basic relations in pharmacology and describes the modelling of pharmacology in anaesthesia. The use of compartment models is discussed along with the use of physiologically–based pharmacokinetic models. The graphical representation of pharmacokinetic models using the bond graph model representation technique is then explained.

Chapter 4 describes the physiological and physicochemical parameterisation of a physiologically–based model of isoflurane pharmacokinetics. Physiologically, the model is based upon data presented by other authors. Physicochemically, it makes use of in–vitro experimental data available in the literature.

Chapter 5 describes the use of the model derived in Chapter 4 to produce a scheme for the estimation of cardiac output and tissue tensions in patients undergoing surgery. A procedure for matching the pharmacokinetic model to the patient using only simple measurements is described. The simulated and on–line performance of the estimation scheme are illustrated.

Chapter 6 of the thesis describes the homeostasis loops and stress response of the body which are relevant to anaesthesia. A model of homeostasis and the stress response based upon the qualitative descriptions of physiology is described. The model is intended to predict the compensation of the body for a range of physiological stresses. The performance of a prototype implementation of the model is illustrated.

Chapter 7 describes the use of the model of homeostasis and the stress response in the assessment of the anaesthetic state of the patient. A preliminary version of this reversed model has been implemented. Its off–line performance on logged

data and its on–line performance in theatre are presented.

Chapter 8 concludes the work described in the thesis in assessing the achievements made and the lessons learned during development. The thesis presents two different techniques for use in anaesthesia and this chapter outlines an architecture which allows their combination in order to provide control of the anaesthetic state. Trials of this architecture are not documented in the thesis and these are therefore suggested, along with other topics, as areas of future development.

Chapter 2

Anaesthesia

SUMMARY

This chapter introduces Anaesthesia and the equipment used in the work described in this thesis. A brief historical introduction precedes description of the physiological bases of pain and anaesthesia. General anaesthesia is specifically discussed and working definitions provided for use in the remainder of the thesis. Monitoring during general anaesthesia is outlined and the chapter concludes with discussion of specialised hardware and software used later to test prototype schemes.

2.1 Anaesthesia

2.1.1 General Definition

The word anaesthesia means "absence of sensation". General anaesthesia is the absence of all sensation and is associated with unconsciousness. In a clinical context, anaesthesia entails both absence of sensation for the patient and the provision of suitable operating conditions for the surgeon.

2.1.2 Historical Perspective

The first successful demonstration of anaesthesia was given by William Morton in 1846. Morton administered ether vapour to a patient having a tumour in his neck removed. At the time, Morton termed the process "etherisation".

An onlooker at the demonstration, Oliver Wendell Holmes, suggested that the term "anaesthesia" should be adopted. Holmes also introduced the phrases "anaesthetic state" and "anaesthetic agent".

Relatively soon afterwards, in 1847, chloroform was used as an anaesthetic by James Young Simpson in Edinburgh. The use of ether as an anaesthetic preceded both the use of antiseptics and the development of the hypodermic syringe.

Following Morton's demonstration, the use of ether became prevalent with chloroform also being readily applied. The use of anaesthesia permitted more lengthy surgery without compromising the patient. Surgical techniques developed accordingly, in parallel with developments in the use of existing and new anaesthetic agents.

Prior to the use of anaesthesia, pain relief for the patient was inadequate and consisted of alcohol or opium ingestion. Surgical conditions were created by physical restraint of the patient, and the surgeon relied upon speed of operation to minimise the patient's suffering.

2.2 Pain: The Perception of Noxious Stimuli

"Pain is the conscious perception of a noxious stimulus" [80]. The perception of pain occurs when tissues are being damaged and provokes action to remove the painful stimulus. The body contains receptor cells which are sensitive to a variety of stimuli such as mechanical deformation, temperature, chemicals and tissue damage. The receptors involved in the detection of pain are sensitive to the physical or chemical damage of tissues and are called *nociceptors*. Nociceptors

are responsive to stimuli which can damage tissue but can be stimulated by *any* stimulus of sufficient magnitude. There are three types of pain receptor present in skin; mechanosensitive pain receptors are activated by intense mechanical stimulation, mechanothermal pain receptors are activated by mechanical and thermal stimulation, and polymodal pain receptors are responsive to mechanical, thermal and chemical stimuli.

Pain receptors generate nerve impulses in response to stimulation. The frequency of the impulses depends upon the severity of the stimulus. The nature of the perceived pain depends upon the nerve fibres in which the impulses from the pain receptors travel. Mechanosensitive and mechanothermal pain receptors transmit impulses via $A\delta$ fibres. Polymodal pain receptors transmit impulses through C fibres. $A\delta$ fibres conduct nerve impulses at high velocities (6 to 25 m/sec) and give rise to a perceived stabbing pain. C fibres conduct impulses more slowly (0.5 to 2 m/sec) and give rise to burning or aching pain.

Pain impulses are conducted from pain receptors in the skin or in other structures, to the spinal column. Nerve impulses then pass along the spinothalamic tract which consists of nerves running along the spinal column to the thalamus. The thalamus is an area of the brain which, amongst other tasks, is responsible for the routing of pain impulses from the spinothalamic tract to other brain centres. The thalamus routes impulses to the somesthetic area of the cerebral cortex which is responsible for the interpretation of the location of the painful stimulus, assessment of its severity, and determination of the nature of the pain.

The transmission pathways involved in the perception of pain are represented in the schematic Figure 2.1.

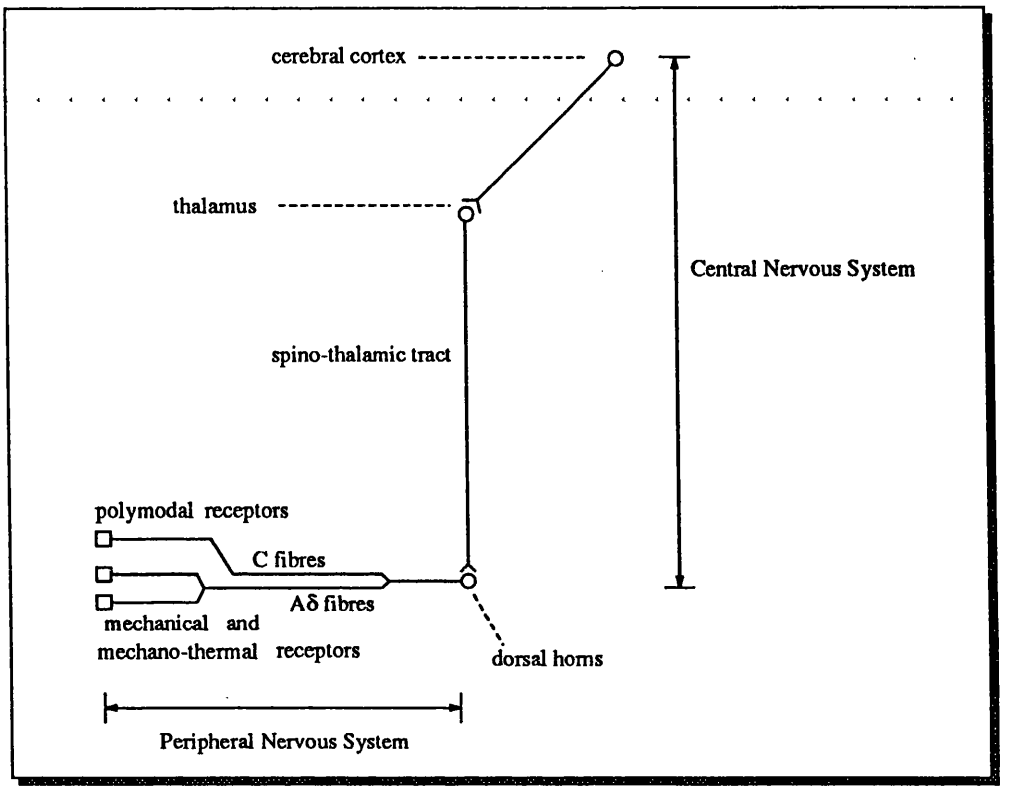

Figure 2.1: The Anatomy of Sensory Pathways

2.3 Drugs which alter the Perception of Noxious Stimuli

The perception of noxious stimuli requires that an intact and functional pathway exists between active nociceptors, through primary afferent neurons into the spinal column, up the spinothalamic tract to the thalamus, and from the thalamus to the somesthetic area of the cerebral cortex. Alterations in the perception of a noxious stimulus can be brought about via the inhibition or impairment of function of the components involved in the generation, transmission and interpretation of nerve impulses due to noxious stimulation. Such effects can be produced using local anaesthetic, analgesic and general anaesthetic drugs. Each of these drug types alters the function of one area of the sensory pathway between the nociceptors and the cerebral cortex.

2.3.1 Local Anaesthetic Drugs

Local anaesthetic agents block the initiation and propogation of nerve impulses in and along neurons. The initiation and propogation of impulses in a neuron depends upon the presence of sodium channels and potassium channels in the cell membrane. These channels can open and close in response to voltage changes between the cell's interior and exterior. At rest, the interior of a neuron has a potential of between -60 and -90 mV relative to the exterior. In this state, the cell is said to be polarised. Additionally, the environments of the cell and its surroundings are such that the concentration of sodium ions (Na^+) is 14 times greater outside the cell than inside, and the concentration of potassium ions (K^+) is 18 to 20 times larger inside the cell than outside it. In the polarised state, the sodium channels in the cell membrane are closed and the potassium channels are very nearly closed. A stimulus from a receptor, such as a pain receptor, or a propogating impulse in the neuron cause the potential of the interior of the cell to rise to around -50mV relative to the exterior. In this range of potential difference, the sodium channels of the membrane begin to open allowing sodium ions to move inside the cell due to electrical and concentration gradients. The influx of positive sodium ions further reduces the potential difference across the cell membrane. This process is called depolarisation. As the voltage of the interior of the cell reaches around -30 mV the sodium channels close preventing further movement of sodium ions. Also, during the depolarisation process, the potassium channels open further, but open much more slowly than the sodium channels. This allows potassium to move out of the neuron thus making the potential difference between interior and exterior return towards the initial value. This process is repolarisation. The flux of ions involved in this process establishes local currents around the membrane which cause propogation of the impulse along the neuron. A graph of the changes in the potential of the interior of a neuron with respect to the exterior for a local region of the membrane is given in Figure 2.2.

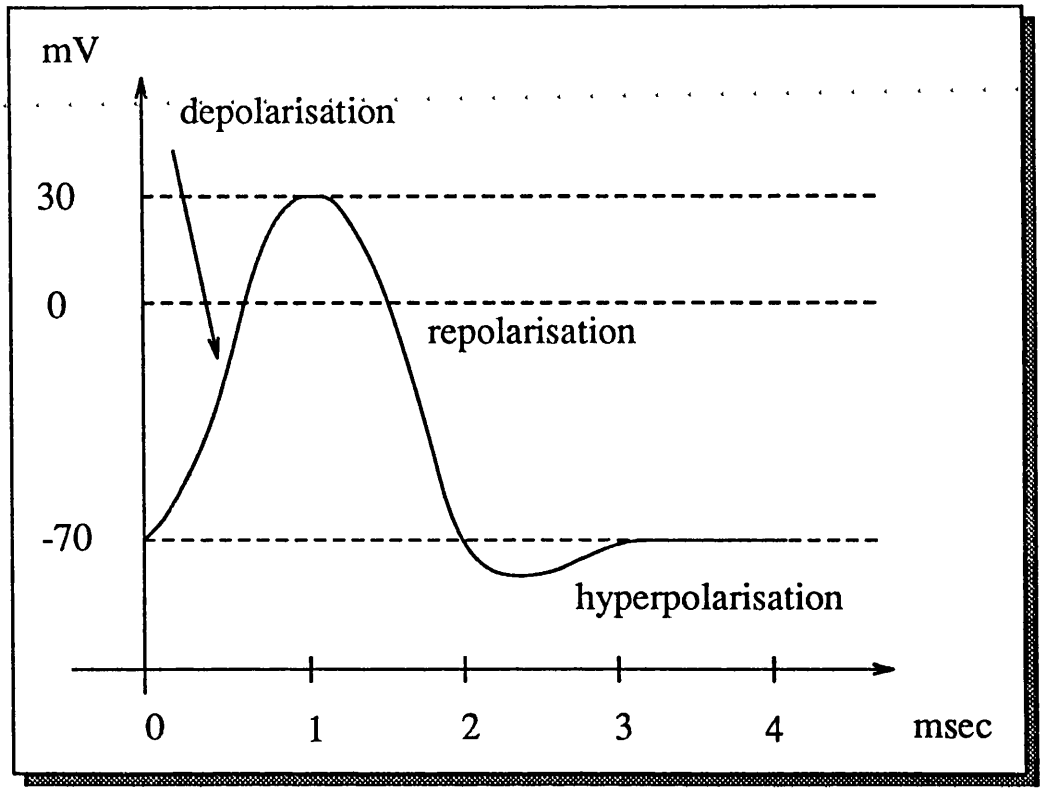

Figure 2.2: Potential Changes during Nerve Impulse Conduction

The dominant action of local anaesthetics is to block sodium channels in the neuron membrane. The membrane then cannot depolarise, impulses cannot be propogated along the neuron, and the transmission of nerve impulses from pain receptors to the brain along the nerve containing the affected neurons is prevented. By a similar mechanism, local anaesthetics also inhibit the generation of impulses by receptor cells.

2.3.2 Analgesic Drugs

Some analgesic drugs increase the permeability of potassium channels in neurons causing the hyperpolarisation of the cell membrane [29]. The hyperpolarisation of the cell membrane causes transmission of impulses along the neuron to be more difficult as additional effort is required to depolarise the membrane. Analgesic drugs also act at the junction or *synapses* between neurons. The pathway between a nociceptor and the cerebral cortex involves synapses between the peripheral

sensory neuron and the spinothalamic tract, and between the spinothalamic tract neurons and those connecting the thalamus and cerebral cortex. In most central nervous system nerves, nerve impulse transmission across a synapse involves chemicals known as neurotransmitters. At such a chemical synapse, the arrival of a nerve impulse at the synapse causes release of some neurotransmitter into the synaptic cleft between the presynaptic end bulb and the postsynaptic structure (Figure 2.3).

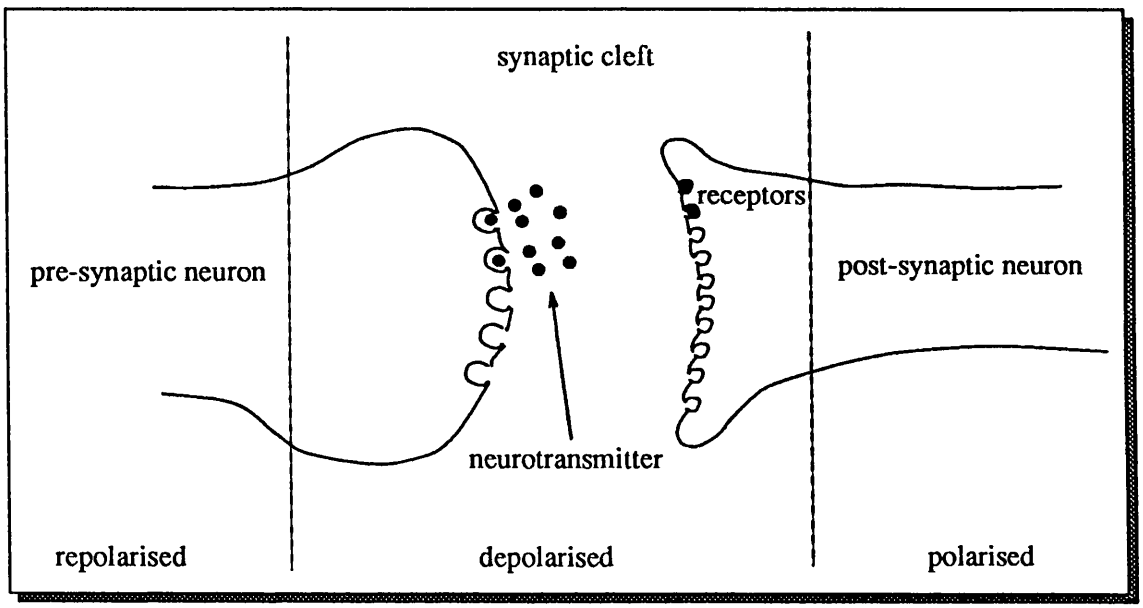

Figure 2.3: Neurotransmitter Function at a Synapse

The postsynaptic structure contains receptors for the neurotransmitter. Depending upon the neurotransmitter, the neurotransmitter–receptor interaction can either be excitatory or inhibitory. In an excitatory interaction, the postsynaptic neuron moves closer to depolarisation. Neurotransmitters which cause excitatory interaction do so by either increasing the membrane permeability to sodium ions directly, or by activating an enzyme called adenylate cyclase which participates in a chemical reaction resulting finally in increased membrane permeability to

sodium ions.

An inhibitory neurotransmitter–receptor interaction causes hyperpolarisation of the post–synaptic neuron by increasing the membrane permeability to potassium. This makes the conduction of an impulse across the synapse more difficult. A further mechanism for inhibiting nerve impulse conduction occurs when an inhibitory neuron synapses with another presynaptic neuron. The release of inhibitory neurotransmitter by the inhibitory neuron suppresses the release of excitatory neurotransmitter by the other neuron causing a decrease in the stimulation of the postsynaptic neuron.

Analgesic drugs can cause presynaptic inhibition to occur thereby reducing the conduction of impulses from nociceptors to the cerebral cortex. The activation of receptors for opioid analgesics, which exist on neurons, causes inhibition of adenylate cyclase activity thus reducing excitatory effects in the postsynaptic neuron.

Analgesics therefore cause reduced transmission of nerve impulses from nociceptors by a combination of effects which include;

1. hyperpolarisation of neurons,

2. pre–synaptic inhibition and

3. reduction of post–synaptic excitatory activity.

2.3.3 General Anaesthetic Drugs

General anaesthetics produce inhibition of the conduction of a nerve impulse along a neuron, and can also inhibit transmission across a synapse. To inhibit conduction along a neuron requires higher concentrations than those required to inhibit synaptic transmission [29]. Similarly, surgical levels of anaesthesia cause little or no inhibition of impulse transmission in peripheral nerves (i.e., outside the brain and spinal chord). While these observations are accepted, the exact mechanism

of action of anaesthetics is not known and several competing hypotheses exist. Anaesthetics have been observed to cause reductions in the release of excitatory neurotransmitter, to reduce the sensitivity of the post–synaptic neuron to the neurotransmitter, and to reduce the electrical excitability of the post–synaptic neuron [29]. Anaesthetics have also been found to inhibit the metabolic breakdown of an inhibitory neurotransmitter (gamma–aminobutyric acid, GABA) [27].

These effects do not occur in equal potency throughout the central nervous system. The loss of consciousness and amnesia caused by anaesthetics probably result from anaesthetic effects in the reticular formation and hippocampus regions of the brain at lower concentrations. Higher concentrations cause effects upon the motor centres which control movement, and the centres involved in the regulation of the body's physiological variables.

General anaesthetics exert their effects by inhibiting the transmission of impulses. This occurs more easily in the central nervous system than in the peripheral nervous system, and more easily in the brain centres concerned with consciousness and short–term memory than in others.

2.4 Types of Anaesthesia

The previous section described the mechanisms of drug action for local anaesthetic, analgesic and general anaesthetic drugs. The drugs are obviously categorised in terms of the effects which they produce. Although there are only three subdivisions of drug types, the use of different drugs gives rise to several different anaesthetic techniques. These are summarised below.

2.4.1 Local and Regional Anaesthesia

A local anaesthetic drug, as described earlier, is capable of inhibiting the generation of nerve impulses by a receptor and the transmission of nerve impulses

along a nerve. This effect allows the transmission of impulses between a site of noxious stimulation and the cerebral cortex to be interrupted and the sensation of pain in response to the noxious stimulation is avoided. Figure 2.1 illustrated the functional characteristics of the body's sensory pathways. Anatomical knowledge supports the inhibition of nerve impulse transmission at different places in the body, with different effects.

The inhibition of receptor activity is involved in topical anaesthesia and infiltration anaesthesia. Topical anaesthesia requires that local anaesthetic is applied to a mucous membrane. Infiltration anaesthesia requires deposition of the drug beneath the skin or a membrane.

The inhibition of nerve impulse transmission in the peripheral nervous system can be used to produce anaesthesia for a region of the body. The deposition of drug around a nerve prevents all receptors which transmit nerve impulses along that nerve from passing information to the brain.

The administration of drug around the spinal column can produce anaesthesia for large areas of the body without causing other undesirable effects such as unconsciousness. This is spinal anaesthesia.

2.4.2 General Anaesthesia

While a local or regional anaesthetic involves the introduction of a drug in the vicinity of an anatomical site, general anaesthetic drugs are administered either by intravenous injection or by inhalation, and reach all tissues of the body. As described earlier, general anaesthetics have their most potent effects within the central nervous system and produce comparatively minor effects in the peripheral nervous system at clinical doses. In depressing brain activity, general anaesthetics interrupt the interpretation of nerve impulses transmitted from a site of noxious stimulation, to the brain. Once again, the pathway between the nociceptors and the cerebral cortex is functionally interrupted and prevents the conscious

perception of pain. The remainder of this thesis is concerned with general anaesthesia and more extensive discussion of this is given below.

2.5 General Anaesthesia

In the first anaesthetics administered, using ether or chloroform, the anaesthetic vapour was the only drug used. As such, it was required to produce not only anaesthesia, but also other effects which supported the surgeon. As drugs developed, including more specific general anaesthetics, analgesics and muscle relaxants, it became necessary to control the administration of several drugs in order to manage the anaesthetic. The evolution of new drugs continues and the anaesthetist is routinely responsible for the administration of general anaesthetic and analgesic drugs during anaesthesia, along with the administration of blood or fluids when needed. If surgery is to be assisted by muscle relaxation, the respiratory muscles of the patient will also be paralysed. Because of this, the anaesthetist must initiate and control the artificial ventilation of the patient. the anaesthetist inherits responsibility, not only for the administration of muscle relaxant but also for the ventilation of the patient.

These processes are further complicated by the range of patients undergoing surgery. This range is extensive both in terms of the physical condition of the patients and in terms of their co-existing disease and medication.

While the skills of anaesthetists have been extended to cope with the capacity to manipulate effects using a combination of drugs, the concepts and definitions of anaesthesia have been slow to follow.

2.5.1 Debate in General Anaesthesia

Perhaps the most widely accepted definition is that of anaesthesia. Prys-Roberts [80] suggests that "the state of anaesthesia can be defined as that in

which, as a result of drug–induced unconsciousness, the patient neither perceives nor [subsequently] recalls noxious stimulation". The important aspects of this definition are that it is defined for the *patient*, and that it encompasses both perception during a procedure and recall afterwards. As pointed out by Robb [61] " 'anaesthesia' is a retrospective diagnosis".

Debate continues, however, in consideration of the features of an "anaesthetic". Robb states that the anaesthetist "aims to produce a reversible state which includes:

1. "Hypnosis...
2. Maintenance of physiological variables...
3. Reflex suppression...
4. A safe and comfortable post–operative recovery..."

Pinsker [81] argues that "paralysis, unconsciousness and attenuation of the stress response are the necessary and sufficient components of the anesthetized state". Woodbridge [82] suggested that the components of anaesthesia were hypnosis, analgesia, muscle relaxation and the suppression of reflexes. Prys–Roberts [80] argues that "Analgesia, muscle relaxation and suppression of autonomic activity, are not *components* of anaesthesia. Rather they should be considered as desirable supplements to the state of anaesthesia as a means to enable surgery to be performed".

2.5.2 Definitions used in this Thesis

In recognition that there is no single set of consistent, universally–accepted definitions of terms related to anaesthesia, the following definitions will be adopted and used in the remaider of the thesis:

Anaesthesia

The definition given by Prys-Roberts is adopted i.e.,

> "the state of anaesthesia can be defined as that in which, as a result of drug–induced unconsciousness, the patient neither perceives nor [subsequently] recalls noxious stimulation".

Anaesthetic

As discussed, the features of an "anaesthetic" or of "anaesthesia" are the subject of continuing debate. Until a more suitable term evolves which encompasses all of the activities of the anaesthetist in theatre, confusion is inevitable. The use of the term "anaesthetic" to cover the activities of the anaesthetist will not be used in the remainder of the thesis.

The Goals of an Anaesthetist

The goals of an anaesthetist are defined so as to encompass all of the activities of the anaesthetist. The goals of an anaesthetist are therefore considered to be, to provide a reversible state including;

1. anaesthesia for the patient,
2. maintenance of a stable physiological state for the patient and,
3. the provision of suitable conditions for surgery.

Depth of Anaesthesia

Depth of anaesthesia is a concept used to classify the anaesthesia provided for the patient. Depth of anaesthesia is considered to be a continuum with "light anaesthesia" and "deep anaesthesia" being at either end of the clinically useful range. Light anaesthesia exists when the patient is receiving inadequate general

anaesthetic drug for the current level of surgical stimulation. Deep anaesthesia exists when the patient is receiving excessive general anaesthetic drug for the current level of surgical stimulation.

The Anaesthetic State

The anaesthetic state of the patient is considered to be composed of both the patient's physiological state and their pharmacological state. This definition of anaesthetic state is adopted to emphasise the mutual dependence of physiological and pharmacological events in anaesthesia.

Anaesthetic State Imbalance

The patient's anaesthetic state was defined to consist of both physiological and pharmacological states. The goals of the anaesthetist are to provide an appropriate anaesthetic state. Because work in this thesis is intended to provide support for the control of anaesthesia, a definition for an appropriate anaesthetic state is desirable. Such a definition is, however, not available. Anaesthetists, while being unable to agree upon an appropriate anaesthetic state, seem to have quite consistent opinions on the characteristics of an inappropriate anaesthetic state. An anaesthetic state may become inappropriate due to a change in the patient's physiological state e.g., a reduced circulating blood volume following bleeding, or due to a change in the patient's pharmacological state e.g., the anaesthetic delivery is reduced and the anaesthetic becomes light.

To support the development of a controller for the anaesthetic state, an anaesthetic state imbalance is therefore considered to be an inappropriate condition of a component of the anaesthetic state which can be remedied by a change in the physiological or pharmacological states of the patient. A physiological anaesthetic state imbalance can be rectified by a change in the physiological state of the

patient e.g., a reduced circulating blood volume can be remedied by the administration of blood of fluids. A pharmacological anaesthetic state imbalance can be rectified by a change in the pharmacological state of the patient e.g., inadequate muscle relaxation can be remedied by further administration of muscle relaxant; deep anaesthesia may be remedied by the reduction of anaesthetic administration.

Appropriate Anaesthetic State

Following on from the previous definition, an appropriate anaesthetic state is defined to exist when there are no anaesthetic state imbalances.

2.5.3 The Phases of General Anaesthesia

The phases of general anaesthesia are the individual components involved in the overall assessment and management of a patient before, during and after general anaesthesia. There are five phases [83] and these are summarised as follows:

Pre-operative Assessment

The anaesthetist requires to assess the state of each patient prior to administering an anaesthetic. The anaesthetist aims to anticipate the effect of surgery and the anaesthetic upon the patient and also establish any changes which the patient will require in the anaesthetic technique. The surgical procedure to be carried out will dictate the anaesthetic state required and also give an estimate of the recovery time for the patient.

The pre-operative assessment is used to establish basic anatomical information about the patient so as to determine ease of intubation, ease of access to veins for cannulation, and ease of ventilation.

Investigation of the previous illnesses of the patient give indication of other complications due to cardiovascular or respiratory disease. History of previous anaesthetics highlight drug sensitivity or allergy. The degree of anxiety or

apprehension of the patient gives an indication of the need for pre-operative sedation.

Pre-operative Medication

Pre-operative medication is intended to make the time before surgery comfortable for the patient, and to forestall potential problems following surgery.

The main complication prior to surgery is normally the anxiety of the patient. Pre-operative administration of a sedative drug in the hours before surgery can reduce anxiety. Other drugs may be administered to cope with co-existing disease of the patient, to reduce post-operative vomitting (anti-emetics) or to reduce salivation (anti-sialogogues).

Induction

Induction represents the most dramatic change in the physiological state of the patient during the anaesthesia process. The aim of induction is to rapidly and safely achieve a depth of anaesthesia appropriate to the performance of surgery.

Prior to induction, a cannula is inserted into one of the patient's veins to allow ease of administration of intravenous drugs and fluids. Following induction, an endotracheal tube may be inserted in the patient's trachea. An endotracheal tube secures access to the patient's lungs and prevents passage of any foreign material into the lungs.

Maintenance of Anaesthesia

The initial depth of anaesthesia achieved during induction is usually produced using a fast acting barbiturate drug (e.g. thiopentone). The maintenance of an appropriate depth is achieved by administration of volatile (gaseous) or intravenous anaesthetics.

Initially, following induction, it is necessary to attach the patient to drug

delivery systems, attach necessary instrument sensors to the patient and place the patient in the correct operating position.

The transition from the conscious patient prior to induction to the unconscious, anaesthetised patient involves significant changes in the physiological state of the patient. The measurements made in the period immediately following induction show wide variation as the combined effects of changes in physical position and the influences of drugs interact.

When the anaesthetist is satisfied that the patient is adequately anaesthetised and that no other complications exist, surgery can proceed. The anaesthetist is now responsible for changes in delivery of drugs and fluids to the patient in accordance with the anaesthetic state of the patient and, if muscle relaxants are being used, the control of muscle relaxation and ventilation.

Drug delivery is stopped as surgery reaches completion and the patient is disconnected from instrumentation and drug systems when a satisfactory level of protective reflexes has been attained.

Recovery

The patient is transferred to the recovery room for observation until a safe level of protective reflexes has returned. In the initial part of recovery, the patient still has a significant amount of anaesthetic present in the body. This is likely to reduce the respiratory drive of the patient. Continual, vigilant observation of the patient in the recovery room is thus essential.

2.6 Monitoring during General Anaesthesia

During the maintenance of anaesthesia, the anaesthetist is concerned with the monitoring of four distinct areas. These are

1. the anaesthesia machine and drug delivery devices,

2. the physiological state of the patient,

3. the depth of anaesthesia of the patient and,

4. the conditions provided for surgery.

Obviously, unreliable or faulty performance of the anaesthesia machine or a drug delivery device can cause subsequent alteration in the physiological state of the patient or in their depth of anaesthesia. Similarly, inappropriate depth of anaesthesia can compromise the physiological state of the patient. These three areas are therefore inter–dependent. Similarly, inappropriate surgical conditions will hinder the surgeon and make surgery more difficult.

The provision of appropriate surgical conditions such as muscle relaxation has not been pursued in the work described in this thesis. Aspects of the monitoring of surgical conditions are therefore not discussed further.

2.6.1 Monitoring the Anaesthesia Machine and Drug–delivery Devices

The Anaesthesia Machine, Vaporiser and Circle System

The anaesthesia machine is used to administer metered amounts of gases to the patient. The anaesthesia machine may operate solely on supplies of gases from cylinders, or may use pipeline supply with the cylinders on the machine acting as emergency reserves. Controls on the anaesthesia machine allow the flow rates of oxygen, nitrous oxide, carbon dioxide and air in the inspired mixture to be altered. This mixture of gases can then be passed through a vaporiser which adds a volatile anaesthetic vapour to the gas stream. The flow of oxygen, air, carbon dioxide and nitrous oxide is measured using "rotameter" flowmeters[84]. In a rotameter flowmeter, a bobbin is suspended in the gas stream in a tube of tapered diameter as shown in Figure 2.4. The gas flow is calibrated at a particular

temperature and pressure and this is incorporated on the flowmeter tube. The rotameter flowmeter is a simple device but because the bobbin is suspended in the gas stream, it is comparatively easy to determine whether there is actually a flow in the device.

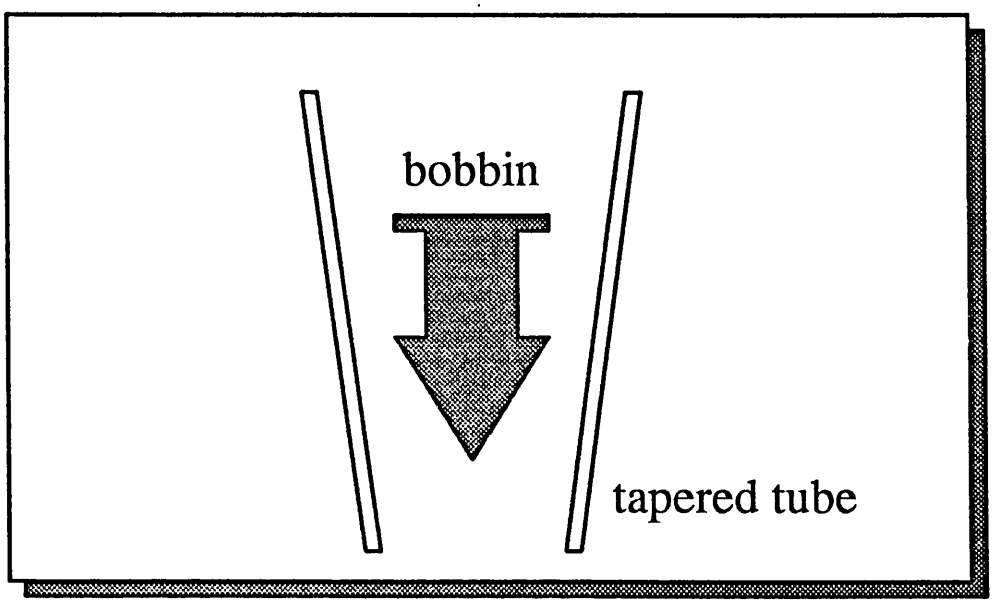

Figure 2.4: A Cross–section of a Rotameter Flowmeter

The combined gas stream flows into a vaporiser. In the vaporiser, some of the gas is passed over liquid volatile agent and then recombined with the remainder of the gas which bypassed the liquid. This process is calibrated over a range of flow rates and is temperature compensated. This arrangement is schematically represented in Figure 2.5.

The anaesthesia machine also features an automatic ventilator to permit ventilation of patients when that is appropriate. When used, the ventilator draws gas from the gas mixture leaving the vaporiser and passes the gas into the patient's lungs according to pressure or volume settings. The patient's expiration during ventilation is passive due to the elasticity of the lungs and chest wall. The ventilator can be bypassed when the patient breathes spontaneously. Ventilators generally employ bellows to perform ventilation. The frequency and amplitude of the bellows movement determine the characteristics of the ventilation. An

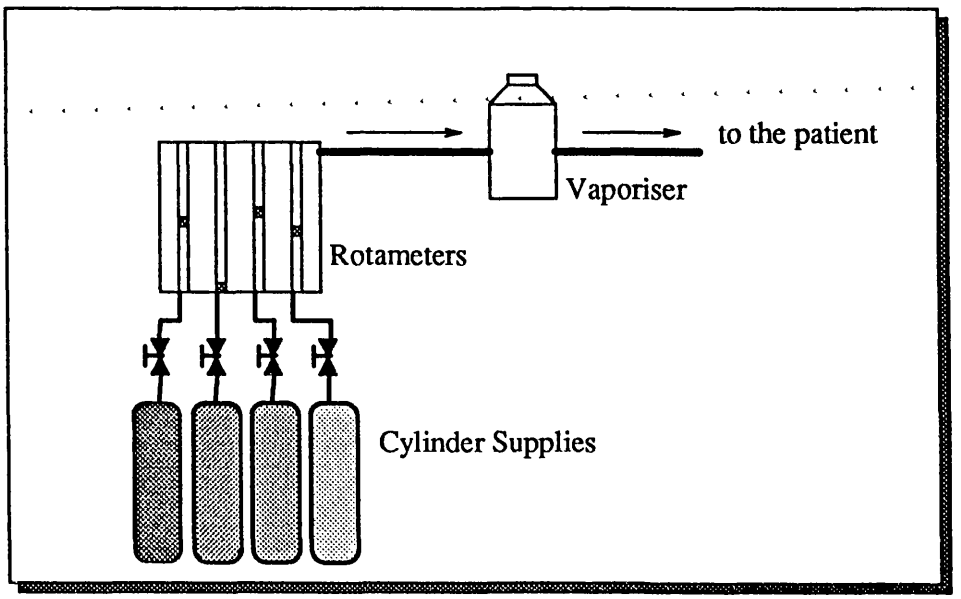

Figure 2.5: A Schematic of the Anaesthesia Machine

additional feature of bellows ventilators is that their movement can be easily observed thus providing vital information on ventilator function.

In many anaesthetics, a circle breathing system is used. A circle breathing system conserves anaesthetic gases and therefore reduces both cost and atmospheric pollution A typical arrangement is shown in Figure 2.6. The inspiratory and expiratory valves are typically placed in clear plastic housings which enable their movements to be observed.

Due to the volume of the circle system, the penalty for the reduced cost and pollution is a delayed change of inspired concentration after a change of the vaporiser concentration setting or other fresh gas component and the dependence upon soda lime for the removal of carbon dioxide.

Correct Anaesthesia Machine Function

A correctly functioning anaesthesia machine and delivery system will ensure that the gas flows measured by the flow meters enter the vaporiser where the volatile agent joins the fresh gas flow. The vaporiser, if functioning correctly, ensures that the concentration of volatile agent entering the gas stream is the same as that on

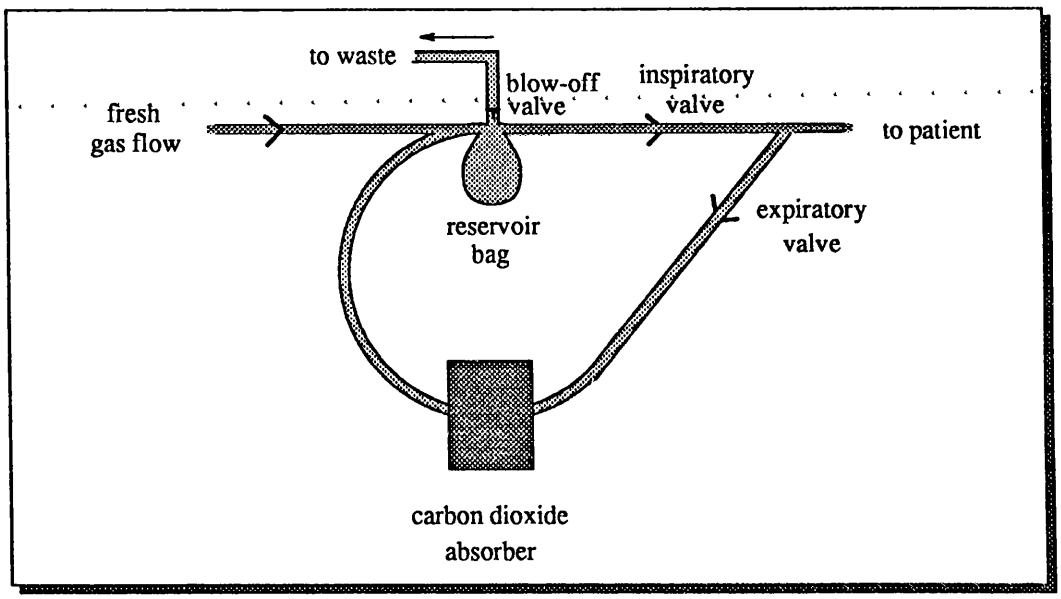

Figure 2.6: A Schematic of a Circle Breathing System

the vaporiser dial. If a ventilator is used, it should deliver the requested volume of gas at the requested rate and without exceeding pressure limits. If a circle breathing system is employed, gas flow should be unidirectional in the circle if the valves are functioning correctly. The carbon dioxide absorber should be capable of removing all expired carbon dioxide from the patient's exhaled gas.

Anaesthesia Machine Monitoring

The ability to monitor the function of the anaesthesia machine is greatly enhanced by monitors which can measure inspired gas concentrations. Using monitors of this type, allows measurement of inspired (and end-tidal) oxygen, carbon dioxide, nitrous oxide and volatile anaesthetic. Therefore, if the anaesthesia machine has been set up to deliver 1 litre/minute oxygen and 1 litre/minute nitrous oxide, the inspired oxygen and nitrous oxide concentrations would then be 50% if no circle system was present. The inspired volatile anaesthetic agent concentration measurement can be used to monitor the function of the vaporiser. The inspired carbon dioxide measurement indicates the efficacy of the carbon dioxide absorber in removing carbon dioxide from the exhaled gas.

Despite the uncomplicated layout of the anaesthesia machine and breathing circuit, their use appears to be the source of a large number of problematic incidents in anaesthesia. In a study of avoidable problems during anaesthesia, Cooper et al. [85] found that 19% of incidents were due to ventilation or breathing circuit problems, 19% were related to the use of the anaesthesia machine and 7% were related to infusion devices. This would imply that more effective monitoring of the anaesthesia machine and drug delivery equipment could significantly reduce the incidence of untoward events.

Approaches to the Automatic Monitoring of the Anaesthesia Machine

The Utah Anesthesia Workstation described by Loeb et al. [86] has been designed to assist in the monitoring and control of the anaesthesia machine. Associated with this development is a set of monitor functions which are capable of correctly identifying many anaesthesia machine faults including; disconnections, blockages, leaks, empty cylinders etc. This system incorporates a graphical display to illustrate, where appropriate, both the fault and its location. The system uniquely and correctly identified 88% of all faults presented to it in a trial. This kind of approach may be used to significantly reduce the incidence of anaesthesia machine related mishaps in anaesthesia.

2.6.2 Monitoring the Physiological State of the Patient

Greenburg and Peskin [87] state that "The primary objective of monitoring is the early detection of physiologic instability."

Physiological instability is the deviation of physiological variables from stable values. Stable values are those which can be maintained adequately by regulatory loops of the body. When a regulatory loop is unable to maintain a value through either already exerting maximal effect or through impaired ability to compensate, the regulated variable becomes unstable. The early detection of a physiologic

instability allows compensatory therapy to be initiated so as to minimise or avoid subsequent effects.

The regulatory loops of the body are highly complex and also interact significantly. It is however convenient to group regulatory loops together in 'systems'. In considering monitoring in a surgical intensive care unit, Greenburg and Peskin [87] suggest the 10 systems listed below.

1.	Respiratory	6.	Metabolic
2.	Cardiovascular	7.	Renal
3.	Oxygen Transport	8.	Hepatic
4.	Fluid and Electrolyte	9.	Gastrointestinal
5.	Haematologic/Coagulation	10.	Neurologic

Of these, the first four are of greatest importance during anaesthesia largely because changes in the condition of these systems occur quickly and are associated with a rapid change in the condition of the patient. The aims and extent of monitoring for these systems is described in the following sections.

Monitoring the Respiratory System

The respiratory system is responsible for the uptake of oxygen into the body, and the removal of carbon dioxide from it. Failure to either take up sufficient oxygen or remove sufficient carbon dioxide causes stimulation of sympathetic nervous system activity and results in significant changes in clinical signs. During anaesthesia with inhalational agents, the respiratory system additionally provides the mechanism for the uptake and removal of inhaled drugs. Ensuring correct function of the respiratory system is therefore vital to both the physiological state of the patient and to the administration of an anaesthetic.

As described in the previous section, the anaesthesia machine and gas delivery system can, in faulty conditions, either fail to deliver the required amounts of

oxygen, nitrous oxide or volatile agent, or can fail to remove carbon dioxide from exhaled gas. Adequate monitoring of the anaesthesia machine is therefore prerequisite to assuring appropriate respiratory function.

Benumof [88] suggests that an "essential monitoring system" for the respiratory system involves:

- checking the anaesthesia machine
- monitoring the oxygen–delivery system
- monitoring apnea
- monitoring minute ventilation
- monitoring gas exchange
- monitoring airway mechanics
- monitoring cardiovascular changes
- monitoring muscle relaxation and,
- monitoring temperature.

Assuming that the first two of these activities are performed during the monitoring of the anaesthesia machine and drug delivery devices, the monitoring of apnea, minute ventilation and gas exchange are usually most important. These are discussed below.

1. Monitoring of Apnea

   Apnea exists when the patient ceases to breathe. The most effective determination of apnea is achieved by listening to breathing sounds with a stethoscope. Breathing can also be assessed by observing the patient's chest movement and the movements of the anaesthesia machine reservoir bag. Typical respiration monitors calculate respiration rate using the gas

stream carbon dioxide concentration. This has the form shown in Figure 2.7

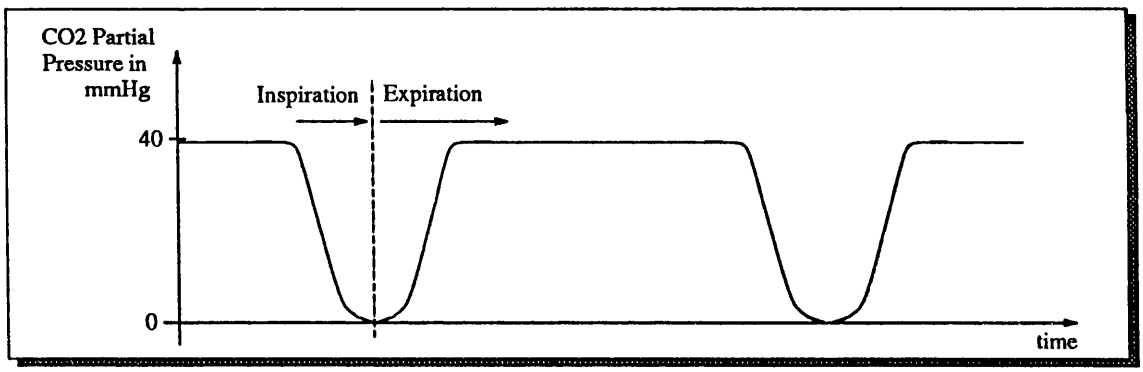

Figure 2.7: An Example End–Tidal Carbon Dioxide Waveform

Dips in carbon dioxide concentration occur during inspiration where very little carbon dioxide is expected to be inspired. The peaks in carbon dioxide concentration result from the measurement of carbon dioxide in exhaled gas. In the event of reduced ventilation or perfusion of the alveoli due to disease of obstruction, the rate of rise of the CO_2 waveform during expiration decreases. This is because gas which has been unable to equilibrate with blood is present in greater quantities than with normal ventilation and perfusion. Respiration monitors calculate respiration rate from the period of the carbon dioxide concentration waveform, and deduce apnea when the wave features no oscillations.

2. Minute Ventilation.

   Minute ventilation is the product of respiratory rate and tidal volume. The tidal volume is the amount of gas passing into the patient in each inspiration. An adequate minute ventilation ensures that sufficient gas is delivered to the

lungs to equilibrate with the blood.

More correctly, it is the gas delivery to perfused alveoli which is important and this is called alveloar minute ventilation. Alveolar minute ventilation is less than minute ventilation due to anatomical and physiological deadspace.

Anatomical deadspace is composed of the areas of the mouth, nose, trachea and bronchi where inspired gas reaches but which cannot equilibrate with the blood. Physiologic deadspace exists because not all alveoli are perfused at all times. Inspired gas in the vicinity of unperfused alveoli cannot equilibrate with the blood passing through the lungs.

In circumstances where the tidal volume is decreased, minute ventilation can be maintained by increasing respiratory rate. In such circumstances, however, although minute ventilation is maintained, the alveolar minute ventilation is decreased. This is illustrated by an example; Let MV_1, RR_1 and TV_1 be a minute volume, a respiratory rate and a tidal volume respectively, with

$$MV_1 = RR_1 \cdot TV_1$$

Now let $RR_2 = 2 \cdot RR_1$ be a new respiratory rate, and $TV_2 = 0.5 \cdot TV_1$ be a new tidal volume. The new minute volume is then

$$MV_2 = RR_2 \cdot TV_2 = MV_1$$

But, let the combined physiological and anatomical deadspace be DS, then for the first instance, the alveloar ventilation AV_1 is,

$$AV_1 = RR_1 \cdot (TV_1 - DS) = MV_1 - RR_1 \cdot DS. \tag{2.1}$$

For the second case, the alveloar ventilation AV_2 is given by

$$AV_2 = RR_2 \cdot (TV_2 - DS) = MV_1 - 2 \cdot RR_1 \cdot DS. \tag{2.2}$$

Thus, the maintenance of minute ventilation does not ensure the maintenance of alveloar minute ventilation.

The anaesthesia machine generally features sufficient instrumentation to allow measurement of respiration rate, tidal volume and minute volume. Using estimates for physiological and anatomical deadspace allow alveloar minute ventilation to be estimated.

3. Gas Exchange.

As stated earlier, it is essential to deliver sufficient oxygen to tissues and to remove sufficient carbon dioxide from them. It is possible to measure the oxygen saturation in blood reaching the fingers using a finger probe. The probe is calibrated so as to give a reading in % saturation of Haemoglobin. Oxygen is bound to Haemoglobin to allow its transport around the body. The oxygen–haemoglobin saturation curve depicts the relationship between percent saturation of haemoglobin and the arterial oxygen partial pressure and is shown in Figure 2.8.

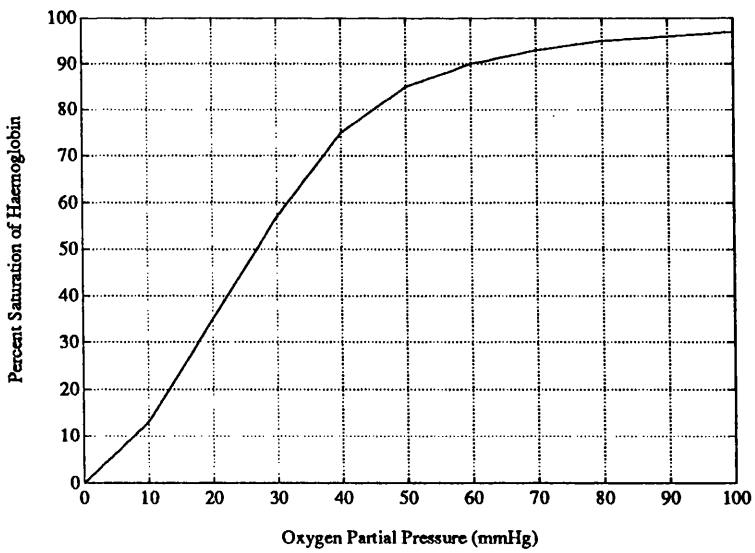

Figure 2.8: Oxygen–Haemoglobin Saturation Curve

Thus values of oxygen partial pressure of 80 mmHg or more result in 95% saturation of haemoglobin.

In contrast to oxygen, carbon dioxide is in solution in blood. Physiologically,

appropriate values for carbon dioxide partial pressures are also known. Expected values for arterial carbon dioxide are in the range 35 to 45 mmHg. The measurement of end-tidal carbon dioxide correlates well with arterial carbon dioxide measurements and can thus provide a good non-invasive estimate of arterial carbon dioxide partial pressure.

Monitoring the Cardiovascular System

The aim of monitoring the cardiovascular system [89] [90] is to ensure that all tissues receive an adequate supply of oxygenated blood at all times. Normal function of the respiratory system allows oxygen to be taken up by the body and carbon dioxide removed from it. The uptake and later elimination of inhaled anaesthetics also relies upon the respiratory system. The process of delivering oxygen and drugs to tissues and removing carbon dioxide and drugs from them depends upon the cardiovascular system.

Normal function of the cardiovascular system requires the normal function of the heart, which pumps blood around the body, and of the blood vessels through which the blood is pumped.

1. Monitoring the Heart.

   The heart pumps blood through the blood vessels thereby delivering oxygen and other nutrients to tissues and removing carbon dioxide and other waste products from them. The heart functions as a pulsatile pump and thus discrete volumes of blood are ejected into the arterial system by the heart on each heart beat. The pulsatile nature of the heart allows a 'pulse' to be felt in the arteries of the body. The function of the heart can be routinely and non-invasively measured using the following;

   (a) Peripheral Pulse

   Observing a pulse in a peripheral tissue site, e.g. the wrist, establishes

that the heart is functioning. Further information is available from the characteristics of the pulse. This information gives an indication of the state of the heart and blood vessels.

The presence of a peripheral pulse suggests that the heart, brain and other vital organs will be receiving adequate blood supply. If the oxygen saturation in the peripheral tissues is adequate, the vital organs will be adequately oxygenated.

(b) Electrocardiogram (ECG)

The mechanical activity of the heart reflected in the peripheral pulse results from the contraction of the muscle walls of the heart. Associated with muscle contraction are electrical currents and hence potential differences. The ECG measures the potential differences on the surface of the body which reflect the polarisation and depolarisation of heart muscles. In the presence of a peripheral pulse, with adequate oxygen saturation, the ECG can be used to provide heart rate information. In the event of irregular peripheral pulse or another problem, the ECG can be used to determine the cause of the problem.

The ECG is responsive to changes in ion concentrations in the blood and the oxygenation of the heart muscle and so can be used to assist the recognition of such problems.

2. Monitoring Blood Pressure

Arterial blood pressure reflects the flow of blood through the resistance offered by the blood vessels. For a constant cardiac output (flow), an increase in the vascular resistance will cause an increase in pressure. A decrease in vascular resistance will cause a pressure decrease. Similarly, if the vascular resistance remains constant, a decrease in cardiac output will cause a blood pressure decrease and an increase in cardiac output will cause

a blood pressure increase. Blood pressure therefore reflects the activity of the heart and blood vessels and is a valuable measurement.

The systolic arterial pressure is the highest pressure in the arteries, the diastolic pressure is the lowest. The heart muscle is perfused between contractions of ventricles and its oxygenation depends upon the diastolic pressure. All other tissues depend upon the systolic pressure for adequate perfusion. Low systolic pressure can prevent some organs from being perfused, low diastolic pressure prevents the heart from being adequately perfused.

Because blood pressure results from the flow of blood in the vascular resistance, blood pressure can be maintained in conditions of low flow by increasing the vascular resistance. This is acheived in the body by contracting the muscle walls of arteries, arterioles and veins so as to provide increased resistance to flow. This process, however, reduces the blood flow in the peripheral tissues so that the peripheral pulse weakens.

The presence of a satisfactory peripheral pulse and a normal arterial pressure indicate that blood flow and vascular resistance both possess normal values.

3. Monitoring Central Venous Pressure (CVP)

The central venous pressure, is the pressure in the large veins which enter the heart. If the blood volume increases from normal, the central venous pressure increases as does cardiac output. If blood volume decreases, CVP and cardiac output decrease. In the presence of normal heart function, measurement of CVP can thus give an indication of the blood volume status of the patient and provide a means of determining if fluid delivery is required. Monitoring of the CVP is advisable for individuals with cardiovascular disease or those undergoing major surgery.

2.6.3 Monitoring the Depth of Anaesthesia

The use of measurements and observations supports assessment of the physiological state of a patient. Some other observations, in addition to many of the measurements and observations employed to assess the physiological state, can be used to assess the depth of anaesthesia for a patient.

In the absence of noxious stimulation, any anaesthetic is too deep. In the presence of surgical or other noxious stimuli, anaesthetic depth is assessed using the signs of the patient. The most accessible and commonly used signs are eye signs, blood pressure, pulse rate and rhythm, respiration, muscle relaxation and sweating [91] [92].

Eye Signs

Eye signs such as pupil size, pupil response to light, eye movement and eyelash reflex have historically been considered to be useful indicators of the depth of anaesthesia. Eye signs are sensitive to drugs being used and do not offer reliable indication of the depth of anaesthesia [91] [92] [61].

Cardiovascular Signs

the cardiovascular signs of routine use in the assessment of depth of anaesthesia are the blood pressures and heart rate.

1. Blood Pressures

   Changes in blood pressure reflect the status of the cardiovascular system as described in Section 2.6.2. If it is established that no significant physiological imbalances exist in the cardiovascular system, then the blood pressure can be employed as an indicator of anaesthetic depth. Generally, increasing depth of anaesthesia causes a decrease in systolic arterial pressure [27] [91] [93]. This effect is however agent specific. The effects of several anaesthetic

agents and combinations are summarised in Table 2.1[27].

Agent	1 MAC	1.5 MAC	2 MAC
Halothane	80	70	60
Isoflurane	75	65	45
Isoflurane + N_2O	85	80	75

Table 2.1: Systolic Arterial Pressures as a Percentage of Awake Values for different Agents and Concentrations

2. Heart Rate

Heart rate changes also reflect the cardiovascular status of a patient (Section 2.6.2). If no significant cardiovascular imbalance is present, heart rate can serve as an indicator of depth of anaesthesia. A summary of the effects of several agents and combinations upon heart rate is given in Table 2.2[27].

Agent	1 MAC	1.5 MAC	2 MAC
Halothane	100	100	100
Isoflurane	120	120	120

Table 2.2: Heart Rates as a Percentage of Awake Values for different Agents and Concentrations

Respiration Signs

Assuming otherwise normal respiratory function, changes in respiration can indicate changes in depth of anaesthesia. many inhalational agents cause decreases in tidal volume with increasing depth of anaesthesia. This is often accompanied by a compensatory increase in respiration rate so as to maintain minute ventilation. Despite this, as outlined in Section 2, the alveolar minute volume is likely to be decreased.

Drugs such as narcotic analgesics cause reductions in respiratory rate but tend not to alter tidal volume. As anaesthetic depth increases the breathing patterns change and ultimately respiration ceases.

The value of respiration as an indicator of anaesthetic depth is dependent upon the effects of the anaesthetic agent(s) being used. When muscle relaxants are being used respiration information is clearly not available and cannot be used.

Sweating and Lacrimation

Robb [61] concluded that sweating and lacrimation were too dependent upon pharmacological and environmental factors to be objectively assessed as indicators of depth of anaesthesia.

Movement

Movement of a patient in response to surgery provides the most categorical indication of light anaesthesia. It is however likely that cardiovascular signs will indicate the presence of light anaesthesia before movement occurs [71]. For procedures involving the administration of muscle relaxants, patient movement is prevented thus removing movement as an indicator of anaesthetic depth.

Other Measurements

Aside of the use of clinical signs to assess anaesthetic depth, many other indicators have been proposed. These were summarised in the Chapter 1. Further appraisal of these measures was made by Thomas and Runciman [92].

2.7 Specialised Equipment used in this Work

The overall aim of the work described in this thesis has been to develop techniques which support the automatic control of anaesthesia. Although the remainder of

the thesis is devoted to the description of the development, implementation and performance of these techniques, some more fundamental activities have been carried out during the timescale of the work described in this thesis.

2.7.1 Specialised Hardware Development

Two items of specialised equipment had already been designed and built for use in the control of anaesthesia and these were made available at an early stage for this work. Firstly, an interface box was available for a Datascope 3100 monitor. The Datascope 3100 provides measurements of heart rate, blood pressures, temperatures and oxygen saturation. The interface box coverts the Datascope standard bus output to RS–232 standard which can then be directly connected to the RS–232 port of a computer.

Secondly, a servo–vaporiser developed by W.M. Gray and staff of the West of Scotland Health Boards' Department of Clinical Physics and Bioengineering and described by Nieman et al. [94] was available. This device consists of a stepping–motor and gearbox mounted on a standard vaporiser. In its original form, the servo–vaporiser controller was interfaced to a parallel port of a small computer. The computer was required to generate direction line information, all of the pulses for each vaporiser movement and a safety 'watchdog' signal waveform. In recognition that the generation of the motor drive pulses presented a significant programming overhead, an interface board was designed to interface a computer with the existing controller. The interface board was designed so that the computer needed only to load the number of pulses to be generated to it. The new interface board then automatically generated that number of pulses. This board has been implemented by the West of Scotland Health Boards' Department of Clinical Physics and Bioengineering.

2.7.2 Specialised Software Development

In addition to the servo-vaporiser described above, this work has involved the use of a Braun Perfusor Secura syringe pump, a Datascope 3100 monitor and a Datex Ultima monitor. As described previously, the servo-vaporiser requires a parallel communication interface to a computer. Both monitors and the syringe pump require serial interfaces. Each of the serial devices operates at a different baud rate and with a different protocol.

In recognition that this combination of monitors and drug delivery devices allows automatic measurement of a wide range of clinical signs and manipulation of multiple drug inputs, the Closed-Loop Anaesthesia Support System (CLASS) libraries have been developed. The CLASS libraries provide virtual devices to allow safe, reliable and efficient communication with the devices described above. To maximise processor utilisation, interrupt-driven communications have been employed. To make the use of the libraries as easy as possible, all hardware and communication protocol details are hidden from the user. For instance, the CLASS library device which handles the servo-vaporiser automatically generates watchdog pulses of the correct form. The structure of the CLASS virtual devices is illustrated in Figure 2.9.

A Viglen III/LS PC clone has formed the basis for the implemented techniques described in this thesis. In order to interface this machine to each of the devices, three serial ports and one parallel port are required. Because interrupt-driven communications were used, each port was required to generate independent interrupts. The PC therefore had the following added to it;

- Amplicon PC 47 AT Dual Independent RS-232 Serial Port Interface Board
- Amplicon PC 36 LP 24 line Parallel Input-Output Interface Board

The CLASS libraries are currently implemented in C++ using the Zortech C++ compiler to generate code for 286 processors. Further details of the programmers'

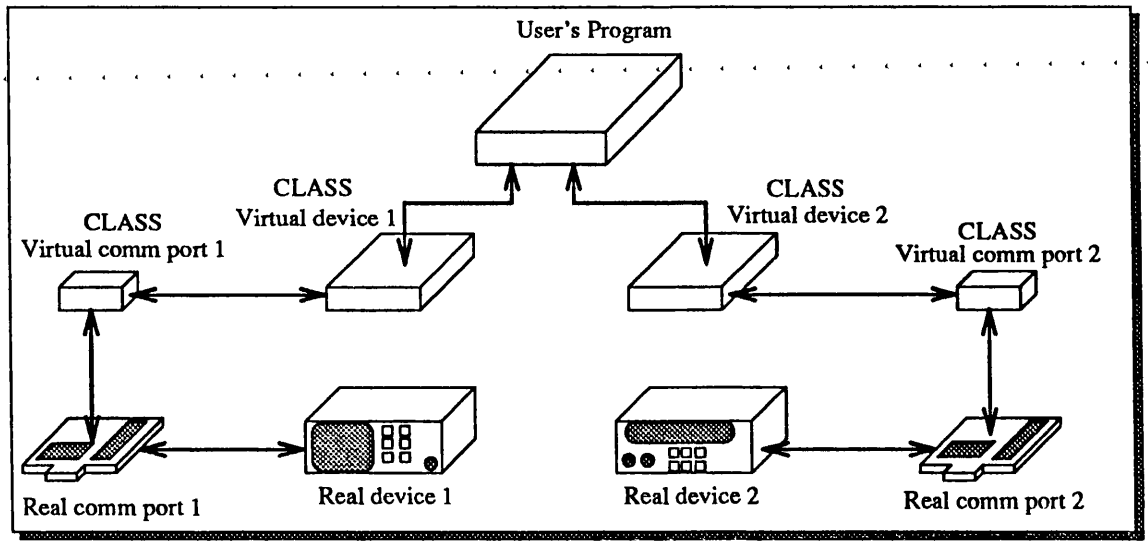

Figure 2.9: The Structure of the CLASS Virtual Devices

interfaces provided by the CLASS libraries are included in Appendix A.

Chapter 3

Modelling the Pharmacology of Anaesthesia

SUMMARY

This chapter introduces the concepts and relations of pharmacology. Approaches used to model pharmacokinetics are described, in particular, the use of physiologically–based pharmacokinetic models. The use of bond graphs to represent physiologically–based pharmacokinetic models of both inhaled and injected drugs is described following the introduction of bond graph notation and the derivation of the bond graph representation for compartment models.

3.1 Pharmacology

Pharmacology is the study of the manner in which the function of living systems is affected by chemical agents [29]. Anaesthetists employ a subset of the available drugs to provide an appropriate anaesthetic state. This includes anaesthesia, analgesia, muscle relaxation and also rapid and safe anaesthetic induction. Models of the pharmacology of drugs used in anaesthesia can satisfy several goals.

These goals include promoting better understanding of the mechanisms of drug distribution and action and developing better ways of using the drugs. Within pharmacology, pharmacodynamics describe the relationship between the drug concentration at the site of action, and its effect. Pharmacokinetics describe the relationship between an administered dose and its route of administration, and the concentration established at the site of action.

3.2 Pharmacodynamics

For a drug to create an effect, it must alter the behaviour of cells. For many drugs, the effect created can be described in terms of cellular changes resulting from the binding of drug molecules to 'receptors'. There are many different types of receptors in the cells of the body and many more are likely to be found. Each type of receptor is responsible for specific effects when it has a drug bound to it. The variation in receptor types and densities in different tissues of the body can cause the same drug to exert different effects in each tissue. As an example, there are five groups of receptors associated with the effects of opioid analgesics such as morphine and fentanyl. These receptor types are μ_1,μ_2, δ, κ and σ receptors. The binding of the opioid drugs to these receptors causes different effects. The specific effects of each opioid drug can be explained in terms of the receptors to which it binds.

When the production of a drug effect does depend upon the binding of drug molecules to receptors, the binding reaction can be represented as follows. For a drug A and receptors R,

$$A + R \overset{k_1,k_2}{\rightleftharpoons} AR \tag{3.1}$$

k_1 and k_2 are the forward and reverse reaction rate constants respectively, AR is the drug–receptor complex. Let N_a be the number of occupied receptors, N_t the total number, and x_a the concentration of drug A. From the Law of Mass Action,

at equilibrium,

$$k_1 \cdot x_a \cdot (N_t - N_a) = k_2 \cdot N_a \quad (3.2)$$

therefore,

$$N_a = \frac{x_a \cdot N_t}{x_a + \frac{k_2}{k_1}} = \frac{x_a}{x_a + K_a} N_t \quad (3.3)$$

with $K_a = \frac{k_2}{k_1}$.

This gives the relationship between receptor site occupancy (i.e. the fraction of sites occupied) and drug concentration as shown in Figure 3.1.

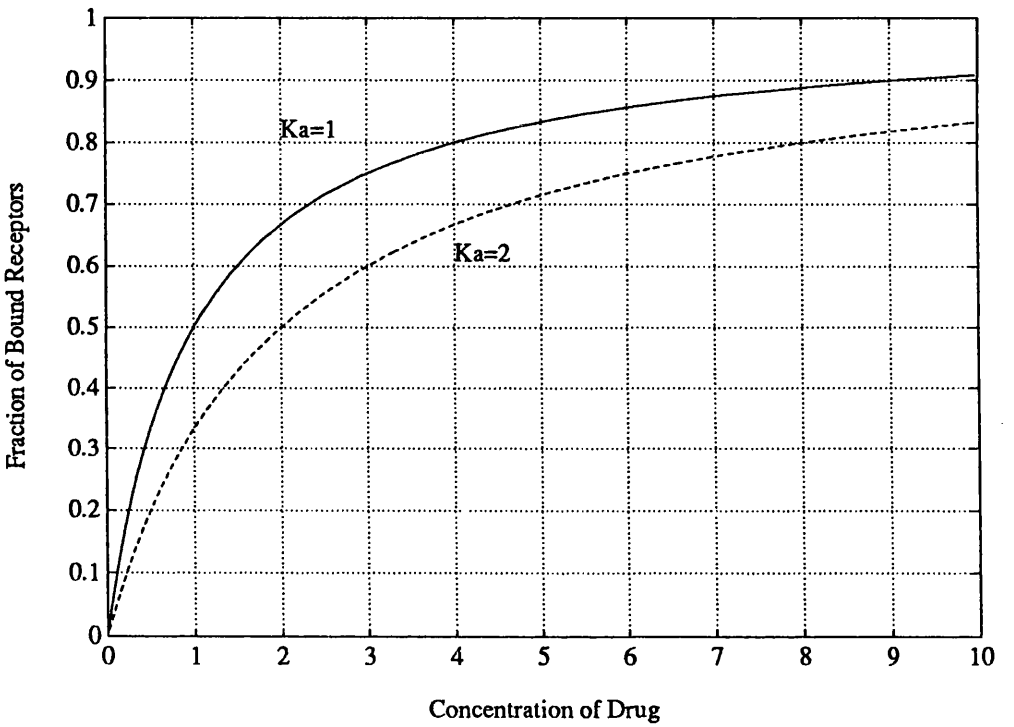

Figure 3.1: Graph of receptor occupancy versus drug concentration

The relationship in Equation 3.3 describes only the number of receptor sites occupied at various drug concentrations. It is possible for two drugs to produce different effects even when they occupy the same receptors with the same occupancy. Some drugs are capable of producing a maximal physiological effect even without occupying all the receptors. These drugs are termed *full agonists.* Drugs which bind to the receptors but which cannot exert maximum effect at any

occupancy are termed *partial agonists.* An *antagonist* is a drug which binds to a receptor without producing any effects.

Several different drugs can bind to the same receptor sites. If two or more of such drugs are present simultaneously, they 'compete' for the receptor sites. Taking, as an example, two drugs A and B with receptor binding reactions

$$A + R \overset{k_{1a},k_{2a}}{\rightleftharpoons} AR$$

and

$$B + R \overset{k_{1b},k_{2b}}{\rightleftharpoons} BR$$

respectively. Let the concentration of drugs A and B be x_a and x_b respectively, let N_a be the number of receptors bound to drug A, N_b the number bound to drug B, and N_t the total. Again, by the Law of Mass Action, at equilibrium,

$$k_{1a} \cdot x_a \cdot (N_t - N_a - N_b) = k_{2a} \cdot N_a$$

and

$$k_{1b} \cdot x_b \cdot (N_t - N_a - N_b) = k_{2b} \cdot N_b$$

These give

$$N_a = \frac{x_a}{(x_a + K_a) + x_b \cdot \frac{K_a}{K_b}} N_t \tag{3.4}$$

where $K_a = \frac{k_{2a}}{k_{1a}}$ and $K_b = \frac{k_{2b}}{k_{1b}}$. Thus increasing concentrations of drug B displace drug A from the receptor sites. If drug B is an antagonist, the total drug effect will be reduced due to the reduced occupation of receptor sites by drug A. An example of this effect for hypothetical drugs A and B with $K_a = 1$ and $K_b = 1$ or $K_b = 10$ is shown in Figure 3.2. In this example, the concentration of drug A varies between 0 and 10 units. The concentration of drug B is kept constant at 5 units.

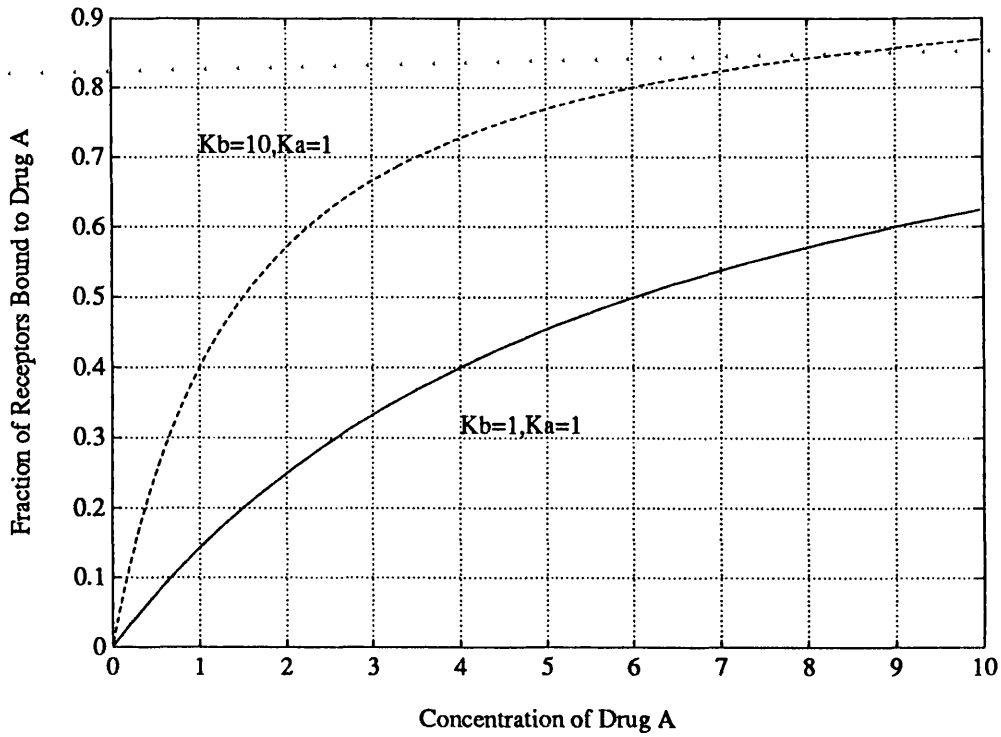

Figure 3.2: Competitive Binding between Drugs

3.3 Pharmacokinetics

The effect of the drug depends upon the number of receptors occupied and the extent to which the drug can exert effects. The occupation of receptors depends upon the existence of sufficient drug concentration in the vicinity of the receptors as described by Equation 3.3. Pharmacokinetics describes the relationship between the administered dose and the concentration at the site of effect.

During anaesthesia, drugs are administered most commonly via inhalation or intravenous injection. A drug administered intravenously flows through the vein in which it is administered to join venous blood returning to the heart. The heart pumps venous blood through the lungs and then into the arteries. Once in the arteries, the drug is distributed throughout the tissues of the body and ultimately to the sites at which it exerts its effects.

An inhaled drug is mixed with the gas breathed in by the patient. The drug is then able to reach the alveoli of the lungs and, according to its physicochemical properties, to pass into the blood passing through the lungs. The inhaled drug is then distributed to the tissues of the body in the same way as injected drugs.

The transport of a drug by the blood allows it to reach all tissues of the body. This process does not result in equal delivery to all tissues. The most important organs and tissues of the body receive the largest blood supply in both absolute terms and in terms of the perfusion per gramme of tissue. Some example tissues are shown in Table 3.1[27].

Tissue	% cardiac output	perfusion $\frac{ml/min}{g}$
kidneys	18.8	4.5
liver	6.9	0.26
brain	11.5	0.55
muscle	17.7	0.021
fat	5.3	0.024

Table 3.1: The Relative Perfusion of Selected Tissues

These differences in perfusion allow concentrations of drug to build up more quickly in the well perfused organs (kidneys and brain) than in the less well perfused organs (muscle and fat). The perfusion of an organ or tissue is therefore a main determinant of the concentration timecourse.

The second main determining factor of the drug concentration timecourse is the ability of the drug to enter cells by crossing cell membranes. The ability to cross cell membranes allows the drug to *diffuse* into other tissues. In some parts of the body, drug can only enter tissues by diffusion. This is the case for drugs which must enter the brain from the bloodstream. In contrast to the blood vessels in other parts of the body, those of the brain have a continuous wall. A drug must therefore travel through the walls of the cells in the brain blood vessels in order to enter the brain.

Cell membranes are largely composed of lipid material. In order to diffuse

across a membrane, a drug must therefore be lipid soluble. More lipid soluble drugs can establish high concentrations in the membrane and thus support high concentration gradients across the membrane and rapid diffusion. Less lipid soluble drugs establish lower concentrations in the membrane, lower concentration gradients across it and less rapid diffusion.

Most of the drugs employed in general anaesthesia are highly lipid soluble so that the build up of concentration across a cell membrane depends upon the rate of delivery of drug to the diffusion site. The rate of delivery of drug is determined by the perfusion of the site. In such an instance, the equilibration of drug concentrations is said to be *perfusion limited.* If the limiting step in the process was the rate at which the drug could diffuse across the membrane, the process would be *diffusion limited.*

While the bloodstream provides the mechanism for transporting drug around the body in order to diffuse across membranes, other effects alter the amount of drug and timecourse of drug concentration at receptor sites. In general, drugs can dissolve in fat, can bind to proteins and can form ionised species. The overall equilibration of a drug involves equilibration between these forms.

3.3.1 Partition into Fat

Many drugs are capable of dissolving in fat (more correctly lipids). In the body, amounts of fat are present in and around all tissues and sum to a total of between 3% and 60% of body weight in the population. The relative solubility of a drug in fat is expressed in terms of its fat:water partition coefficient. Therefore,

$$C_{fat} = \lambda \cdot C_{water} \tag{3.5}$$

where C_{fat} is the concentration of the drug in fat, C_{water} is the concentration of the unionised drug in the water with which the fat is in equilibrium, and λ is the partition coefficient.

3.3.2 Protein Binding

Drugs can bind to protein molecules in the blood and tissues. In general, more lipid soluble drugs are also more highly bound to protein. Protein binding involves the reversible binding of drug molecules to protein molecules. The relationships involved can be described using the Law of Mass Action to give

$$[D] + [S] \overset{k_1,k_2}{\rightleftharpoons} [DS] \tag{3.6}$$

where [D] is the free drug concentration, [S] the concentration of free binding sites, [DS] the concentration of bound sites, and k_1 and k_2 are the forward and backward rates of reaction respectively. Let the free drug concentration be x_d, N_b be the number of bound sites and N_t be the total number of binding sites then by the Law of Mass Action.

$$k_1 \cdot x_d \cdot (N_t - N_b) = k_2 \cdot N_b$$

Thus,

$$N_b = \frac{k_1.x_d}{k_2 + k_1.x_d} N_t = \frac{x_d}{x_d + \frac{k_2}{k_1}} N_t = \frac{x_d}{x_d + K_a} N_t \tag{3.7}$$

where $K_a = \frac{k_2}{k_1}$, the equilibrium constant. If P is the concentration of protein in the tissue or fluid, the concentration of bound drug is then

$$C_b = \frac{N_b}{N_t} \cdot P = \frac{x_d}{x_d + K_a} \cdot P \tag{3.8}$$

This has the form of a rectangular hyperbola as illustrated in Figure 3.3.

The precise description of the protein binding relationship for a drug requires knowledge of the specific protein sites to which the drug binds, the concentration of those binding sites, and the concentration of the drug in the vicinity of the sites. The lack of specific knowledge of the protein binding sites often dictates that estimates of protein binding are made. As examples, thiopentone is estimated to be 70% bound to plasma proteins at therapeutic concentrations. Morphine is estimated to be about 30% bound to plasma proteins at therapeutic concentrations.

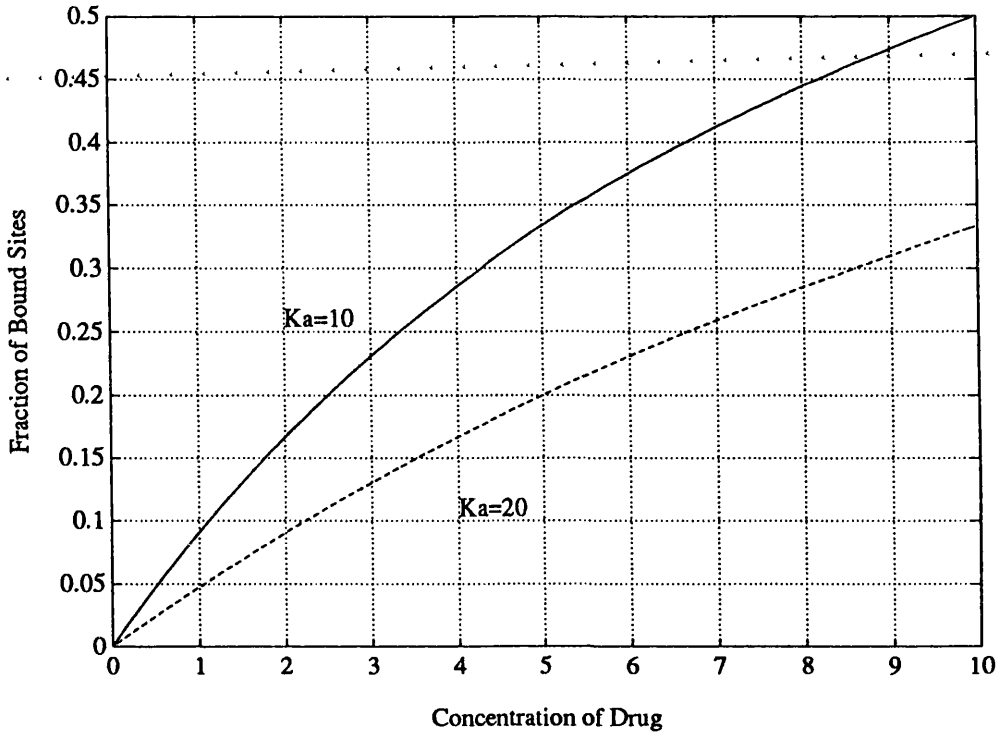

Figure 3.3: Relationship between Drug Concentration and Bound Protein Sites

3.3.3 Ionisation

The third main determinant of drug concentration is the ionisation of the drug. Ionisation involves the establishment of equilibrium between the unionised form of a drug and its ionised species. The equilibrium position depends upon the physicochemical properties of the drug and the pH of the fluid in which it is present. Ionisation is described by the Henderson–Hasselbach equations which are; for a base,

$$BH^+ \overset{K_a}{\rightleftharpoons} B + H^+$$

$$pK_a = pH + log_{10}\frac{[BH^+]}{[B]} \tag{3.9}$$

for an acid,

$$AH \overset{K_a}{\rightleftharpoons} A^- + H^+$$

$$pK_a = pH + log_{10}\frac{[AH]}{[A^-]} \qquad (3.10)$$

where $[BH^+]$ is the concentration of ionised base, $[B]$ is the concentration of unionised base, $[AH]$ is the concentration of unionised acid, $[A^-]$ is the concentration of ionised acid, and $[H^+]$ is the hydrogen ion concentration.

3.3.4 Equilibration within a Tissue or Fluid

Each fluid or tissue contains amounts of water, fat and proteins. A drug will therefore be able to ionise, dissolve in lipids and bind to protein in order to establish equilibrium. Symbolically, this can be represented as shown in Figure 3.4

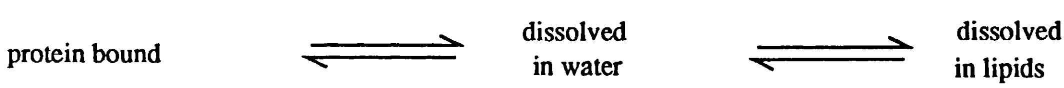

Figure 3.4: Equilibration within a fluid space

Of course, the part of the drug dissolved in water is divided between unionised and ionised fractions as described by the Henderson-Hasselbach equations (3.9) and (3.10). Equation (3.7) relates the drug dissolved in tissue water to that bound to protein. Equation (3.5) relates drug in fat to that in the tissue water. If d is the total amount of a basic drug in the tissue or fluid, x_s is the concentration of the free unionised form of the drug in water, W_T is the mass of the tissue or fluid, P is the concentration of protein in the tissue, F_f and F_w are the mass fractions of fat and water respectively and λ is the fat:water partition coefficient, then equations

3.7, 3.5 and 3.9 can be combined to give,

$$d = W_T \cdot \{\frac{x_s}{x_s + K_{pb}} \cdot P + \lambda \cdot x_s \cdot F_f + x_s \cdot F_w + 10^{(pKa-pH)} \cdot x_s \cdot F_w\} \quad (3.11)$$

This equation contains terms in x_s on both the numerator and denominator. Solution of the equation for x_s therefore requires iteration in order to establish the equilibrium point.

For some drugs, however, the degree of binding to protein is relatively constant throughout the therapeutic range of concentrations. This is the case for drugs which occupy only a small proportion of the available protein sites at therapeutic concentrations. For such drugs, the relationship between the concentration of free drug and the concentration of bound drug can be approximated by a linear relationship. This approximation is possible because when only a small number of protein binding sites are occupied, the term x_d is much smaller than K_a in Equation 3.7. The equation therefore approximates to

$$N_b = \frac{x_d}{K_a} N_t$$

Equation 3.8 then gives

$$C_b = \frac{x_d}{K_a} \cdot P. \quad (3.12)$$

and Equation 3.11 then becomes

$$d = W_T \cdot \{\frac{x_s}{K_{pb}} \cdot P + \lambda \cdot x_s \cdot F_f + x_s \cdot F_w + 10^{(pKa-pH)} \cdot x_s \cdot F_w\} \quad (3.13)$$

Because x_s only appears in the numerator of this equation, knowledge of the drug amount in a tissue or fluid space can be used to directly solve for the free unionised concentration of the drug.

3.3.5 Equilibration between Tissues or Fluids

Only the unionised form of a drug can diffuse through cell membranes. Equilibration between two tissues therefore depends upon the unionised drug concentration

on either side of the membrane, and the solubility of the drug in the membrane. The equilibration of two fluid spaces separated by a cell membrane can be schematically represented as shown in Figure 3.5.

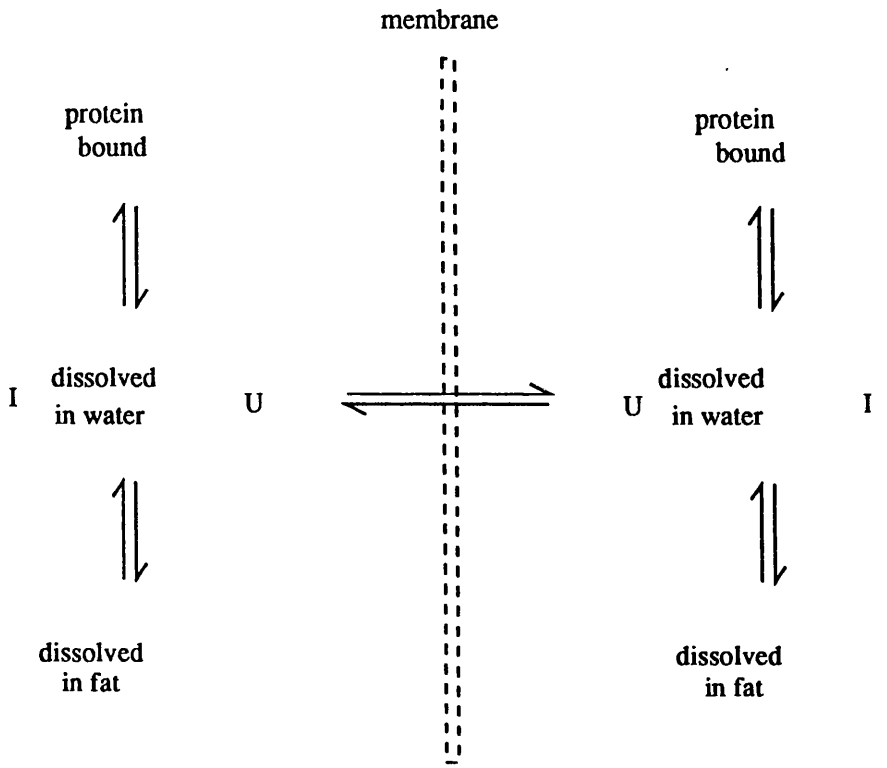

Figure 3.5: Equilibrium of Drug Across a Membrane

Thus, at equilibrium,

- Free, unionised parts have equal concentrations either side of the membrane.
- The total amount of drug contained in the system is unchanged

This assumes that a negligible amount of drug becomes stored in the membrane and that equilibration is complete. Thus, using Equation 3.11, for the drug in fluid 1 before equilibration

$$d1 = W_{T1} \cdot \{\frac{x_{s_1}}{x_{s_1} + K_{pb1}} \cdot P_1 + \lambda \cdot x_{s_1} \cdot F_{f1} + x_{s_1} \cdot F_{w1} + 10^{(pKa - pH_1)} \cdot x_{s_1} \cdot F_{w1}\} \quad (3.14)$$

for the drug in fluid 2 before equilibration

$$d1 = W_{T2} \cdot \{\frac{x_{s_2}}{x_{s_2} + K_{pb2}} \cdot P_2 + \lambda \cdot x_{s_2} \cdot F_{f2} + x_{s_1} \cdot F_{w2} + 10^{(pKa - pH_2)} \cdot x_{s_2} \cdot F_{w2}\} \quad (3.15)$$

after equilibration, the concentration of unionised fractions of the drug is the same on either side of the membrane. Therefore,

$x_{s_1} = x_{s_2} = x_s$

Because no drug has been added to or removed from the system,

$$\begin{aligned} d1 + d2 \;=\; & W_{T1} \cdot \{\frac{x_{s_1}}{x_{s_1} + K_{pb1}} \cdot P_1 + \lambda \cdot x_{s_1} \cdot F_{f1} + x_{s_1} \cdot F_{w1} \\ & + 10^{(pKa - pH_1)} \cdot x_{s_1} \cdot F_{w1}\} \\ & + W_{T2} \cdot \{\frac{x_{s_2}}{x_{s_2} + K_{pb2}} \cdot P_2 + \lambda \cdot x_{s_2} \cdot F_{f1} + x_{s_1} \cdot F_{w1} \\ & + 10^{(pKa - pH_2)} \cdot x_{s_2} \cdot F_{w2}\} \end{aligned} \tag{3.16}$$

Assuming that the pH values, pH_1 and pH_2 of both tissues are known, or can be estimated, the amount of drug in each form can be derived. If drug delivered to or removed from the tissues is included, the timecourse of concentrations, and amounts of drug unionised, ionised, protein bound, dissolved in fat and transferring between tissues can be derived. The equation for the equilibration between two tissues (Equation 3.16) requires iterative solving. If the approximation used to generate Equation 3.13 is valid, then once again, a solution for the free unionised concentration of the drug can be found directly.

In general, the unionised species of the drug is required to bind to a receptor in order to exert the effect. The concentration of unionised drug in the vicinity of the receptors may however be much less than the notional concentration. This process can be illustrated by considering two examples.

1. Thiopentone.

   Thiopentone is a weak acid with a pKa of around 7.5 and is approximately 70% bound to plasma protein at therapeutic concentrations. Thiopentone is highly lipid soluble and has a fat:water partition coefficient of about 10. The equilibration of thiopentone is described as follows: let d mg of thiopentone

be added to the V_b litres of blood. Using data from Davis and Mapleson [45], the blood is assumed to be composed of 80% water, 0.65% fat and 18% protein and to have a pH of 7.4. Let the free unionised concentration of thiopentone be C_s then, the concentration in fat $C_{fat} = 10 \cdot C_s$. The ionised and unionised concentrations of thiopentone in water are related by the Henderson–Hasselbach equation for an acid drug (Equation 3.10). The concentration of the ionised drug in water C_i is then

$$C_i = C_s \cdot 10^{(pH-pKa)} = 10^{-0.1} \cdot C_s = 0.7943 \cdot C_s$$

Because 70% of the drug is protein bound, only 30% remains dissolved in fat or water. Thus, using equation (3.11)

$$0.30d = 0.0065 \cdot C_{fat} \cdot V_b + 0.80 \cdot C_i \cdot V_b + 0.80 \cdot C_s \cdot V_b = 1.50 \cdot C_s \cdot V_b$$

so,

$$C_s = \frac{0.30d}{1.50 \cdot V_b} = 0.20 \cdot \frac{d}{V_b}$$

The free concentration is thus only 20% of the notional blood concentration. This concentration forms the concentration gradient across cell membranes.

2. Morphine.

   Morphine is a weak base with a pKa of around 8.5. Approximately 30% of morphine is bound to plasma proteins at therapeutic concentrations. Morphine is lipid soluble and has a fat:water partition coefficient of around 0.4.

   Consider d mg of morphine injected to V_b litres of blood. Let the free unionised concentration of morphine be C_s. The free ionised concentration of morphine is related to the free unionised concentration by the Henderson–Hasselbach equation for a weak base (Equation 3.9). Therefore,

$$C_i = C_s \cdot 10^{(pKa-pH)} = 10^{1.4} \cdot C_s = 25.1189 \cdot C_s$$

As 30% of morphine is protein bound then 70% remains unbound and is dissolved in fat and water. The blood composition was detailed for the thiopentone example. Thus, using equation (3.11),

$$0.7 \cdot d = 0.0065 \cdot (0.4 \cdot C_s) \cdot V_b + 0.80 \cdot C_i \cdot V_b + 0.80 \cdot C_s \cdot V_b = 20.8977 \cdot V_b \cdot C_s$$

The concentration of free, unionised form of the drug is

$$C_s = \frac{0.70 \cdot d}{20.8977 \cdot V_b} = 0.0335 \frac{d}{V_b}$$

and therefore only about 3% of the notional concentration of the drug is contributing to the concentration gradient across cell membranes.

The higher lipid solubility of thiopentone and the greater fraction of free, unionised drug allows it to achieve rapid equilibration with tissues and this is only limited by the perfusion of the tissues. This is consistent with thiopentone's suitability as an induction agent.

Morphine requires a longer time to achieve equilibration due to its relatively smaller lipid solubility and greater degree of ionisation. The smaller fat:water partition coefficient for morphine does however ensure that large reservoirs of the drug do not form in body fat. This is a desirable characteristic and supports rapid recovery.

3.3.6 Removal of Drugs from the Body

In order for the effects of a drug to reduce, the concentration of the unionised free form of the drug in the vicinity of the receptors for it must fall. The fall in the free unionised drug concentration shifts the equilibrium of the drug–receptor reaction (Equation 3.1) so as to reduce the concentration of the drug–receptor complex and thus the effects of the drug.

In general, the concentration of a drug falls if the drug is either *metabolised* by the body to form other products which do not exert effects, or if the drug is *excreted* and hence leaves the body.

The main site in the body where metabolism occurs is the liver. Some drugs are however metabolised in blood plasma, the lungs, or the lining of the gastrointestinal tract. Metabolism involves the transformation of a drug into a metabolite via a chemical reaction. The metabolite may be pharmacologically active and also exert effects, may be pharmacologically inactive, and may be excreted from the body.

The excretion of drugs can be achieved by the kidneys or the liver. The kidneys pass drugs into urine and the liver passes the drug into bile. Inhaled agents can leave the body via the lungs. For many inhaled anaesthetic agents, this route is the only mode of elimination because they are highly lipid soluble thus resisting excretion by the kidneys and they are only insignificantly metabolised.

3.4 Compartmental Models of Pharmacokinetics

Pharmacokinetic studies often provide only plasma (or blood) drug concentration data. In the absence of knowledge of drug concentrations in other tissues and fluid spaces, it is difficult to develop a model to represent the pharmacokinetics of those tissues. Most pharmacokinetic models therefore aim to produce plasma concentration estimates which match experimental data. Typical experimental work involves either injecting a drug bolus or infusing the drug for a period of time. The plasma drug concentration timecourse is then measured and used to generate a model.

The most commonly applied modelling scheme is compartmental modelling. Using the definition of Cobelli [95]:

> "A compartmental model represents the system by a finite number of components, the compartments, and by the material exchange between them. A compartment is an amount of material which acts

> kinetically in a homogeneous and distinctive manner; it is characterised by its physico-chemical state, its location or both. ... The flux of material between compartments corresponds either to physico-chemical conversion of one metabolite to another in the same location or the transport of a substance from one location to another without change of form"

The most commonly used compartmental models have either two or three compartments. Given that excretion and absorption can be considered to occur in each compartment of the model, several arrangements are possible for combinations of compartments. As examples, two possible configurations of a two compartment model are shown in Figure 3.6.

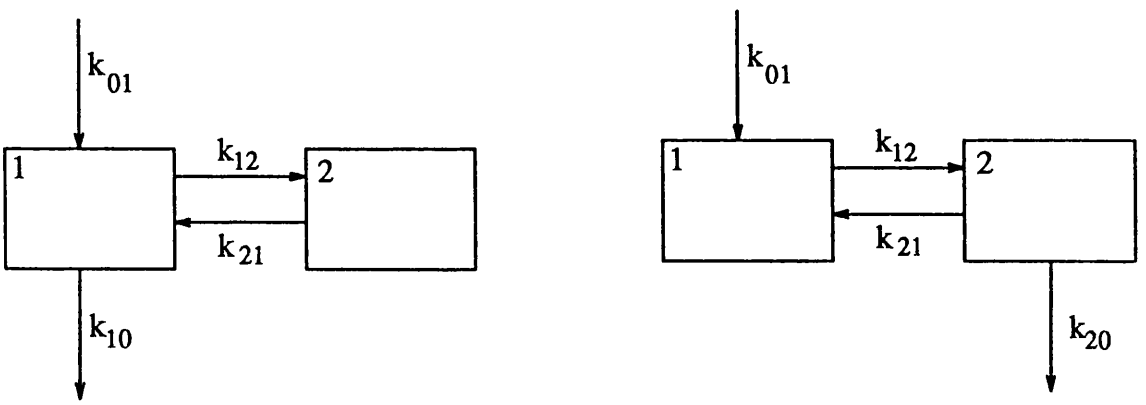

Figure 3.6: Two Possible Arrangements of a Two Compartment Model

Conceptually, compartment models are often considered to be composed of a central compartment which notionally contains intravascular fluid and well perfused tissues such as the kidneys, liver, heart, brain and lungs. The volume of the central compartment is however generally calculated from experimental data and is not chosen to reflect the volumes of the tissues considered to exist within it. The remainder of body's tissues are considered to exist in one of the other

compartments which also have volumes which are not necessarily directly related to the tissue components.

Mathematically, compartmental models are arranged so that transfers between and out of compartments are related to the amount of drug within the compartment. This gives rise to an exponential term for each compartment. e.g. for the two compartment model shown in Figure 3.7, if x_1 is the amount of drug in compartment 1 and x_2 is the amount of drug in compartment 2, the rate of change of these amounts is given by

$$\frac{dx_1}{dt} = -(k_{10} + k_{12}) \cdot x_1 + k_{21} \cdot x_2$$

and

$$\frac{dx_2}{dt} = k_{12} \cdot x_1 - k_{21} \cdot x_2$$

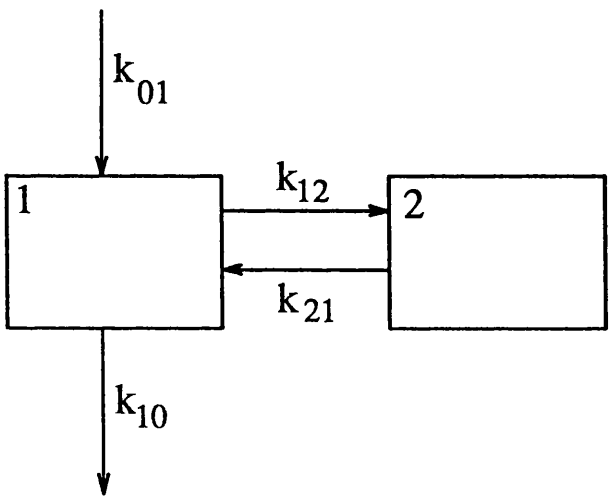

Figure 3.7: A Two Compartment Model

The solution for the amount of drug in the central compartment is therefore the summation of two exponential decays. An example for a hypothetical drug has compartment volumes $V_1 = 10$ and $V_2 = 30$, transfer coefficients $k_{10} = 0.1$, $k_{12} = 0.3$ and $k_{21} = 0.04$. A simulation of this system for an initial bolus dose of drug in the central compartment gives the curves for compartment amounts shown in Figure 3.8. The bolus was represented by the deposition, instantaneously, of 5 units of mass in the central compartment.

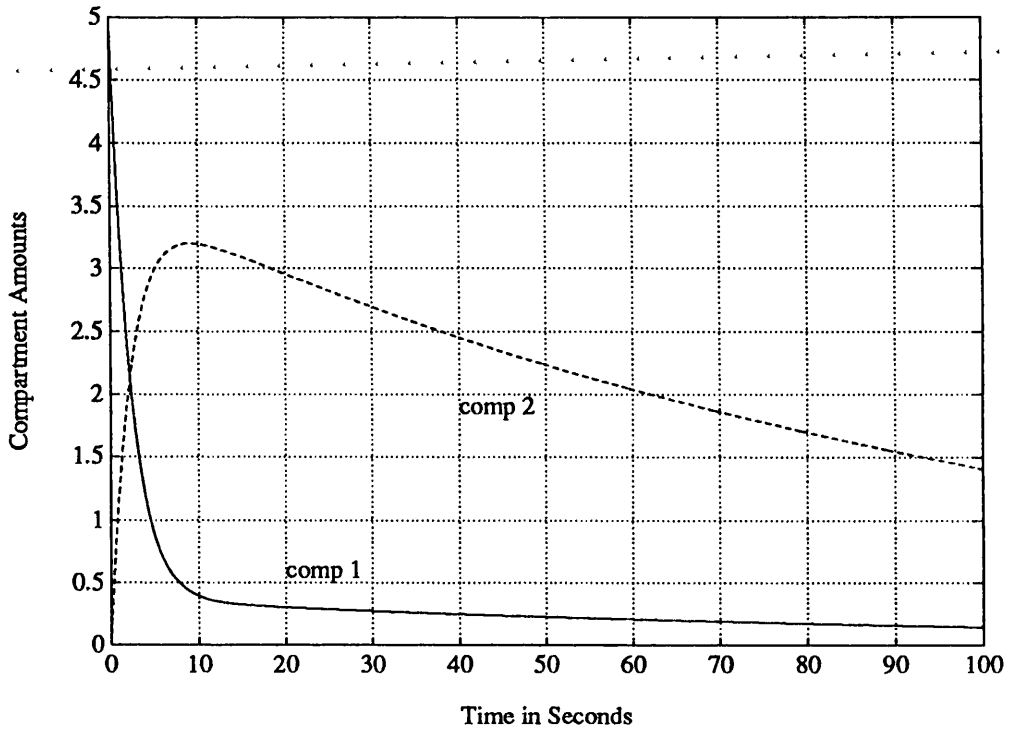

Figure 3.8: Compartment Amounts of Drug versus Time

Compartmental models are often developed to represent the pharmacokinetics of drugs in the population. Development of such models involves the measurement of the responses of a representative range of individuals. From this collection of information, the parameters of a population pharmacokinetic model can be selected. This procedure is outlined in standard compartmental model texts such as [96] and [97]

Compartmental models offer a simple representation of drug pharmacokinetics which supports the development of dosing strategies. The limitation to the practical development of compartmental models lies in the difficulty associated with identifying compartmental models using experimental data. Some solutions to this problem are presented by Godfrey [97] and Godfrey and DiStefano [98].

Despite some limitations, the use of compartment models provides conceptual and mathematical simplicity and they are therefore widely applied. Work such as that of Vajda et al. [99] aims to generate "parameter space boundaries" for

unidentifiable compartmental models thereby constraining the number of possible solutions. Such effort significantly reduces the problems associated with these models.

3.5 Physiologically–based Models of Pharmacokinetics

A physiologically–based model represents the tissues of the individual in order to predict drug handling by the individual. The level of modelling dictates whether tissues are represented individually or are lumped together in tissue groups. Because tissue perfusion is represented in a physiologically–based model, changes in perfusion can be investigated. The representation of tissue masses and volumes allows investigation of the effects of altered body composition.

3.6 Physiologically–based Models of Inhaled Agent Pharmacokinetics

Inhaled anaesthetics are added to the gas mixture breathed by the patient during surgery. For some inhaled drugs, a very small concentration of the agent is adequate to cause the necessary anaesthetic effect in the patient, other drugs require larger concentrations. The inhaled drug enters the lungs as the patient inspires, and equilibrates in the alveoli. The alveoli of the lungs are highly perfused areas of tissue where, in normal circumstances, oxygen is taken up by the blood passing through each alveolus, and carbon dioxide is removed. The equilibration between alveolar gas and the blood passing through each alveolus is rapid and complete in normal circumstances. An inhaled drug is similarly capable of entering the bloodstream through the alveoli. Inhaled anaesthetics are readily able to cross the walls of the alveoli therefore achieving rapid equilibration with the alveolar

blood. If a large concentration of the inhaled anaesthetic is present, absorption of the agent into the blood will cause a decrease of the gas volume in the lungs. In reality, this volume will be made up by a further inflow of gas mixture to the lungs. In such a case, a greater flow of drug into the lungs, and to the alveoli, occurs allowing increased movement of drug into the blood. This effect is known as the *concentration effect.* A similar increase in uptake can occur when one agent is administered in the presence of another. A typical example is the administration of a small concentration of a volatile anaesthetic agent (e.g. 3% isoflurane) in a large concentration of nitrous oxide (around 50%). The uptake of nitrous oxide causes a further inflow of gas mixture including the volatile agent. The rate of inflow of the volatile agent is therefore greater than it would be in the absence of nitrous oxide. This effect is known as the *second gas effect.*

The amount of inhaled anaesthetic crossing the alveoli depends upon the solubility of the drug in blood and the concentration of the agent in both alveolar gas and in the blood of the alveoli. Drug moves across the alveoli until the *tension* of the agent in the alveolar gas equals that in the blood. The tension of anaesthetic in a gas mixture is the partial pressure of the anaesthetic gas. The tension, or partial pressure, of an anaesthetic agent in a liquid is "the partial pressure of the agent in the gas phase with which the liquid is or would be in equilibrium." [39].

Inhaled anaesthetics have different solubility in different tissues. Different concentrations of drug are therefore present when two different tissues equilibrate. A *partition coefficient* describes the ratio of concentrations in two media at equilibrium. Partition coefficients are generally stated for blood:gas, tissue:gas and tissue:blood interfaces. As an example, considering equilibration between a gas volume V_g, and a blood volume V_b with blood:gas partition coefficient λ_{bg}. If there is initially no agent in the blood but amount d in the gas then, assuming the concentration in the gas after equilibration to be c,

$$d = c \cdot V_g + \lambda_{bg} \cdot c \cdot V_b$$

and,

$$c = \frac{d}{V_g + \lambda_{bg} \cdot V_b}$$

Arterial blood which has equilibrated with alveolar gas is pumped, by the heart, to the tissues of the body. Each tissue equilibrates with the arterial blood anaesthetic tension according to its tissue:blood partition coefficient, the volume of the tissue, and its blood flow. A simplified grouping of the body's tissues into four groups is shown in Table 3.2 [27]. Clearly, as tissue volume increases,

Tissue Group	% of Body Mass	% of cardiac Output
Vessel-Rich Group	10	75
Muscle Group	50	19
Fat Group	20	6
Vessel-Poor Group	20	< 1

Table 3.2: Relative Masses and Perfusions for Tissue Groups

more drug must enter the tissue in order for it to equilibrate with arterial blood. Also, highly perfused tissues receive a large blood supply which also delivers large amounts of drug. Well perfused tissues are therefore able to equilibrate more rapidly than less well perfused tissues for equal volume. The tissue:blood partition coefficient dictates the ratio of drug concentrations in the tissue and in the blood at equilibrium. As the tissue:blood partition coefficient increases, more drug must enter the tissue in order to achieve equilibrium concentration. These factors are summarised in Table 3.3.

Factors Increasing Rate	Factors Decreasing Rate
low tissue:blood partition coefficient	high tissue:blood partition coefficient
small tissue volume	large tissue volume
large blood flow	small blood flow

Table 3.3: Factors Affecting the Rate of Tissue Equilibration

Recovery from anaesthesia requires the removal of drug from the tissues and

blood. The removal of drug from each tissue depends upon the same factors as the rate of equilibration during uptake. The factors which increase the rate of equilibration also increase its rate of removal of the drug. Those which decrease the rate of equilibration slow down the removal of drug from the tissue. Removal of drug from the blood requires equilibration between alveolar gas and the blood in the alveoli as for uptake, except that the drug moves out of the blood.

Mapleson [37] derived differential equations describing the uptake of inhaled anaesthetic by the tissues of the body in terms of alveolar ventilation, cardiac output, tissue perfusion, tissue:gas and blood:gas partition coefficients and tissue volumes. Mapleson derived an electric analogue of anaesthetic uptake which consisted of the passive electrical network shown in Figure 3.9. As indicated in this diagram, the component values were all based upon the physiological characteristics of the individual and the physicochemical properties or the drug. As a result of this, currents in the analogue actually correspond in value to mass flows of drug in the patient.

Mapleson [38] further developed the theory proposed in [37] to accommodate the concentration and second-gas effects. The incorporation of these effects within the electrical analogue (Figure 3.9) was also described. In [37], Mapleson acknowledged that the electrical analogue did not represent either the time taken for the blood, at alveolar tension, to travel from the lungs to each tissue, or to travel from each tissue, at tissue tension, back to the lungs. In fact, these transfers were assumed to be instantaneous.

In [40], Mapleson proposed an overall model structure which is reproduced in the schematic, Figure 3.10. In this model, each tissue, or tissue group possesses an 'artery' and a 'vein'. The artery and vein are considered to contain a sequence of fractional stroke volumes which move from the lungs, along the artery, through the tissue, along the vein and back to the lungs. On each heart beat, a fractional stroke volume moves one step around the loop. The arteries and veins contain

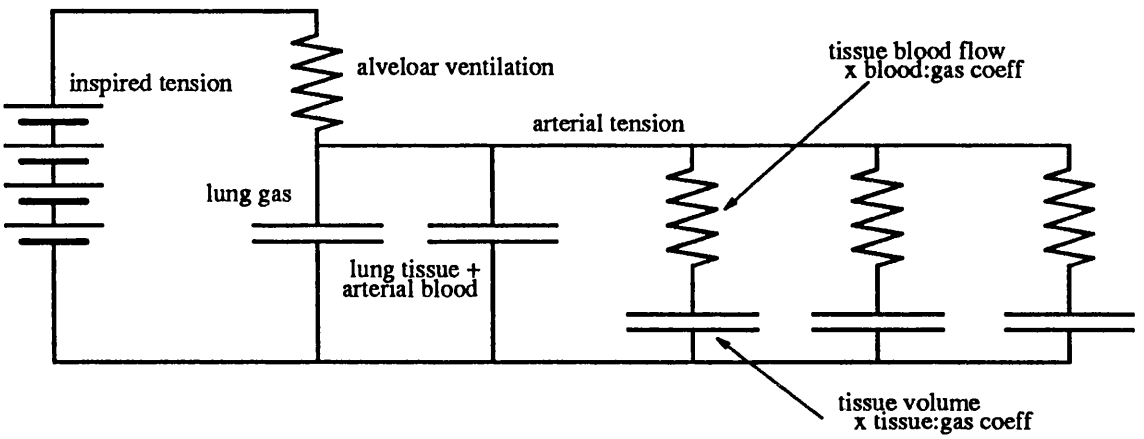

Figure 3.9: Mapleson's Electrical Analogue for Inhaled Agent Uptake

sufficient fractional stroke volumes to represent the circulation time of the tissue. The circulation time for the model is assumed to be the mean transit time for the tissue which is given by

$$\text{mean transit time} = \frac{\text{volume of blood between two points}}{\text{flow rate}}$$

Because circulation times vary between tissues, the number of fractional stroke volumes in the arteries and veins of each tissue also varies.

Mapleson also proposed four approximations to this model for use in the computation of tissue tensions. These models were named model O, F, M and P [40]. In model O, all blood from the 'arteries' was placed in the lung compartment and blood from each vein was placed in the appropriate tissue. The explicit representation of circulation time is therefore lost, but because inspired gas must equilibrate with all arterial blood, some delay is imposed. In model F, all arteries and veins are reduced to the length of the shortest artery and all arteries are then

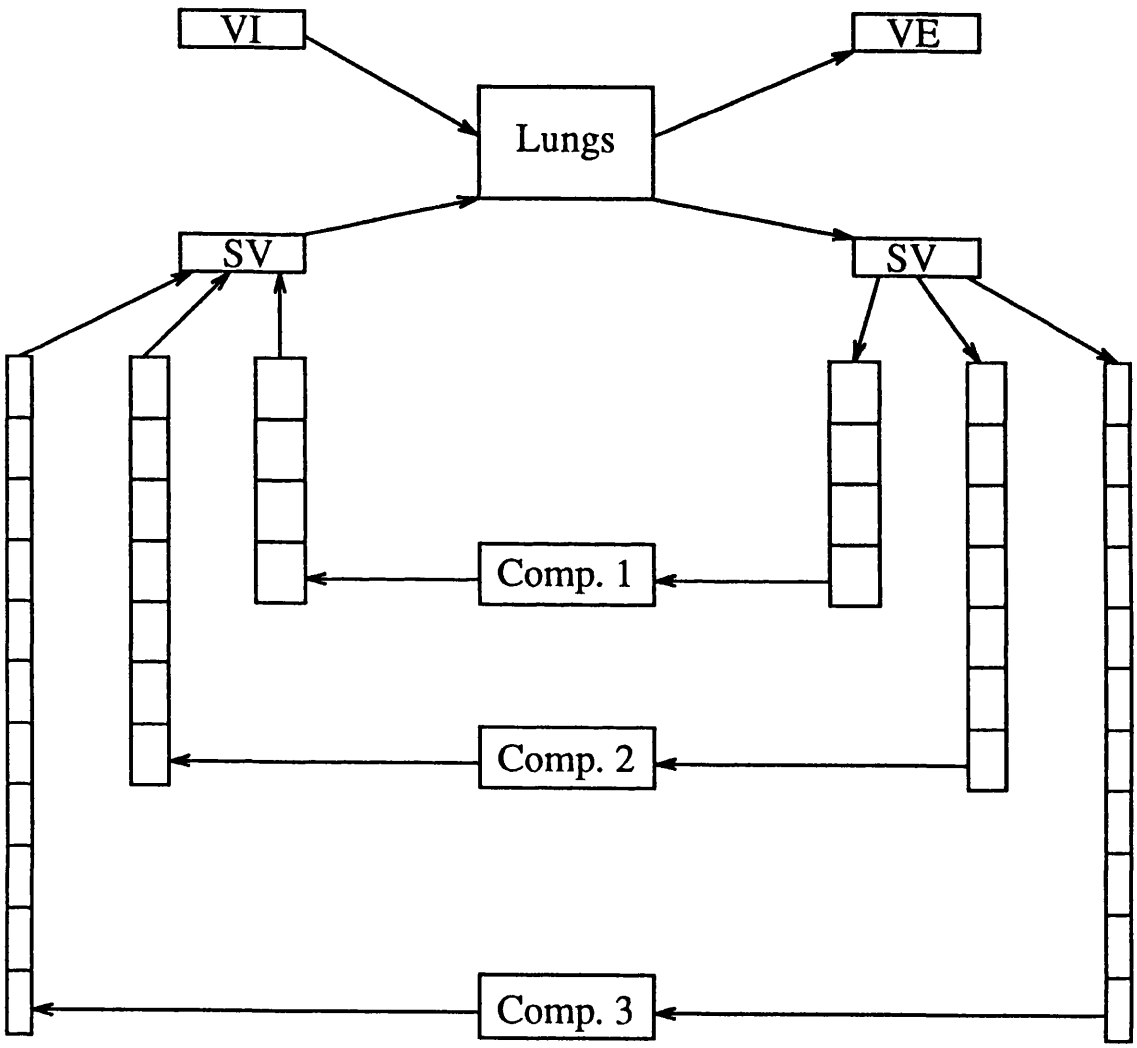

Figure 3.10: Mapleson Circulation Time Model

joined together. Blood from the truncated parts of the longer arteries and veins is placed in the appropriate tissue compartment. In this model there is explicit representation of circulation time for the fastest tissues. Model M adopts the approach of model F with respect to the truncation of arteries and veins. Model M differs from model F in that the longitudinal mixing of blood in the arteries and veins is allowed and is modelled. Model P is also derived from model F but differs in that instead of the artery and vein being composed of a finite number of non-communicating stroke volumes, they become single well mixed pools.

Mapleson compared each approximation and concluded that the differences between models F, M and P were small so that model P presented the simplest and most convenient approximation to the original model (Figure 3.10). Using data from the International Committee for Radiological Protection, Mapleson parameterised each model to give tissue volumes, associated blood volumes for each tissue, and tissue perfusions. Assuming the pulmonary circulation time of 7.5 seconds, and a "highway" circulation time of 5.5 seconds given by Mapleson [40], each circulation has a component of circulation time of 13 seconds. The sizes of arterial, venous and tissue blood pools are then calculated. This is done by first calculating the total blood volume associated with each tissue using the equation

$$\text{associated blood volume} = \text{circulation time} \cdot \text{tissue blood flow}$$

The total blood volume is then the sum of the associated blood volumes for each tissue. Of this, one quarter was assumed by Mapleson to be arterial and the remainder was therefore assumed to be venous blood. These volumes were further subdivided to give local tissue pools and the arterial and venous pools so as to accurately reproduce the local and 'highway' circulation times for each tissue. The circulation schematic diagram for Mapleson's model P is shown in figure 3.11.

Other related work in this area has largely stemmed from the multiple model structure proposed by Beneken and Rideout [44]. A multiple model is

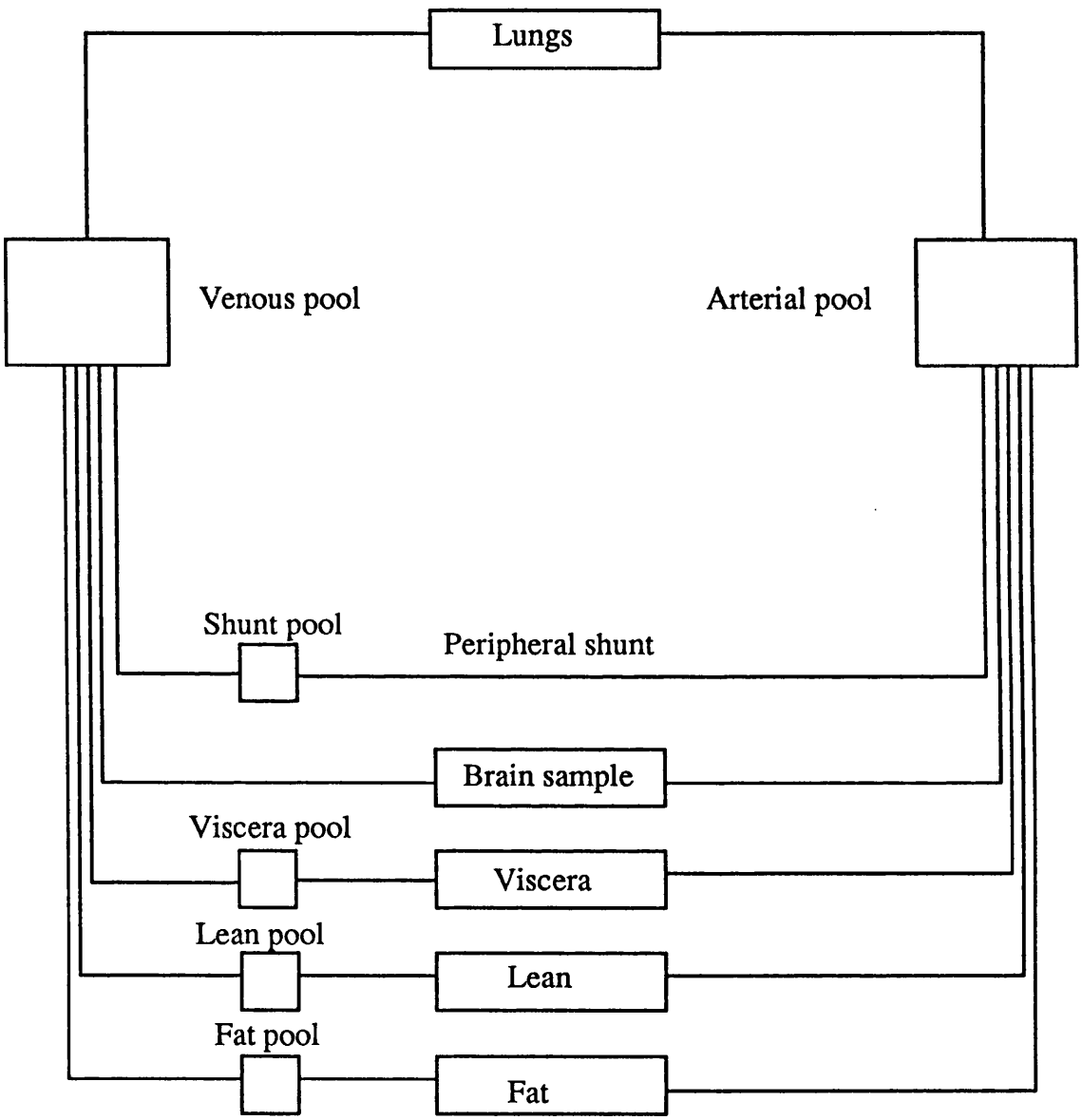

Figure 3.11: Circulation Schematic for Mapleson's Model P

composed of multiple interacting submodels. For instance, the original model described by Beneken and Rideout contained a circulation model and a second model for a substance transported in the blood. Zwart, Smith and Beneken [100] [43] developed an electrical analogue of a multiple model to represent the interaction between halothane uptake and circulation. In this model, halothane concentrations caused alterations in cardiac output and vascular resistance which has further effects upon halothane uptake. Ventilation was assumed to be constant. This model suggested that significant changes occurred as a result of the interaction between halothane uptake and the circulation. Fukui and Smith [41] [42] described a multiple model with representation of respiration, circulation and the uptake and distribution of halothane. This model used pulsatile flows in blood vessels and used halothane concentrations in one, or a combination, of three compartments to modulate circulatory and respiratory performance.

The model of Schwid [101] also employed a multiple model consisting of a pharmacokinetic–pharmacodynamic model, a circulatory model, and a carbon dioxide and oxygen transport model. Schwid's model aimed to represent the effects and interactions between inhaled and injected drugs in the simulated patient.

3.7 Physiologically–based Models of Injected Agent Pharmacokinetics

Injection of a drug can be to various anatomical sites. Intramuscular injection deposits drug in a muscle from which it enters the circulation. Intravenous injection places a drug directly in the blood in a vein. The drug then flows in the venous blood to the heart and is pumped into the arteries and through the tissues of the body. An intraarterial injection places drug in an artery allowing significant concentrations of the drug to be developed in the tissues served by the artery. The distribution of drug following injection depends upon:

1. the physico–chemical properties of the drug

   and,

2. the physiological characteristics of the body tissues.

The physico–chemical properties of the drug include its pKa, its protein binding characteristics and its solubility in lipids. Physiological characteristics of relevance include the perfusion of the tissue, the volume of the tissue, and its components as fat, water and protein.

As the drug enters the blood, from an injection site, equilibration occurs between free unionised, free ionised, protein bound and lipid dissolved drug. As blood passes through a tissue, drug may diffuse between the tissue and the blood of may pass through spaces in blood vessel walls. The net flow of drug may be either into or out of the blood depending upon the equilibration. Blood leaving the tissue after equilibrating with it mixes with other venous blood in the large veins. Further equilibration occurs in these vessels. Description of injected agent pharmacokinetics requires representation of each stage in each equilibration process. This equilibration process within a tissue or fluid space was schematically represented in Figure 3.5.

In comparison with the processes for inhaled anaesthetics, injected agents present more complex calculations. The concept of anaesthetic tension allowed simple manipulation of inhaled agent concentrations. The use of tensions is a realistic approximation for most inhaled agents because inhalational agents do not ionise to any significant extent in solution. There is similarly no evidence of the *binding* of inhaled anaesthetic drugs to specific sites in proteins. All of the drug is therefore dissolved in either fat, water or protein [102] and the tissue or fluid space can therefore be represented as a volume with an associated tissue:gas partition coefficient. Equilibration therefore results in the tensions in all tissues reaching the same levels. For injected agents, only unionised drug can dissolve in fat and, depending upon the drug, either unionised, ionised or both unionised and

ionised forms of the drug may bind to proteins [103]. It is therefore not possible to consider a partition coefficient which will represent the 'capacity' of a tissue or fluid for a drug. The expression of such a parameter would be dependent upon pH, temperature and many other factors.

As an example, Equation 3.11 expresses the total amount of a basic drug in a tissue or fluid space in terms of the free unionised form of the drug. Reproducing this equation for clarity,

$$d = W_T \cdot \{\frac{x_s}{x_s + K_{pb}} \cdot P + \lambda \cdot x_s \cdot F_f + x_s \cdot F_w + 10^{(pKa-pH)} \cdot x_s \cdot F_w\}$$

The ratio of the free unionised form of the drug to the total drug amount is then given by

$$\text{ratio} = \frac{F_w}{\frac{P}{x_s+K_{pb}} + \lambda \cdot F_f + (1 + 10^{(pKa-pH)}) \cdot F_w}$$

If this ratio is taken as a partition coefficient, it is therefore dependent upon the pH and the concentration of the drug and must be recalculated at each stage.

Davis and Mapleson [45] proposed a model for the pharmacokinetics of injected agents. The model was based upon Mapleson's model P [40] with slight alteration of data to incorporate the 1975 ICRP standard man. Davis and Mapleson added explicit portal, liver and kidney circulation paths to support representation of excretion and metabolism. The single venous pool of Mapleson's model P was split into two parts in order to "permit accurate representation of i.v. injections" [45]. The ICRP standard man of 1975 included data on the composition of each tissue in the body in terms of water, protein and fat. The circulation path schematic diagram of Davis and Mapleson's model is shown in Figure 3.12.

In his Ph.D. Thesis [46], Davis described the steps involved in the simulation of injected agent pharmacokinetics and used pethidine as an example. Davis separated the body into two 'regions': blood and tissue. Each region had two sub–regions; red cells and plasma for blood and tissue cells and interstitial fluid for tissue. Each sub–region was itself composed of specified amounts of water, fat and

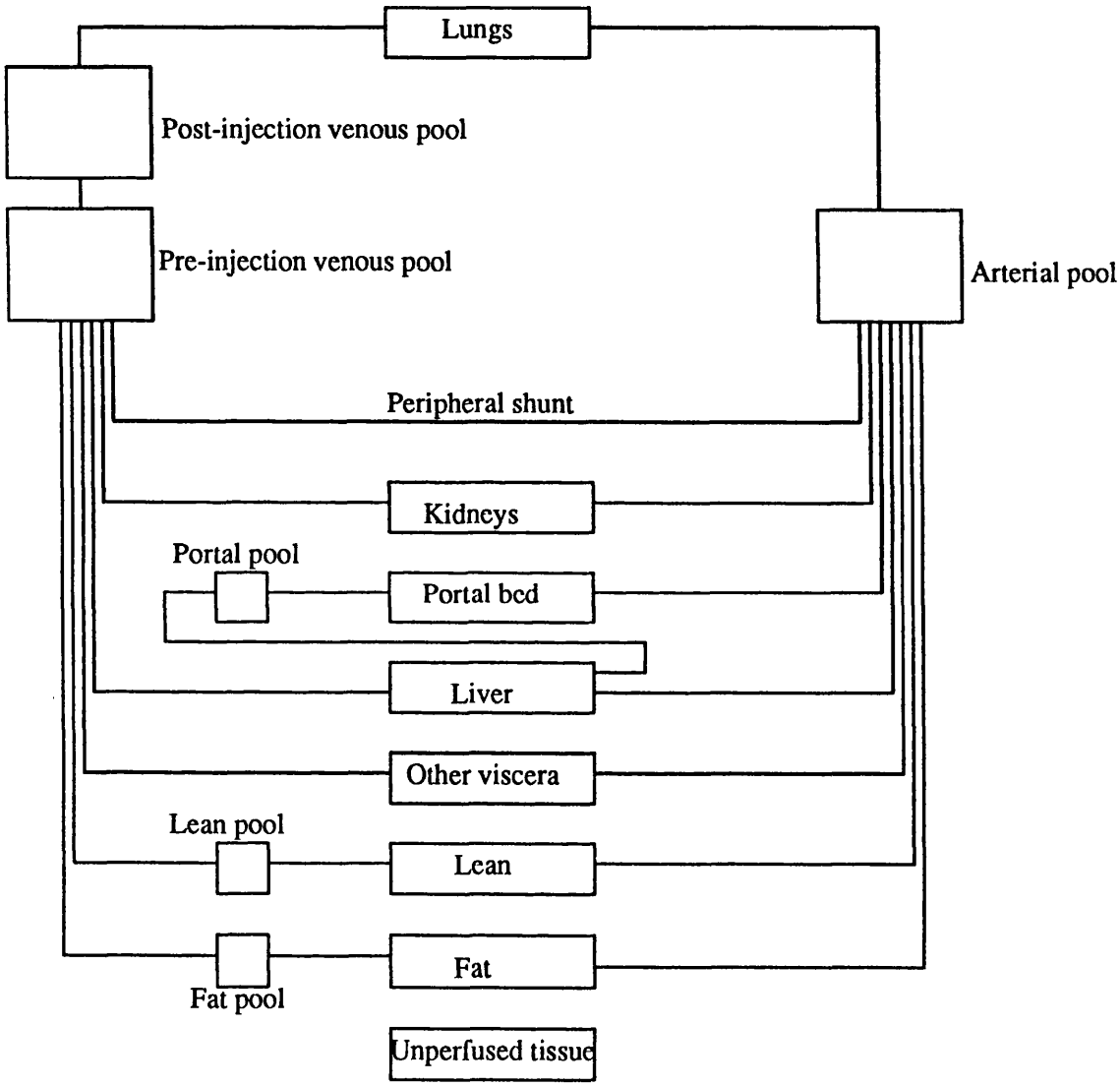

Figure 3.12: The Circulation Path Schematic for Davis and Mapleson's Model

protein. Davis described relevant pharmacokinetic data describing the ionisation, protein binding and partition into fat of pethidine, and chose representations of each relationship according to the quality of the data available. Davis derived equations for the rate of change of total drug amount in a sub–region with respect to the concentration of the free unionised form. The available data for pethidine, and experimental work carried out by Davis required that protein binding was represented by a relationship of the same form as Equation 3.8. In consideration of the amount of drug in a tissue, Davis used equations of the form of Equation 3.11 to derive the amount of the drug in the plasma, red cells, tissue cells and interstitial fluid of each tissue. The change in drug amount was calculated as the difference in drug content caused by the arrival of a new drug bolus and the departure of an old one. The free unionised concentration was then calculated by iteration so as to make the estimated amount in the tissue, based upon the estimated free unionised concentration, move within a specific tolerance of the actual amount of drug in the tissue which was kept via tallying.

Davis represented the metabolism of pethidine using a simple empirical relationship in which a constant fraction of the drug amount in the blood arriving at the liver was removed. This relationship was chosen because information available on pethidine metabolism did not support quantification of a more specific relationship. Excretion of pethidine was also represented empirically but included the effects or urine pH.

Higgins [103] used Davis's model for pethidine as the basis for a physiologically–based model of fentanyl pharmacokinetics. Higgins added a new nasal compartment to the pethidine model to allow for the modelling of intranasal administration of fentanyl. The ionisation, protein binding and dissolution into fat of fentanyl was represented in accordance with existing studies in the area. The metabolism of fentanyl was represented by removing a constant fraction of the drug from the

blood entering the liver. Excretion of fentanyl by the kidneys was represented differently to that in Davis's model and allowed for a concentrating effect in the renal tubule along with variation according to urine pH. Fentanyl apparently binds to a small proportion of the available protein binding sites. The Scatchard equation which relates the protein bound and free forms of a drug is

$$C_b = \frac{n \cdot k \cdot C_s}{1 + k \cdot C_s} \tag{3.17}$$

where n is the number of protein binding sites per protein molecule, k is the binding constant, C_b is the ratio of mmol bound drug to mmol protein and C_s is the concentration of the free form in mmol drug per g water. When the drug binds to only a small fraction of the available protein sites, the term $k \cdot C_s$ is small and equation 3.17 approximates to

$$C_b = n \cdot k \cdot C_s$$

The generation of the free unionised concentration of fentanyl in Higgins' model therefore uses equations of the form of Equation 3.13 to represent the distribution of a drug amount within each tissue. In this form, the free unionised concentration can be directly obtained given the amount of drug in the tissue. This removes the need for computationally expensive iteration.

In contrast to the work of Davis and Higgins, the model employed by Schwid [101] was described as having the capacity to represent pharmacokinetics and pharmacodynamics of morphine, thiopentone, fentanyl, lidocaine, succinylcholine, pancuronium, atracurium and neostigmine. Schwid describes an eight tissue group model where the tissue groups are defined in terms of mass, oxygen consumption and carbon dioxide production. The equilibration of injected drugs within the model is modelled by assigning a tissue:blood partition coefficient for each drug. From Schwid's description of the drug model, it is unclear whether tissue perfusions, blood volume and circulation times are reliably represented in

the model. The basis of selection of the partition coefficient for each tissue for each drug is not described.

In summary, the physiologically–based models developed by Mapleson [40], Davis and Mapleson [45], Davis [46] and Higgins [103] each employ realistic parameters to represent tissue volumes and masses, compositions and perfusions. The data available for the physico–chemical properties of the drugs appears to present current limitations to the quality of the modelling. Davis [46] actually performed some experiments in order to determine physicochemical data. Higgins [103] required to arbitrate between often inconsistent data in the available literature. It appears therefore, that the performance limitations of physiologically–based models of pharmacokinetics are largely due to the lack of good quality physicochemical data. If physiologically–based models become more widely used in the analysis of drug pharmacokinetics, the systematic evaluation of physicochemical parameters through good experimental design and performance should follow.

3.8 Representation of Physiologically–Based Pharmacokinetic Models

In a recent editorial, Hull [104] suggested that in order to analyse drug disposition data, "the most satisfying approach is to derive a physiological model that emulates, as far as possible, what actually happens in the body". Hull suggests that the main advantage of this approach is that physiologic changes can be accommodated. He also concedes that the main disadvantage of these models is that "numerical values must be assigned to their many parameters". A further limitation to the utility of physiologically–based models is the lack of an appropriate model representation.

Physiologically–based models have been developed by several workers including Mapleson [40], Davis and Mapleson [45], Davis [46] and Higgins [103]. These models have employed textual description and graphical schematics to express the important concepts of the models. Without exception, however, the actual *representation* of the model has involved mathematical equations written in computer code.

To an individual, unfamiliar with either programming or physiologically–based modelling, it is not simple to separate the important aspects of the model from the mechanisms of the program. In such a case, the representation of the model actually detracts from its utility. The following sections introduce Bond Graphs for the representation of models. Their use will be illustrated for the representation of compartment models first and then for physiologically–based pharmacokinetic models.

3.9 Bond Graph Model Representation

Bond graphs [105] provide a means of graphically representing system models. They were originally used to represent engineering models but have been used in many other areas [106]. For instance, Karnopp and Rosenberg [107] describe the use of bond graphs for mechanical, electrical, thermal and acoustic systems. Bond graphs have also been used to represent biological models. As examples, Plant and Horowitz [108] used bond graphs to represent chemical reactions and ion transport; Karnopp and Azarbaijani [109] introduced bond graphs for generalised compartmental models; Lefevre and Barreto [110] used a combination of block diagrams and bond graphs to represent biochemical models and Thoma and Atlan [111] represented osmosis using bond graphs. Further diverse applications are described by Thoma [112].

These applications illustrate the utility of the bond graph representation

technique. Given this utility, the bond graph technique has therefore been used to represent the physiologically–based models described earlier in the chapter.

3.9.1 Bond Graph Notation

This section is intended to provide an informal introduction to bond graph elements and their notation. Of course, full description of the notation is given in standard text books such as [107] and [113]. Bond graphs consist of components, junctions and their interconnections. Common to all bond graphs are the concepts of effort and flow which can also be termed 'across variables' and 'through variables'. A simple example is voltage as an effort variable and current as a flow variable for an electrical system. In some bond graphs, true power bond graphs, the product of effort and flow gives the instantaneous power flow in the system. This is the case in the electrical example. In other situations, the effort–flow product does not have the dimensions of power and these bond graphs are termed pseudo bond graphs. Bond graph components can represent loss, storage, or transformation of quantities appropriate to the system model being represented. Bond graph junctions provide no loss or storage but conserve material or energy.

Component and Junction Interconnections

1. Bonds.

   A bond represents an ideal connection which possesses no loss, storage or transformation of matter or energy. Each bond therefore has one effort and one flow associated with it. A bond is illustrated in Figure 3.13. The half arrow on the bond signifies the assumed positive direction of energy or material flow. As indicated in Figure 3.13, horizontal bonds have their effort variable written above them and their flow variable below. Non–horizontal bonds have their effort to the left of the bond and their flow to the right.

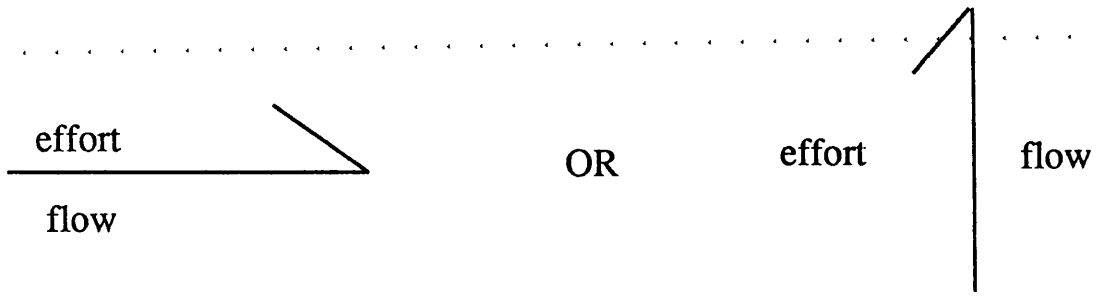

Figure 3.13: A Bond and its Notation

2. Signals.

   Signals allow one way transfer of information. Signals are usefully employed to represent the transport of material and this feature is exploited in later examples. The difference between a bond and a signal is illustrated later following introduction of the remaining bond graph notation.

Junctions

There are two types of bond graph junction. A common effort or '0' junction is characterised by each of the bonds attached to it having the same effort and the net sum of the flow variables on the bonds attached to it being zero. A common flow or '1' junction is characterised by each of the bonds attached to it having the same flow and the net sum of the effort variables on the bonds attached to it being zero. The notation of bond graph junctions is summarised in Figure 3.14. To further illustrate their use, Figure 3.15 gives a simple electrical example of two resistors either in series or in parallel. The parallel pair have the same voltages across them (a common effort) and the total current in the resistors is the sum of the individual currents (net flow sum is zero). This arrangement can be represented using a common effort junction. In the series combination, both resistors have the same current (a common flow) and their individual voltage drops sum to the total applied voltage. This arrangement can be represented using a common flow

junction.

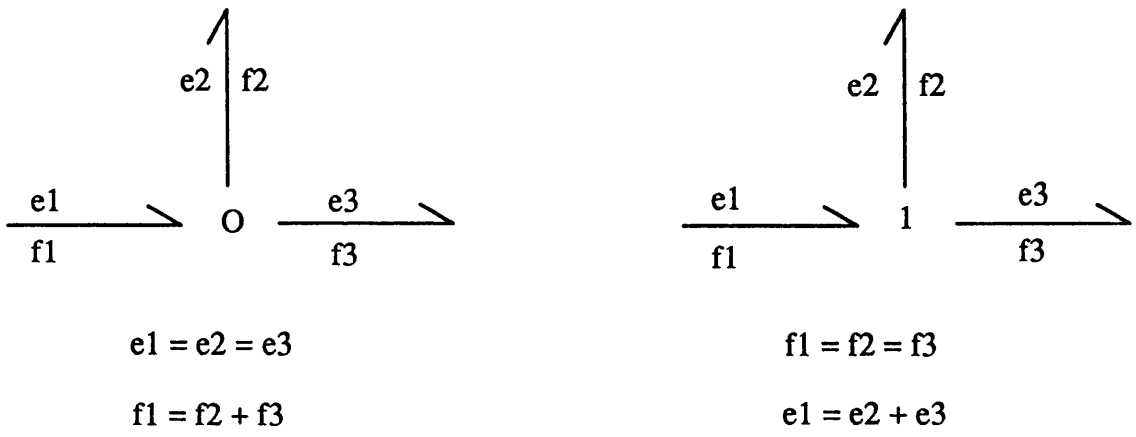

Figure 3.14: Bond Graph Junctions and their Notation

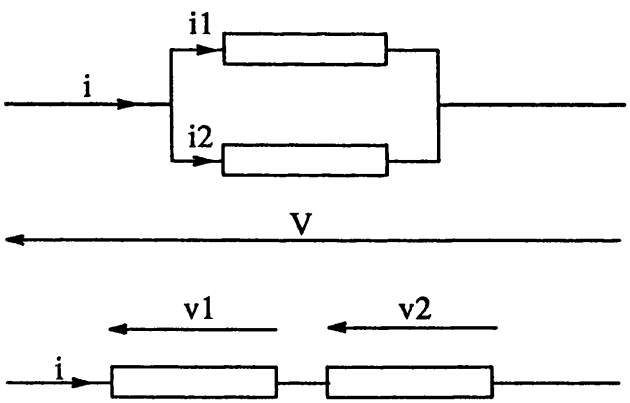

Figure 3.15: An Electrical Example for Illustration of Junction Types

Components

1. The Resistor.

   This component is used to represent resistance to flow and dissipation. Electrically, a voltage applied across a resistor causes a current through

it. Conversely, a current flowing through a resistor causes a voltage to be established across it. Similarly, the diffusion of a drug across a membrane (a flow) depends upon the existence of a concentration gradient across the membrane (an effort). In power bond graphs, the product of the effort and flow variables associated with a resistor gives the power dissipated in it. Some examples of different uses of bond graph resistors are shown in Figure 3.16.

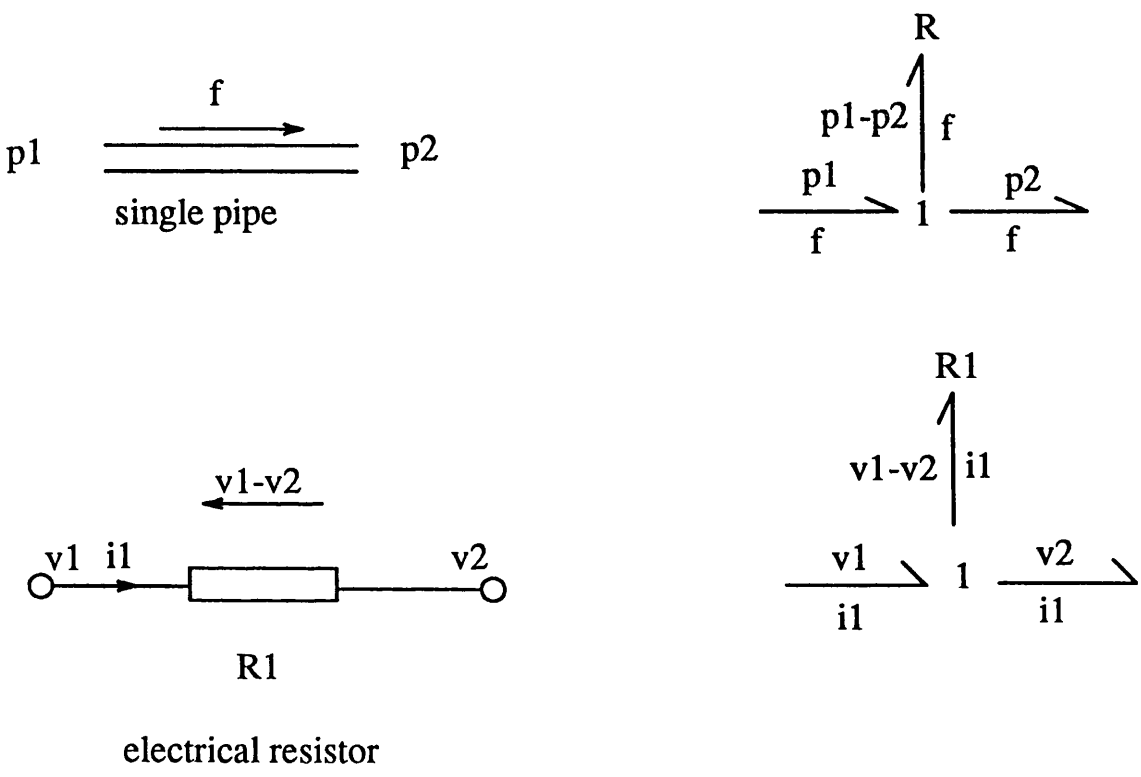

Figure 3.16: The Resistor and its Notation

2. The Flow Store

The flow store is illustrated by the fluid system of Figure 3.17. In this example, the fluid accumulated in the tank (flow store) causes a pressure at the bottom of the tank (an effort). Because the pressure in the pipes entering and leaving the tank is the same as that in the tank, the bond graph representation for the tank involves a common effort junction. In more

abstract terms, a linear flow store can be considered to have the relationship

$$\text{effort} = \frac{1}{C} \cdot \int \text{flow dt} \tag{3.18}$$

where C is a constant (e.g., capacitance) with dimensions appropriate to the selection of effort and flow variables.

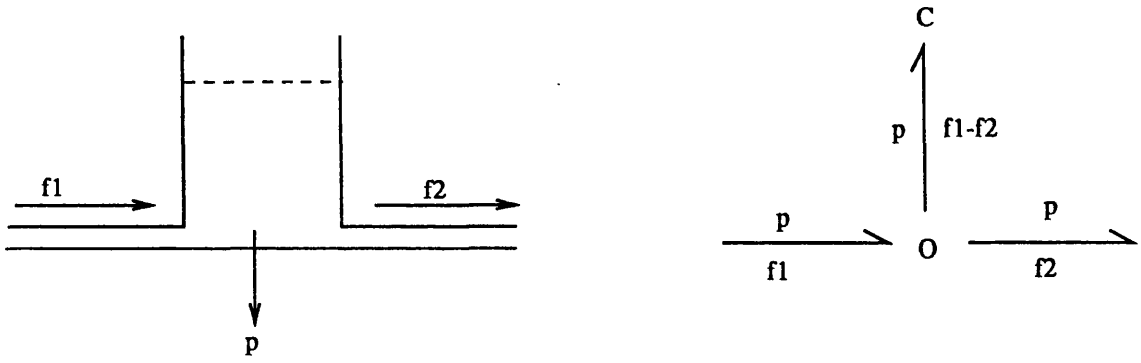

Figure 3.17: The Flow Store and its Notation

3. The Effort Store.

   The effort store is the dual of the flow store therefore,

$$\text{flow} = \frac{1}{I} \cdot \int \text{effort dt} \tag{3.19}$$

   where I is a constant (e.g., inertance) with appropriate dimensions.

   Effort stores are rare in physiological systems.

The Difference between Bonds and Signals

Figure 3.18 illustrates the differences between bonds and signals. In the diagram on the left of the Figure, the flow out of the first tank depends upon the pressure

difference between the tanks. In other words, the second tank can apply a back-pressure to the outflow of the first tank. In the diagram on the right, the pressure in the second tank has no effect on the outflow of the first and the flow therefore depends only upon the pressure in the first tank. Portions of a bond graph representation for these systems are included in the Figure. Note that when the flow from the tank depends upon both the forward and back pressures, a bond is used. When it depends only upon the forward pressure, a signal is used.

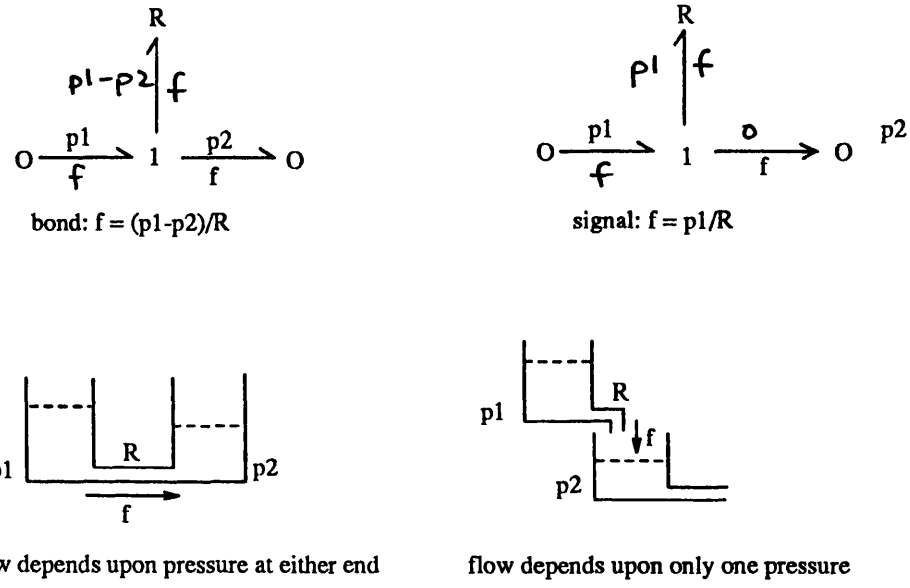

Figure 3.18: Comparison of Bonds and Signals

Causality

One of the central themes of bond graph representation is that of causality. Causality, in this context, means computational causality, which determines the order in which the equations of the system must be solved. A simple example is that of a resistor. The relationship defining the characteristics of the resistor can be expressed as either of

$$\text{effort} = \text{flow} \cdot \text{resistance}$$

or

$$\text{flow} = \frac{\text{effort}}{\text{resistance}}$$

Causality determines whether the equations of the system should be solved so as to determine the effort or flow for such a component first. The appropriate version of the relationship is then applied. In a bond graph containing sources of effort or flow or both, causality is defined for each source and cannot be changed. This is illustrated for effort and flow sources in Figure 3.19 An effort source

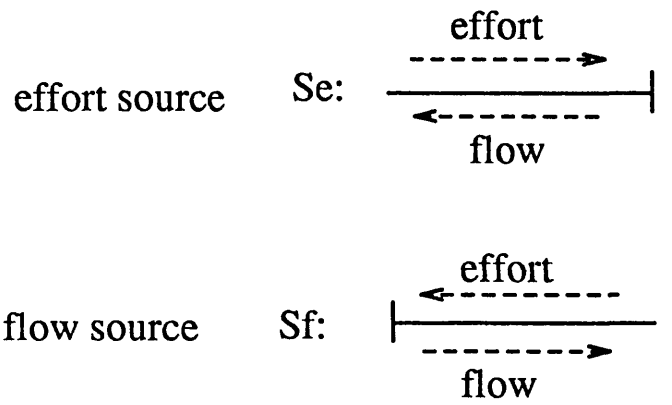

Figure 3.19: Causality of Effort and Flow Sources

determines the effort input to the system but the system determines the flow through the source. A flow source determines the flow through the system but the system determines the effort across the source.

Flow stores and effort stores have preferred causality as shown in Figure 3.20. It is clear that for a flow store, it is desirable that the flow into the store is determined by the system and that the effort returned by the store is determined by the store. The opposite is true for an effort store.

A further effect of causality is manifested at junctions. At a common effort junction, all bonds share a common effort. It is not possible for more than one bond to convey this effort to the junction. All bonds except one therefore accept the effort value from the junction. Conversely, for the common flow junction, only one bond may apply the flow to the junction, all others must accept it. These situations are illustrated in Figure 3.21.

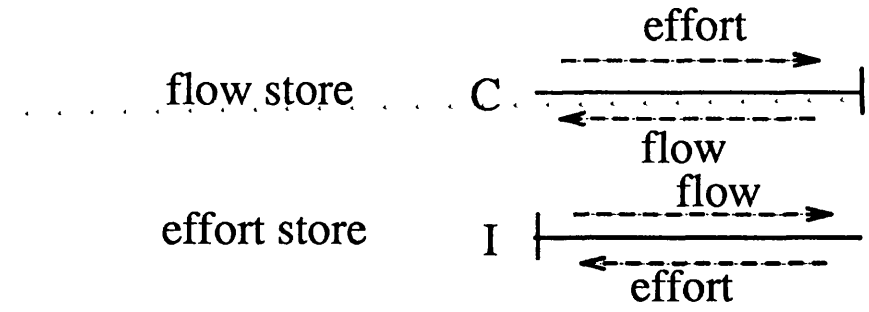

Figure 3.20: Causality of Effort and Flow Stores

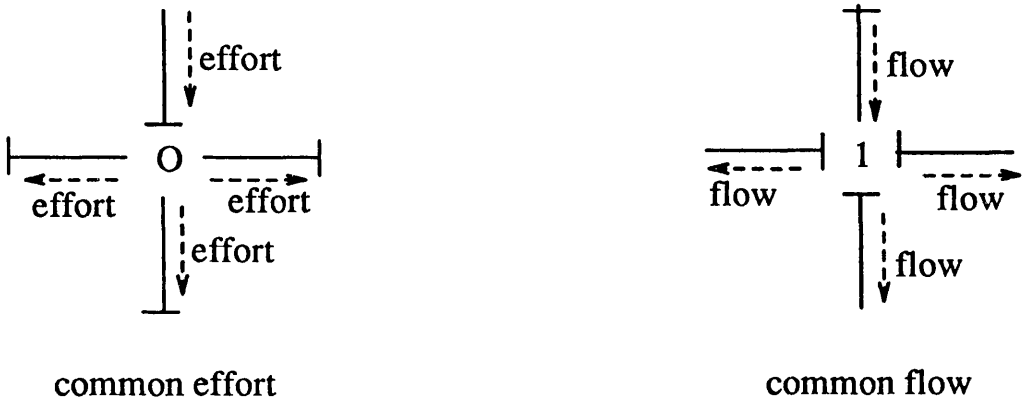

Figure 3.21: Causality of Bond Graph Junctions

Constitutive Relations

The constitutive relation of a component is a physical or empirical law which describes its behaviour. In discussion so far, only linear relationships have been considered. In general, any non-linear relationship can form the constitutive relationship for a component. The use of non-linear constitutive relationships is illustrated later.

3.10 Bond Graph Representation of Compartment Models

In this section, the bond graph representation of compartment models is derived. This serves to illustrate the use of bond graph bonds, signals, junctions and components in the representation of a well-known class of models. In this way,

the characteristics of the representation are made distinct from the characteristics of the model. First, the bond graph for a two–compartment model is derived. The bond graphs for different arrangements of two–compartment models are then given for comparison. The bond graph for a three–compartment model is then used to derive simulation equations. These are parameterised using data on the population pharmacokinetics of propofol and simulation results are presented. The compartmental model notation employed in this section is that suggested by Hull [114].

3.10.1 Developing the Representation for a Two-Compartment Model

The schematic diagram for a two-compartment model is shown in Figure 3.22. The compartmental model implied by this schematic consists of the following parts: two compartments (labelled 1 and 2), a drug source (Sf) and three microconstants (labelled k_{12}, k_{21} and k_{10}).

The Compartments

Each compartment represents a notional amount (volume or mass) of a tissue. The injection or infusion of drug into the compartment results in an amount and a concentration of drug in the compartment. The concentration is given by $conc = \frac{x}{V}$ for drug amount x and compartment volume (or mass) V. The compartment is analogous to a water tank, since a flow of water into the tank results in pressure at the base of the tank.

In bond graph notation, this behaviour is displayed by a *capacitance*. The constitutive relationship for a capacitance in the context of compartment models is shown in Figure 3.23.

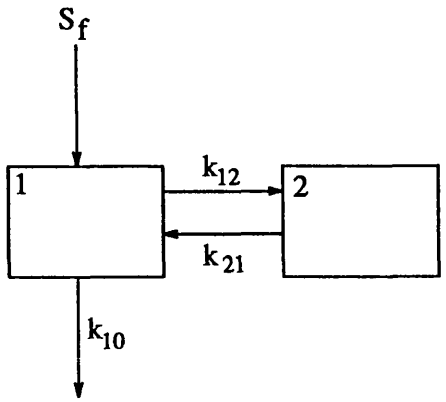

Figure 3.22: A Two-Compartment Model

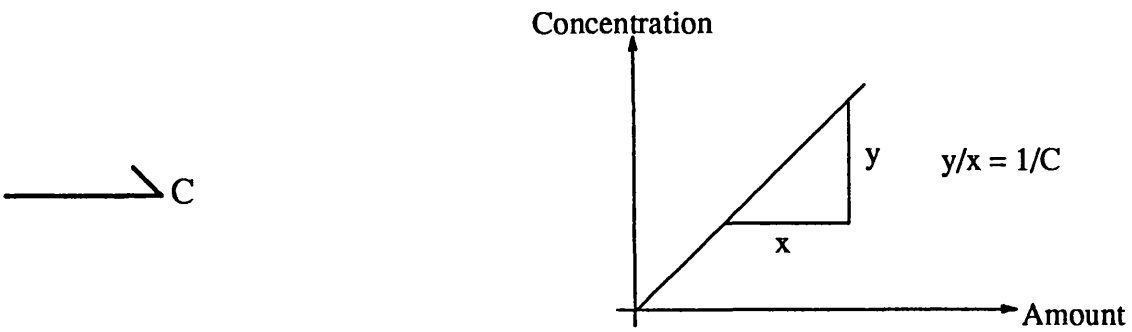

Figure 3.23: A Capacitance in Pharmacological Context

Microconstants

Microconstants define transfers between compartments. With x_1 mg of drug in compartment 1, and a microconstant k_{12} s^{-1} describing the transfer from compartment 1 to compartment 2, the rate of drug flow from compartment 1 to compartment 2 is $k_{12} \cdot x_1$ mg/sec. This transfer depends only upon the amount of drug in compartment 1, but not upon that in compartment 2.

In bond graphs, a one way transfer can be represented by a *signal.* The microconstant can be represented using a resistor. An appropriate arrangement is shown in Figure 3.24. In this arrangement, c_1 is the concentration in compartment 1, c_s is the concentration on the signal and f is the flow of drug from compartment 1 to compartment 2. The drug flow is therefore

$$flow_{12} = \frac{c_1 - c_s}{R} = \frac{c_1}{R}$$

But the signal goes from a common–flow junction. It therefore carries flow only and c_s, the effort variable, is therefore zero.

For this representation to be equivalent to the compartmental model, the drug flow values predicted by each representation must equate. This is achieved by selection of R as follows:

if V_1 is the volume of compartment 1 then

$$\frac{c_1}{R} = k_{12} \cdot x_1$$

so

$$R = \frac{c_1}{k_{12} \cdot x_1} = \frac{1}{k_{12} \cdot V_1}$$

The microconstant representing transfer from compartment 2 to compartment 1, k_{21}, can be similarly represented. The microconstant representing clearance from the model, k_{10} is represented in bond graphs as a resistor placed between the first compartment and the environment. The value of this resistor is calculated in the same way as that for the other microconstants.

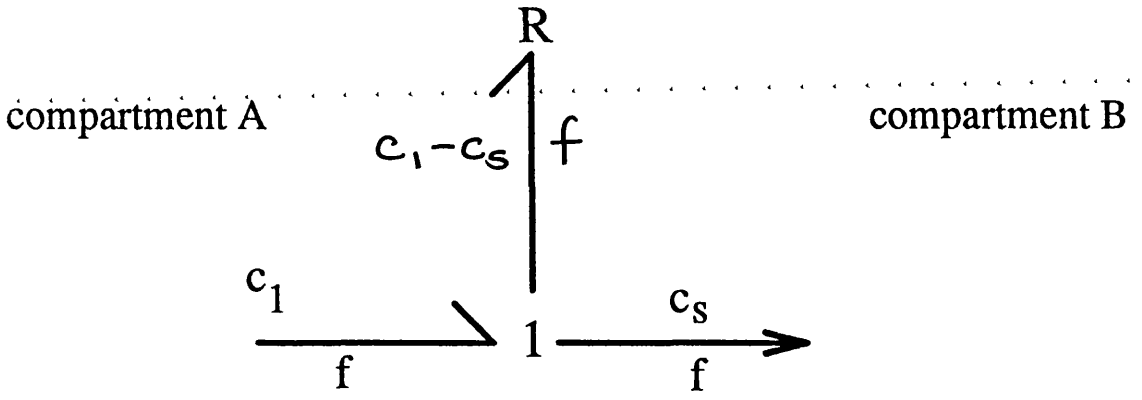

Figure 3.24: Bond Graph Representation of a Microconstant

Overall Representation.

To complete the representation, it is now only necessary to ensure that drug is conserved within the model. Thus, for each compartment, drug flows can be from an external drug source into the compartment, from another compartment, to another compartment, or to the environment. At all times, these flows must sum to zero because drug is conserved within the model. Also the flows from a compartment are all dependent upon the amount in it. In bond graphs, both of these conditions are satisfied by the placement of compartment and microconstant representations about a "0" or "common-effort" junction. This final arrangement is shown in Figure 3.25.

Structural Changes in the Model and Bond Graph

Figure 3.26 shows the schematic diagram for a two compartment model which has drug elimination from the second compartment, and the bond graph for this model. It can be seen that the changes in both the schematic diagram and bond graph are very simple.

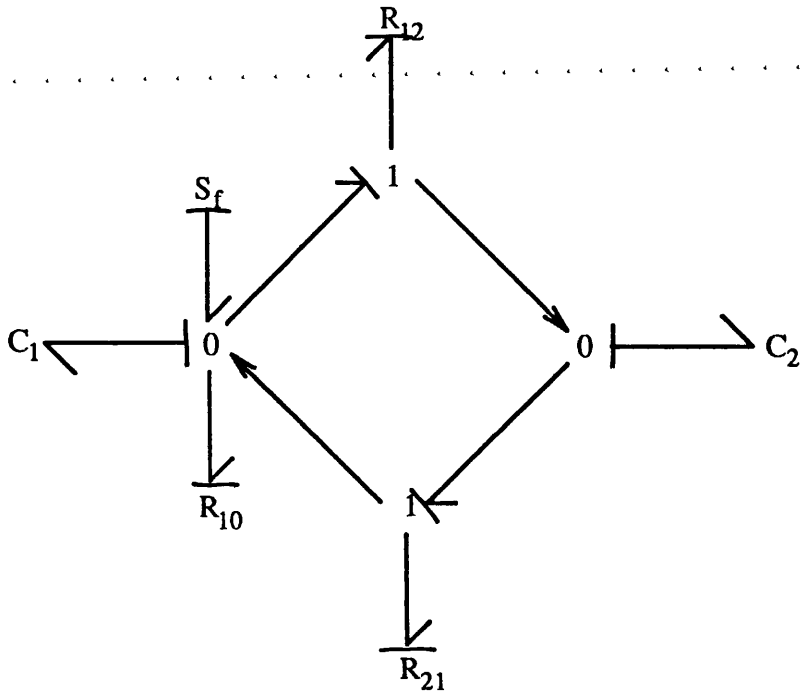

Figure 3.25: Bond Graph of the Two-Compartment Model with Elimination from Compartment 1

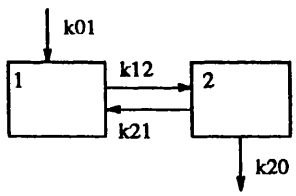

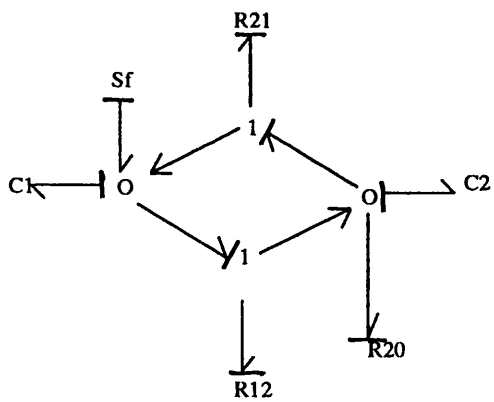

Figure 3.26: A Two Compartment Model with Elimination from Compartment 2 and its Bond Graph

3.10.2 Bond Graph Representation of a Three–Compartment Model

Figure 3.27 is the bond graph of a three compartment model for propofol. Using data from [35], and refinements provided by Marsh et al. [36] the Model Transformation Toolbox (MTT) [115] was used to automatically derive blood concentation estimates in the notional central compartment for a constant rate infusion of 6 mg/kg/hour (Figure 3.28). The simulation results are in agreement with the experimental data published by Gepts et al. [35] as would be expected.

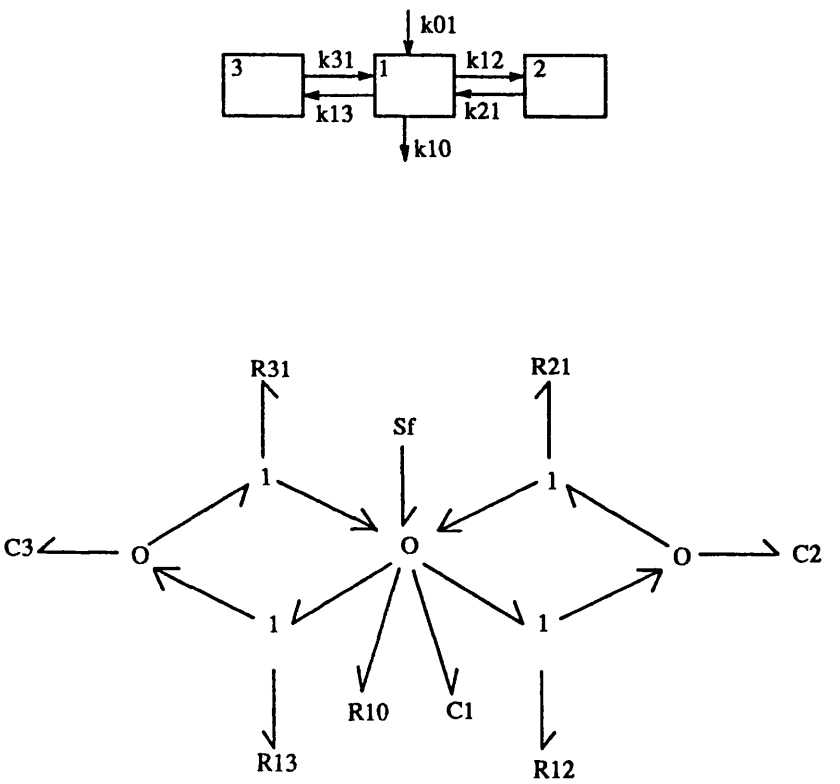

Figure 3.27: Three–Compartment Model and its Bond Graph

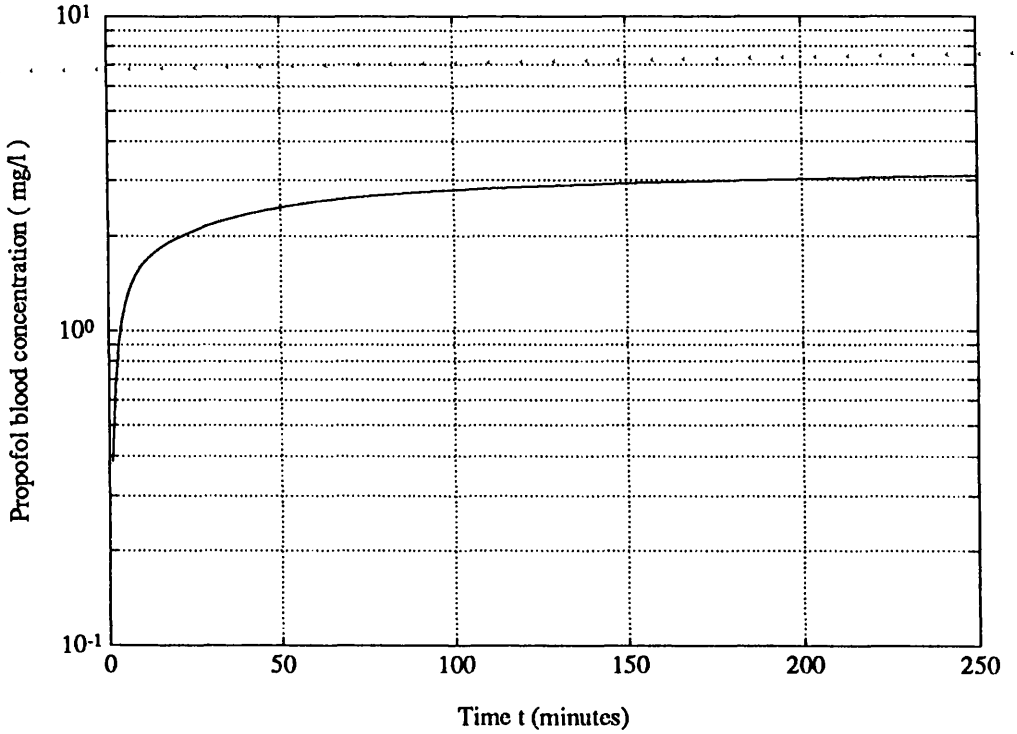

Figure 3.28: Simulated Central Compartment Concentration for Propofol Model

3.11 Bond Graph Representation of Physiologically–based Models of Inhaled Agent Pharmacokinetics

As described in Section 3.8, understanding of physiologically–based pharmacokinetic models is hindered by the lack of an appropriate model representation scheme. Central to the physiologically–based models developed by Mapleson [40] and pursued by Davis [46] and Higgins [103], are the concept of circulation, the use of physiological data to parameterise tissue groups and the use of real physico–chemical data.

In representing the more abstract two–compartment model, sufficient bond graph elements have been used to allow representation of the physiologically–based models. In the Mapleson models, drug is transported to the tissues of

the body in the blood. The models actually represent the movement of drug alone but the parameters used in this process embody both physiological and physico–chemical data. In Mapleson's models, the concept of anaesthetic tension is important because at equilibrium, the tension in all tissues is the same.

The bond graph representation of Mapleson's Model P is presented in Figure 3.29. The bond graph of the model can be compared with its circulation schematic diagram (Figure 3.11). In the bond graph, each tissue group is represented by a capacitance. Where a tissue has a blood pool associated with it, this has been combined with it to reduce the order of the model. This approximation is further described in Chapter 4. The capacitances have been assumed to be linear and have a magnitude which represents the capacity of the tissue group for the drug. For instance, the arterial pool has capacitance given by

$$C_{artpool} = \lambda_{blood} \cdot V_{artpool}$$

where λ_{blood} is the blood–gas partition coefficient and $V_{artpool}$ is the volume of the arterial pool.

Because drug is transported by the blood, the amount of drug being delivered to a tissue group is given by the concentration of the drug in the blood reaching the tissue multiplied by the blood flow to the tissue. This amount does not depend upon the amount or concentration of drug already in the tissue. This is analogous to the behaviour of microconstants in compartment models (Section 3.10.1). The delivery of drug to a tissue group is therefore represented by a bond graph resistor and a signal as shown in Figure 3.30.

In this arrangement, the mass flow of drug between the tissue groups represented by C1 and C2 is from C1 to C2 only and depends upon the anaesthetic tension (an effort) on C1 and the resistance R. The resistance R relates the tension on C1 to the drug flow to C2. R therefore reflects the blood flow of the tissue group represented by C2 and the partition coefficient of the blood.

In contrast to Model P, Mapleson's Model O did not represent circulation time

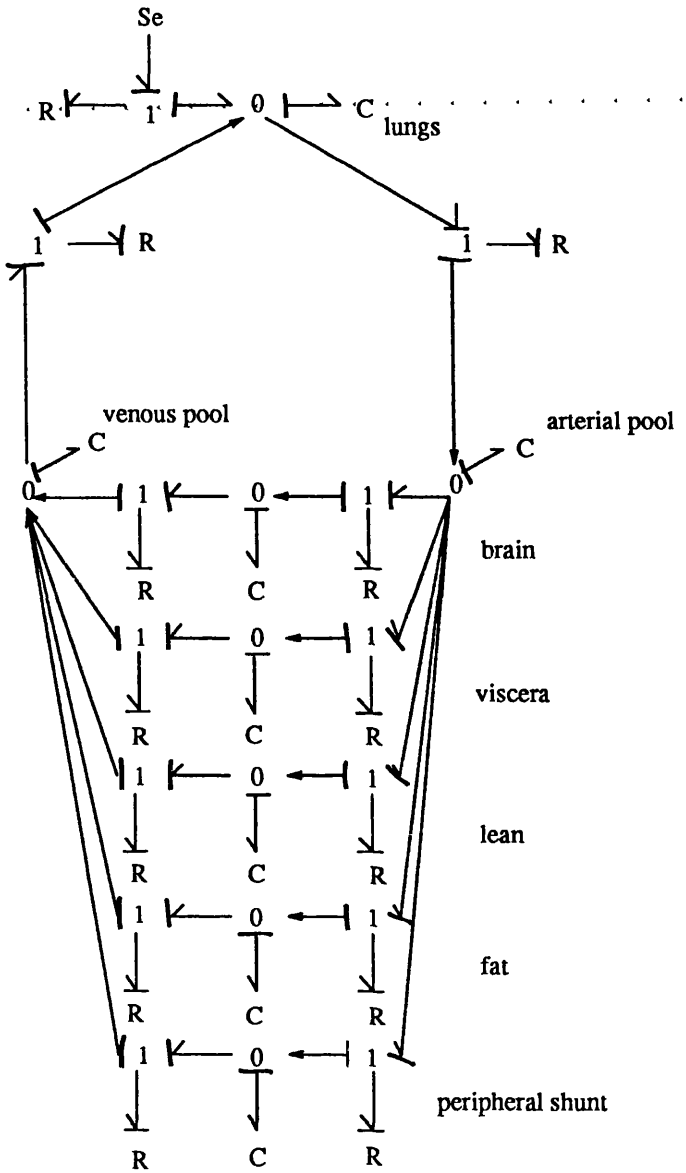

Figure 3.29: Bond Graph for Mapleson Model P

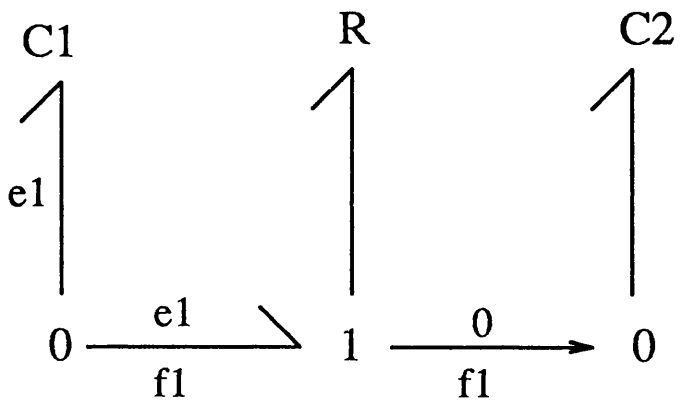

Figure 3.30: The Arrangement used to Represent Drug Transport

delays or make explicit arterial and venous flows. Model O has the fluid analogue illustrated in Figure 3.31. Its bond graph is shown in Figure 3.32. In this case, the bond graph does not require signals due to the absence of circulation in the model. As before, each tissue group is represented by a capacitance which represents the capacity of the tissue group and its associated blood pool for the drug. The blood flow for each tissue and the blood:gas partition coefficient are embodied in the resistance values.

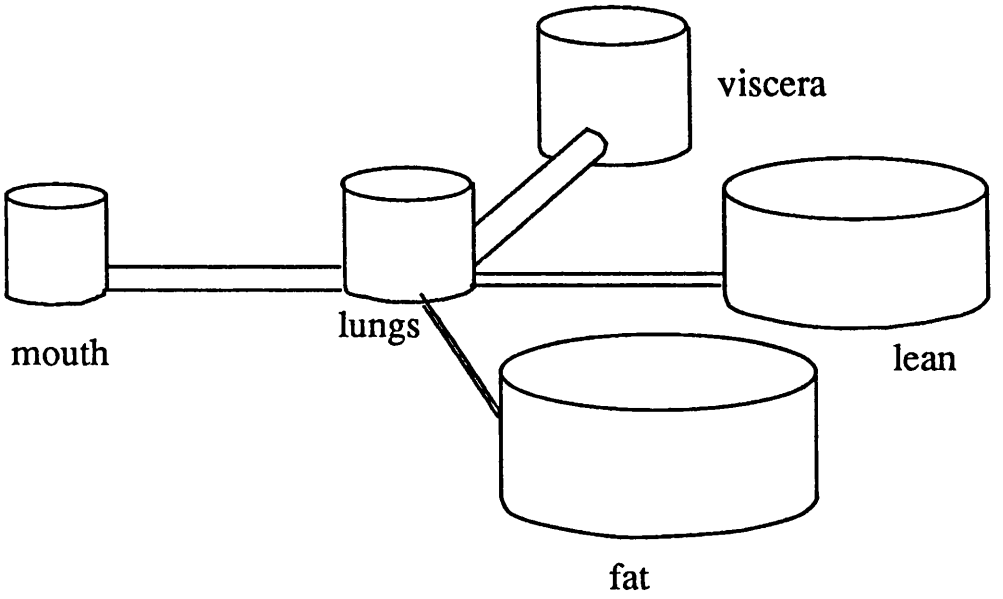

Figure 3.31: The Model O Fluid Analogue

The Model Transformation Toolbox (MTT) [115] was used to automatically generate MATLAB simulation equations for both Model O and Model P from a graphical representation of their bond graphs. Comparison of their respective brain tension values for a step input of nitrous oxide at time 0 concentration are shown in Figure 3.33. The effect of representing circulation times accurately in Model P are clear in comparison to the approximation of circulation times used in Model O.

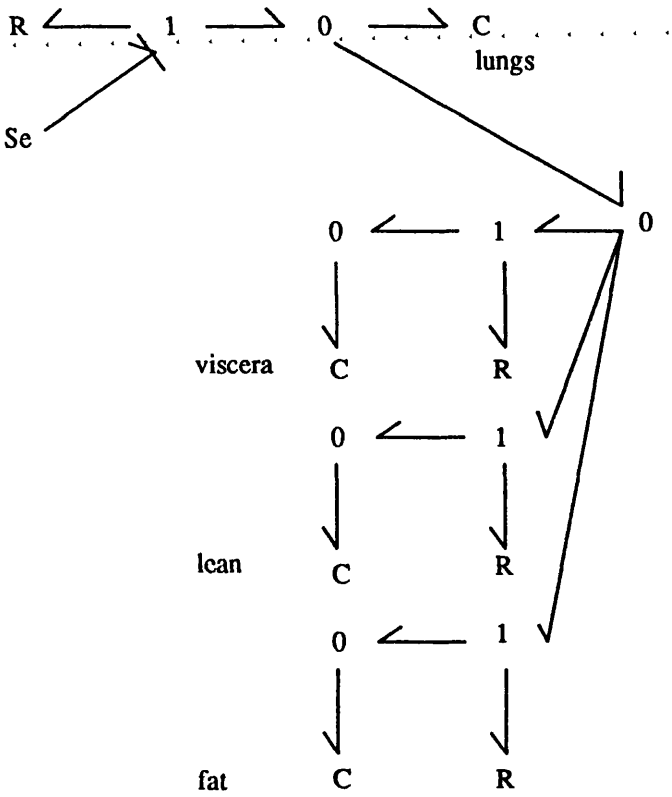

Figure 3.32: The Model O Bond Graph

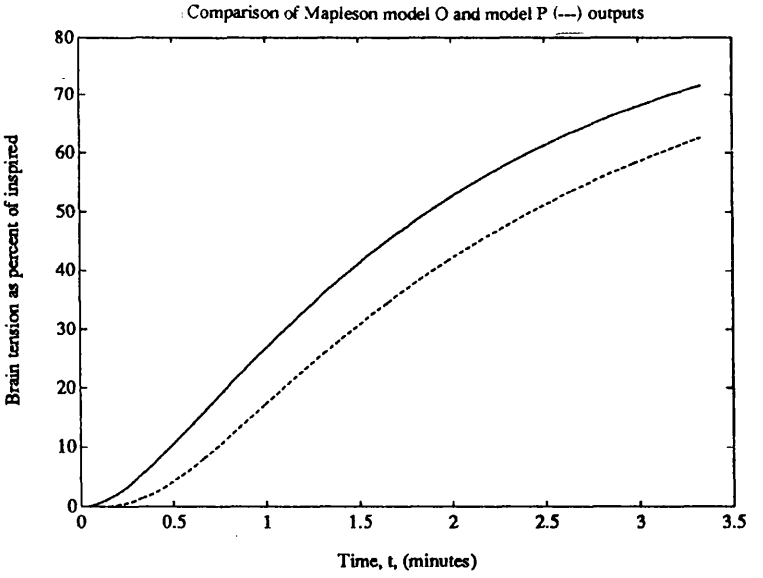

Figure 3.33: Comparison of Model O and Model P Brain Tensions

3.12 Bond Graph Representation of Injected Agent Pharmacokinetics

Equation 3.11 described the amount of drug in a fluid space in terms of the amounts unionised in water, ionised in water, bound to protein and dissolved in fat. Given that both ionised and unionised drug may bind to protein, equilibration may be schematically illustrated as shown in Figure 3.34.

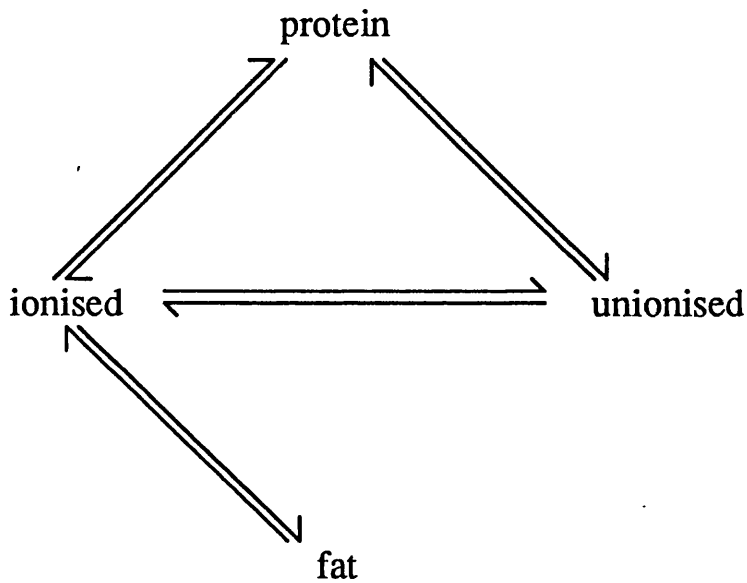

Figure 3.34: Schematic for the Equilibration of Drug in a Fluid Space

Figure 3.35: The Notation for a Bond Graph Transformer

In the current bond graph approaches, the effort variable has been assumed to be concentration and the flow variable is the mass flow of the drug. Representation using these choices can proceed using a bond graph *transformer*. The generalised bond graph transformer is drawn as shown in Figure 3.35 and its behaviour is

described by an equation of the form of Equation 3.20.

$$\begin{bmatrix} e_1 \\ f_2 \end{bmatrix} = \begin{bmatrix} a & 0 \\ 0 & b \end{bmatrix} \cdot \begin{bmatrix} e_2 \\ f_1 \end{bmatrix} \tag{3.20}$$

It is often assumed that $a = \frac{1}{b}$. If $a \neq \frac{1}{b}$ then more general relationships can be represented. Ionisation, dissolution in fat and protein binding can be represented as follows.

1. Ionisation.

   From Equation 3.10, for an acid drug,

   $$C_i = 10^{(pH-pKa)} \cdot C_s$$

   This can be represented by a transformer with the constitutive relationship

   $$\begin{bmatrix} C_i \\ f_{si} \end{bmatrix} = \begin{bmatrix} 10^{(pH-pKa)} & 0 \\ 0 & 1 \end{bmatrix} \cdot \begin{bmatrix} C_s \\ f_{is} \end{bmatrix} \tag{3.21}$$

   where f_{si} and f_{is} are the mass flows from standard form to ionised form and ionised form to standard form respectively.

2. Fat Solution

   From Equation 3.5,

   $$C_f = \lambda \cdot C_s$$

   This can be represented with the transformer defined by

   $$\begin{bmatrix} C_f \\ f_{sf} \end{bmatrix} = \begin{bmatrix} \lambda & 0 \\ 0 & 1 \end{bmatrix} \cdot \begin{bmatrix} C_s \\ f_{fs} \end{bmatrix} \tag{3.22}$$

   where f_{sf} and f_{fs} are the mass flows from standard form to fat dissolved form and fat dissolved form to standard form respectively.

3. Protein Binding

Equation 3.8 gives,

$$C_p = \frac{C_s}{C_s + K_{pb}} \cdot C_{prot}$$

This can be represented by the transformer defined by

$$\begin{bmatrix} C_p \\ f_{sp} \end{bmatrix} = \begin{bmatrix} \frac{C_{prot}}{C_s + K_{pb}} & 0 \\ 0 & 1 \end{bmatrix} \cdot \begin{bmatrix} C_s \\ f_{ps} \end{bmatrix} \tag{3.23}$$

where f_{sp} and f_{ps} are the mass flows from standard form to protein bound form and protein bound form to standard form respectively.

Considering the general transformer constitutive relationship, Equation 3.20, it is apparent that the effort–flow products are not equal on either side of the transformer unless a=b (left–hand product = $e_1 \cdot f_1$ and right–hand product = $\frac{b}{a} \cdot e_1 \cdot f_1$. In a power bond graph, this would imply that *energy* has been introduced to the system.

For the transformers defined above (Equations 3.21, 3.22 and 3.23) the effort–flow products are not equal on both sides. While this is the case, because the coefficient relating the flow variables is unity in each transformer, there is no 'gain' of drug in the system. Flow through the transformer therefore occurs until the concentrations have equilibrated in accordance with the transformers constitutive relationship.

Using the transformers defined above, a bond graph can be drawn to represent the equilibration of an injected drug within a tissue or fluid space. This bond graph has the general form shown in Figure 3.36. In this figure, C:cp1 and C:cp2 are capacities representing the available protein binding sites for the unionised and ionised forms of the drug respectively. The capacitors C:cw represent the water within the tissue or fluid and the capacitor C:cf represents lipids. Transformers TF:tsp and TF:tip have the form of Equation 3.23. The resistor elements in

Figure 3.36 can be used to represent the finite rate of equilibration between the various phases. Alternatively, if the model considers equilibration to be near instantaneous, the resistor elements are given very small values. In the limit case, equilibration is assumed to be instantaneous and the resistor elements are removed from the bond graph and the bond graph represents only the steady–state of the system.

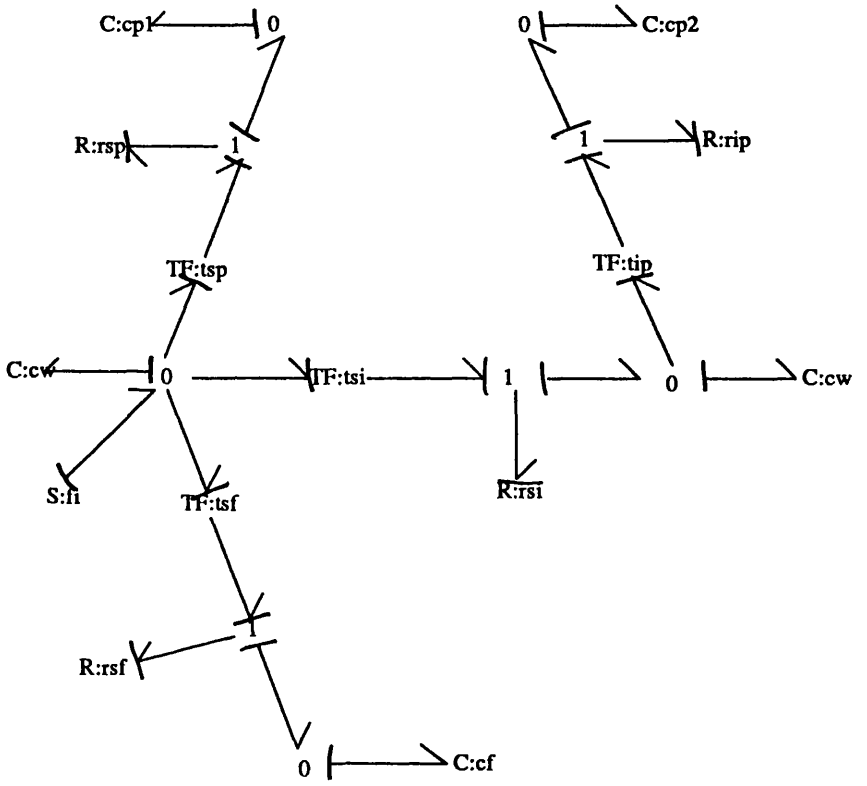

Figure 3.36: The Bond Graph for Injected Agent Equilibration in a Fluid Space

To illustrate this approach to the representation of drug equilibration, a bond graph has been created to represent the equilibration of fentanyl in plasma. The bond graph is based upon the model described by Higgins [103] and parameter values are taken from the same source. Higgins found that it was necessary to model the ionisation of fentanyl along with the binding of both unionised and ionised forms of the drug to plasma proteins. The inclusion of lipid dissolution was not found to be necessary. Higgins also found that, for fentanyl, protein

binding in plasma could be realistically approximated by the linear equations;

$$C_{boundi} = P \cdot C_i \cdot k_i$$

and

$$C_{bounds} = P \cdot C_s \cdot k_s$$

where C_{boundi} is the concentration of ionised bound drug, C_{bounds} is the concentration of unionised bound drug, P is the concentration of plasma protein sites, C_i is the concentration of ionised drug, C_s is the concentration of unionised drug and k_i and k_s are constants chosen so as to match experimental results. The bond graph of Figure 3.36 therefore reduces to that of Figure 3.37. Using data given

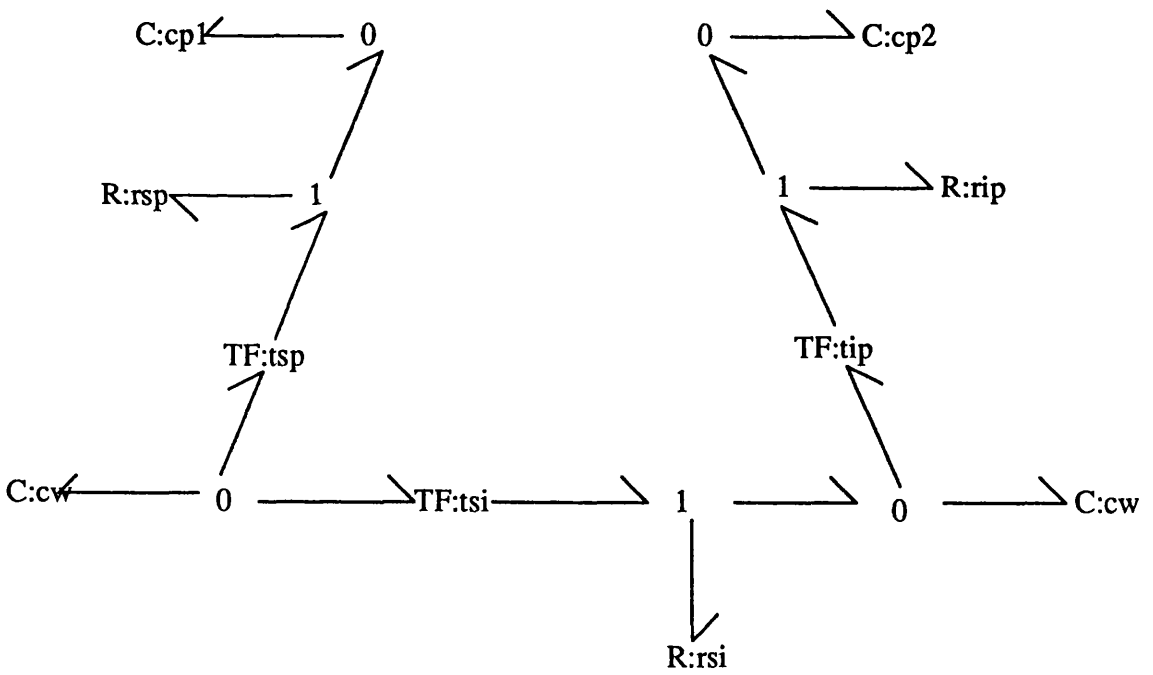

Figure 3.37: The Bond Graph for Fentanyl Equilibration in Plasma

by Higgins [103] gives

P = 747 μmol/kg

k_i = 1.246 x 10^{-3}

k_s = 1.9121 x 10^{-2}

pKa = 7.85

and there are assumed to be 68 grammes of proteins per kilogram of plasma and 915.5 grammes of water per kilogram of plasma.

The Model Transformation Toolbox was used to automatically generate SIMULAB code for the fentanyl model. This code was then used to simulate fentanyl pharmacokinetics in plasma. The simulation could be performed at any pH value and the value of pH could be changed during simulation. Figure 3.38 shows the ratios of free ionised to free unionised concentrations and of bound unionised to free unionised concentrations at a pH of 7.4. Figure 3.39 shows the ratio of bound ionised to free ionised concentrations at a pH of 7.4.

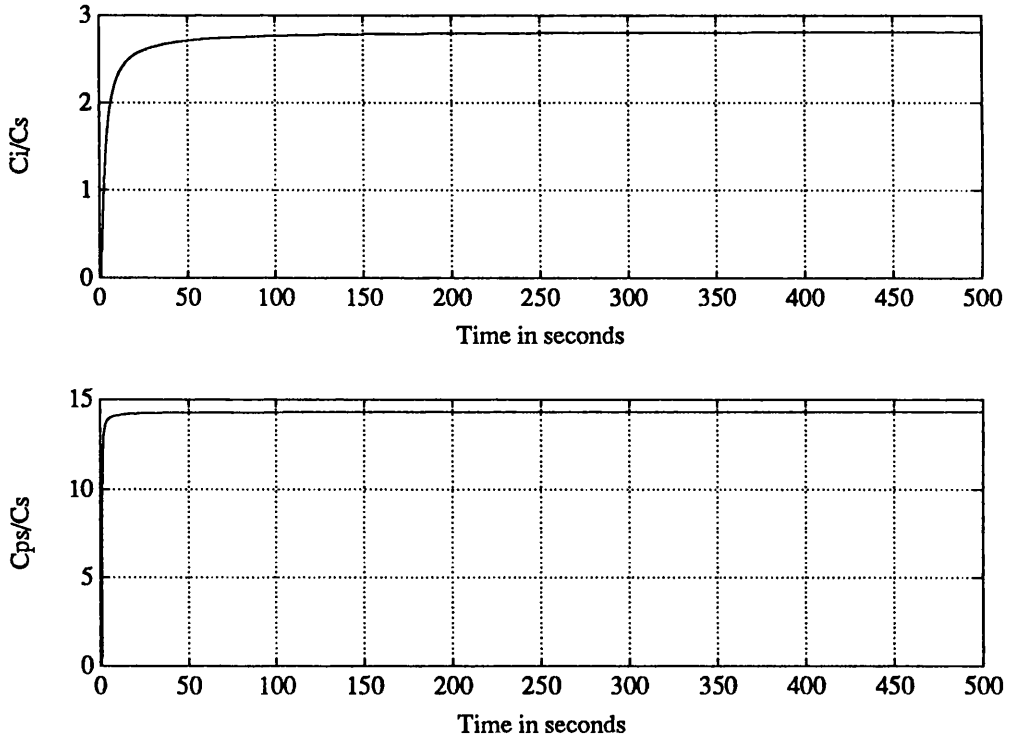

Figure 3.38: Fentanyl Distribution in Plasma at pH 7.4

With a pH of 6.0, the ratio of free ionised to free unionised concentrations

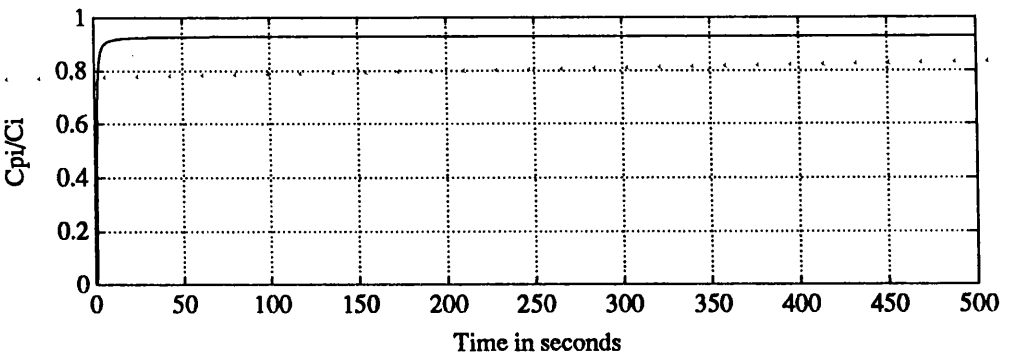

Figure 3.39: Fentanyl Distribution in Plasma at pH 7.4

changes as shown in Figure 3.40. The ratios of bound unionised to free unionised concentrations and bound ionised to free ionised concentrations do not change as shown in Figure 3.40 and 3.41. These results, which have been *automatically* generated following definition of the transformer constitutive relations and construction of the bond graph, are in complete agreement with those presented by Higgins. This clearly demonstrates the utility of the bond graph representation technique.

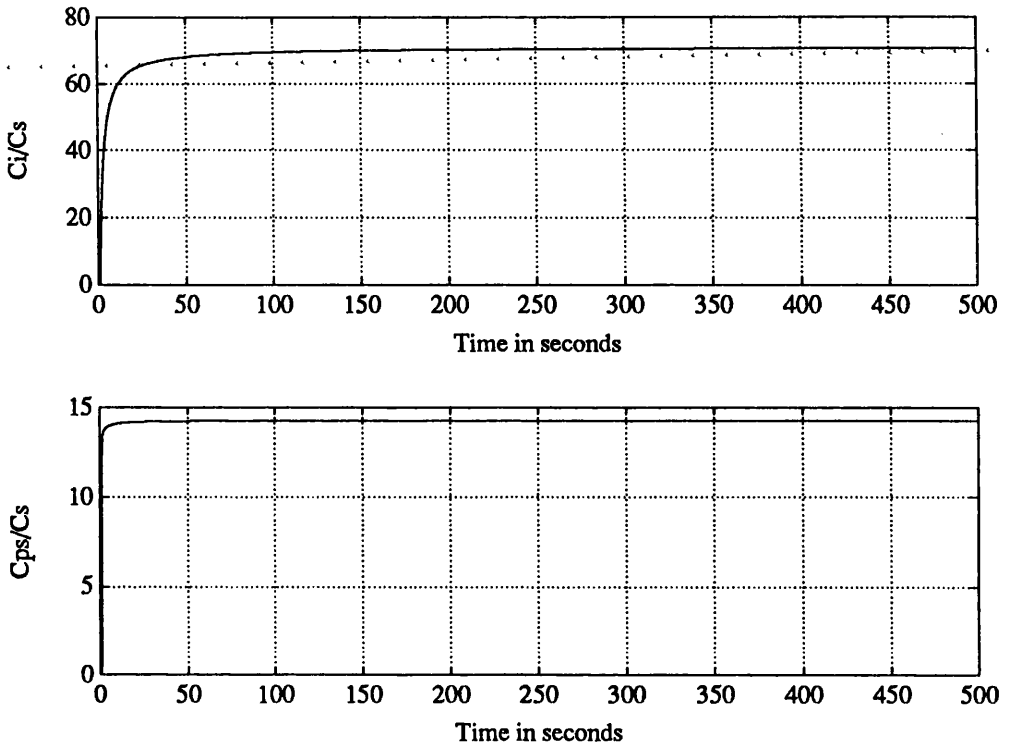

Figure 3.40: Fentanyl Distribution in Plasma at pH 6.0

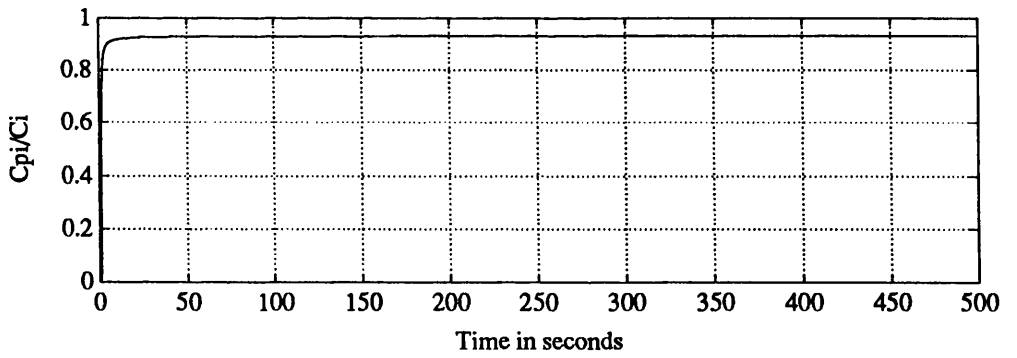

Figure 3.41: Fentanyl Distribution in Plasma at pH 6.0

Chapter 4

A Physiologically–Based Model of Isoflurane Pharmacokinetics

SUMMARY

This chapter derives a physiologically–based model of isoflurane pharmacokinetics using physiological and physico–chemical data available in the literature. The model is represented using a bond graph and the determination of the bond graph component values is described. Using equations automatically generated from the bond graph, the effects of intra–individual and inter–individual physiological changes upon isoflurane pharmacokinetics are investigated via simulation.

4.1 The Structure and Quantification of a Physiologically–Based Model of Isoflurane Pharmacokinetics

Isoflurane is a commonly used inhalational anaesthetic agent. Despite this, physiologically–based models of isoflurane pharmacokinetics have only recently

been developed [116][117]. A physiologically–based model of isoflurane pharmacokinetics has been developed to support work in this thesis. The model is intended to allow:

- representation of the effects of physiological changes within the individual on isoflurane pharmacokinetics and,
- representation of the effects of body composition differences, between individuals, on isoflurane pharmacokinetics.

4.1.1 Model Structure

The structure of the model is schematically represented in Figure 4.1. The model is based upon Mapleson's Model P and therefore incorporates blood pools for the slower tissues. The model groups the tissues of the body into a visceral group, a lean group and a fat group, the lungs are explicitly represented, as is a peripheral shunt. The blood volume is distributed between an arterial blood pool, a venous blood pool, and tissue blood pools. A sample brain tissue compartment has been added to allow investigation of brain tension. The quantification of the model is as follows:

4.1.2 Physiological Quantification

Davis and Mapleson [45] adopted the circulation schematic of Figure 3.12 to allow representation of the pharmacokinetics of both injected and inhaled agents. The main difference between the schematic of the model for injected and inhaled drugs and those of the earlier schematics [40] is the explicit representation of the kidneys and liver and their circulations. This alteration directly supported the representation of the metabolism and excretion of drugs. This model was parameterised using data from the ICRP and was described by Davis and Mapleson [45].

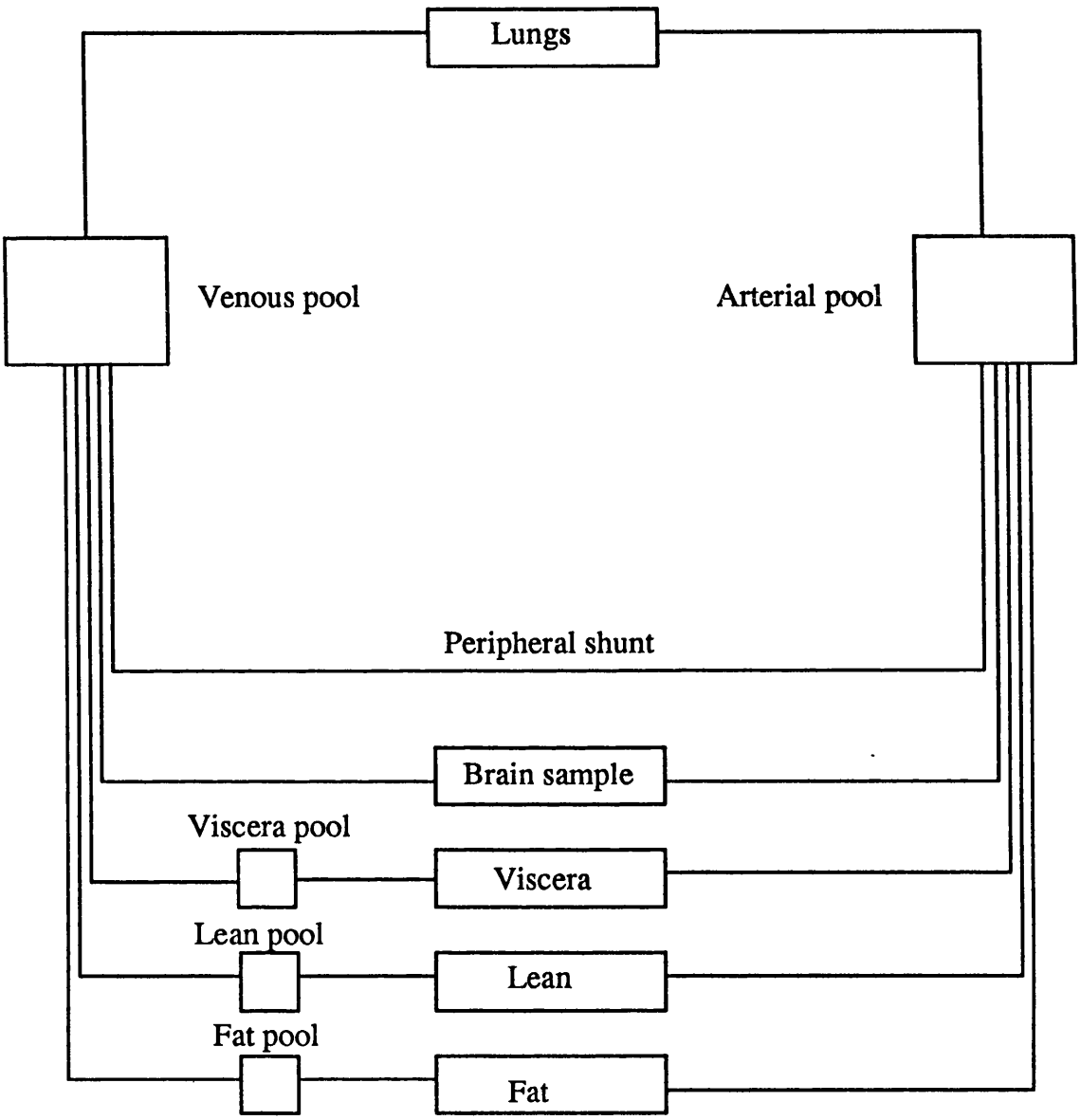

Figure 4.1: Circulation Schematic for the Isoflurane Model

In generating a physiologically–based model of isoflurane pharmacokinetics, there is no requirement for the explicit representation of the liver and kidneys because isoflurane is not significantly metabolised or excreted. In the model developed here, the kidneys, liver and portal circulation are therefore incorporated within the visceral tissue group. This returns the model to the form of Mapleson's Model P [40].

The volumes, blood flows and blood volumes associated with the tissue groups were described by Davis and Mapleson and are summarised in Table 4.1.

Tissue	Volume (ml)	Perfusion (ml/min)	Associated Blood Volume (ml)
Viscera	5067	4012	2117
Lean	34955	1147	2115
Fat	14786	342	631
Shunt	0	979	326
Total	54808	6480	5189

Table 4.1: Summary of Tissue Group Characteristics

The breakdown in blood volume is made in order to accommodate the circulation times for each tissue group. The circulation time for each tissue is taken to be the mean transmit time for the tissue and is given by

$$\text{circulation time} = \frac{\text{associated blood volume}}{\text{blood flow}}$$

Table 4.2 gives the resulting circulation time for each tissue group.

Tissue Group	Circulation Time (secs)
Viscera	31.66
Lean	110.6
Fat	110.7
Shunt	19.98

Table 4.2: Tissue Group Circulation Times

In deriving the "simplified scheme" of their model, Davis and Mapleson calculated the circulation time for the combination of the fastest visceral tissue

to be 18.7 seconds. This time was subtracted from the total circulation time for each tissue group and local blood pools were added to each tissue group with a total circulation time greater than 18.7 seconds. The local tissue pools were sized so as to represent the difference between the total circulation time for the tissue group and the assumed minimum circulation time (18.7 seconds).

In Table 4.2, the fastest total circulation time is that of the peripheral shunt. The circulation time of this tissue group is approximately 20 seconds. Using the same approach as that of Davis and Mapleson, a 'central' circulation time of 20 seconds has been assumed and local pools created to represent the additional local circulation times. The blood pool volumes for each tissue are chosen using the formula:

pool volume = (total circulation time −central circulation time)·tissue blood flow

Table 4.3 gives the resulting local circulation times and blood pool sizes for each of the tissue groups.

Tissue Group	'local' circulation time	blood pool volume (ml)
Shunt	0	0
Viscera	11.66	780
Lean	90.6	1733
Fat	90.7	517
Total		3030

Table 4.3: Local Blood Pool Volumes

Davis and Mapleson state that 25.9% of the total blood volume (5189 ml) is arterial and that 17.2% of the blood in the tissue pools is arterial. The total amount of arterial blood is therefore $0.259 \times 5189 = 1344$ml. The amount of arterial blood within the local tissue pools is $0.172 \times 3030 = 521$ml. The remaining arterial blood volume is therefore $1344 - 521 = 823$ml and this is placed in the arterial blood pool. The remaining blood is therefore $5189 - (3030 + 823) = 1336$ml and this is placed in the venous blood pool. Using these values and those

of Tables 4.1 and 4.3, the physiological characteristics of the model can be summarised as shown in Table 4.4.

Tissue Group	Volume (ml)	Blood Flow (ml/min)	Blood Pool Volume (ml)
Shunt	—	979	0
Viscera	5067	4012	780
Lean	34955	1147	1733
Fat	14786	342	517
Lungs	464	—	0
Arterial Pool	—	—	823
Venous Pool	—	—	1336
Totals		6480	5189

Table 4.4: Summary of Tissue Group Characteristics

Addition of a Brain Sample Compartment

Davis and Mapleson state that the total circulation time for the brain is 20.5 seconds. The model described above assumes a 'central' circulation time, common to all circulations, of 20 seconds. Therefore, a brain sample tissue may be added without further representation of local circulation time. The concept of tissue samples of very small volumes and perfusions was described by Mapleson [40]. Taking the values from those models, a brain sample can be added to the model without significantly altering any behaviour in other tissues, or the blood, but providing brain tension information. A brain sample of volume 0.7 ml (identical to that originally described by Mapleson) has therefore been added to the model. The perfusion of the sample is proportional to that of the whole brain. The brain has a volume of around 1300 ml and receives about 741 ml/min of blood flow. These figures give the the perfusion of the brain sample as $741 \times \frac{0.7}{1300} = 0.4\text{ml/min}$.

4.1.3 Physicochemical Quantification

The physiological quantification of the model provides a basis for the prediction of the behaviour of any agent if appropriate physicochemical data are available. Isoflurane is not significantly metabolised or excreted in humans. Knowledge of the tissue:gas and blood:gas partition coefficients for isoflurane therefore allow quantitative representation of its pharmacokinetics.

Only five distinct sources of data on blood:gas and tissue:gas partition coefficients have been found. Regrettably, there is a wide range of derived partition coefficients. It is difficult to suggest that one set of results should be considered better than the others and the coefficients chosen to provide the physico–chemical parameterisation for this model are therefore the result of arbitration between experimentally derived results in the literature. Table 4.5 summarises the partition coefficients suggested by each source. The partition coefficients for the model were chosen as follows:

Partition Coefficient	[118]	[119]	[116]	[120]	[121]
blood:gas	1.4	1.37	1.5	—	1.4
brain:gas	—	2.26	3.6	2.09	1.9
heart:gas	—	2.64	2.25	2.18	—
liver:gas	—	2.99	3.45	2.34	4.1
kidney:gas	—	—	1.95	1.39	2.1
muscle:gas	—	2.82	2.25	4.40	2.4
fat:gas	68	76.75	94.5	64.2	69
lung:gas	—	—	2.7	—	1.6

Table 4.5: Summary of Isoflurane Partition Coefficient Data

1. Blood:gas Partition Coefficient

   Based upon data from Fiserova–Bergerova et al. [121], Lerman et al.[119] and and Steward et al.[118], a blood:gas partition coefficient of 1.4 has been selected.

2. Brain:gas Partition Coefficient

   The estimates of the brain:gas partition coefficient of Fiserova–Bergerova et al., Yasuda et al.[120] and Lerman et al. each have similar values. That of Lerou et al.[116] is higher. Taking account of the differences, a brain:gas partition coefficient of 2.1 has been assumed.

3. Heart:gas Partition Coefficient

   The estimates of heart:gas partition coefficient are reasonably close in the data given by Yasuda et al., Lerman et al. and Lerou et al. A partition coefficient of 2.3 has therefore been assumed for the heart.

4. Liver:gas Partition Coefficient

   Estimates of liver:gas partition coefficient range from 2.34 (Yasuda et al.) to 4.1 (Fiserova–Bergerova et al.). A partition coefficient of 3.0 has been assumed.

5. Kidney:gas Partition Coefficient

   Estimated kidney:gas partition coefficients occupied a range from 1.39 (Yasuda et al.) to 2.1 (Fiserova–Bergerova et al.). A value of 1.8 has been assumed for use in the model.

6. Muscle:gas Partition Coefficient

   For muscle tissue, the partition coefficient estimates of Yasuda et al. are higher than those of other groups. This was also the case for their muscle:gas partition coefficients for halothane. Notably, the standard deviation quoted by Yasuda et al. was also very large in comparison to that derived by other groups. In recognition of the uncertainty associated with the data from Yasuda et al., a muscle:gas partition coefficient has been derived from primarily considering the data of other groups. The muscle:gas partition coefficient has therefore been chosen as 2.8.

7. Fat:gas Partition Coefficient

   Estimated fat:gas partition coefficients range from 64 (Yasuda et al.) to 94.5 (Lerou et al.). The value of Lerou is significantly higher than those of other authors. A fat:gas partition coefficient of 70 has therefore been assumed.

8. Lung:gas Partition Coefficient

   Lerou et al. and Fiserova–Bergerova et al. are the only sources of lung:gas partition coefficient estimates. Because the figures quoted by Lerou et al. are consistently higher than those of other groups, the estimate of Fiserova–Bergerova has been chosen. The lung:gas partition coefficient is thus assumed to be 1.6.

To ease comparison, the coefficients provided in the literature (Table 4.5) have been listed alongside those selected for use in this model in Table 4.6.

Partition Coefficient	[118]	[119]	[116]	[120]	[121]	New
blood:gas	1.4	1.37	1.5	—	1.4	1.4
brain:gas	—	2.26	3.6	2.09	1.9	2.1
heart:gas	—	2.64	2.25	2.18	—	2.3
liver:gas	—	2.99	3.45	2.34	4.1	3.0
kidney:gas	—	—	1.95	1.39	2.1	1.8
muscle:gas	—	2.82	2.25	4.40	2.4	2.8
fat:gas	68	76.75	94.5	64.2	69	70
lung:gas	—	—	2.7	—	1.6	1.6

Table 4.6: Summary of Isoflurane Partition Coefficient Data

Selection of Partition Coefficients for the Model

The partition coefficient estimates for the tissues derived above result from *in vitro* measurements. Ideally, values for functioning tissue in patients would be available. Steward et al. [122] found that the differences between *in–vivo* and *in–vitro* partition coefficients was small, suggesting that partition coefficients resulting from *in–vitro* experiments are appropriate for the parameterisation of a model.

A further requirement is that a partition coefficient is available for each of the tissue groups in the model i.e. blood, lungs, lean, fat, viscera and brain sample. For these, the value described in the previous section can be used except for the partition coefficient of the visceral tissue group. Allottet al. [123] used *in-vitro* estimates of blood:gas, muscle:gas, fat:gas, lung:gas and brain:gas partition coefficients to provide partition coefficients for the blood, lean, fat, lung and brain components of a physiologically-based model. They then derived a partition coefficient for the visceral tissue group in a weighted summation, according to the tissue masses, of the measured partition coefficients for the brain, heart, kidneys, liver and gut. Steward et al. [124] found partition coefficients for halothane in the dog. They found that the partition coefficient for the gut was greater than those of the heart and kidneys, but less than those of the brain and liver. As an approximation, without any other available information, the partition coefficient of the gut has been assumed to be the same as that of the brain in humans, i.e., 2.1.

The partition coefficient for the visceral tissue group can therefore be calculated as:

$$\lambda_{viscera} = \frac{W_k \times \lambda_k + W_l \times \lambda_l + W_g \times \lambda_g + W_h \times \lambda_h + W_b \times \lambda_b}{W_k + W_l + W_g + W_h + W_b} \tag{4.1}$$

where $\lambda_{viscera}$ is the viscera:gas partition coefficient, W_t symbolises the mass of tissue t, λ_t is its tissue:gas partition coefficient and k,l,g,h and b are subscripts for the kidneys, liver, gut, heart and brain respectively. Therefore, using data from [45] and the partition coefficients derived above,

$$\lambda_{viscera} = \frac{284 \times 1.8 + 1721 \times 3.0 + 1391 \times 2.1 + 316 \times 2.3 + 1339 \times 2.1}{284 + 1721 + 1391 + 316 + 1339} = 2.4023 \tag{4.2}$$

The partition coefficients which are to be used in the model for isoflurane

pharmacokinetics are summarised in Table 4.7.

Tissue	Tissue:gas Partition Coefficient
Blood	1.4
Lungs	1.6
Viscera	2.4
Lean	2.8
Fat	70
Brain	2.1

Table 4.7: Model Partition Coefficients

4.2 Bond Graph Representation of the Isoflurane Model

The schematic for the isoflurane model (Figure 4.1) illustrates the allocation of tissue and blood volumes in the model. The exact numerical specification of each volume and flow was described earlier. In order to simulate, or further analyse the model, it is desirable to represent it in a form which assists the production of system equations, or other forms of the model. The bond graph representation of physiologically–based models was introduced earlier in Chapter 3. This technique has been used to represent the isoflurane model described above. The bond graph for the isoflurane model is shown in Figure 4.2. In the bond graph, ventilation and perfusions are regarded as continuous, steady flows so as to be consistent with the approach of Mapleson. The bond graph, however, allows derivation of *continuous time* equations for the model whereas Mapleson's models adopted discrete time equations to ease computation.

The bond graph for the model has a lot in common with the original electrical analogue of Mapleson [37] [38] and Figure 3.9. In the analogue, flow into the lung capacitors is dependent upon the inspired tension, alveolar tension, and a resistor which has a value determined by alveolar ventilation. Flow from the lung

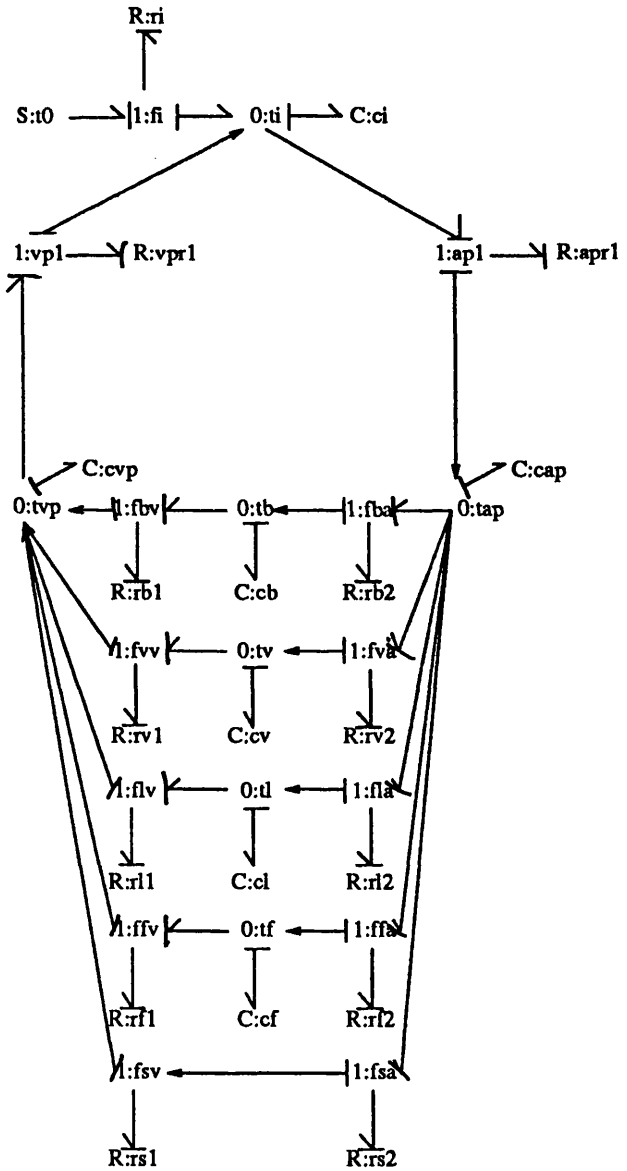

Figure 4.2: The Bond Graph Representation of the Isoflurane Model

capacitors to the tissues depends upon the alveolar tension, the tissue tension, and a resistor which has a value dependent upon the tissue volume, tissue perfusion and the tissue:gas partition coefficient. Of course, Mapleson's analogue made no distinction between arterial and venous circulation but this was incorporated in later models [40].

4.2.1 Determination of Component Values

The bond graph representation of the model (Figure 4.2) adopts anaesthetic tension as the effort variable and mass flow of anaesthetic drug as the flow variable. This is consistent with Mapleson's original selections is his electrical analogue [38]. In consideration of these choices, the values of each component in the bond graph are as follows.

1. Inspiration

   The models of Mapleson [40] and Davis and Mapleson [45] have assumed an alveolar minute ventilation of 4 l/min for a 70 kg man. If a tension, t_o, of an agent is present in the inspired gas stream, then the flow of agent into the patient, f_i is $4 \times t_o$ l/min assuming the alveolar gas concentration to be zero. If the concentration in alveolar gas is t_i then the net flow of drug, f_i into the alveolar gas is

   $$f_i = 4 \times (t_o - t_i)\text{l/min} = \frac{1}{15} \times (t_o - t_i)\text{l/sec.}$$

   This relationship is represented using the resistance labelled R:ri on the bond graph. The resistor is assumed to be linear and has value calculated as

   $$R = \frac{\text{effort}}{\text{flow}} = \frac{(t_o - t_i)}{f_i} = 15. \tag{4.3}$$

2. Tissue or Pool Capacities

   The variation of agent solubility between tissues allows different concentrations to be established in each tissue at equilibrium. The capacity of a tissue

for drug is related to its partition coefficient by

$$C_t = \lambda_t \times V_t \tag{4.4}$$

where C_t is the tissue capacity, λ_t is its partition coefficient and V_t is its volume. In the model, equilibration in the lung involves the equilibration of alveolar gas and lung tissue. Because the partition coefficient of gas is unity, the capacity of the lung is

$$C_i = V_A + \lambda_{lung} \times V_{lung}$$

where V_A is the volume of alveolar gas, λ_{lung} is the lung tissue:gas partition coefficient and V_{lung} is the volume of lung tissue. Using data from Davis and Mapleson [45] and the partition coefficients derived above,

$$C_i = 2.5 + 1.6 \times 0.464 = 3.24$$

For a blood pool, the capacity is simply

$$C_{pool} = \lambda_{blood} \times V_{pool}$$

The arterial pool therefore has capacity

$$C_{cap} = \lambda_{blood} \times V_{ap} = 1.4 \times 0.823 = 1.15$$

and the venous pool has capacity

$$C_{cvp} = \lambda_{blood} \times V_{vp} = 1.4 \times 1.336 = 1.8704.$$

When a tissue group has a blood pool associated with it, the combination of the pool in series with the tissue may be approximated by combining their capacities. The tension in the combined capacity does not therefore correspond exactly to the tension in the tissue only, but the use of a sample compartment can avoid that problem. In this model, the viscera, lean and

fat tissue groups have associated blood pools. For the combination of a tissue t with volume V_t and partition coefficient λ_t with an associated blood pool of volume V_{pt} and blood:gas partition coefficient λ_{blood}, the combined capacity is given by:

$$C_t = \lambda_t \times V_t + \lambda_{blood} \times V_{pt}$$

The capacities for the viscera, lean and fat tissue groups are therefore calculated as

$$C_v = \lambda_v \times V_v + \lambda_{blood} \times V_{vp} = 2.4 \times 5.067 + 1.4 \times 0.780 = 13.25$$

$$C_l = \lambda_l \times V_l + \lambda_{blood} \times V_{lp} = 2.8 \times 34.955 + 1.4 \times 1.733 = 100.30$$

$$C_f = \lambda_f \times V_f + \lambda_{blood} \times V_{fp} = 70 \times 14.786 + 1.4 \times 0.517 = 1035.74$$

The only remaining tissue capacity is that of the brain sample tissue, it is given by

$$C_b = \lambda_b \times V_b = 2.1 \times 0.0007 = 0.00147$$

3. Flow between the Lungs and the Arterial and Venous Pools

   The common effort junction labelled 0:ti in Figure 4.2 has the tension of the lungs as its effort variable. Blood flows into the lungs from the large veins at mixed venous tension and this is represented in the bond graph by a mass flow of drug, in one direction, from the venous pool to the lungs. Blood flows from the lungs, at arterial tension, into the arterial blood pool. This flow is also represented by a mass flow, in one direction, between the lungs and the arterial pool.

   (a) Mass Flow from Venous Pool to Lung Capacitance

   The mass flow from the venous pool to the lungs depends upon the venous pool tension. The mass flow of drug is given by

$$\begin{aligned} \text{mass flow} &= \text{blood flow} \times \text{drug concentration in the blood} \\ &= \text{blood flow} \times \lambda_{blood} \times \text{drug tension} \end{aligned}$$

The resistance value R:vpr1 is therefore chosen to be

$$R : vpr1 = \frac{\text{tension}}{\text{mass flow}} = \frac{1}{\text{blood flow} \times \lambda_{blood}}$$

Given that the whole cardiac output (6480 ml/min) flows through the venous pool, the value is therefore

$$R : vpr1 = \frac{1}{\frac{6480}{60} \times 1.4} = 6.61$$

Note that the use of a signal between the common flow junction 1:vpl and the common effort junction 0:ti ensures that mass flow between the venous pool and the lungs depends only upon the tension in the venous pool.

(b) Mass Flow from the Lung Capacitance to the Arterial Pool

By analogy with the mass flow from the venous pool to the lungs, the resistor value R:apr1 is similarly defined to be

$$R : apr1 = \frac{1}{\frac{6480}{60} \times 1.4} = 6.61$$

4. Mass Flow between the Arterial Pool and Tissues and Tissues and the Venous Pool

The representation of circulation dictates that the mass flow of drug between the arterial pool and each tissue depends only upon the tension of the arterial pool. Again, this has been represented using signals on the bond graph (Figure 4.2). For a tissue t, the mass flow of drug into it depends upon its blood flow and the drug concentration of the blood. If the tissue receives a fraction, k_t, of the cardiac output then the mass flow of drug into t is given by

$$\text{mass flow into t} = k_t \times \text{cardiac output} \times \lambda_{blood} \times \text{blood tension}$$

The resistances between the arterial pool and the tissues are therefore defined using the form:

$$R = \frac{\text{tension}}{\text{mass flow}} = \frac{1}{k_t \times \text{cardiac output} \times \lambda_{blood}}$$

Using blood flow data from Table 4.1, the resistances for the arterial sides of each tissue are

$$R{:}rb2 = 107142$$

$$R{:}rv2 = 10.68$$

$$R{:}rl2 = 37.36$$

$$R{:}rf2 = 125.31$$

$$R{:}rs2 = 43.77$$

By analogy, the resistances between the tissues and the venous pool are defined in the same way. Hence,

$$R{:}rb1 = R{:}rb2$$

$$R{:}rv1 = R{:}rv2$$

$$R{:}rl1 = R{:}rl2$$

$$R{:}rf1 = R{:}rf2$$

$$R{:}rs1 = R{:}rs2$$

The use of signals between the tissue common effort junctions and the venous pool ensures that mass transfers are only from the tissues to the pool.

4.2.2 Generation of Other Model Forms

The representation of the model using bond graph notation allows automatic generation of symbolic and numerical model forms. Using a public domain figure editor, on a Sun workstation, the bond graph shown in Figure 4.2 was drawn. The Model Transformation Toolbox (MTT) toolbox [115] was then used to generate other model forms. MTT can produce symbolic and numerical transfer functions, state–space matrices and other model forms. Significantly, MTT is able to produce state–space matrices for a bond graph which can be read into MATLAB. MATLAB can then be used to simulate and analyse the model's behaviour. In using MTT, it is possible to generate entirely symbolic representations of systems, or to make partially numeric representations, or to produce fully numeric output. This allows characteristics of the model e.g., cardiac output or ventilation to be retained as a symbol in the generation of state–space matrices. Simulation of the model for varying parameters can therefore be achieved within the simulation environment.

4.3 Simulating the Effects of Physiologic Changes on Inhaled Agent Pharmacokinetics

The use of a physiologically–based model allows direct investigation of the interactions between physiological quantities and pharmacokinetics. Two types of physiological change are considered here:

1. Intra–individual Changes

   These are short–term variations in the physiological performance of the individual.

2. Inter–individual Changes

   These result from the inate differences between people.

4.3.1 Intra–individual Changes I. Ventilation

Ventilation or; more specifically, alveolar ventilation provides the flow of inhaled agent into the body. As ventilation increases, so too does the amount of drug brought to equilibrate with alveolar blood. Conversely, if alveolar ventilation decreases, the amount of drug being brought into the lungs to equilibrate decreases.

In consideration of the bond graph of the isoflurane model (Figure 4.2) there is only one component which has a value directly related to the alveolar ventilation. The component is the resistor labelled R:ri which is related to the alveolar ventilation as described by Equation 4.3. The effects of changes in ventilation can therefore be investigated by modulating the value of this resistor. Figure 4.3 shows the simulated arterial and brain tensions for alveolar ventilations of 3, 4 and 5 litres per minute with all other variables assuming the values described in the previous sections.

It is apparent that changes in ventilation affect the *rate* of increase of both the arterial and brain tensions, and change the tension at which the tensions equilibrate. While it is not possible to measure alveolar ventilation, the total minute ventilation can be measured and from this an estimate of alveolar ventilation can be derived for the individual. It should be noted that even though the simulated alveolar ventilations deviate by $\pm 25\%$ from the assumed normal ventilation of 4 litres per minute, the arterial tension deviates by only about $\pm 10\%$.

4.3.2 Intra–individual Changes II. Cardiac Output

The effective circulation of blood around the body is required to deliver drugs to each tissue. In the bond graph (Figure 4.2), all resistors except R:ri depend upon the blood flow to the associated tissue group or blood pool. Clearly, a reduction in cardiac output dictates that the blood flow in some of the tissues

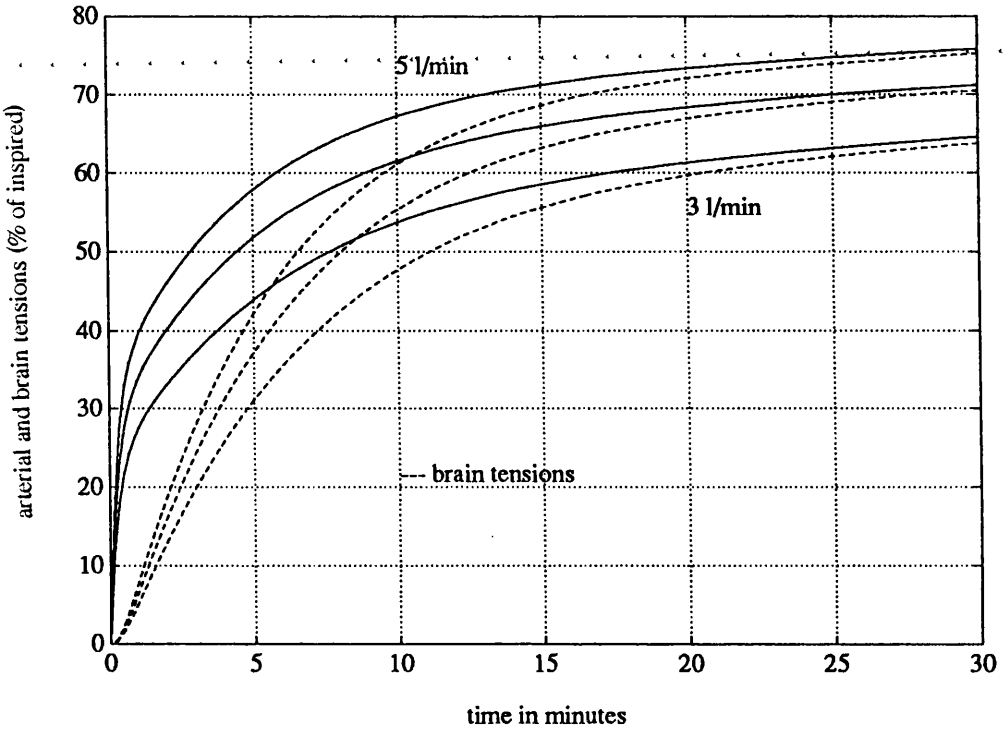

Figure 4.3: The Effects of Alveolar Ventilation on Brain and Arterial Tensions

must also reduce. In order to simulate the effects of cardiac output changes upon the pharmacokinetics of isoflurane, the following steps were taken.

1. It was assumed that at each cardiac output to be simulated, that the blood flow in each tissue group was proportional to the cardiac output.

2. A range of cardiac output values from 4 litres per minute to 10 litres per minute was chosen as a suitable range.

3. The alveolar and brain tension timecourses of the simulated isoflurane model were recorded for a step input of inspired concentration.

The results of the simulation for three cardiac output values are shown in Figure 4.4. It can be seen that as the cardiac output increases, the arterial tension decreases and therefore, tissue tensions are also somewhat lower. It is also apparent that the rate of rise of tissue tensions increases with cardiac output.

Qualitatively, for constant alveolar ventilation, larger cardiac outputs cause the alveolar gas to equilibrate with a larger blood volume. The end-tidal and hence arterial tensions are therefore lower although the uptake of the drug will actually be greater. While the arterial tension may well be lower with a higher cardiac output, the equilibration of the tissues with this tension is quicker. This is directly due to the perfusion limited nature of inhaled agent distribution. Obviously, as cardiac output increases, the blood flow to each tissue increases allowing a greater mass flow of drug to enter the tissue and therefore speeding up equilibration. The arterial and brain tensions for various cardiac output values (4.0 l/min, 6.5 l/min and 10.0 l/min) shown in Figure 4.4 assume a constant alveolar ventilation of 4.0 litres per minute.

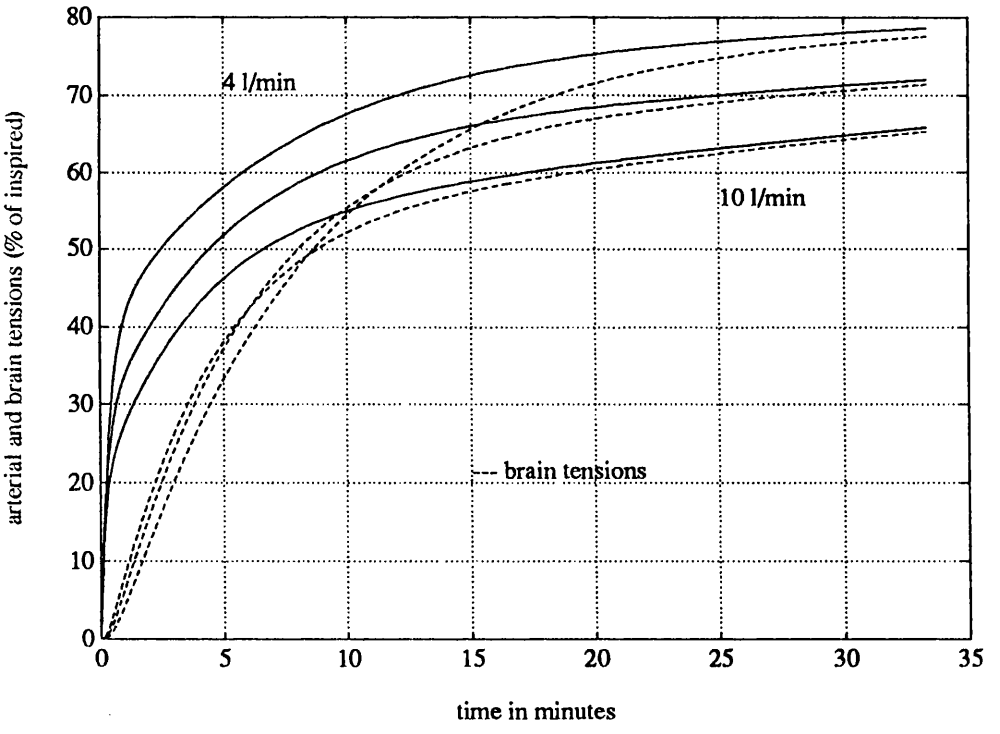

Figure 4.4: The Effects of Cardiac Output on Brain and Arterial Tensions

4.3.3 Comparison of the Model's Predictions with Experimental Results

The work of Frei et al. [125] investigated the effects of ventilatory and circulatory changes on the pharmacokinetics of isoflurane and halothane in the dog. During hyperventilation, the authors reported an increase in the ratio of end-tidal anaesthetic concentration to inspired concentration. For a constant inspired anaesthetic concentration, this implies that the end-tidal concentration increases with ventilation. The simulation results presented in Figure 4.3 are therefore in agreement with this experimental finding.

Frei et al. also reported that an increase in cardiac output caused a decrease in the ratio of end-tidal concentration to inspired concentration of the anaesthetic agent. For a constant inspired concentration, this would result in lower end-tidal concentrations as cardiac output increased. The simulation results presented in Figure 4.4 are therefore also in agreement with the experimental result.

The work of Frei et al. has provided experimental evidence of the effects of ventilatory and circulatory changes on the pharmacokinetics of isoflurane in the dog. These results are in agreement with the results predicted by simulation of the physiologically-based model derived in this chapter. The experimental work therefore provides validation of the model's representation of intra-individual changes and their effects on pharmacokinetics.

4.3.4 Inter-individual Changes: Body Composition

Within the population, physiologic differences can result from age and disease but can also be a result of natural variation. The standard man data used by Mapleson [40] and Davis and Mapleson [45] describe, in specific detail, the body composition of one individual. Patients are somewhat different from the standard man in terms of health but also in terms of physiology. Some pharmacokinetic changes are a

product of changes in body composition. Typically, it would be expected that the pharmacokinetics of an inhaled agent in an elite marathon runner would be different from those of an obese, sedentary individual even if they were the same age and sex.

In order to investigate the effects of body composition changes on pharmacokinetics, a version of the standard man has been adopted as a basis but the amount of tissue in the lean and fat tissue groups has been made variable to simulate different compositions.

1. Simulation Model Approximations and Assumptions.

   It has been assumed, for the purposes of this investigation, that common to all simulated individuals is a visceral tissue group of the same size and that the lung and peripheral shunt components of the model are also common. Around these basic common features, variable amounts of lean and fat tissue group material are added. This is obviously an approximation to reality but is necessary in the absence of any quantitative information on the masses and volume of tissues in individuals of varying body composition. Because each of these common components equilibrates very quickly with arterial blood, their uptake after the first 15 minutes or so of an anaesthetic is minimal and so will be their impact upon the arterial and brain tensions. A less valid approximation made here is that alveolar ventilation will be constant in the range of individuals simulated. Qualitatively, larger bodies provide larger metabolic demands at rest than smaller bodies. It would seem reasonable therefore to increase alveolar ventilation according to some parameter related to body size. While this is straightforward, its omission allows observation of the effects of changes in body composition alone.

   In consideration of physiologic ranges in body composition, it is unlikely that an individual should have less body fat than about 5% of body mass, or an amount of muscle less than about 15% of body mass. While observing

5% body fat simultaneously with 15% muscle mass is not likely (5% body fat might be associated with an elite endurance athlete and greater muscle mass is therefore expected), the combination provides a minimum point from which further muscle and fat may be added. The model therefore consists of a core person with a normally perfused viscera, lungs and peripheral shunt, and a minimum amount of muscle and fat.

The maximum body fat is perhaps 60% of body mass in an obese, immobile individual. The maximum muscle may approach 60% in a body builder. The simultaneous combination of 50% fat and 60% muscle is not possible but these may serve as upper limits for physiological ranges.

The lean group of the standard man represents about 36.7 kg (52%) of the 70 kg body mass. The fat group is about 13.7kg (20%). Given the assumed minima and maxima discussed above, ranges of fat group masses between 5 kg and 30 kg and ranges of lean group mass between 20 kg and 60 kg were selected for simulation.

2. Blood Volumes and Cardiac Output.

The addition of lean and fat tissue to the model, without changing blood volume or cardiac output causes pharmacokinetic changes alone due to the relatively reduced perfusion of each tissue. In an attempt to present a realistic representation of the addition of lean and fat tissue, any tissue added has been accompanied by:

(a) An increase in cardiac output.

(b) An increase in blood volume.

The model's cardiac output is increased to ensure that the added tissue is perfused to the same extent as the existing tissue of the same type. The

blood volume is increased by adding blood to the blood pools of the lean and fat groups. This has been done in order to keep the circulation times of these tissues constant.

3. Results.

Simulations were performed to investigate the effects of

(a) changing the amount of fat with a constant lean group mass,

(b) changing the amount of muscle with constant fat group mass, and

(c) changing the amounts of both muscle and fat.

Figure 4.5 shows the arterial and brain tension curves resulting from simulation of the standard man with varying quantities of fat. The fat compartment varied in mass between 5 kg and 30 kg while the lean group mass remained constant at 40 kg. It is clear that increasing amounts of fat tissue cause an increased uptake of drug into that tissue and results in lower arterial and brain tensions.

Figure 4.6 shows the arterial and brain tensions resulting from simulation of the standard man with muscle mass between 20 kg and 60 kg with a constant fat group mass of 12.5 kg. It is clear from the graphs that as muscle mass increases, the increased uptake of drug into the muscle causes lower arterial and brain tensions.

Figure 4.7 shows the simulated arterial and brain tensions for the complete range of lean group and fat group masses described earlier. The figure contains three sets of curves; one for a simulation with 5kg fat and 20 kg muscle, one with 30kg fat and 60 kg muscle and one for the standard man (12.5 kg fat, 40 kg muscle). These curves define the range of pharmacokinetic behaviour resulting from physiologic changes.

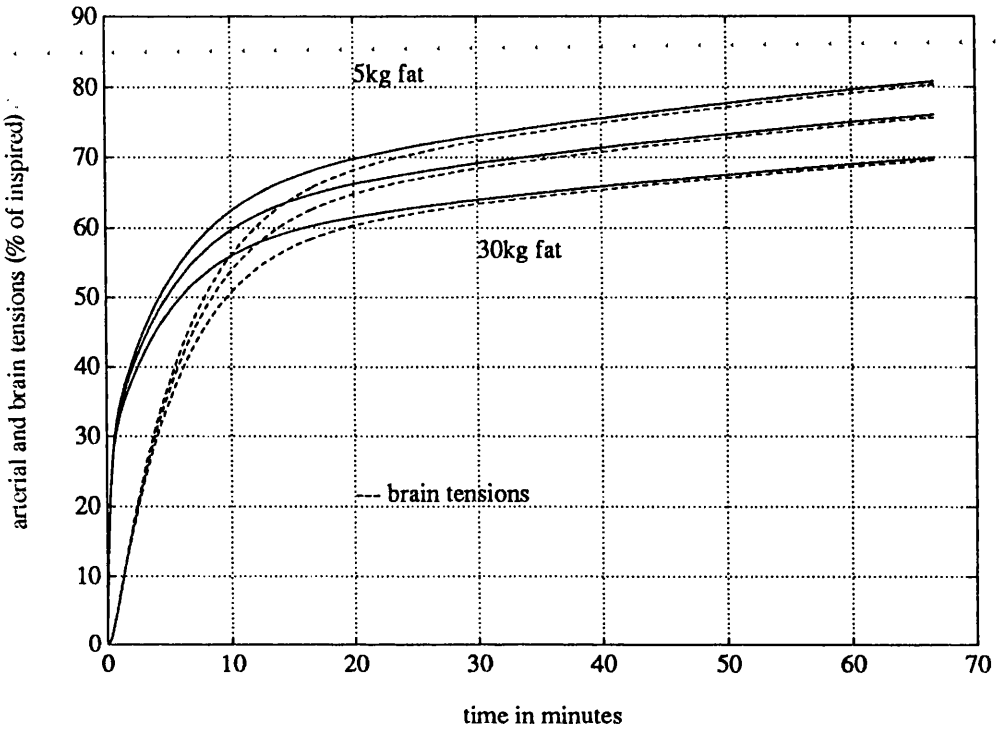

Figure 4.5: The Effects of Fat Mass on Brain and Arterial Tensions

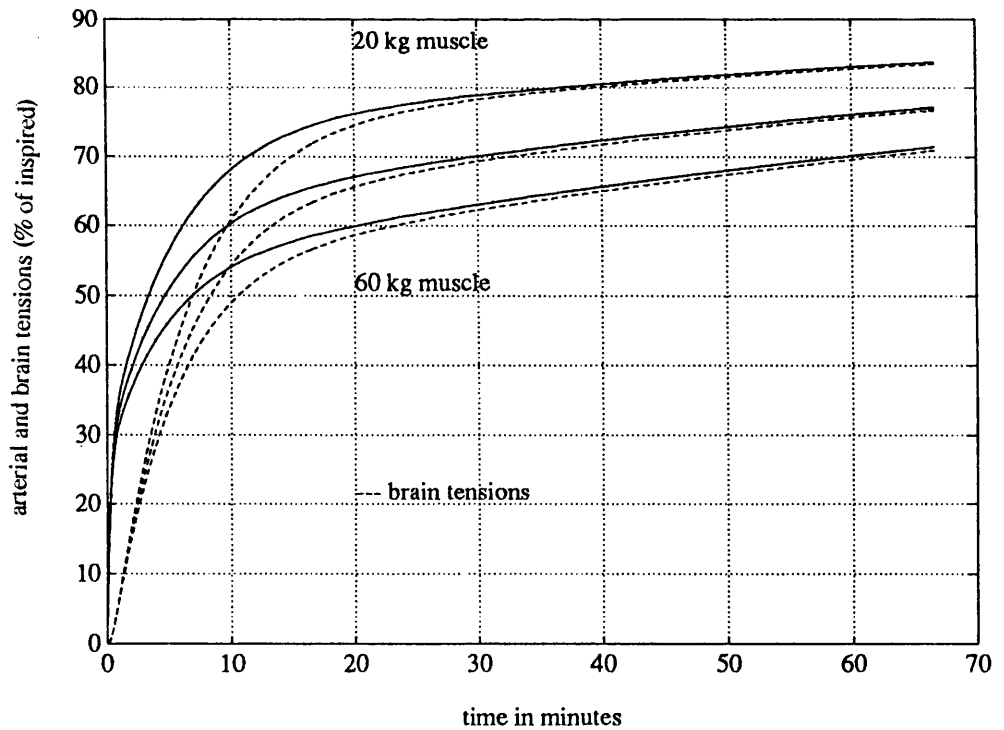

Figure 4.6: The Effects of Muscle Mass on Brain and Arterial Tensions

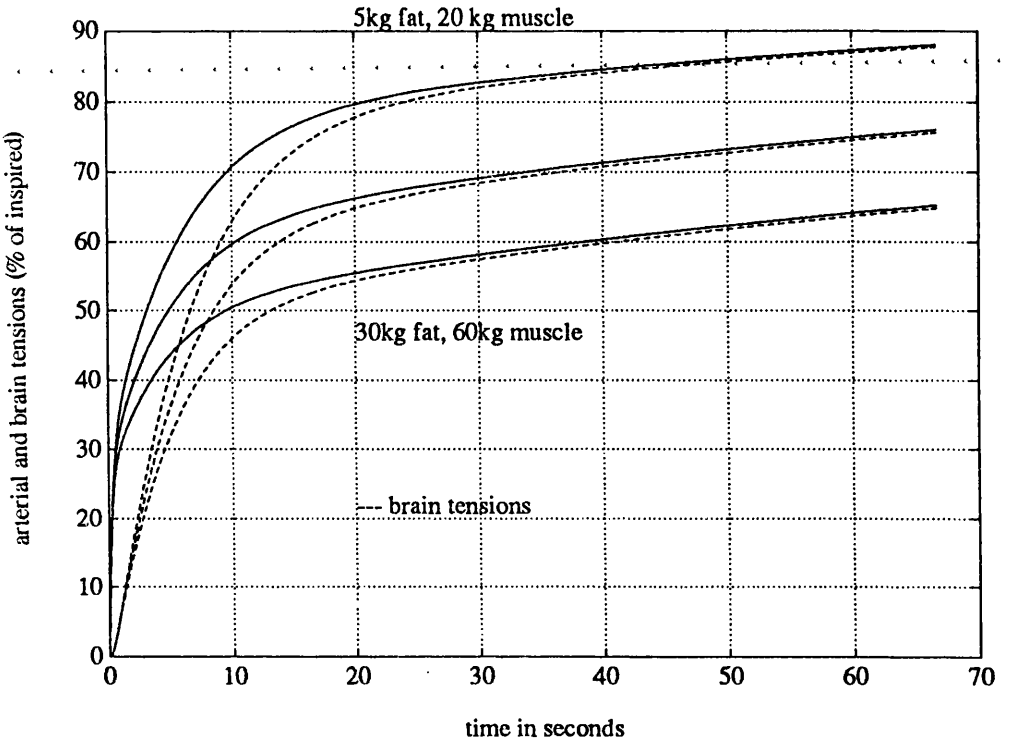

Figure 4.7: The Effects of Body Composition on Brain and Arterial Tensions

It has been demonstrated that physiological changes cause changes in the pharmacokinetics of inhaled drugs in individuals. These pharmacokinetic changes alter both the rate of tissue equilibration and the rate of arterial blood equilibration with the inspired concentration. As an illustration of the comparative effects of body composition upon pharmacokinetics, Figures 4.8 and 4.9 show the brain tension 30 minutes after a step change in inspired concentration from 0%. After 30 minutes, the faster tissues (visceral group) have practically completely equilibrated with arterial blood but the lean and fat groups have significant uptake.

The effect of changes in muscle mass is clearly greater than that of fat mass in altering the equilibration of arterial blood. Despite this, small changes in muscle mass, or fat mass, do not have large effects upon the pharmacokinetic properties. As an example, assuming a fat mass of 12.5 kg (Figure 4.9 middle curve), and a muscle mass of 40 kg, changes in the muscle mass of $\pm 10\%$

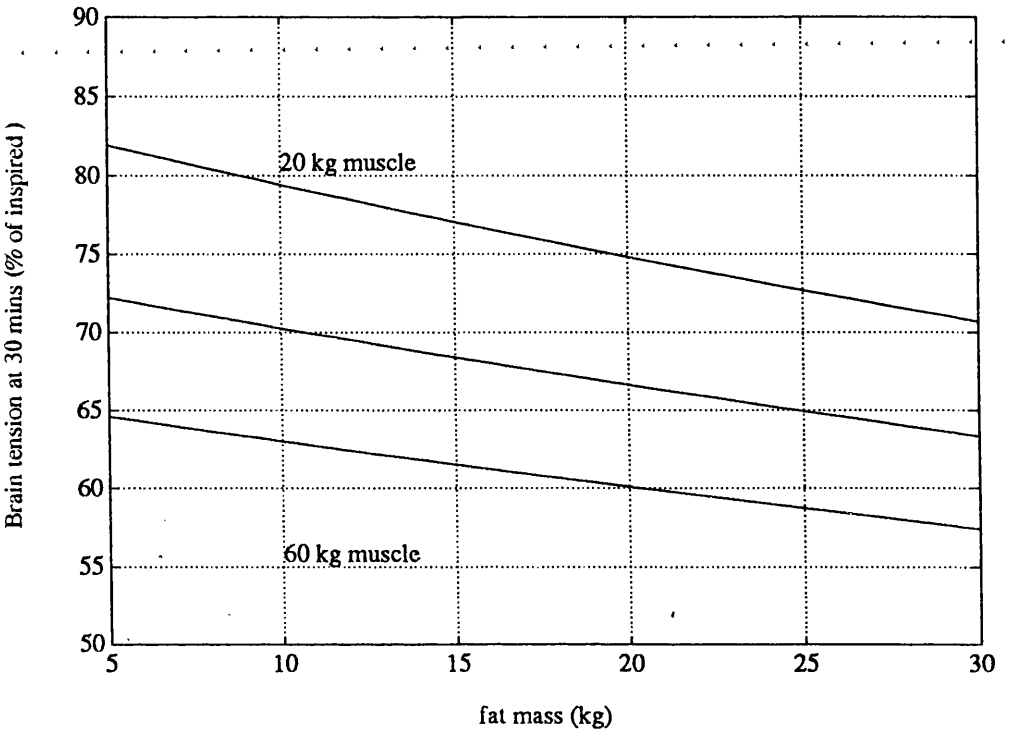

Figure 4.8: Brain Tensions after 30 minutes for different body compositions

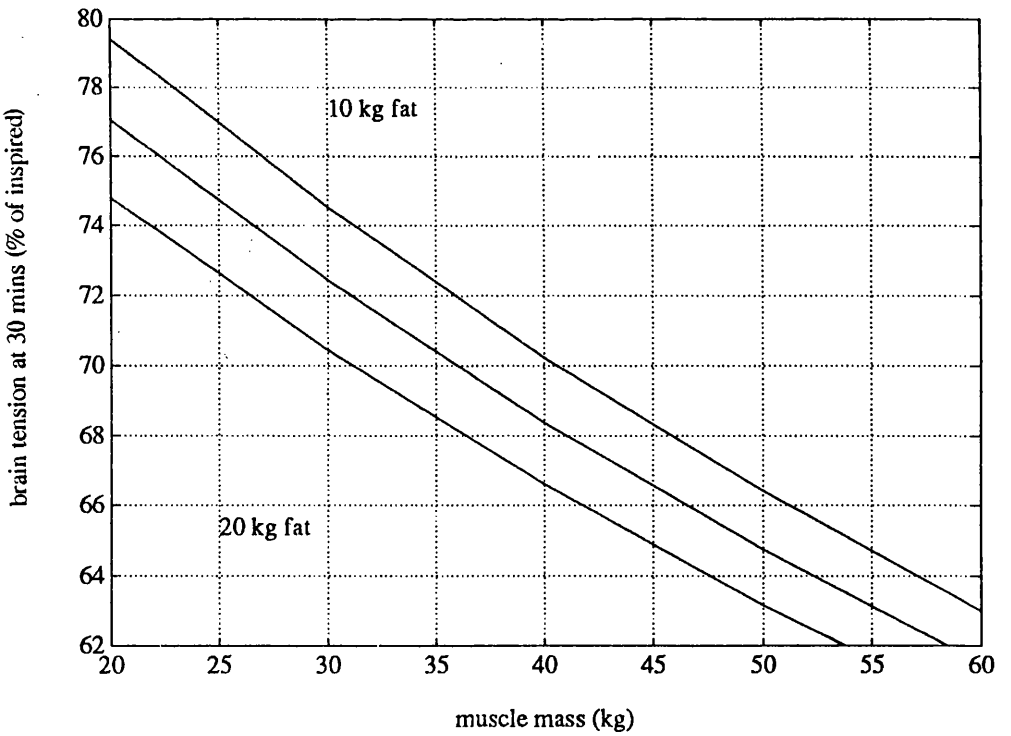

Figure 4.9: Brain Tensions after 30 minutes for different body compositions

cause changes in the brain tension at 30 minutes of only ±2.5%.

Chapter 5

Model–Based Estimation of Tissue Tensions

SUMMARY

This chapter introduces an estimation scheme intended to provide estimates of tissue anaesthetic tensions. The scheme is based upon a physiologically–based model and a scheme for matching the model to the patient using only simple, routinely applicable measurements is proposed. The estimation scheme is described and its performance in both continuous–time and discrete–time with matched and mismatched models are illustrated by simulation. Finally, some experimental results from prototype application of the scheme in the operating theatre during anaesthesia are presented.

The structure of the physiologically–based model described in Chapter 4 allows for representation of both individual body composition and of physiologic changes such as changes in cardiac output. Assuming that sufficient data can be provided, or measurements made, such a model can be matched to an individual person. Applying the inspired anaesthetic tension of a patient undergoing surgery to a model of the pharmacokinetics of the agent, matched to the patient,

would therefore allow tissue anaesthetic tensions to be estimated for the patient. Knowledge of the tissue anaesthetic tensions would allow quantitative information to be available at all times during an anaesthetic. Such information would be useful during induction and recovery but also during maintenance of general anaesthesia.

When considering the automatic control of anaesthesia, Chilcoat, Lunn and Mapleson [79] decided that "in any one individual, a closer correlate of depth of anaesthesia is brain tension." If this is the case, an estimate of brain tension could form the basis of a controller for anaesthetic depth. This was the approach developed by Chilcoat, Lunn and Mapleson as described in [79]. In this work, a physiologically-based model of halothane pharmacokinetics was matched to a dog and the model's brain tension was used to determine the required halothane doseage. The matching of the model to the patient has three phases;

1. The matching of the tissue masses and volumes of the model and its blood:gas partition coefficient. This phase occurs once only.

2. The update, every 10 seconds of the model using estimates of alveolar ventilation and cardiac output.

3. The measurement, every 30 minutes, of arterial tension and the subsequent adjustment of the model's cardiac output so as to match the model's arterial tension with the measured value.

The only drawback in this scheme is the requirement for measurement of arterial tension. The following sections describe a procedure which provides an estimate of tissue tensions in a patient undergoing surgery. This scheme requires only non-invasive measurements in order to function.

5.1 Matching the Model to the Patient

Matching a physiologically-based model to a patient ideally requires;

1. estimation or measurement of tissue masses, volumes and perfusions
2. estimation or measurement of tissue:gas and blood:gas partition coefficients
3. estimation or measurement of alveolar ventilation
4. estimation or measurement of cardiac output.

The estimation of tissue partition coefficients requires invasive measurements and is therefore impractical. As an approximation, the partition coefficients derived for the isoflurane model and listed in Table 4.7 will be assumed for all individuals. The measurement of cardiac output is not routinely applied and is generally invasive. Such a measurement will not be pursued. The scheme developed to estimate tissue tensions therefore requires the following steps to match the model;

1. estimation of tissue masses, volumes and perfusions
2. estimation of alveolar ventilation
3. estimation of cardiac output

5.1.1 Estimation of Tissue Masses, Volumes and Perfusions

In matching their pharmacokinetic model for the dog, Allott, Steward and Mapleson [123] actually measured the masses of the main organs and estimated partition coefficients so as to produce a 'standard' dog. The standard dog was used in their later work [79] to provide individual parameterisation for each dog. As a first approximation, it is conceivable that the 'standard man' such as that

detailed by Davis and Mapleson [45] could be simply scaled to an individual patient, on the basis of body mass, to produce tissue masses, volumes, perfusions, blood pools and a cardiac output for a matched model. Unfortunately, the range of body composition in humans is extensive. Furthermore, there are fundamental differences between the body composition of men and that of women. This makes straightforward scaling of the standard man's proportions to a patient's body mass inadvisable.

The non–invasive assessment of body composition in humans generally assumes the body to be composed of two compartments: the body fat and the fat–free mass [126]. The body fat is assumed to have a constant density of around 0.90 kg/l and and the fat–free compartment compartment is assumed to have density of around 1.10 kg/l. Body fat contains no potassium or water. The fat–free mass contains both potassium and water. These characteristics allow estimates of the masses or fractions of both compartments to be made by measuring total body potassium, total body water or body density.

The measurement of total body potassium and total body water requires laboratory analysis and special preparations. The measurement of body density can be achieved using underwater weighing (see Durnin and Rahaman [127] for details) but this is not routinely applicable.

The measurement of skinfold thickness and body density has been used to derive tables of percentage body fat versus skinfold thickness for different age classes. This approach has been described by Durnin and Womersley [126]. In producing estimates of percentage fat from skinfolds, these workers measured body density by underwater weighing. Assuming that the body is composed of two compartments of different density d_1 and d_2, the fraction of body weight made up by material 1, w_1 is related to the total body density, D by

$$w_1 = \frac{1}{D} \cdot \frac{d_1 \cdot d_2}{(d_2 - d_1)} - \frac{d_1}{(d_2 - d_1)}$$

This equation is derived by Brozek et al. [128]. This fraction was then used to

derive regression equations for use in tables relating the skinfold thickness to fat percentage. This approach is limited by the assumption of constant density in the body fat and fat-free compartments. As described by Durnin and Womersley [126], this has greatest effect in individuals with very low or very high proportions of bone in their fat-free mass.

Accepting these limitations, it is apparent that the measurement of skinfolds can offer a simple and effective means of assessing the body composition of an individual. The technique requires four measurements using skinfold calipers, no laboratory analysis and the results are drawn from standard tables.

The scheme proposed for matching a physiologically-based model to a patient is illustrated in Figure 5.1. The scheme requires only the input of the patient's mass and percentage fat.

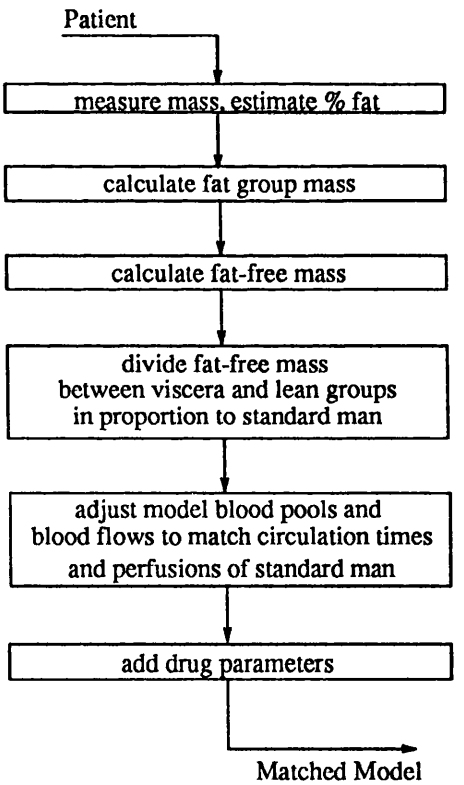

Figure 5.1: Schematic of the Model Matching Scheme

This scheme has been implemented for use with the on-line estimator and takes the patient's sex, mass and percentage body fat as arguments. If the percentage fat

is unknown, the program assumes a value dependent upon the sex of the patient. 15% body fat is assumed for a man and 25% for a woman. Following the model matching procedure, the tissue group masses and volumes, blood pool volumes and tissue group partition coefficients are each determined. Full parameterisation also depends upon alveolar ventilation and cardiac output.

5.1.2 The Estimation of Alveolar Ventilation

Equation 2.1 relates the alveolar ventilation to the respiratory rate, tidal volume, minute volume and deadspace volume. Instrumentation available on the anaesthesia machine measures respiration rate, tidal volume and expired minute volume. Unfortunately, these cannot be automatically collected from the instrument as it has no external interface. The measurement can however form the basis of an estimate of alveolar ventilation. When ventilation is controlled, more precise estimation is viable because each 'breath' is the same. In the on-line estimator originally implemented, the alveolar ventilation was assumed constant at 4 litres per minute. This assumption introduced unacceptable error to the estimation process and a means of establishing and changing the alveolar ventilation estimate during estimation was later added to the implementation. This modification and the factors which necessitated it are described later.

5.1.3 The Estimation of Cardiac Output

The accurate estimation of cardiac output is a complex procedure and the most reliable methods currently available are invasive. Even approximate methods such as impedance cardiography present practical problems in their use [79]. In the estimation scheme described in this chapter, the estimation of cardiac output is an explicit step in the estimation of tissue tensions and involves non-invasive techniques.

5.2 The Estimation Scheme

In their scheme for the control of brain tension, Chilcoat, Lunn and Mapleson [79] used measured arterial tensions to modify the cardiac output of their model. The end-tidal anaesthetic tension is a reasonable approximation to the arterial anaesthetic tension and can be more readily measured. This characteristic has been exploited to form an estimation scheme which, using a matched physiologically-based model, modulates the cardiac output of the model so as to make its end-tidal tension match that of the patient. The scheme is illustrated in Figure 5.2

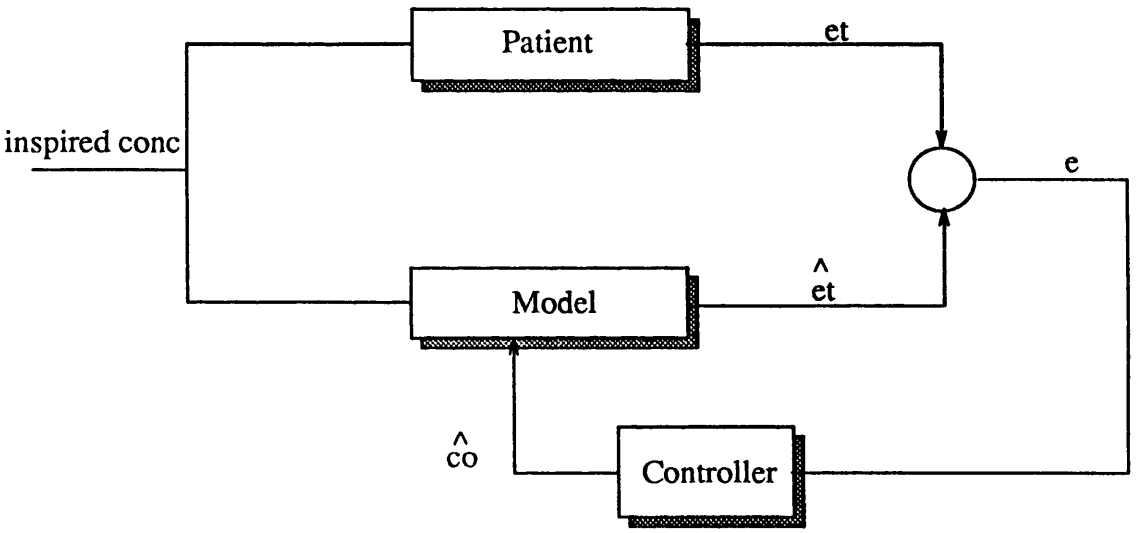

Figure 5.2: Tissue Tension Estimator Scheme

As indicated, a controller is employed to drive the error, e, between the measured end-tidal tension, *et*, and that of the model, $\hat{et}$ to zero. The function of the estimator is based upon the monotonic changes in end-tidal tension caused by cardiac output changes (see Figure 4.4). The model of the patient therefore

depends upon the cardiac estimate produced by the controller.

5.2.1 The Mechanism of Operation of the Estimator

The estimation scheme drives the error between the patient and model end-tidal tensions to zero. If the ventilation of the model is matched to the ventilation of the patient, the uptake of the model will equate with that of the patient. If the tissue masses, relative blood flows and partition coefficients are consistent with those of the patient, the uptake in each of the tissue groups of the model will be the same as those of the patient if the model's estimate of cardiac output is correct. The correct estimation of cardiac output therefore depends upon the model being well-matched to the patient.

If the model is not well-matched to the patient, errors will arise in the estimation of cardiac output and ultimately in the estimated tissue tensions. For instance, if the model assumes an alveolar ventilation greater than that present in the patient, the notional flow of drug into the model is greater than that into the patient. This, in isolation, would tend to increase the end-tidal tensions of the model above that of the patient all other things being equal. In order to compensate for this situation, the estimator will increase the model's cardiac output so as to increase the uptake of drug by each tissue group and therefore reduce end-tidal tension. The model's cardiac output estimate will therefore be too large. In a similar manner, an overestimate of tissue group volumes in the model will result in greater uptake in the tissue groups of the model than in the tissue groups of the patient. This causes the model to have a lower mixed-venous tension and subsequently lower end-tidal tension. To maintain end-tidal tension matching, the estimator would underestimate cardiac output in this situation. These effects will be illustrated later.

5.3 Simulated Performance of the Estimation Scheme

In order to test the validity of the estimation scheme, its performance in a range of tests has been evaluated. In evaluating the scheme, one version of the isoflurane model derived in Chapter 4 has been used to represent the patient and another has been manipulated by the estimation scheme. The tests involved changing the cardiac output of the patient model and observing the behaviour of the estimator. These tests were carried out using MATLAB and consist of;

1. The continuous-time performance of the estimator with a perfectly matched model.

2. The discrete-time performance of the estimator with a perfectly matched model. (discretely available estimator input)

3. The continuous-time performance of the estimator with mismatched tissue groups.

4. The continuous-time performance of the estimator with mismatched alveolar ventilation.

5.3.1 Continuous-Time Performance with a Perfectly Matched Model

To demonstrate the performance of the estimation scheme, a continuous-time version of the estimator has been simulated using MATLAB. The controller within the estimator (see Figure 5.2) has been implemented as a simple PI controller. The controller gains have been adjusted manually to produce acceptable performance during simulation. The aim of the adjustment has been to produce a fast response of the cardiac output estimate without excessive overshoot or oscillation. In the

tests described below, the proportional gain is fixed at 0.3 and the integral gain is 0.06. The use of the integral term ensures that the error between the model and patient end–tidal tensions is reduced to zero.

In each of the tests featured below, step changes occur in both the inspired concentration to the simulated patient and in the cardiac output of the patient model. In each case, the estimator's initial cardiac output estimate is 6 l/min and the patient model's cardiac output is 7.2 l/min initially. In each test, the inspired concentration either varies between 1% and 3% or 3% and 1% after 20 minutes. After 30 minutes, the cardiac output either changes from 7.2 l/min to 8.0 l/min or from 7.2 l/min to 6.0 l/min. The timing of the cardiac output changes is so as to allow equilibration of the faster tissue groups of the patient model. The gradient of the end–tidal curve is consequently reduced and the amount of information available to the estimator is much less than in the initial 15 minutes. This presents a useful performance test which simulates the timescale in which the estimator would be most useful if used in the automatic control of anaesthesia. The conditions of each test and the figures illustrating their results are listed in Table 5.1 In each of the figures, the upper graph shows the patient model cardiac output as a dashed line and the estimated cardiac output as a solid line. The lower graph of each figure shows the patient model and estimated brain tensions. The patient model brain tension is the dashed line and the estimated brain tension is a solid line. It is apparent from these results that the estimation scheme is capable of providing satisfactory estimation performance.

5.3.2 Discrete–Time Performance with a Perfectly Matched Model

In the operating theatre, continuous information on inspired and end–tidal tensions cannot be automatically collected without specialised hardware. The Datex Ultima monitor, for which there is a CLASS library virtual monitor, can

Test	T_i	T_f	CO_i	CO_f	Figure
1	1%	3%	7.2	8.0	5.3
2	1%	3%	7.2	6.0	5.4
3	3%	1%	7.2	8.0	5.5
4	3%	1%	7.2	6.0	5.6

Note:T_i and T_f are the initial and final inspired concentrations respectively and CO_i and CO_f are the initial and final cardiac outputs of the patient model respectively

Table 5.1: Summary of Continuous–Time Estimator Tests

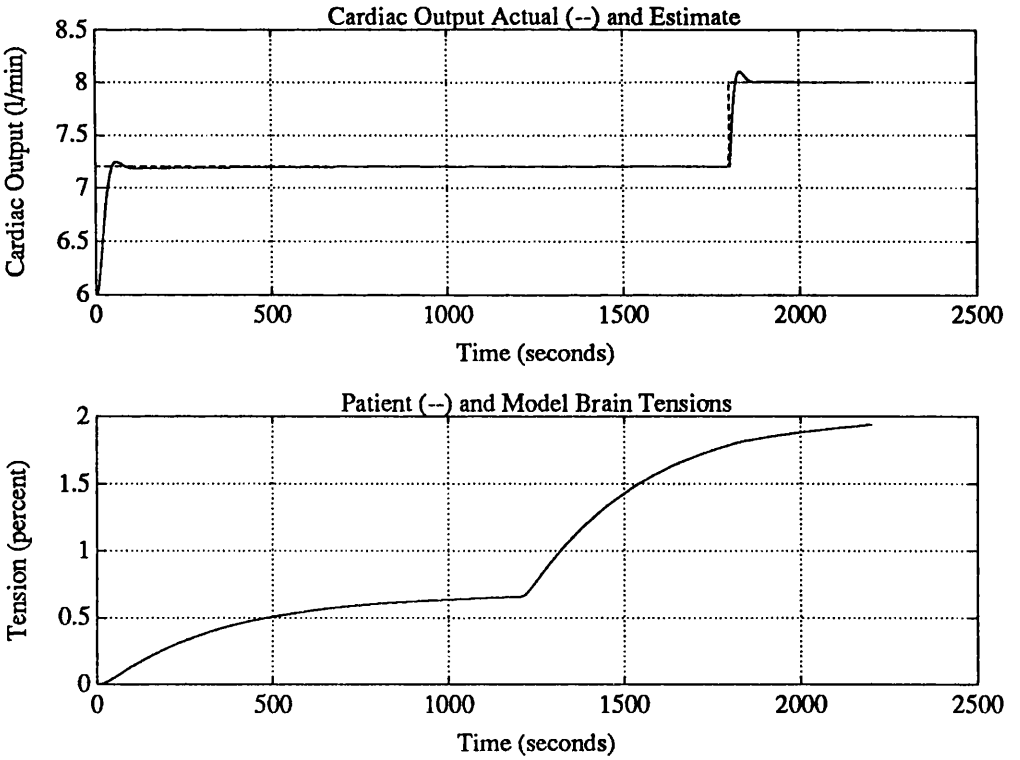

Figure 5.3: Continuous–Time Test 1

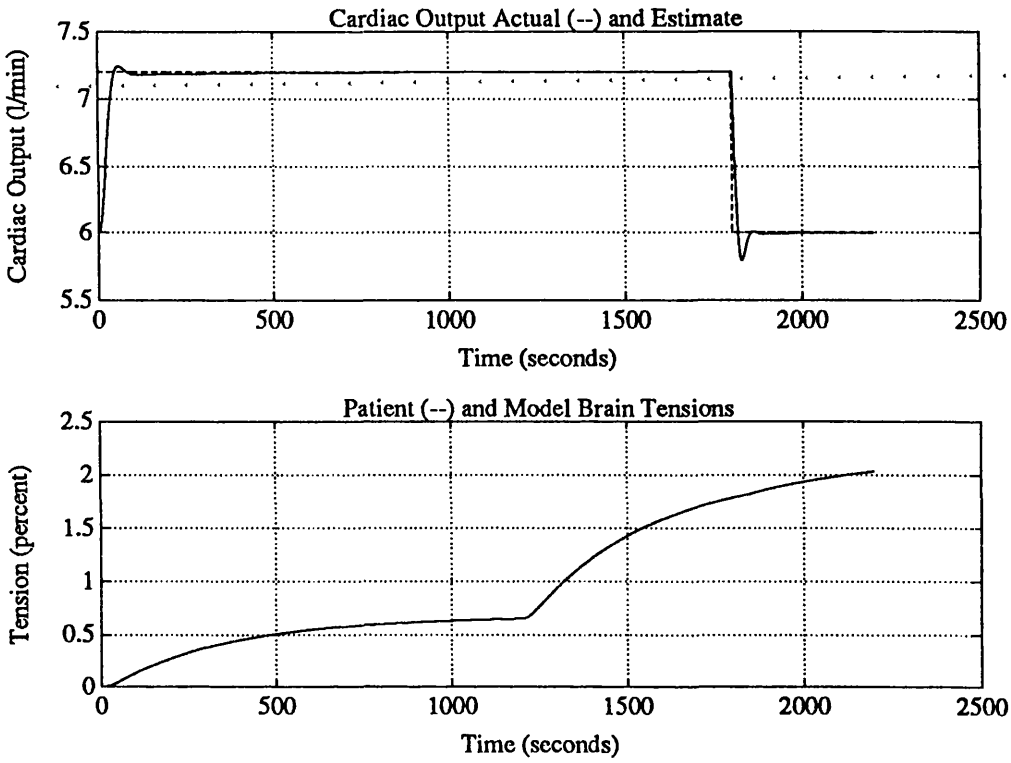

Figure 5.4: Continuous–Time Test 2

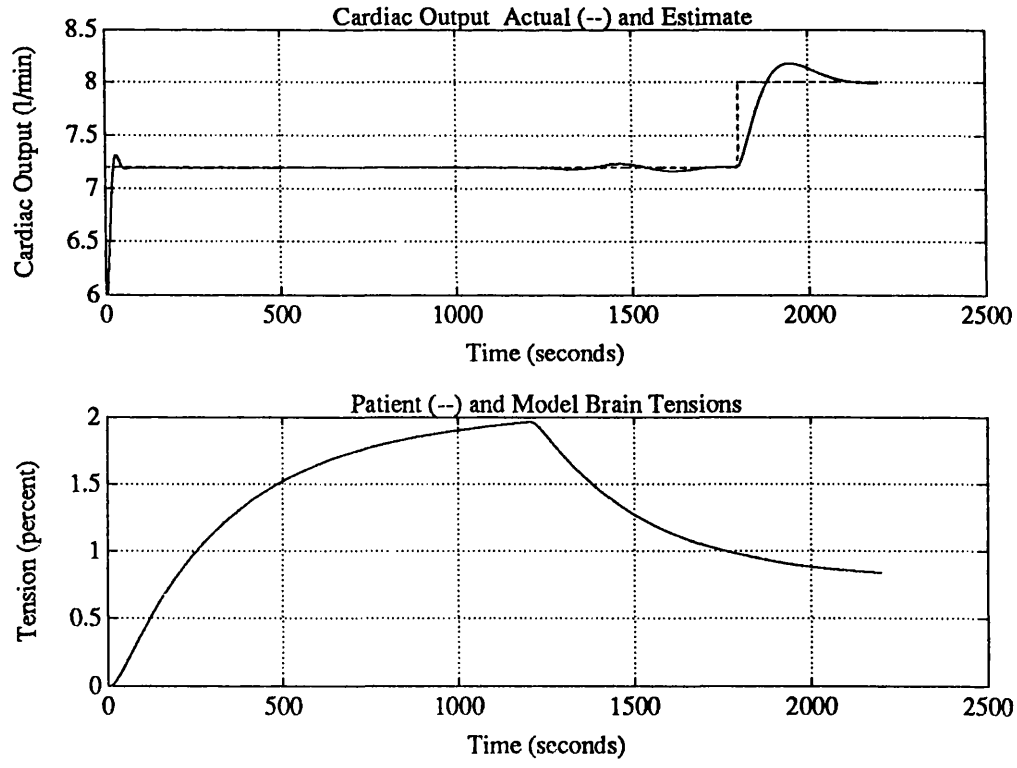

Figure 5.5: Continuous–Time Test 3

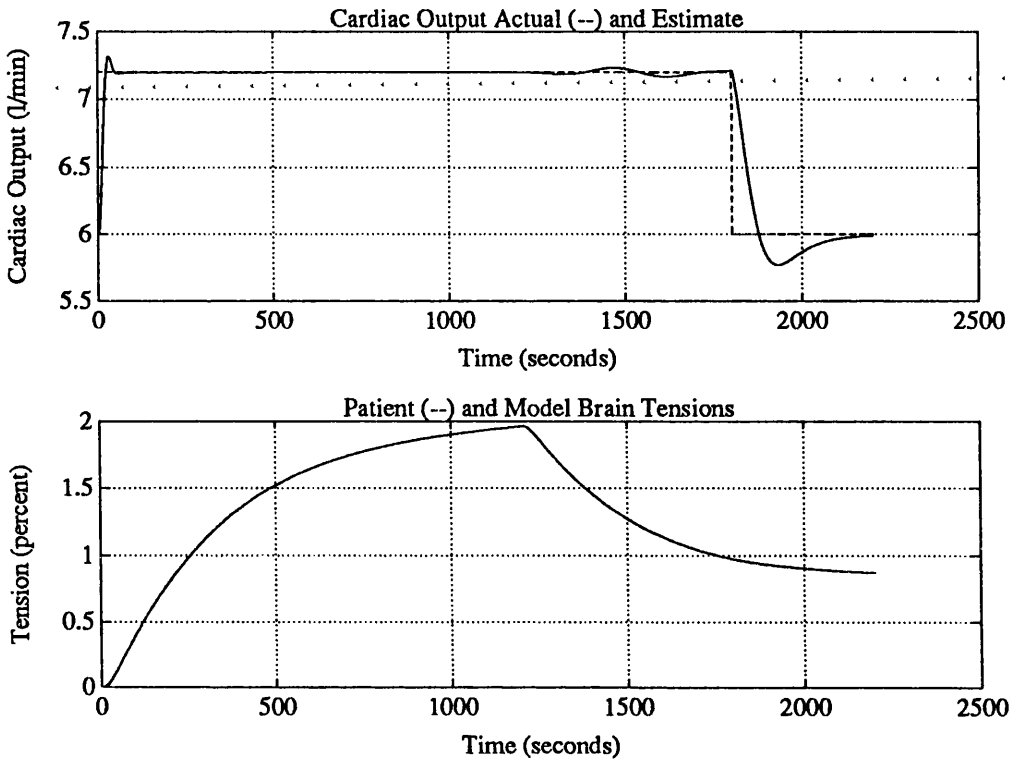

Figure 5.6: Continuous–Time Test 4

provide such information every 10 seconds in a data string output at its RS–232 data port. The estimation scheme code used in the continuous–time tests has been modified so as to provide estimator updates in multiples of 10 seconds. In an initial investigation, the performances of estimators producing estimates every 10, 20 and 30 seconds were compared. Updates every 30 seconds were not considered satisfactory. The following tests used updates every 20 seconds to simulate using every second Datex string. This, of course, allowed the use of every Datex string as a further refinement if required. The testing scheme followed the same format as the continuous–time tests for the first four tests and these are summarised along with their figure numbers in Table 5.2. In addition, the performance of the estimator in following a ramp–up and ramp–down of cardiac output from 5 l/min at 20 minutes to 8 l/min at 25 minutes and back to 5 l/min at 30 minutes with a constant 3% inspired isoflurane is shown in Figure 5.11. The arrangement of each of these graphs is identical to that of the continuous–time tests. In each of these

tests, the controller was once again a PI type with proportional gain = 0.1 and integral gain = 0.25. These tests indicate that a discrete–time implementation of the estimator, designed to take account of the practical limitations of data collection, can produce satisfactory estimation performance.

Test	T_i	T_f	CO_i	CO_f	Figure
1	1%	3%	7.2	8.0	5.7
2	1%	3%	7.2	6.0	5.8
3	3%	1%	7.2	8.0	5.9
4	3%	1%	7.2	6.0	5.10

Note:T_i and T_f are the initial and final inspired concentrations respectively and CO_i and CO_f are the initial and final cardiac outputs of the patient model respectively

Table 5.2: Summary of Discrete–Time Estimator Tests

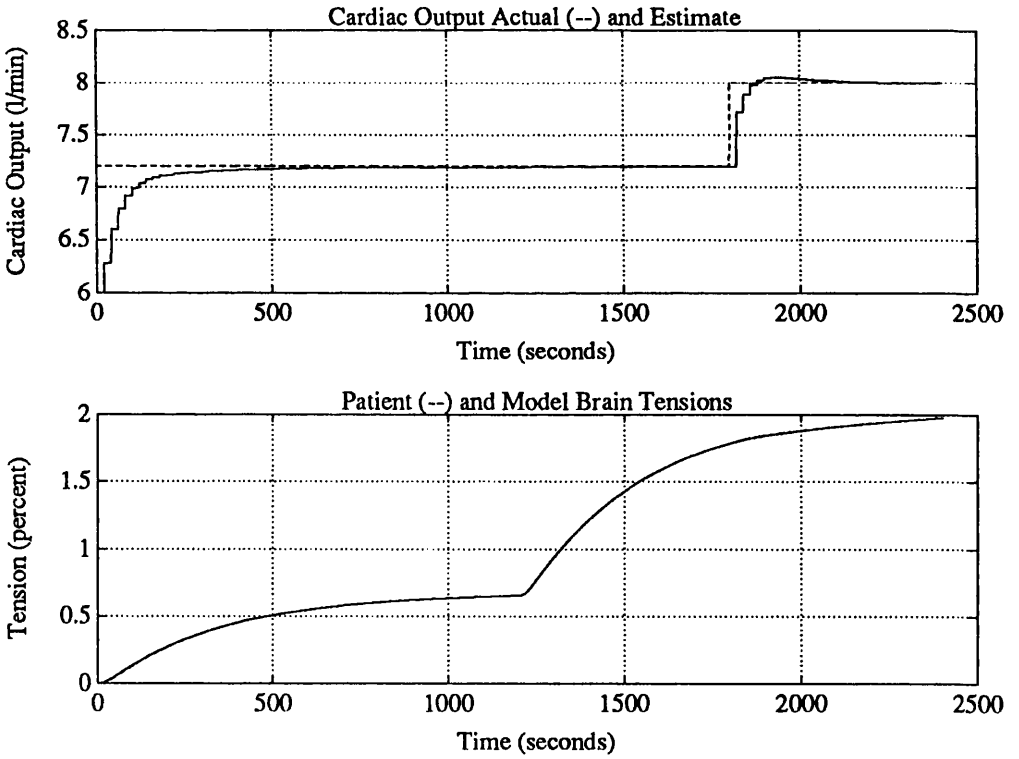

Figure 5.7: Discrete–Time Test 1

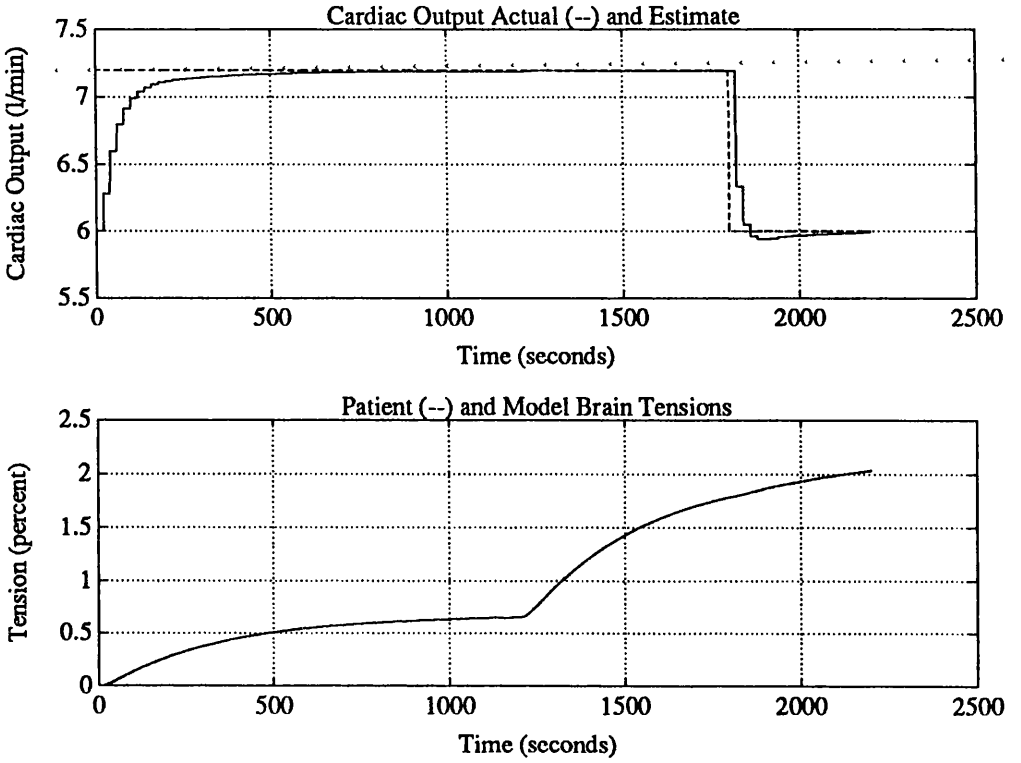

Figure 5.8: Discrete–Time Test 2

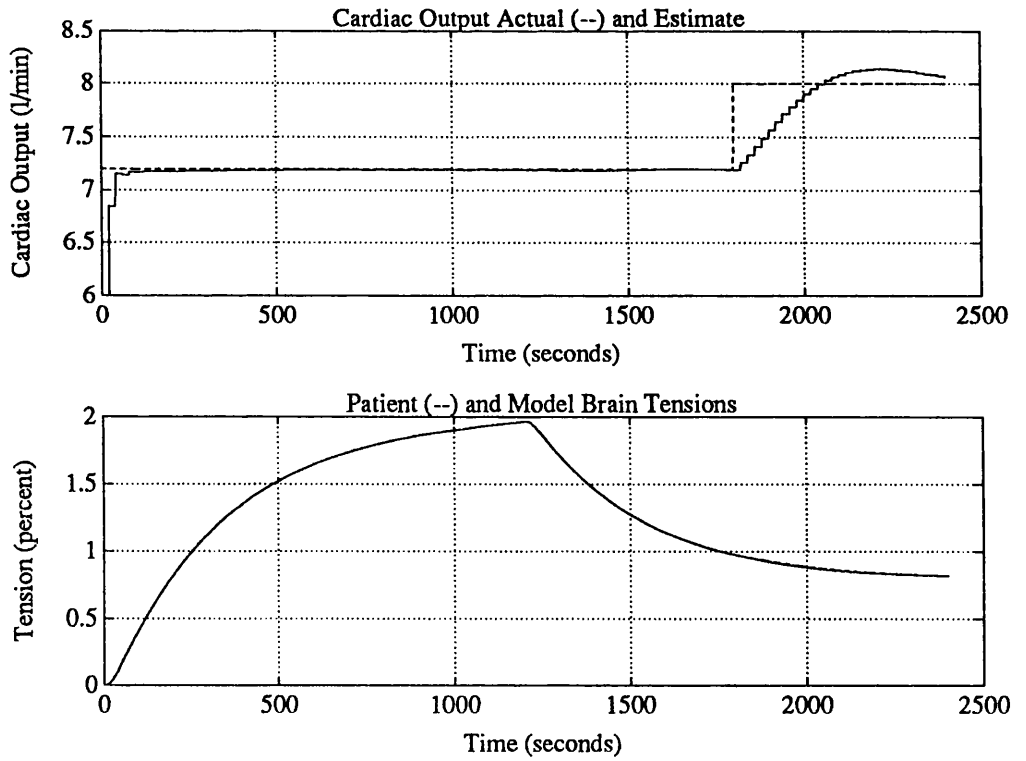

Figure 5.9: Discrete–Time Test 3

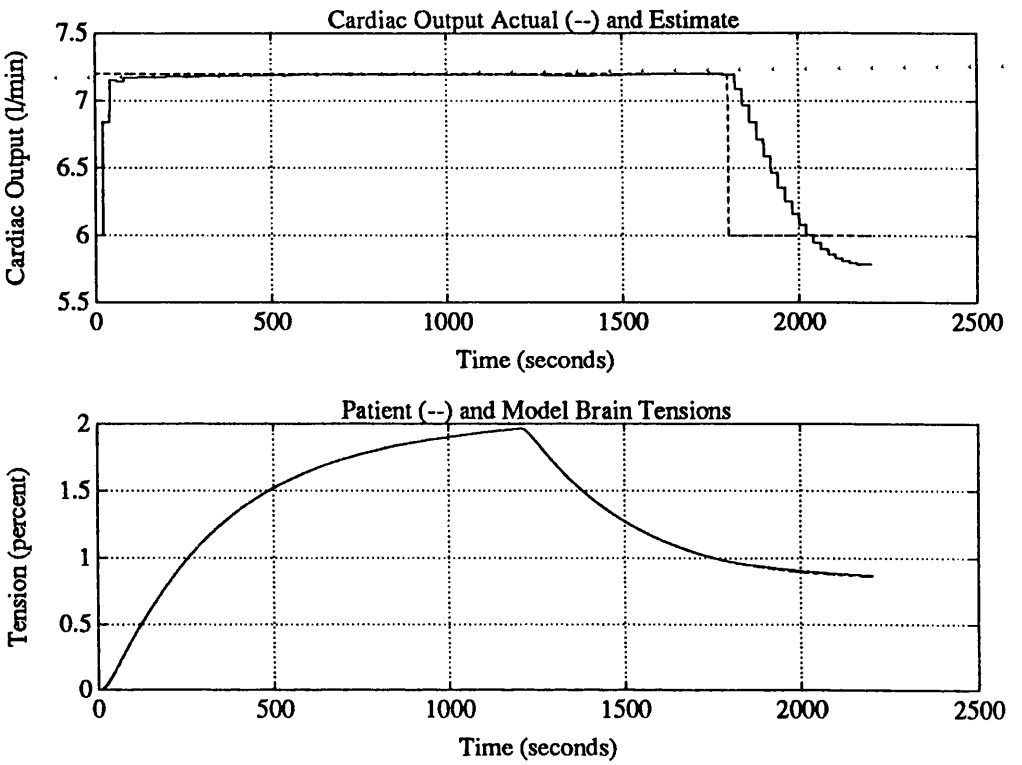

Figure 5.10: Discrete–Time Test 4

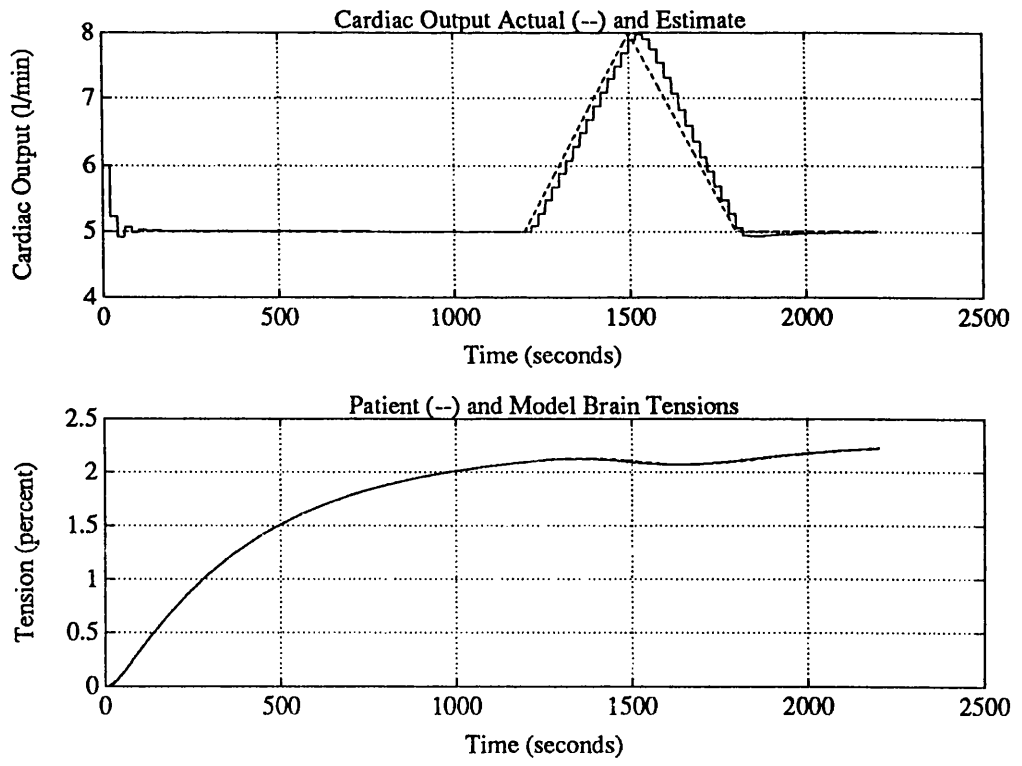

Figure 5.11: Discrete–Time Ramp Test

5.3.3 The Effects of Mismatched Body Composition Estimates

Estimates of body fat and body muscle cannot be made very precisely. Any estimate made is therefore likely to introduce errors into the estimation scheme. In this case, the interpretation of the results of the estimation changes.

In matching end–tidal concentrations, the estimation scheme actually attempts to ensure that the *uptake* of the model is the same as that of the patient. If all the tissue masses employed in the model are correct, having the model uptake the same as the patient's uptake dictates that the model's cardiac output is also the same as that of the patient. This ceases to be the case when model tissue masses are not the same as those of the patient.

Early in the estimation process, the brain sample, visceral group, lean group and fat group all require significant uptake of drug in order to equilibrate with the arterial blood. After about 15 minutes, the faster tissues (brain and viscera) have very nearly equilibrated with arterial blood and no longer contribute significant uptake. After this time, further changes in cardiac output only alter the rate of uptake of drug in the slower lean and fat groups. In matching the uptake of the patient, the estimator will place the correct amounts of drug within the tissue groups (assuming correct circulatory parameterisation). If there is an error in calculating or measuring the mass or volume of a tissue group, there will also be an error in the tension estimated for that group. A further complication arises from the error in the tissue volume estimates: because tissue uptake increases with its capacity for the drug which, in turn, increases with the tissue volume (see equation 4.4), an error in the tissue volume estimate causes an error in the cardiac output estimate. This is because in order to equate the uptake of two tissues of different mass, the smaller of the two must be more highly perfused.

These effects are illustrated in Figures 5.12, and 5.13. Figure 5.12 shows the effects of a 10% underestimate of the lean group volume and a 10% underestimate

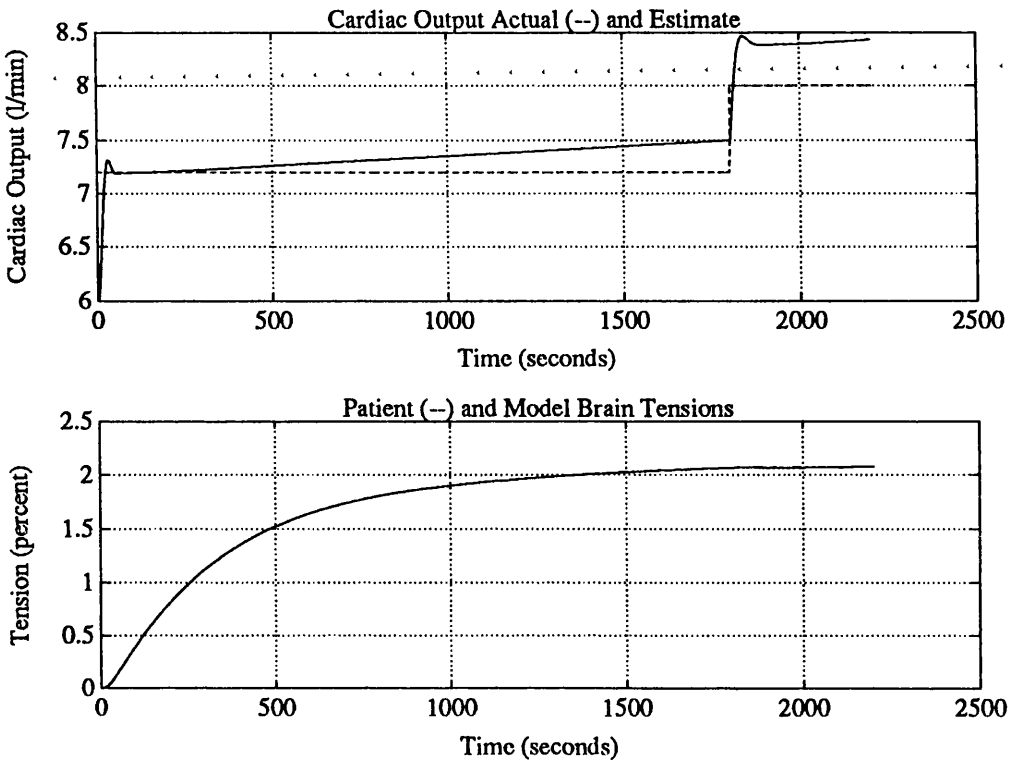

Figure 5.12: Mismatched Tissue Test 1

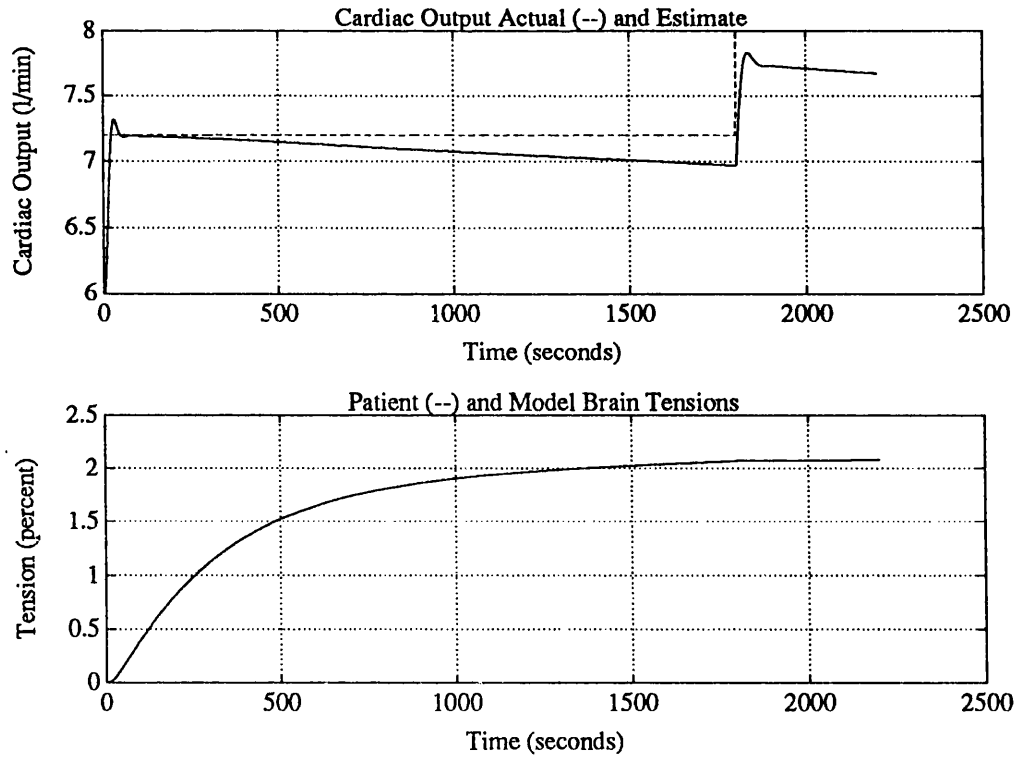

Figure 5.13: Mismatched Tissue Test 2

of the fat group volume in the model employed by the estimator. Figure 5.13 shows the effects of a 10% overestimate of the lean group volume and a 10% overestimate of the fat group volume in the model employed by the estimator. In both cases, the end-tidal curves are well matched as would be expected. The brain tension curve is well matched to the actual patient simulation brain tension, but the cardiac output estimate is no longer reliable due to the mismatched models.

It can be noted, however, that the error in the cardiac output estimate in both cases is still only 5% after 30 minutes for a 10% error in both the lean and fat group volumes.

5.3.4 The Effects of Mismatched Alveolar Ventilation Estimates

Alveolar ventilation cannot be directly measured but can be estimated in consideration of either minute volume or tidal volume and respiration rate. Alveolar ventilation is minute ventilation minus the ventilation of physiologic and anatomical deadspace (see Equation 2.1). Such an estimate will also have an error associated with it.

The alveolar ventilation determines the rate of delivery of drug into the patient. If the alveolar ventilation increases, the end-tidal and tissue tensions also increase as shown in Figure 4.3. A mismatch between the model and patient alveolar ventilations therefore causes errors in the subsequent estimation.

If the patient's alveolar ventilation is larger than that of the model, the end-tidal concentration predicted by the model will be lower than that of the patient. The estimation scheme will compensate by reducing model tissue uptakes in order to raise the end-tidal tension. This will be achieved by reducing the cardiac output. If the model has an underestimate of alveolar ventilation, it will subsequently underestimate both cardiac output and tissue tensions. Conversely, if the model assumes an alveolar ventilation greater than that of the patient,

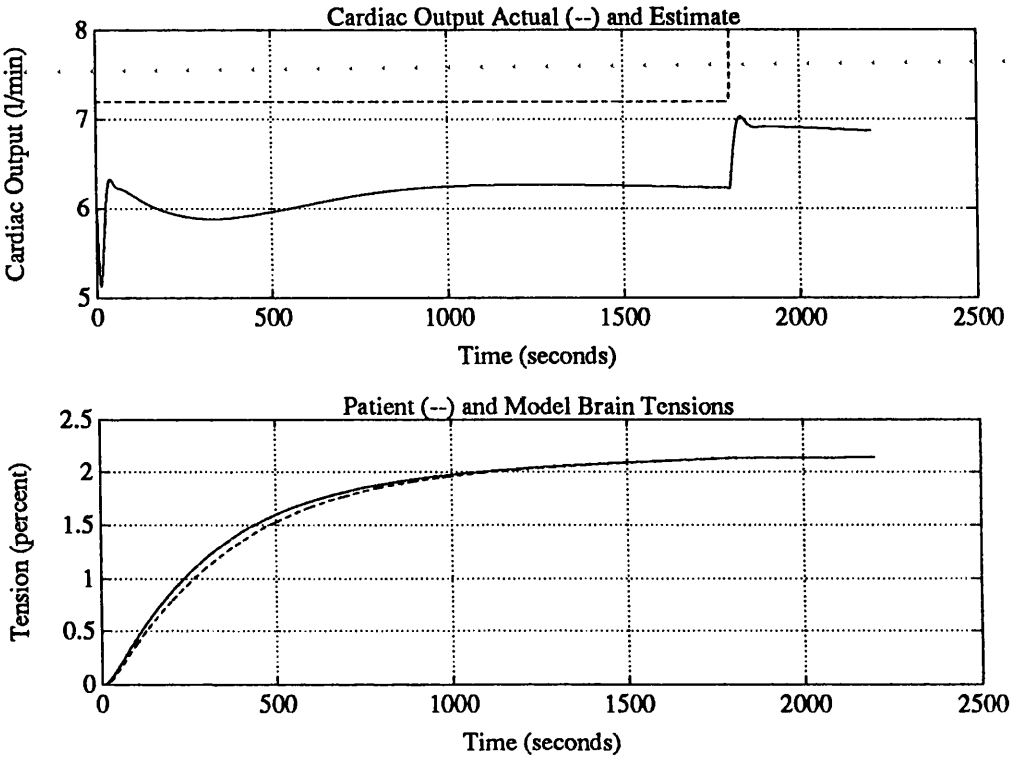

Figure 5.14: Mismatched Ventilation Test 1

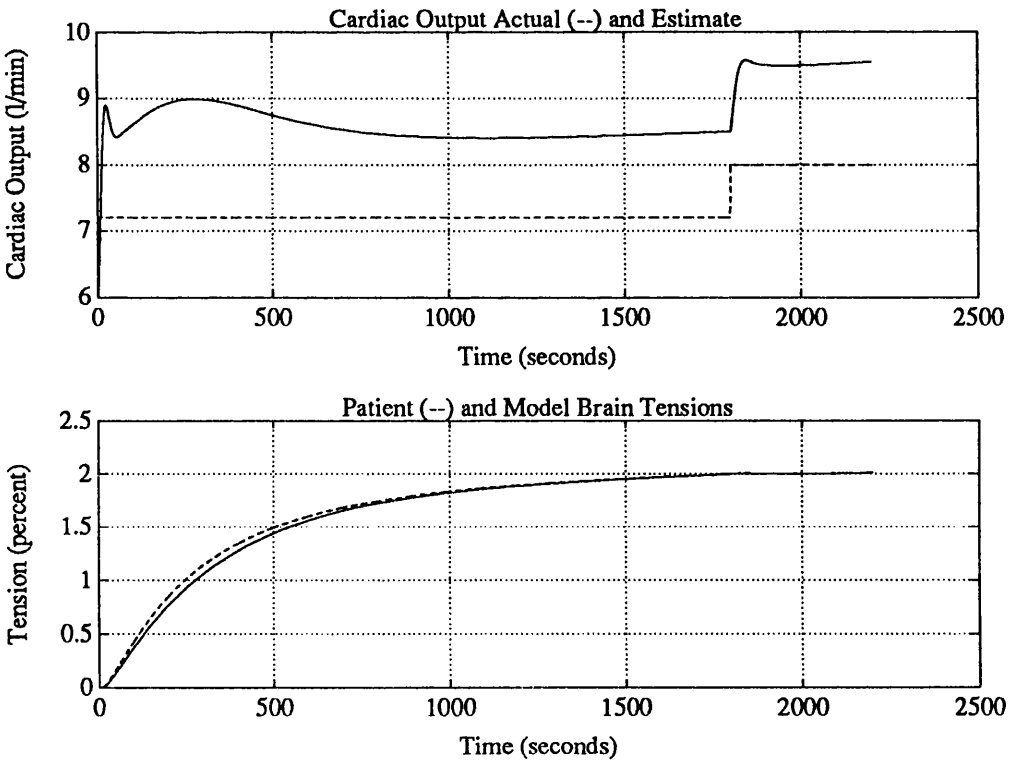

Figure 5.15: Mismatched Ventilation Test 2

the model end-tidal tension will be higher than that of the patient and in compensating for the difference the estimator will produce cardiac output and tissue tension estimates which are too high.

These effects are illustrated in Figures 5.14 and 5.15. Figure 5.14 shows the results of assuming an alveolar ventilation in the model which is 10% below that of the patient simulation. This results in an underestimate of cardiac output and an underestimate of brain tension. The error in the brain tension estimation is however not very large. Figure 5.15 shows the performance of the estimator when the model assumes an alveolar ventilation 10% greater than that of the patient simulation. In this case, the estimator over estimates the cardiac output and brain tension. Once again the error in the estimated brain tension is not too large.

5.4 Actual Performance of the Estimation Scheme

The simulation of the estimator scheme contributed greatly to the refinement of the approach. Further areas where refinements are necessary have been highlighted following the use of the estimation scheme in theatre. The potential problems described earlier which are due to mismatching of the model's ventilation and tissue groups become apparent in practice. Further complicating factors have also arisen, in particular, the characteristics of the inspired and end-tidal concentration measurements.

5.4.1 Experimental Equipment

A prototype version of the estimation scheme has been implemented as part of the Glasgow Anaesthesia Estimation Libraries (GAEL). These libraries contain code to perform model matching and the initialisation and updating of an estimation scheme with a PI controller. Using the CLASS libraries, a virtual monitor for the Datex Ultima monitor was created. This allowed inspired and end-tidal

anaesthetic concentrations to be measured and passed to the estimation scheme. As described in Chapter 2, the code is written in C++, compiled with the Zortech C++ 3.0 compiler running on a Viglen III/LS machine. The estimation scheme has been set up to produce a physiologically-based model of isoflurane pharmacokinetics matched to the patient. In theatre, isoflurane, nitrous oxide and oxygen are delivered via a circle system. To minimise interference with conventional anaesthesia practice, the estimation scheme was used in conjunction with this arrangement.

5.4.2 Inspired and End-Tidal Isoflurane Concentration Measurements

After a limited amount of preliminary investigation, it became apparent that the measured end-tidal concentration timecourses did not appear as expected. When using closed-circuit anaesthesia, it is customary for the circuit to be 'primed' by delivering isoflurane and other fresh gases through the circuit to a test bag which simulates the patient so as to distribute the fresh gas mixture throughout the circuit. This ensures that the patient breathes a mixture close to that set on the vaporiser and gas flowmeters. In addition to this, an appreciable amount of anaesthetic gas is stored in the circuit during priming and this acts as a buffer during the initial large uptake of the patient.

The patient may also be presented with a gas mixture including the volatile agent at induction. In estimating tissue anaesthetic tensions using the estimation scheme, it is essential to have an 'empty' patient i.e., a patient having breathed none of the agent being used to drive the estimation. Estimator tests were however upset by apparently high end-tidal tensions at an early stage in the patient's uptake. Without a reliable physiological explanation for this, it was decided that the monitor should be tested in a range of combinations. The changes in both inspired and end-tidal concentrations were therefore measured during anaesthetics

in which the patient and the anaesthetic circuit could either be 'primed' or 'empty'. Three tests were performed as summarised in Table 5.3. The figure number for the graphs showing the results of these tests is also given in the table. In these figures, the solid line represents the inspired concentration of isoflurane in percent and the dashed line represents the end-tidal concentration also in percent as recorded by the Datex monitor.

Test	Circuit	Patient	Figure
1	primed	primed	5.16
2	primed	empty	5.17
3	empty	empty	5.18

Table 5.3: Summary of Concentration Measurement Tests

It is apparent, from these figures, that when the circuit is primed, the end-tidal concentration measurement rises very rapidly initially and then tends to follow the inspired tension. This would suggest that the monitor's measurement of end-tidal tension does not accurately reflect the end-tidal tension of the patient. The precise reason for this is not clear. In contrast, the concentration-time curves for the empty circuit and empty patient (Figure 5.17) produce an end-tidal curve which is more realistic. Although it is apparent that the monitor's end-tidal measurement may not accurately reflect the patient's end-tidal anaesthetic concentration, the use of an empty circuit and empty patient (i.e., none of the measured agent in the circuit or the patient at the start of measurements) has been adopted so as to minimise these effects. A further effect can be observed in Figure 5.17. Following the reduction of the inspired concentration at around 1300 seconds, the end-tidal value falls very rapidly. Once again, it seems pharmacologically and physiologically unlikely that such a rapid reduction in end-tidal concentration could occur after 20 minutes of anaesthesia. Regrettably, this characteristic of the measurement is not avoidable because such reductions in the inspired concentration are necessary at the end of an operation.

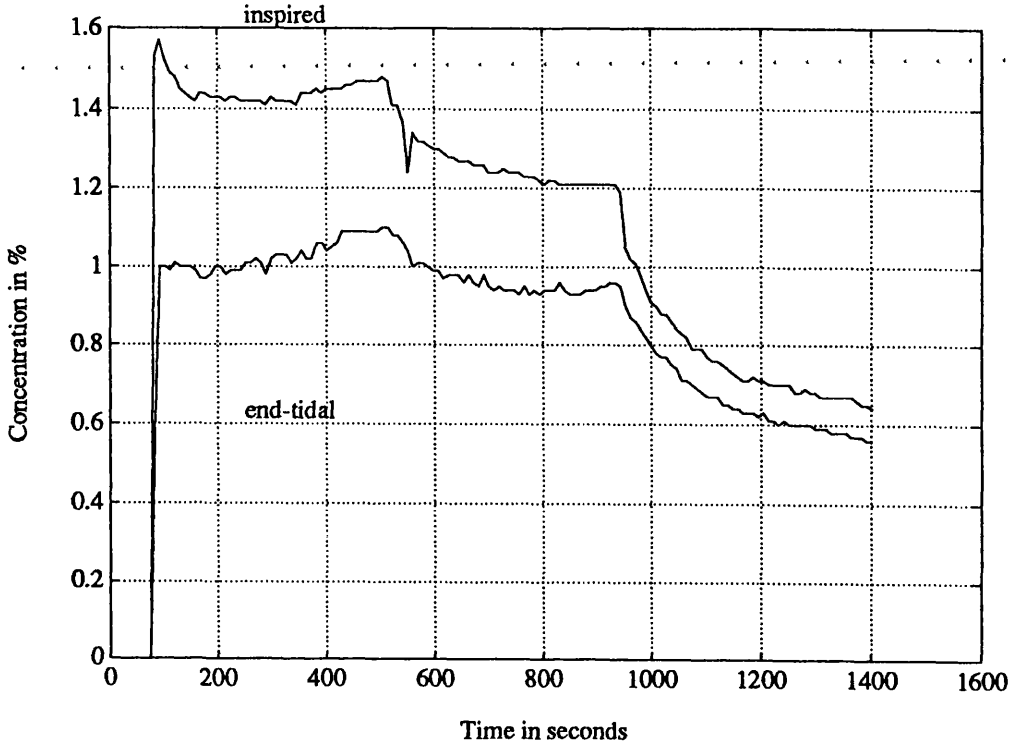

Figure 5.16: Monitor Test: Primed Circuit, Primed Patient

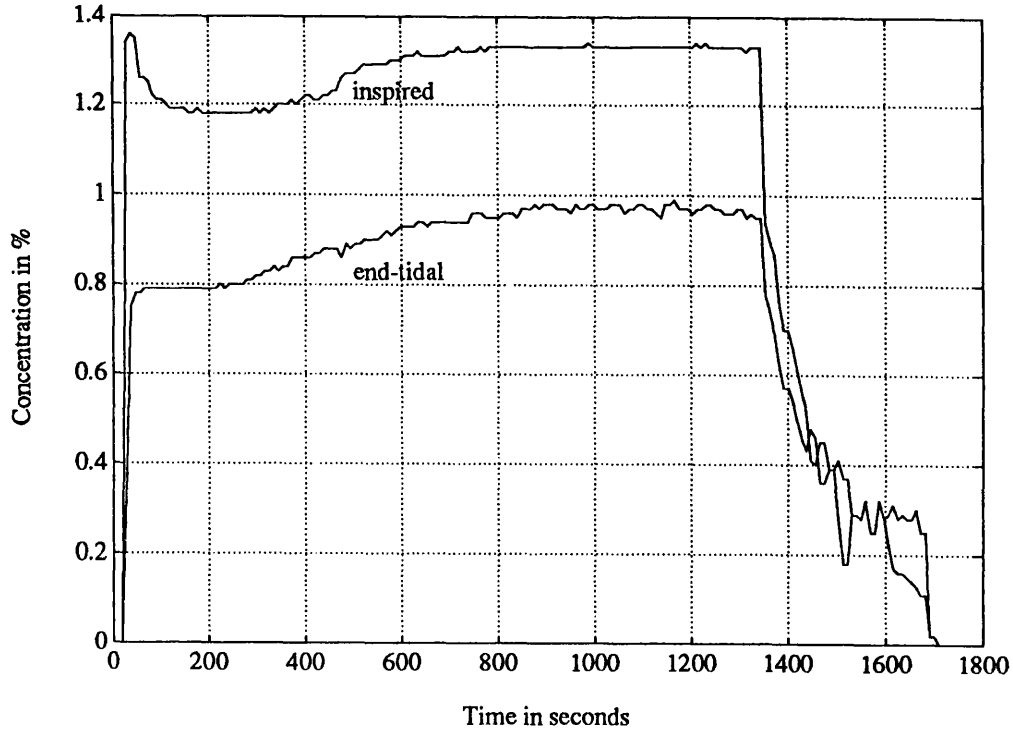

Figure 5.17: Monitor Test: Primed Circuit, Empty Patient

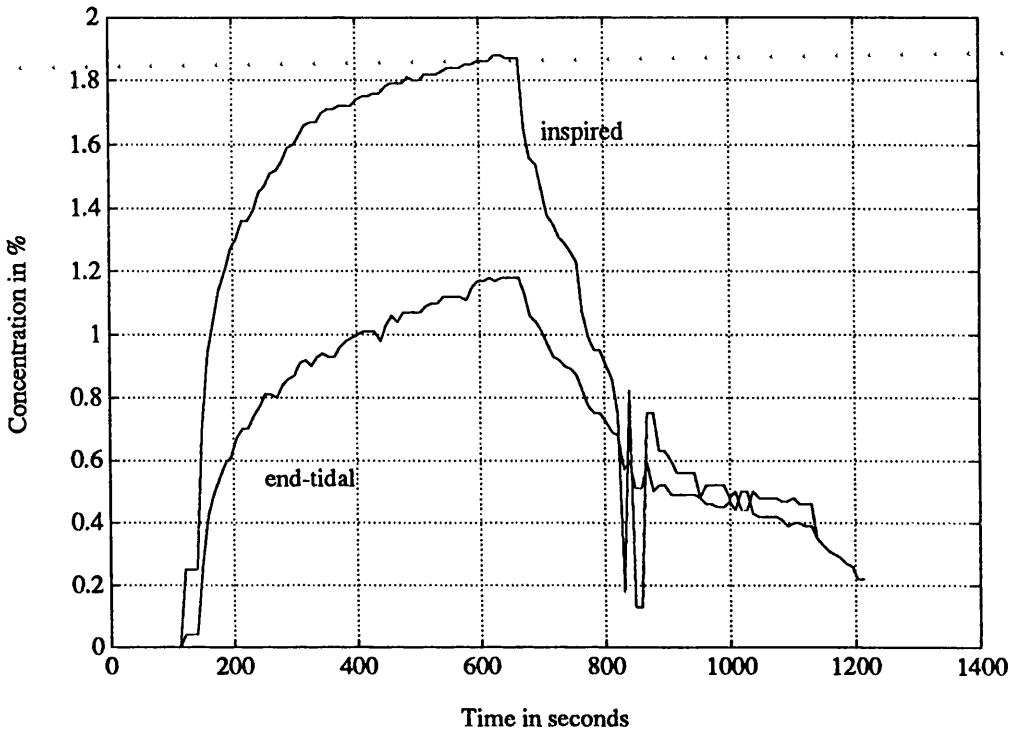

Figure 5.18: Monitor Test: Empty Circuit, Empty Patient

5.4.3 Estimation Scheme Theatre Test Results: Version 1

This section discusses the characteristics of three tests of the estimator in the operating theatre. As stated earlier, each patient was not given any isoflurane prior to their positioning on the operating table and the connection of the monitor. The anaesthetic circuit was also flushed so as to ensure that no isoflurane remained in the circuit. The characteristics exhibited by each test are summarised below.

Test A

This test took place during an operation on a 64kg man to relieve haemerrhoids. Estimates of the patient's percentage body fat were not available and the estimation was set up to assume that the patient's body fat was in the same proportion as that of the standard man. Figure 5.19 shows the measured inspired

and end-tidal concentrations (expressed as a percentage) as continuous lines. The end-tidal concentration produced by the estimator is shown as a broken line on the lower graph of Figure 5.19. The estimation scheme has succeeded in following the patient's end-tidal concentration as would be expected. In Figure 5.20, the

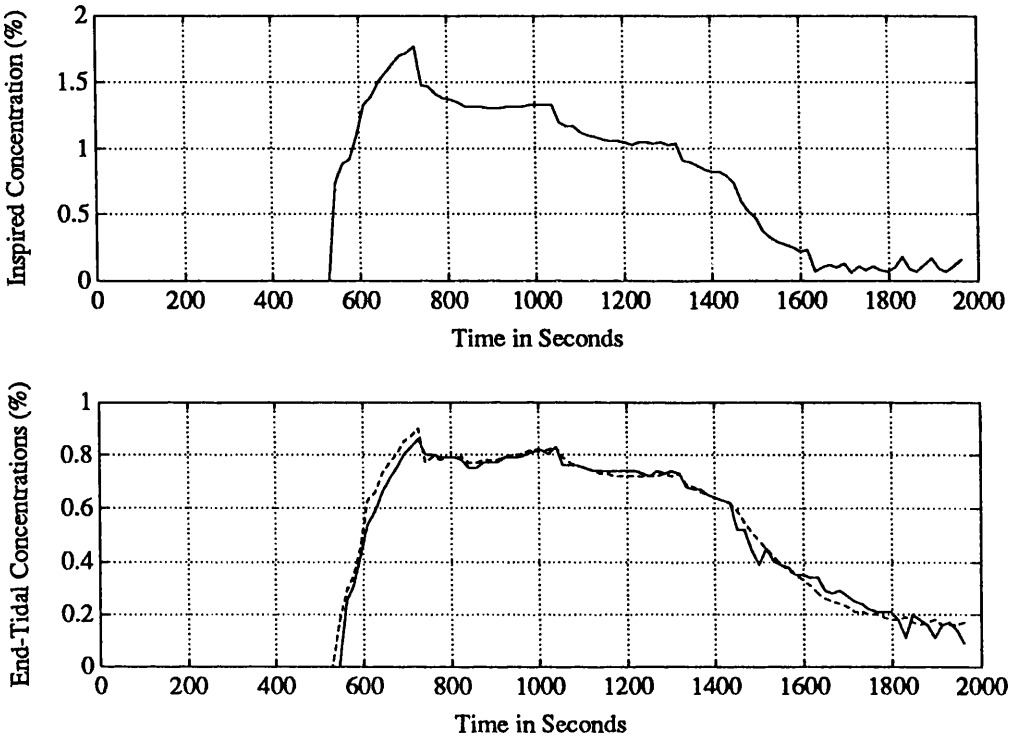

Figure 5.19: Test A: Inspired and End-Tidal Concentrations (Model End-Tidal Value is the Broken Line)

upper graph shows the brain tension estimate produced by the scheme. While is is probably unwise to suggest that this plot is an accurate representation of the actual brain tension, it does seem to present a plausible relationship. The estimated cardiac output of the estimation scheme is shown in the lower graph of Figure 5.20. The initialisation of the estimation scheme provides an initial value of 6.5 l/min for cardiac output. As data arrives and is processed by the estimator (at about 550 seconds), the cardiac output estimate changes. The initial estimates are low as the estimation scheme attempts to track the patient's end-tidal tension rise. The complementary case exists after around 1400 seconds

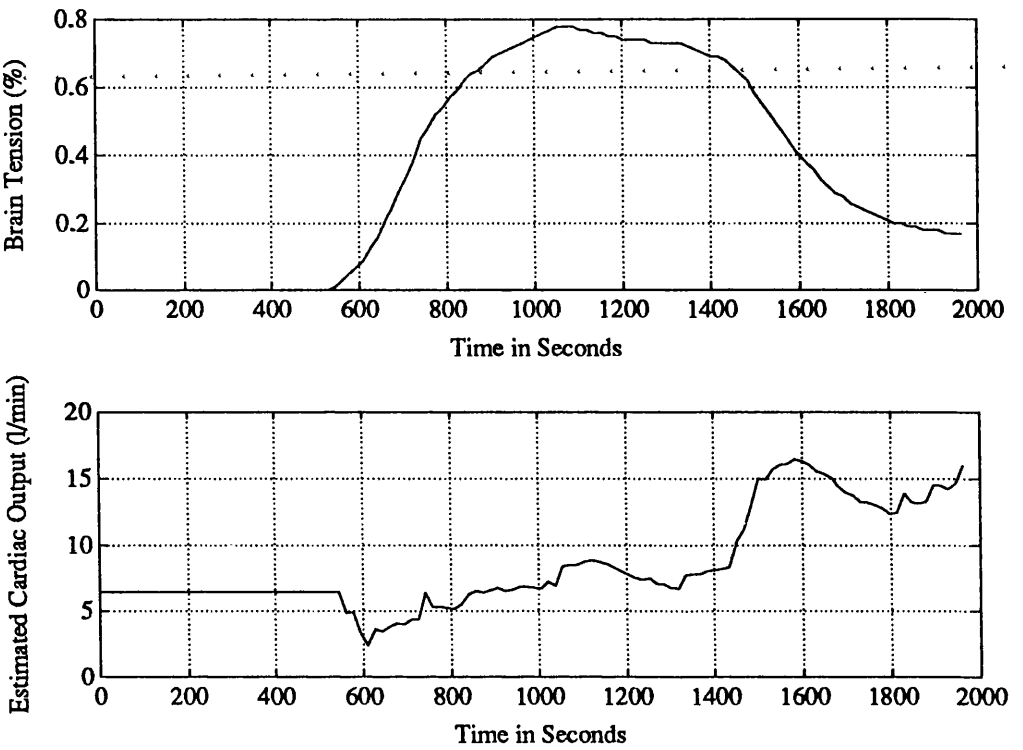

Figure 5.20: Test A: Brain Tension and Cardiac Output Estimates

when the estimator increases the cardiac output estimate to unrealistic values in attempting to match the decreasing end-tidal concentration at the end of the anaesthetic. The operation of the estimator between 800 seconds and 1400 seconds provides cardiac output estimates in a physiologically acceptable range and is more likely to be accompanied by reliable estimates of tissue tensions.

Test B

This operation took place on a male patient weighing 67.6 kg. The patient was assumed to have the body fat in proportion to the standard man. In Figure 5.21, the inspired and end-tidal measured concentrations of isoflurane are shown using continuous lines and the end-tidal estimate of the estimation model is shown using a broken line. Tracking of the patient's end-tidal concentration was good from about 500 seconds until the vaporiser was turned off just before 2000 seconds. Tracking was not as good from switch-on up to 500 seconds or after switch-off.

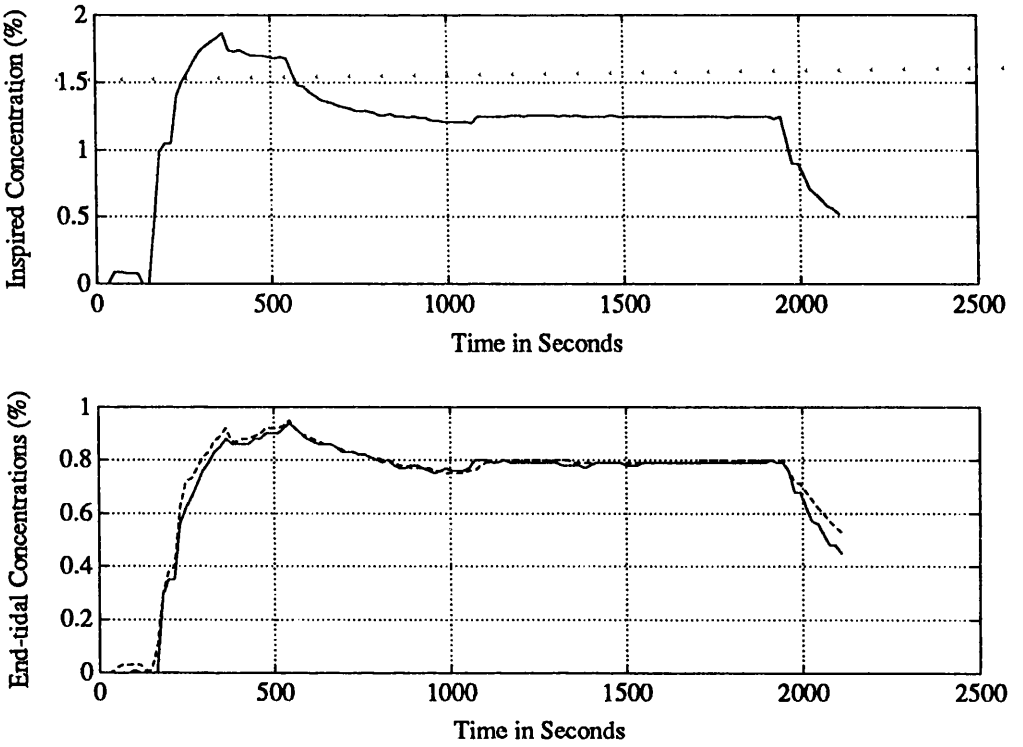

Figure 5.21: Test B: Inspired and End-Tidal Concentrations

Despite this, the brain tension estimate shown in Figure 5.22 seems reasonable. If this estimate is accurate, then the skill of the anaesthetist in controlling brain tension is exemplified by this brain tension response. The cardiac output estimate reflects the effort made by the estimator to match the end-tidal tensions. As with the previous test, the cardiac output estimate is too low in the initial period and, in this case, certainly too high at the end of the test. Between 500 and 2000 seconds, the estimation scheme provided good matching of the patient and model end-tidal tensions. The cardiac output estimate during this period is however too high. The excessive estimate produced during this period was apparent during the test. As considered earlier, cardiac output estimates can be erroneous in the presence of a mismatched model. In this case, the mass of the patient was known so that errors in the masses of tissue groups should have been reasonably small. The other main source of error arises from mismatches in alveolar ventilation. At this point, the estimation scheme assumed, for all patient's, an alveolar ventilation of 4 l/min.

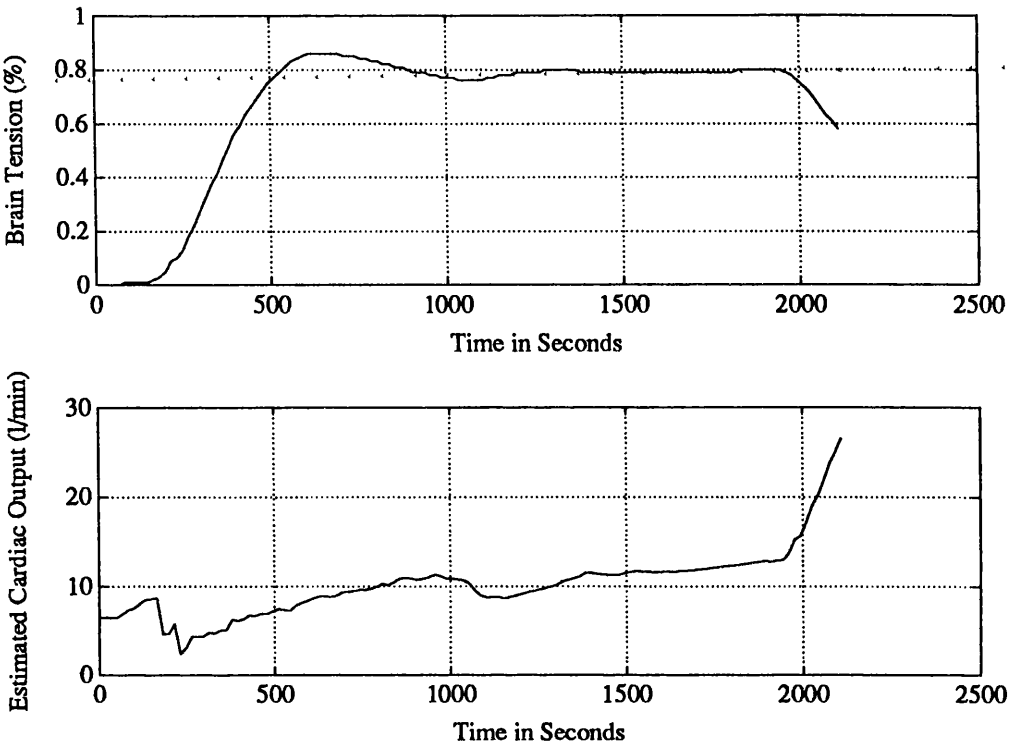

Figure 5.22: Test B: Brain Tension and Cardiac Output Estimates

For this patient, who was artificially ventilated, the ventilator was delivering 10 breaths per minute and the tidal volume was 0.51 litres. This gives a minute volume of 5.1 litres. The alveolar ventilation is determined following subtraction of anatomical and physiological deadspace. As an approximation, the combined deadspace can be estimated as between 2 and 2.5 ml/kg [A.J. Asbury personal communication]. For this patient, this gives a deadspace of between 135ml and 170ml. These figures, in turn, predict alveolar ventilation of between 3.4 l/min and 3.75 l/min. The model has therefore assumed a greater alveolar ventilation than that of the patient. As shown in Figure 5.14, this can result in consistently high cardiac output estimates.

Test C

This operation involved the removal of a cyst on the neck of a male patient estimated to be around 85kg in weight. Without any additional data on the

patient's body fat, he was assumed to have tissue groups and fat in proportion to those of the 70kg standard man. The measured inspired and end–tidal concentrations of the patient are shown in Figure 5.23. The model's end–tidal

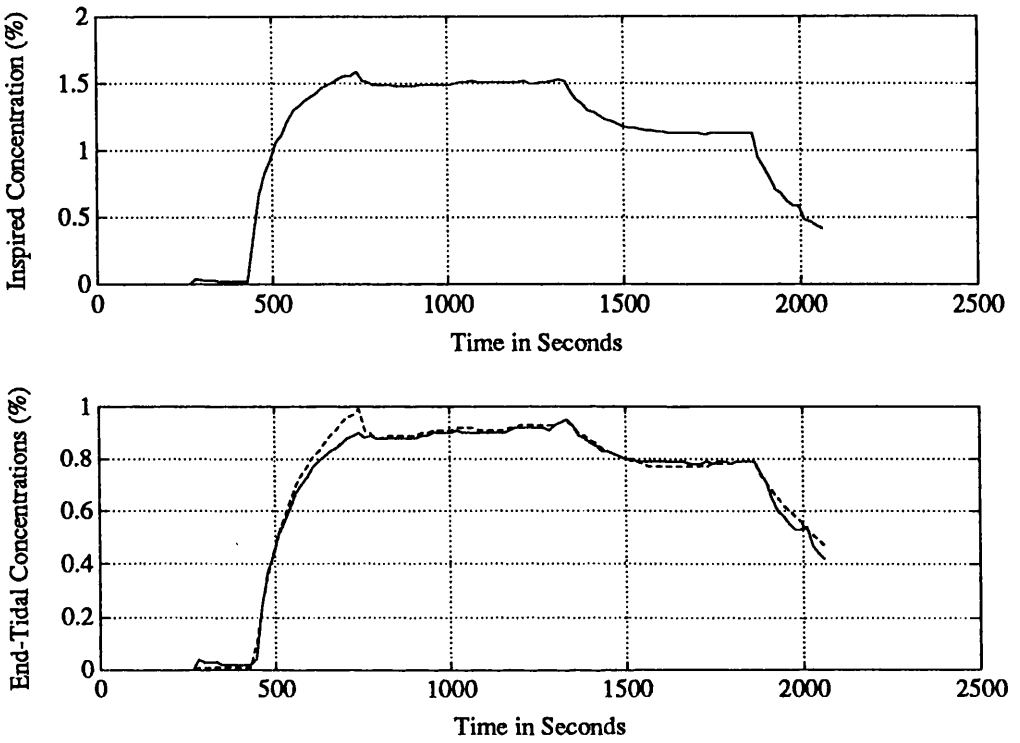

Figure 5.23: Test C: Inspired and End–Tidal Concentrations

tension is shown as a dashed line in the same figure. The cardiac output and brain tension estimates produced during this procedure are shown in Figure 5.24. It is apparent that from about 500 seconds until around 1000 seconds that cardiac output estimate is too low. In fact, a hard limit on the lowest cardiac output permissible in the estimator was set at 2.4 l/min. The cardiac output estimate held this value for some time during the early stages of this procedure. There are many potential sources of error in this case; the mass of the patient and the proportion of body fat were not precisely known, the operation took place with the patient face–down on the table which influences circulation and ventilation and, as in the previous case, the ventilation of the patient differed from that assumed by the model. The model assumed an alveolar ventilation of 4 l/min.

The patient was ventilated at 12 breaths per minute with a tidal volume of 0.65 litres. Deadspace can be estimated as being between 170 and 212 ml giving an alveolar ventilation of between 5.25 and 5.64 l/min. This can account for the systematically low cardiac output estimates.

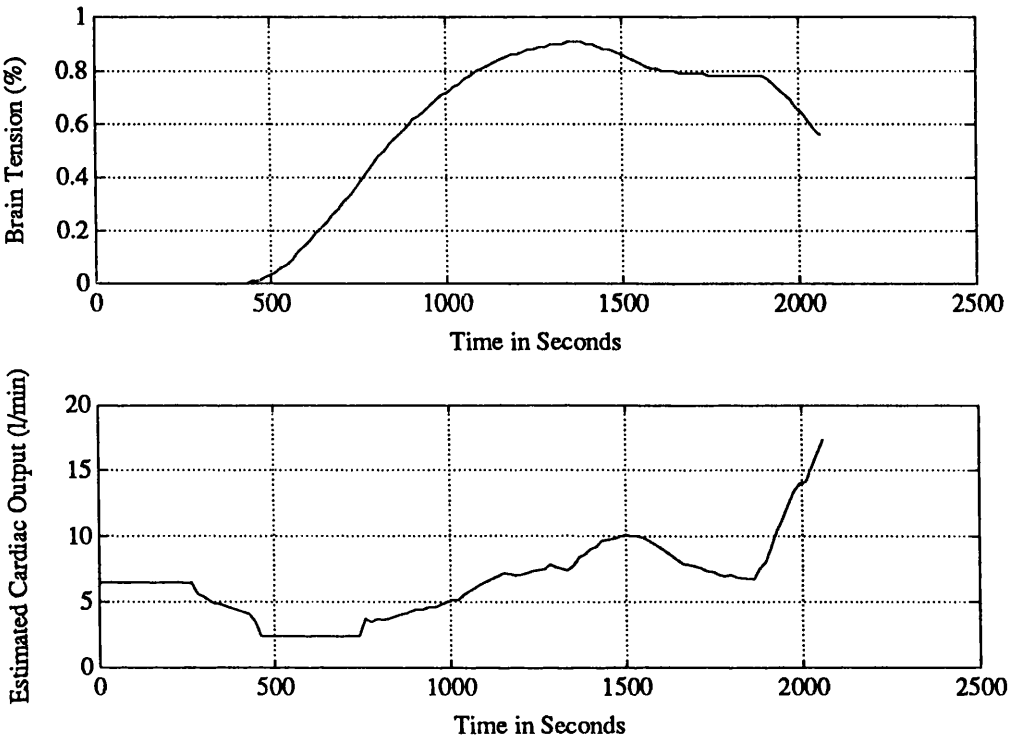

Figure 5.24: Test C: Brain Tension and Cardiac Output Estimates

5.4.4 Estimation Scheme Theatre Test Results: Version 2

It became apparent that the assumption of alveolar ventilation of 4 l/min for the estimation scheme model was inappropriate. This was therefore remedied by adding a menu box to the interface of the program which runs the estimation scheme. In this arrangement, the user could alter the alveolar ventilation in the box during a run of the estimator and this would be used to update the patient model used by the estimator. A limited number of tests have been performed

using this version of the estimator. Two of these are described below.

Test D

This procedure was a kidney transplant to a 57kg female patient. At the start of the procedure, the program was started with some in-line diagnostic code present. This interfered with the interface to the program and necessitated its removal and recompilation. The breathing circuit was then flushed and the estimator re-started. For completeness, the data gathered during the initial abortive stage has been included. The measured inspired and end-tidal concentrations of isoflurane in percent are shown in Figure 5.25 as solid lines. The estimator's matching

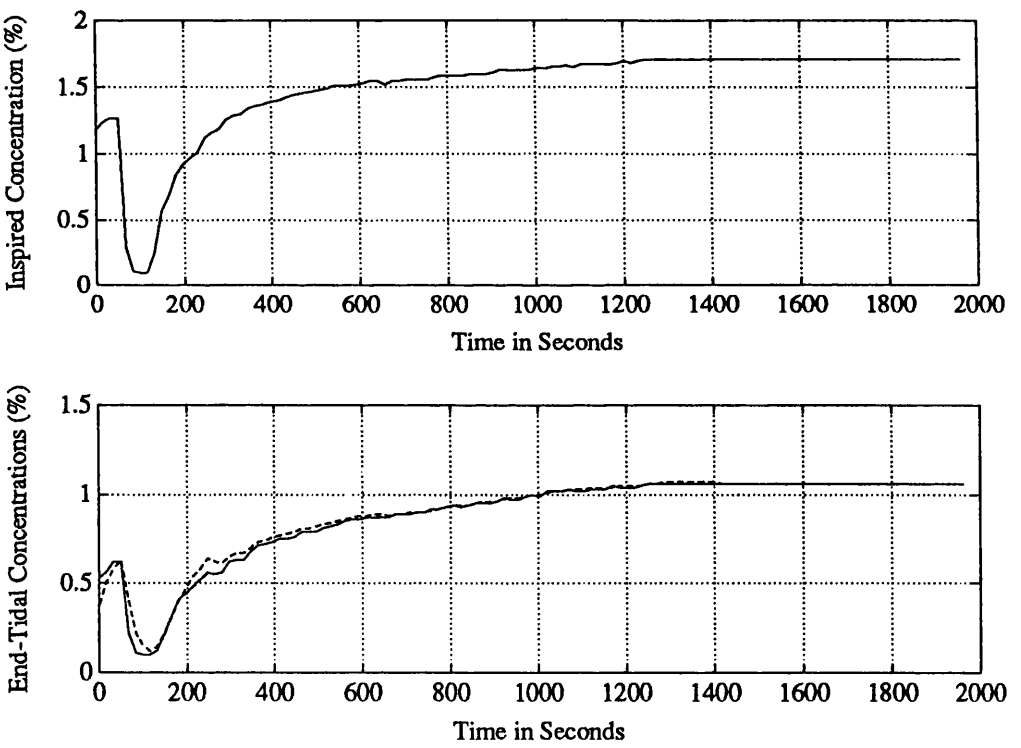

Figure 5.25: Test D: Inspired and End-Tidal Concentrations

of the end-tidal tension is shown as a dashed line in the same figure. The estimator was applied at the start of the procedure and was used for around 20 minutes. It is clear from the graphs of the estimated cardiac output (Figure 5.26) that the incorporation of better matched ventilation† has resulted in more stable,

† (values around 3.3 l/min were input)

physiologically realistic values. Regrettably, just after 1200 seconds, a data collection fault resulted in the estimator being presented with erroneous measured concentration values of about 1.7% inspired and 1.1% end–tidal. Because the estimator model's end–tidal concentration is still rising, the estimator increases cardiac output from this point onwards so as to match the measured end–tidal concentration. Disregarding cardiac output estimates after about 1200 seconds gives an indication of the viability of this approach.

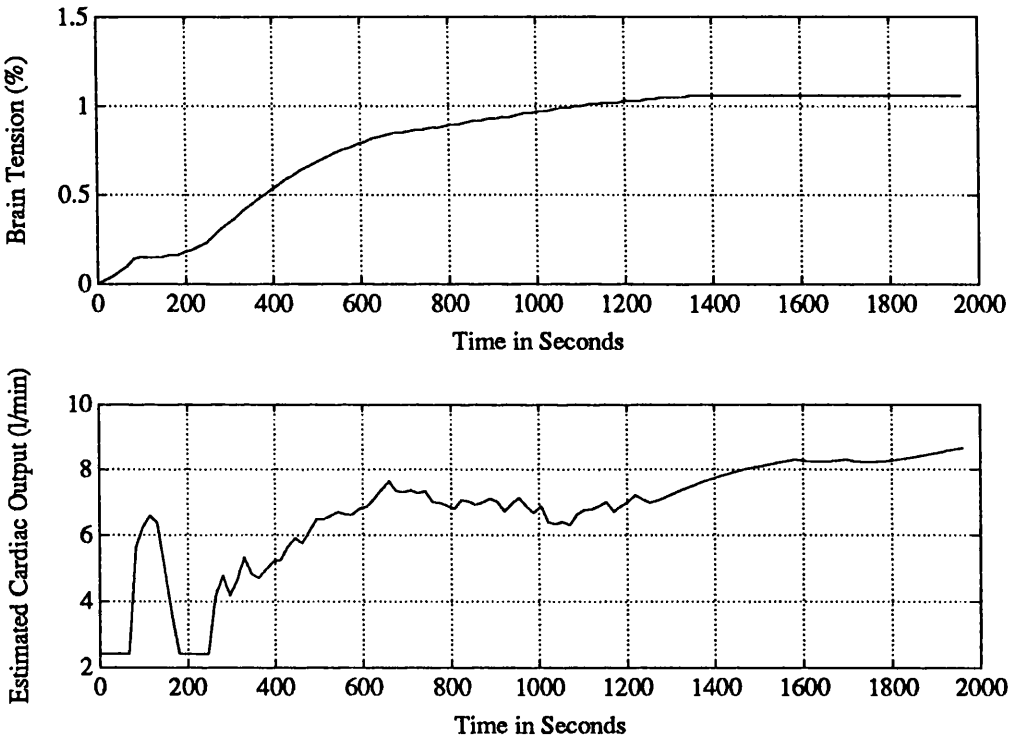

Figure 5.26: Test D: Brain Tension and Cardiac Output Estimates

Test E

This operation was carried out on a 50kg woman to perform a lymph node biopsy. The patient was assumed to have body fat in the same proportion as the standard woman described in the discussion of the estimator. Figure 5.27 shows the inspired and end–tidal measured concentrations as continuous lines on the upper and lower graphs respectively. The estimation scheme model end–tidal concentration is

shown as a broken line on the lower graph of Figure 5.27. It is apparent that the matching of the actual measured end-tidal concentration and that predicted by the estimator is good except in the initial and final stages of the test. The

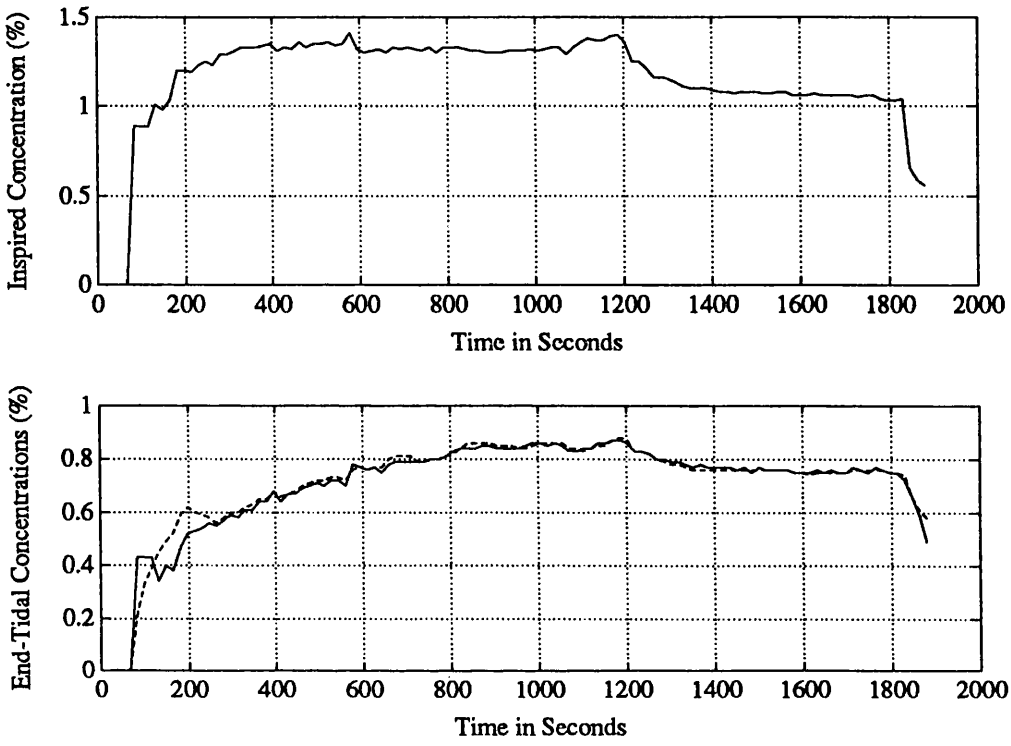

Figure 5.27: Test E:Inspired and End-Tidal Concentrations

cardiac output estimate for this test is shown in the lower graph of Figure 5.28. Following the presentation of data to the estimator, the cardiac output estimate is reduced to its lowest permitted value for a short period. During the period of good matching of end-tidal measurements and predictions, (from about 250 seconds to about 1800 seconds) the estimated cardiac output lies between 3 and 5 litres per minute. This was considered to be a realistic physiologic range for a patient of this size and condition. The good quality of the cardiac output estimate suggests that both the tissue groups and alveolar ventilation of the model are well-matched. It is possible that the cardiac output estimates are a little low but the error is small. An error of this size could easily be introduced by a slight underestimation of alveolar ventilation[†]. The brain tension estimate is shown in the upper graph of

[†] (values around 3 l/min were applied)

is shown in the upper graph of Figure 5.28. Given the quality of the cardiac output estimate, it seems probable that the brain tension estimate is reliable. At

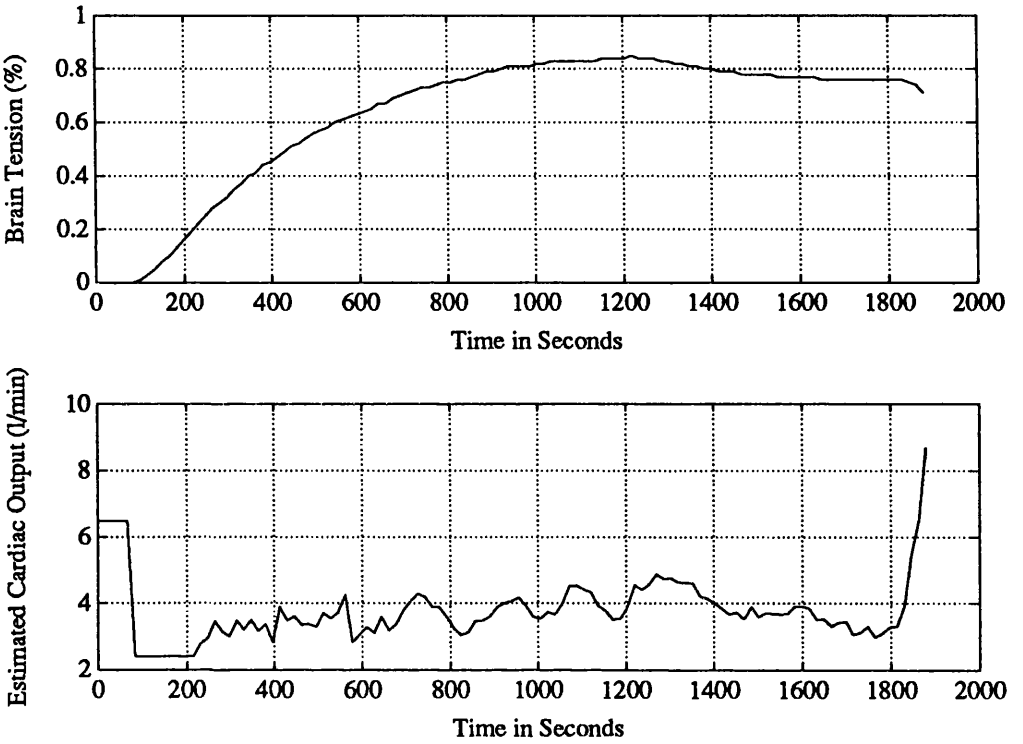

Figure 5.28: Test E:Brain Tension and Cardiac Output Estimates

the end of the procedure, the inspired concentration is reduced sharply and the end-tidal measured concentration follows a similar trajectory. The cardiac output estimate exceeds physiologically realistic values at this time. Although the cardiac output estimate is not entirely satisfactory at the start and end of this test, the performance of the estimation scheme between these times gave, in this case, 25 minutes of reliable performance. This illustrates the capacity of the approach, even in this prototypical form.

5.5 Discussion of Results

Without exception, in each of the practical tests conducted so far, the initial cardiac output estimates have been forced low in order to match the rise in

the measured end-tidal concentration. In a similar manner, in each test where the anaesthetic concentration is reduced at the end of the operation, the cardiac output has been forced up so as to match the fall of the end-tidal measurement. Of course, these events have occurred at the start and end of each test. While the errors in the cardiac output estimate after the initial phase and before the switch-off of the vaporiser have been explained, to a large extent, in consideration of model mismatches, this argument cannot be applied to the behaviour in the initial phase and after switch-off.

The source of these errors appears to lie in the measurements made by the Datex Ultima. Figures 5.16 and 5.17 show that the end-tidal measurement starts high in a primed circuit irrespective of whether the patient is primed or not. This would imply that the end-tidal measurement is altered by the inspired concentration. Figure 5.17 shows that when the vaporiser is switched off and the circuit fresh gas flow is increased so as to rapidly reduce the inspired concentration of volatile agent, the fall in end-tidal concentration follows that of the inspired concentration. This is not as expected. It seems possible, based upon these data that the measured end-tidal concentration is higher than the actual patient end-tidal concentration initially and lower than the actual value on reduction of the inspired concentration. If this is the case, the erroneous behaviour of the estimation scheme is a result of problems associated with the measurements made. This could be remedied by improving the quality of the measurement.

In conclusion, it has been demonstrated that it is possible to produce estimates of tissue tensions of anaesthetic using the estimation scheme described in this chapter. The reliable use of the scheme depends upon the accurate matching of the model used in the estimator to the patient and this concerns both the matching of tissue groups and alveolar ventilation. The tests performed have demonstrated, however, that physiologically realistic values can be produced by the estimator without the need for invasive measurements or extensive effort in

model matching.

A further useful property of the estimation scheme is that cardiac output is produced as an intermediate result. This quantity has real physiological meaning and a 'wrong' value is very apparent to the anaesthetist. It became apparent during the tests that the anaesthetists took a keen interest in the estimate of a *real* value by the scheme. This feature greatly enhanced the acceptability of the scheme to the anaesthetists.

Chapter 6

Modelling Homeostasis and the Stress Response in Anaesthesia

SUMMARY

This chapter describes a model developed to represent homeostasis and the stress response. First, the characteristics of homeostasis and the stress response are described. This is followed by discussion of the effects of general anaesthetics upon them. The motivation for, and development of, an explanatory model of homeostasis and the stress response are then described. The inclusion of drug effects within the model is discussed and results from a prototype implementation of the model are presented.

6.1 Physiological Systems

Anatomy is the study of body structures and the relationship between them. Physiology is the study of the function of, and interaction between body structures. The study of physiology involves consideration of activity at several levels of abstraction. These are summarised in Table 6.1 [129].

Level of abstraction	Description
chemical level	most fundamental
cellular level	most basic structural and functional units
tissue level	groups of similar cells performing a special function
organ level	sets of two or more tissues with special function
system level	groups of organs with a common function
organism level	a living individual

Table 6.1: Levels of Abstraction in Physiology

Considering function at system level is adequate to describe most of the physiologic processes which have relevance during anaesthesia. Tortora and Anagnostakos [129] list the following major body systems:

System	Components
Integumentary	skin,hair,nails,sweat glands, oil glands etc.
Skeletal	bones and joints
Muscular	skeletal muscle tissue
Nervous	brain, spinal chord, nerves, eyes, ears
Endocrine	glands that secrete hormones
Cardiovascular	blood, heart and blood vessels
Lymphatic	lymph, lymph vessels and structures with lymphatic tissue
Respiratory	lungs and respiratory passageways
Digestive	gastrointestinal tract and associated organs
Urinary	organs that produce, collect and eliminate urine
Reproductive	organs that produce, store and transport reproductive cells

Table 6.2: Physiological System of the Body

Each of these systems is involved in the maintenance and performance of bodily function at all times. During anaesthesia, however, the majority of significant effects and events can be explained in terms of the Nervous System, Endocrine System, Cardiovascular System and Respiratory System. In some cases, co–existing disease of the patient may necessitate consideration of other systems. For example, a patient with kidney disease is affected by drugs differently to other patients. This can be explained, to an extent, by consideration of the urinary

system which includes the kidneys.

6.1.1 The Nervous System

The nervous system consists of the brain, spinal column, nerves and sense organs. Functionally, the nervous system performs three types of task; sensory, integrative and motor. The sense organs of the nervous system respond to changes in the body and its external environment; this is the sensory function. The integrative function of the nervous system is the interpretation of the sensory information and determination of appropriate compensatory action. The motor function is the initiation of muscle contractions or glandular secretions in order to achieve compensation. The nervous system transmits information via nerves. Nerve conduction is fast and the nervous system can therefore respond quickly to changes.

The functions performed by the nervous system are wide–ranging and diverse. It is therefore divided into component sub–systems according to function as shown in Figure 6.1.

The central nervous system (CNS) consists of the brain and spinal column and is responsible for the overall control of the nervous system including the interpretation of sensory information and the determination of compensation.

The peripheral nervous system (PNS) consists of the nerves that connect the CNS to sensory organs, muscles and glands. Within the PNS, the afferent system is composed of nerves which conduct impulses from sensory organs to the CNS. The efferent or motor system consists of nerves travelling from the CNS to muscles and glands. The efferent system is further subdivided into the somatic nervous system and the autonomic nervous system. The somatic nervous system comprises nerves travelling from the CNS to skeletal muscle and is used to initiate and control movement. The autonomic nervous system consists of nerves travelling from the CNS to non–skeletal muscle such as that in blood–vessel walls, the

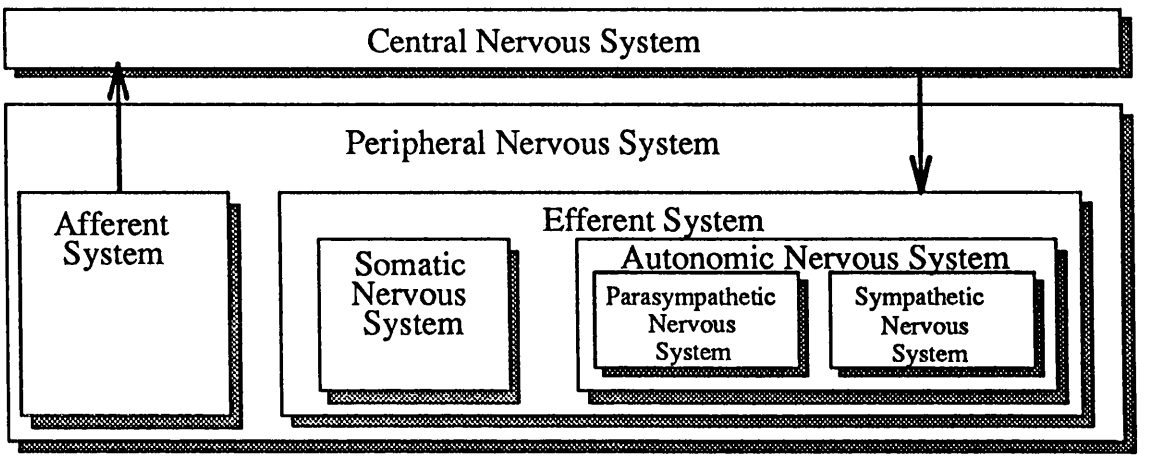

Figure 6.1: Illustration of Nervous System Components

gut and the heart, and also to glands. The activity of the non-skeletal muscle and glands is not considered to be consciously controllable and the autonomic nervous system is therefore considered to only involve involuntary activity. The autonomic nervous system is further divided into the parasympathetic nervous system and the sympathetic nervous system. Overall, the sympathetic nervous system is considered to stimulate or increase the activity of an organ and the parasympathetic nervous system is considered to inhibit or decrease activity. The effects of parasympathetic and sympathetic nervous system activity on various organs and organ systems is summarised in Table 6.3

6.1.2 The Endocrine System

The endocrine system is composed of the endocrine glands. The endocrine glands secrete hormones which enter the bloodstream and are thus carried to all the tissues of the body. A hormone is a chemical substance which acts as a messenger

Site	Sympathetic NS effect	Parasympathetic NS effect
heart		
SA node	increase heart rate	decrease heart rate
AV node	increase conduction speed	decrease conduction speed
His-Purkinje system	increase automaticity	
	increase conduction speed	
ventricles	increase contractility	
	increase conduction speed	
lungs		
bronchial smooth muscle	relaxation	contraction
GI tract		
motility	decrease	increase
secretion	decrease	increase
sphincters	contract	relax
bladder		
smooth muscle	relax	contract
sphincter	contract	relax
eye		
radial muscle	dilate pupil	
sphincter muscle		constrict pupil
ciliary muscle	far vision	near vision
liver	glycogenolysis/gluconeogenesis	glycogen synthesis
salivary glands	increase salivation	large increase in salivation
arterioles		
coronary	constrict (alpha receptors)	relax ?
	relax (beta receptors)	relax
skin and mucosa	constrict	relax
skeletal muscle	constrict (alpha)	relax
	relax (beta)	relax
pulmonary	constrict	relax

Table 6.3: Table showing the relative effects of Sympathetic and Parasympathetic Nervous System Activity

to the tissues of the body. The function of a hormone will fall into one of the following categories:

1. to regulate chemical composition and volume of the body's internal environment,
2. to respond to severe changes in environmental conditions thereby allowing the body to cope with stressors such as infection, dehydration, bleeding and emotional stress,
3. to ensure smooth growth and development,
4. to contribute to reproductive processes, and
5. to regulate metabolism and energy balance.

The effects of hormones take much longer to occur than the effects of the nervous system, but those effects are likely to be present for much longer. Neuronal mechanisms therefore allow the short–term fast responses required to cope with minute–to–minute or faster environmental disturbances. Hormonal, or endocrine, responses provide long–term regulation.

The release of most hormones is governed by the body's own feedback control loops. There are three possibilities.

1. The endocrine gland releases hormone in response to changes in the variable which the hormone affects. This is the case for the control of blood calcium by parathyroid hormone.
2. The endocrine gland releases the hormone in response to nerve impulse stimulation of the gland. This is the case for adrenaline.
3. The hypothalamus (part of the brain) releases a regulating hormone (or regulating factor when the chemical structure is unknown) into the blood.

The regulating hormone either stimulates or inhibits the release of the main hormone by another endocrine gland. This is the case for human growth hormone which is released from the pituitary gland according to blood levels of Growth Hormone Releasing Hormone and Growth Hormone Inhibiting Hormone.

Many hormones have little chance to cause significant changes or effects during the timescale of anaesthesia although some have a major impact upon the recovery from anaesthesia. A summary of relevant hormones and their main effects is given in Table 6.4.

Hormone	Effects
Adrenaline and Noradrenaline	Increase heart rate and contraction strength, constrict blood vessels, dilate respiratory passageways, increase muscle efficiency
Antidiuretic Hormone	Prevents excessive urine production, constricts arterioles in severe bleeding
mineralocorticoids	increase blood water and sodium, decrease blood potassium
glucocorticoids	promote normal metabolism, resistance to stress and reduce inflammation

Table 6.4: Hormones Relevant to Anaesthesia and their Effects

Adrenaline and noradrenaline are both secreted by the medulla (middle) of the adrenal glands. There are two adrenal glands, one above either kidney. Noradrenaline and adrenaline cause effects similar to those produced by sympathetic nervous system stimulation and are therefore termed *sympathomimetic*. The release of adrenaline and noradrenaline results from stimulation of the adrenal glands by the sympathetic nervous system. Therefore, environmental events which cause stimulation of the sympathetic nervous system also cause the release of adrenaline and noradrenaline. These events include physical and emotional stresses.

Antidiuretic hormone is secreted by the posterior pituitary in response to nerve impulses originating in the hypothalamus. ADH is secreted in response to a number of stimuli including; low water concentration in the blood, pain, stress, trauma and anxiety.

Mineralocorticoids are a group of related hormones secreted by adrenal cortex (the outer layers of the gland). There are at least three mineralocorticoids but 95% of secretion is of the hormone aldosterone. The secretion of aldosterone is controlled by several mechanisms including decreased blood volume and increased potassium ion concentration in the fluid surrounding cells.

Glucocorticoids are a group of hormones which influence metabolism and the resistance to stress. Glucocorticoids include hydrocortisone, corticosterone and cortisone. Hydrocortisone contributes 95% of glucocorticoid effects. The glucocorticoids are secreted so as to maintain normal metabolism but are also secreted in response to stress. The effects of glucocorticoids which are useful in responding to stress are; the raising of blood sugar levels and the suppression of the inflammatory response.

6.1.3 The Cardiovascular System

The cardiovascular system consists of the blood, heart and blood vessels. The cardiovascular system is responsible for the delivery of oxygen and nutrients to cells and the removal of carbon dioxide and wastes from them. The cardiovascular system also plays a role in regulating body temperature through changes in skin blood flow. Components within the blood promote blood clotting in wounds, help to maintain acid–base balance and help to provide resistance to disease.

Within the cardiovascular system, the heart acts as a pump and maintains circulation of the blood in blood vessels. The heart has two ventricles and two atria. The right atrium is a chamber which fills with blood from the veins. Once during each heart cycle, the volume of blood in the right atrium is transferred to

the right ventricle. The right ventricle pumps blood into the pulmonary arteries which enter the lungs. In the lungs, as will be summarised later, oxygen enters the blood and carbon dioxide leaves it. Following passage through the lungs, blood enters the left atrium. The left atrium transfers blood to the left ventricle. The left ventricle pumps blood into the aorta which is the largest component of the arterial tree.

Blood vessels are responsible for the transport of blood around the body. The types and characteristics of blood vessels are summarised in Table 6.5. The

Type	Characteristics
Elastic arteries	narrow walls in comparison with diameter, elastic
Muscular arteries	thick muscle walls in comparison to diameter
Arterioles	tiny arteries with limited muscle around them
Capillaries	smallest vessels, allow exchange of nutrients and wastes with cells
Venules	smallest veins, combination of several capillaries
Veins	narrower walls than arteries and less muscle

Table 6.5: Summary of Blood Vessel Types

circulation of the blood around the tissue of the body is schematically represented in Figure 6.2.

6.1.4 The Respiratory System

The respiratory system includes the nose, pharynx, larynx, trachea (windpipe), bronchi and the lungs. Respiration is the process of gas exchange between the atmosphere, blood and cells. Respiration is subdivided into pulmonary ventilation (inhalation and exhalation) , external respiration (gas exchange between the lungs and the blood) and internal respiration (gas exchange between the lungs and cells). The respiratory system is obviously directly involved in both pulmonary ventilation and external respiration.

Gas passing into the lungs first enters the trachea and then either into the left or right primary bronchus. A primary bronchus divides into several secondary

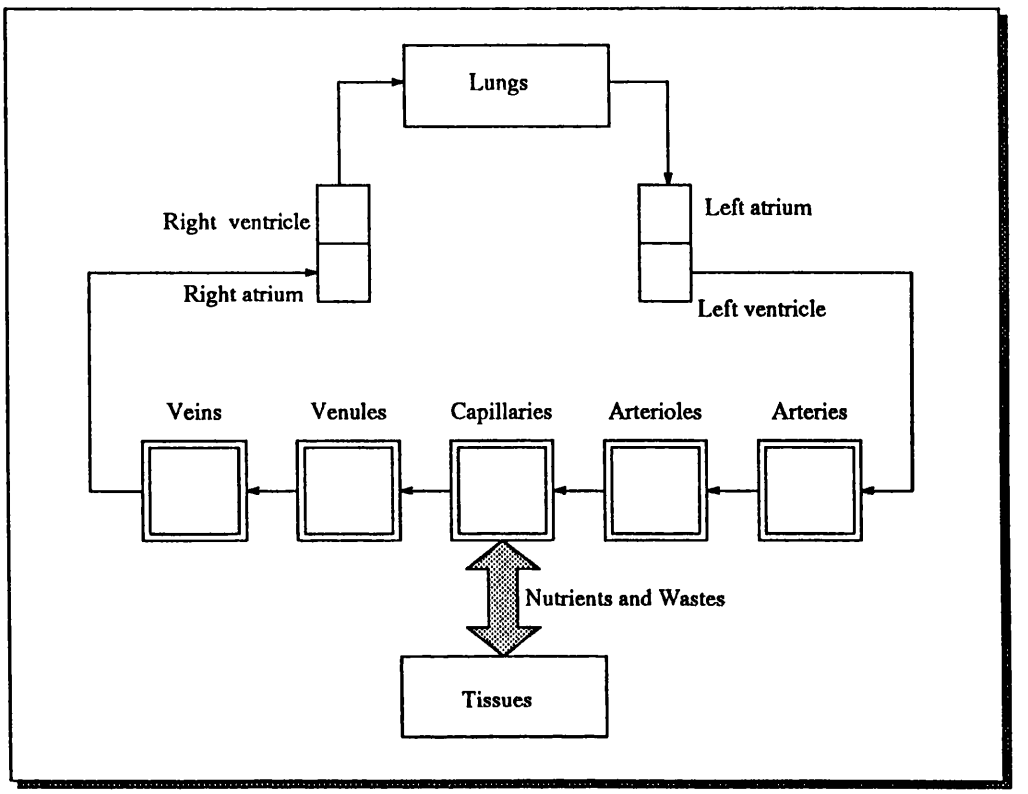

Figure 6.2: Blood Flow in the Heart and Blood Vessels

bronchi and these divide into tertiary bronchi. Tertiary bronchi divide into bronchioles. The bronchioles branch into terminal bronchioles. The division of airways from the trachea to the terminal bronchioles is called the bronchial tree. Each terminal bronchiole divides into microscopic respiratory bronchioles and these, in turn, divide into alveolar ducts. Alveoli surround the alveolar ducts. Gas exchange between the lungs and the blood takes place when oxygen and carbon dioxide diffuse between the gas in the alveoli and the blood in the capillaries which run through the alveoli. The membrane between the alveolar gas and the capillaries around the alveoli is about 0.5μm thick. There are estimated to be about 30 million alveoli together creating a surface area of around 70 m^2 for the exchange of gases between the lungs and blood.

6.2 Homeostasis

The cells of the body contain fluid and are surrounded by fluid. The fluid within the cells is called intracellular fluid and the fluid outside the cells is called extracellular fluid. Extracellular fluid exists either between the cells as interstitial fluid or within blood vessels as intravascular fluid. These are illustrated in Figure 6.3.

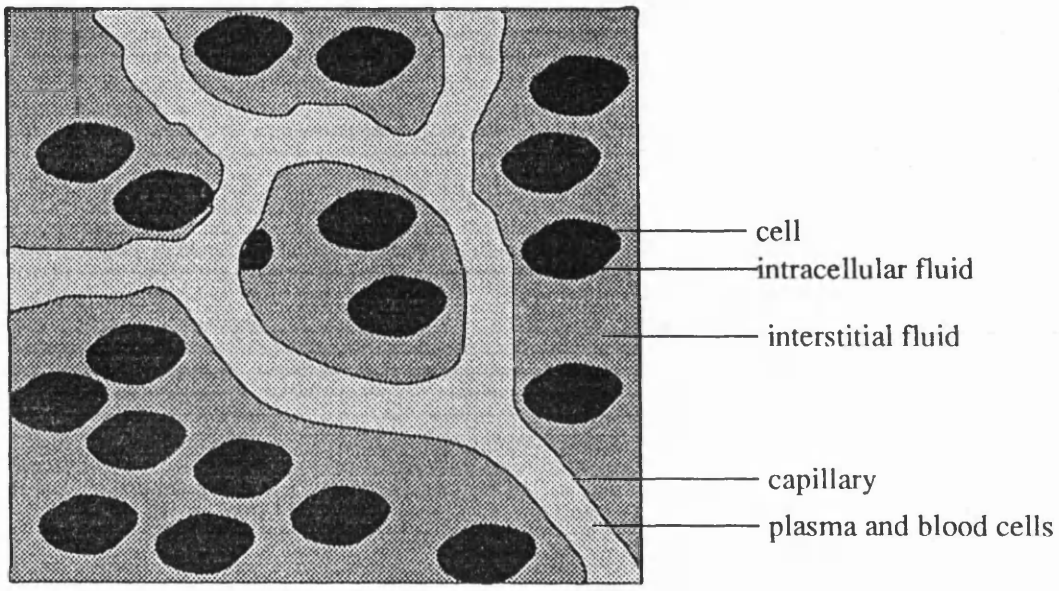

Figure 6.3: Illustration of Body Fluid Subdivisions

Homeostasis is the maintenance of the body's internal environment within physiological limits. The existence of homeostasis requires that the internal environment;

1. contains optimum concentrations of gases, nutrients, ions and water,

2. has an optimal temperature

3. has an optimum pressure

A *stress* is any stimulus which creates an imbalance in the internal environment. Some stresses result from external environmental changes such as extremes of temperature, oxygen deficiency or sudden noises. Others have internal origins

and include pain and high blood pressure. The body has many well–developed regulatory loops which maintain homeostasis. These make use of components in all of the systems listed in Table 6.2.

In the context of anaesthesia, many of the clinical signs reflect the activity of the homeostasis loops or of the stress response. Of the measurements made during anaesthesia, the majority are concerned with either the cardiovascular or respiratory systems although the blood volume affects each. The following sections describe the control of circulation, respiration and the blood volume by the body's control loops.

6.2.1 Control of Circulation

Blood flows through the heart as shown in Figure 6.2. Cardiac output is the total blood flow out of either ventricle and is also the product of heart rate and stroke volume. The stroke volume is the amount of blood ejected by a ventricle during its contraction. The stroke volume is the difference between the amount of blood in the ventricle prior to its contraction (end–diastolic volume) and the amount remaining after contraction (end–systolic volume). The end–diastolic volume can be increased as a result of increased venous pressure which causes greater filling of the ventricles. As heart rate increases, less time is available for the filling of the ventricles and end–diastolic volume will decrease. The end–systolic volume depends upon arterial pressure. The pressure in the ventricle must exceed that in the arteries before blood can flow out of the ventricle into the arterial tree. Raised arterial pressure therefore increases end–systolic volume. Increased force of contraction of the heart muscle causes greater flow from the ventricle into the arterial tree and a reduction in end–systolic volume.

The body has control loops which monitor and regulate both the arterial and venous pressures. These loops employ both neuronal and hormonal mechanisms and can be summarised as follows:

Control of Arterial Pressure

Pressure sensitive cells (baroreceptors) exist in the aorta and in the carotid arteries (which supply blood to the head). The carotid baroreceptors and the associated carotid sinus reflex are involved in the maintenance of normal blood pressure in the brain. The aortic baroreceptors and the associated aortic reflex are involved in the regulation of blood pressure elsewhere in the arterial system.

Increases in blood pressure cause baroreceptors to generate impulses at a higher rate. Impulses from arterial baroreceptors are conducted to the medulla (in the brain stem) and these influence the activity of the cardioacceleratory centre, cardioinhibitory centre and the vasomotor centre. A decreased blood pressure causes a reflex increase in the activity of the cardioacceleratory centre and of the vasomotor centre. The cardioacceleratory centre causes an increase in heart rate and force of contraction thus increasing cardiac output. The vasomotor centre causes constriction of veins, small arteries and arterioles. The constriction of veins increases the flow of blood into the heart thus increasing end–diastolic volume which helps to raise stroke volume. The increase in heart force of contraction reduces the end–systolic volume thereby further increasing stroke volume. The increase in heart rate in combination with the increased stroke volume, increases cardiac output. The constriction of small arteries and arterioles increases peripheral resistance. The increased cardiac output flowing through the increased peripheral resistance increases arterial pressure. These reflexes are responsible for the minute–by–minute regulation of blood pressure.

Control of Venous Pressure

The atria of the heart contain baroreceptors which are sensitive to the lower venous pressures. Increases in venous pressure result in reflex dilation of blood vessels and also a reflex increase in heart rate (Bainbridge Reflex). These changes reduce venous pressure in the short term. A lowered venous pressure results in reciprocal

changes.

In the longer term, the vasodilation or vasoconstriction caused by the atrial reflex also constricts or dilates the arteries entering the kidney. This affects the rate of water loss by the kidney due to changes in perfusion pressure. A further effect of the atrial reflex is modulation of the secretion of anti–diuretic hormone by the hypothalamus. This further influences the water loss by the kidney.

The baroreceptor and atrial reflexes are responsible for the minute–by–minute regulation of arterial and venous pressure. Other factors can also cause changes through a combination of effects on the heart and blood vessels. For example, raised potassium ion or sodium ion concentrations in plasma decrease heart rate and strength of contraction. Increased body temperature increases heart rate and decreased temperature decreases it. Some effects are caused by changes in hormone levels and these are summarised in Table 6.6.

Hormone	Effects
adrenaline	increase heart rate, force of contraction and vasoconstriction
noradrenaline	as above
anti–diuretic hormone	promotes water loss can cause vasoconstriction
angiotensin II	causes vasoconstriction and release of aldosterone
aldosterone	causes water reabsorbtion

Table 6.6: Hormonal Effects on Blood Pressure

6.2.2 Control of Respiration

Respiration ensures that the cells of the body are supplied with oxygen and have carbon dioxide removed from them. Although it is possible, to an extent, to consciously control respiration, the regulation of respiration normally occurs subconsciously. Regulation maintains levels of oxygen and carbon dioxide in the blood. Carbon dioxide levels are reflected in the concentration of hydrogen ions and it is likely that respiration control loops are sensitive to these.

Cells sensitive to levels of chemicals or ions are termed chemoreceptors. Within the medulla, a chemosensitive area is sensitive to carbon dioxide levels. Chemoreceptors in the carotid arteries and the aorta are sensitive to both carbon dioxide and oxygen levels. Increases in blood carbon dioxide cause reflex increases in the rate and depth of respiration allowing more carbon dioxide to be removed from the body and blood levels to be returned to normal.

The chemoreceptors are much less sensitive to arterial oxygen. The normal partial pressure of oxygen in the blood is about 105 mmHg but reflex increase in respiration due to lowered oxygen partial pressure do not occur until about 50 mmHg. The respiratory control centres are responsible for generating a regular breathing rhythm and for changing the rate and depth of respiration. This is achieved by altering the activity of the diaphram and intercostal muscles which are used in respiration.

6.2.3 Control of Blood Volume

The volume of blood in the body reflects the body's overall fluid balance. The inate sensitivity of cells to their environment dictates that the volume and concentration of body fluids is regulated precisely. The control of blood volume takes place in parallel with the control of venous pressure which was discussed earlier. Increased blood volume causes an increase in venous pressure and cardiac output. This is compensated for, in the short term, by reflex vasodilation and reductions in heart rate and contractility. The long term reduction requires the reduction of blood volume. This is accomplished through increased elimination of water by the kidney. This occurs due to two mechanisms; the vasodilation of the kidney arteries which increases kidney filtration pressure and water elimination and, the reduced secretion of anti-diuretic hormone (ADH) which further enhances water elimination. A reduced blood volume results in cardiac and blood vessel changes to compensate in the short term but long term compensation requires the addition of

fluid either by ingestion (the normal process) or by intravenous administration (as used in theatre). The mechanisms involved in the production of vasoconstriction or vasodilation and in the regulation of ADH secretion were described earlier.

6.3 The Stress Response

The hypothalamus is sensitive to changes in the chemistry, temperature and pressure of the blood, and is also directly connected to the emotional and other brain centres. In being responsive to both physical and emotional stresses, the hypothalamus coordinates the stress response. The stress response or General Adaptation Syndrome (GAS) can be initiated by any extreme or unusual stress. While homeostasis loops operate so as to maintain the internal environment, the GAS overrides these to prepare for an emergency. The GAS is considered to have three phases;

1. The initial or alarm response,
2. the resistance reaction, and
3. exhaustion.

The alarm response is characterised by activation of the sympathetic nervous system and the adrenal medulla. This produces a very quick but short–acting response which prepares the body for vigorous physical activity. The effects of the alarm response include increased heart rate and force of contraction, vasoconstriction of blood vessels aside of those in skeletal muscle, the brain and heart, vasodilation of the blood vessels in muscle, the brain and heart, dilation of airways, increased respiration rate, and sweating.

The resistance reaction follows the alarm reaction and relies upon hormones to achieve its goals. The most important hormones are the glucocorticoids and mineralocorticoids which are produced and secreted by the adrenal cortex. These

hormones act so as to maintain blood volume, increase blood sugar, decrease inflammation and sensitise blood vessels to stimuli which cause their constriction.

If the resistance reaction fails to overcome the stressor, the exhaustion stage occurs. This is largely due to the excessive elimination of potassium due to mineralocorticoid activity.

In the absence of anaesthesia, surgery would elicit an alarm response. Inadequate anaesthesia may therefore result in some remnant alarm response becoming apparent. The resistance reaction is essential to a patient's recovery from surgery.

6.4 Drug Effects upon Homeostasis and the Stress Response

A general anaesthetic is administered so as to alter central nervous system activity and produce anaesthesia. However, general anaesthetics have effects in tissues other than the central nervous system and produce other effects as well as anaesthesia. These include effects upon the regulatory loops of the body. The effects are specific to the agents, or chemical group of agents used but are also dose–dependent. The majority of experimental investigation has resulted in empirical description of the effects without explanation of the possible mechanisms. The best explained of the effects are those which alter cardiovascular and respiratory behaviour. The effects of general anaesthesia upon these are summarised below.

6.4.1 The Effects of General Anaesthetics upon the Cardiovascular System

Based upon observation of the effects of inhaled anaesthetics, many circulatory changes are common to to all anaesthetics. Stoelting [27] reviews the effects of the

most commonly used anaesthetics on blood pressure, heart rate, cardiac output, right atrial pressure and peripheral resistance. These effects are summarised in Table 6.7 where changes are from awake values.

Drug Combination	arterial pressure	heart rate	cardiac output	right atrial pressure	peripheral resistance
halothane	decrease	none	decrease	increase	none
enflurane	decrease	increase	decrease	increase	decrease
isoflurane	decrease	increase	small dec.	small inc.	decrease
nitrous oxide	none/inc.	small inc.	increase	increase	small inc.

Table 6.7: Effects of General Anaesthetics upon Cardiovascular Variables

Administration of a volatile agent, such as isoflurane, in nitrous oxide results in a lesser blood pressure decrease than that produced by isoflurane alone. This is due to the slight excitatory effects of nitrous oxide.

The mechanisms of effect of volatile agents are incompletely understood and, although some mechanisms have been discovered, these are not common to all agents. Changes in cardiac output, heart rate and blood pressures can be created by changes in peripheral vascular resistance, the performance of the heart or the performance of the regulatory loops concerned with arterial and venous pressure.

A review of the anaesthetic effects upon the regulatory loops concerned with circulation by Prys–Roberts [130] suggests that anaesthetic agents may sensitise baroreceptors thereby causing more frequent discharges in response to blood pressure changes. The ability of volatile agents to depress the sympathetic nervous system to a greater extent than they depress the parasympathetic nervous system is also noted. Prys–Roberts suggested that volatile agents could produce both a 'resetting' of the baroreceptor reflexes to a new equilibrium pressure and also cause a decrease in the sensitivity of the regulation to changes in pressure.

Further effects of relevance are generated by the direct effects of volatile agents upon the heart and blood vessels. Some volatile agents, especially halothane and enflurane, cause depression of the heart muscle therefore impairing its activity.

The reduction in cardiac output produced during anaesthesia with these agents (see Table 6.7) is consistent with these effects. In contrast, isoflurane has very little depressant effect upon the heart, and cardiac output is relatively constant during isoflurane anaesthesia. The effects of anaesthetic agents on the heart have been reviewed by Smith [131]. An editorial by Marty and Reves [132] discusses the effects of anaesthetics upon the baroreflex control of arterial pressure. The work of Kortly et al. [133] describes the steady–state value and sensitivity of blood pressure regulation for anaesthetic combinations using isoflurane. The work of Takeshima and Dohi [134] compares the steady–state value and sensitivity of the baroreflexes before anaesthesia, during anaesthesia, during anaesthesia and surgery and during recovery after anaesthesia for isoflurane and enflurane. They found that the sensitivity of the baroreflex response increased following the onset of surgery compared to that prior to the onset of surgery with isoflurane anaesthesia. The steady–state arterial pressure also increased at this time. The authors reasoned that isoflurane depressed the sympathetic nervous system and this caused the reduction in arterial pressure, but that the onset of surgery caused further stimulation of the sympathetic nervous system and partial reversal of baroreflex depression.

The effects of general anaesthetic agents on the circulation and cardiovascular system are therefore dependent upon the agents used and may affect combinations of baroreceptors, brain centres, the heart and blood vessels. Surgical stimulation can result in additional sympathetic nervous system activity to increase cardiovascular variables but individual values reflect the existing compensation for physiological imbalances, the effects of the anaesthetic and the effects of surgical stimulus.

6.4.2 The Effects of General Anaesthetics upon the Respiratory System

General anaesthetics cause alterations in the function of respiratory regulation loops. The effects of inhaled anaesthetics on respiration and respiration control are summarised by Stoelting [27]. Nitrous oxide, halothane and enflurane cause dose–related increases in respiration rate. Isoflurane causes an increase in respiration rate in concentrations up to 1 MAC[1] (minimum alveolar concentration) but further increases in dose cause no further change in respiration rate until the inhibition of medullary activity at much higher doses.

Associated with the increases in respiration rate are decreases in tidal volume. The overall alveolar ventilation may therefore be reduced as described in equations 2.1 and 2.2. Arterial carbon dioxide increases and the ventilatory response to this decreases with higher doses. The presence of surgical stimulation causes an increase in minute volume and a corresponding decrease in arterial carbon dioxide. It should be noted that the ventilatory response to low arterial oxygen is completely abolished by anaesthetic concentrations of only about 0.1 MAC.

The effects of general anaesthetics upon respiration are thought to reflect depression of the ventilatory control centres of the medulla although abolition of the ventilatory response to low arterial oxygen may indicate an effect of these agents upon the chemoreceptors. A further action of some agents e.g., halothane, is to alter the function of the intercostal muscles which are used in breathing. It is once again apparent that general anaesthetics can alter respiration by acting at combinations of the tissue sites involved in its control and that these effects are agent specific.

[1]the concentration required to prevent movement in response to incision in 50% of the population

6.5 Quantitative Models of the Circulation and Respiration

The physiologic processes involved in the regulatory and protective reflexes of the body are complex and interact significantly. The effects of drugs on these processes adds further interaction. Despite this, some workers have successfully represented the interactions between the circulatory and respiratory systems and drugs.

The multiple model structure suggested by Beneken and Rideout [44] consisted of one sub–model for circulation and another for the transport of a material in the circulation. Beneken and Rideout, using carbon dioxide transport as an example, suggested a structure for the incorporation of baroreceptor and chemoreceptor reflexes within a multiple model. The model of Smith, Zwart and Beneken [100] [43] incorporated the effects of halothane on circulation. The model of Fukui and Smith [41] [42] had three sub–models, one for each of circulation, ventilation and drug transport. The model represented the interaction between ventilation, circulation and the effects of halothane. The respiratory and circulatory performances of the model are altered by the presence of halothane. The respiratory and ventilatory changes, in turn, alter the further uptake and distribution of halothane.

The model used by Schwid [101] used the multiple model structure of Fukui and Smith and incorporated the effects of more drugs. The model described by Schwid and O'Donnell [135] incorporates both inhaled and injected drugs and their effects. The pharmacokinetics of the injected drugs are represented by simple two compartment models, and their effects by simple empirical relations. The interaction between drug effects in a tissue is assumed to be additive. This model has been used as the basis of a simulator for anaesthesia for the training and assessment of anaesthetists [135].

A model of the cardiovascular system including major blood vessels, the heart and regulatory reflexes has been developed by Leaning et al. [136]. This model represents arteries as elastic vessels and veins similarly except that they are collapsible if the volume of blood within them decreases. The heart is modelled as four chambers with time–varying elastance. The heart model includes representation of the timing of cardiac events. The effects of gravity upon the blood vessels and blood pressure has also been included in the model.

Baroreceptor reflexes were modelled to include effects both proportional to the pressure and also to the rate of change of pressure. To establish the effect of drugs, the circulation model was used to generate the drug concentrations at various sites and empirical relations were then used to establish the effect upon heart rate, peripheral resistance, myocardial contractility and venous volumes and compliances.

In validating the model [137], the authors compared the predictions of the model with experimental data for circulatory changes caused by physiological and pharmacological events. They concluded that the model did not predict behaviour correctly over the desired range of application and that these deviations were due to inadequacies in the model of baroreceptor reflexes. The modelling inadequacy was due to lack of understanding of such reflexes.

6.6 Qualitative Descriptions and Models of Physiology

The range of individual responses to physiologic and pharmacologic changes exhibited by humans precludes quantitative description of effects and mechanisms in all individuals. The majority of models used in physiology are therefore qualitative and descriptive. As an example, the earlier sections of this chapter, which describe the regulatory and protective reflexes of the body, use qualitative

description. To a large extent, these models allow the understanding of many processes without any need for quantification.

Some other models related to physiology have employed Qualitative Reasoning and Qualitative Simulation in order to make assertions and predict behaviour in the absence of quantitative information. Applications of Qualitative Reasoning include the KARDIO system [138] and the work involving Hunter et al. [139] [140] [141] [142].

6.7 Trade-offs between Model Complexity, Applicability and Utility

As discussed, there is a spectrum of models in physiology which range from qualitative, textual, empirical description of events or changes through to fully parameterised, quantitative models of circulation, respiration and pharmacology.

The simpler models provide adequate description of expected changes in a large range of individuals and are readily understood and applied. Such models may, however, prove inadequate when explanation of the interaction between changes is required.

The fully–parameterised, quantitative models provide an opportunity to represent the limit of current understanding and to reveal weaknesses in understanding. For example, the cardiovascular system model described by Leaning et al. [136][137] highlighted the incomplete understanding of central nervous system mechanisms for controlling circulation. Unfortunately, these models require a very large number of parameters in order to make quantitative predictions (the model of Leaning et al. had 178 parameters). Parameterising such a model to match an individual or subrange of individuals is therefore not practical.

Intuitively, a compromise is possible between the simplicity of qualitative description and the complexity of the quantitative models. In the context

of anaesthesia, the anaesthetist does not form quantitative predictions for the values of cardiovascular and respiratory variables. The anaesthetist is aware of physiological regulatory and protective mechanisms and also of the effects of anaesthetic and other drugs. This awareness and understanding, along with clinical experience, allows the successful and effective provision of anaesthesia for patients.

The following sections introduce a model intended to represent the interactions between physiologic and pharmacologic changes and the clinical signs of anaesthesia.

6.8 A Model of Homeostasis and the Stress Response

The previous sections have described the physiologic processes which are involved in the regulation of the physiological state and, the response of the body to extreme stimuli. The effect of general anaesthetics upon these processes has also been described along with some of the mechanisms of action. Unfortunately, description of these loops is normally given as text. In this form, it is difficult to differentiate between structural and functional components and their areas of interaction. In an attempt to resolve these problems, a model of homeostasis and the stress response has been developed to satisfy the following aims;

1. To predict changes in clinical signs resulting from changes in the physiological state.

2. To represent the structural (anatomical) elements of the reflex loops.

3. To represent the functional (physiological) aspects of the structural elements.

4. To illustrate areas of interaction between reflex loops.

5. To allow iterative refinement of the model as more understanding is developed.

Because the description of the regulatory loops and the stress response is most commonly qualitative and textual and because of the difficulty associated with quantitative models of this this form, it was decided that the model should use qualitative values. Similarly, because experimental and theoretical results tend to describe the behaviour of loops in isolation, it has been decided that the model should serve to highlight interactions but the modelling of these interactions has not been attempted due to the lack of information. Given these criteria, the model is then explanatory[2].

6.8.1 Model Development — Understanding the Processes

The author has no formal experience of physiology or pharmacology. Because the development of a model requires an adequate level of understanding of the system to be modelled, the development of a model of homeostasis and the stress response necessitated two tasks:

1. The development of an understanding of the appropriate physiology.

2. The modelling of this understanding.

The first of these tasks was considered to be the most important because it determined the limits of the second. The development of an understanding took place in several stages. Initially, basic physiology textbooks such as [129] [143] [27] were consulted. More specialised texts such as [144] [130] [145] [146] [147] were then chosen so as to enhance the depth of understanding. At this point, it became apparent that to understand the physiological descriptions required

[2]Leaning et al. [136] suggest that a model may be descriptive, predictive, explanatory or pragmatic

a basic degree of familiarity with anatomical and physiological terms. A set of diagrams was therefore produced by the author to accomplish the following:

1. Familiarisation with anatomical and physiological terms.
2. Presentation of the understanding of each loop.
3. Identification of other determining factors.
4. Provision of a platform for discussion and refinement of understanding.

These diagrams have been included in Appendix B. Following their production, they were discussed with Dr. D.P. Gilmore[3] and Dr. A.J. Asbury[4]. The diagrams proved an effective means of satisfying the aims for which they were developed.

6.8.2 Model Development — Representing the Loops

The representation of the loops involved in homeostasis and the stress response should allow the important features of each loop and the common features of loops to become apparent. To an extent, anatomy and physiology already highlight many of the important features. Physiology describes the existence of receptors, integrative centres and effectors. A receptor is sensitive to changes in the internal or external environment of the body e.g., a pressure, a temperature or the chemical composition. The receptor generates nerve impulses which often pass along nerves to an integrative centre. An integrative centre is responsible for the coordination of the body's response to a change in the internal or external environment. The integrative centre achieves compensation by modulating the activity of effectors. The communication of information to the effectors may employ the nervous system or the endocrine system. An effector participates in the compensation for changes

[3]Senior Lecturer, Institute of Physiology, University of Glasgow

[4]Consultant Anaesthetist and Senior Lecturer, Department of Anaesthesia, University of Glasgow

in the body's environment by altering its level of activity. The change in activity can result from changes in the neuronal stimulation of the effector, changes in the hormonal input, or both. Examples of effector actions include the heart pumping at a higher rate and the kidney excreting less water.

The grouping of the elements of the reflex loops as receptors, integrative centres and effectors is on the basis of their function. For each individual loop, there may be one or more groups of anatomically–distinct receptors. There is generally a single, anatomically–distinct integrative centre and the loop may employ several effector sites which are also anatomically–distinct. Using this information allows the construction of a generalised regulatory loop as shown in Figure 6.4. This

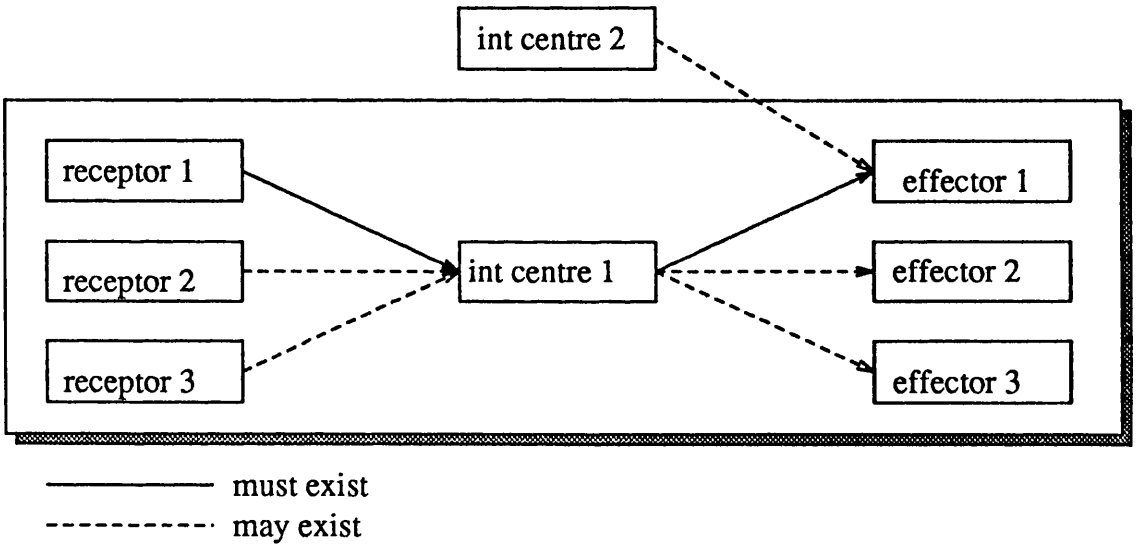

Figure 6.4: The Structure of a Regulatory Loop

figure reflects the existence of physiologically and anatomically–distinct tissue sites. For the general loop under consideration, it is shown that at least one receptor group must exist but that more may also be present. For example, the baroreceptor reflex loops rely upon baroreceptors in both the aorta and carotid arteries. The generalised loop is considered to have a single integrative centre which communicates with at least one effector. In the general loop, no distinction is made between neuronal and hormonal communication. In Figure 6.4, it is also

shown that an effector site may be influenced by at least one integrative centre and possibly more. Each of these integrative centres will operate to control one aspect of the regulatory or protective reflexes. As an example, the heart's activity is modulated by many different loops including the baroreceptor reflexes and the stress response.

A further characteristic of regulatory loops is that their receptors are sensitive to the internal or external environment and the actions of their effectors are often visible or measurable. The physiological state of the body has been assumed to consist of both those variables which are regulated by the body and also those which reflect effector activity. Each loop will therefore be sensitive to some of the variables of the physiological state and will alter others. This interaction is schematically represented in Figure 6.5.

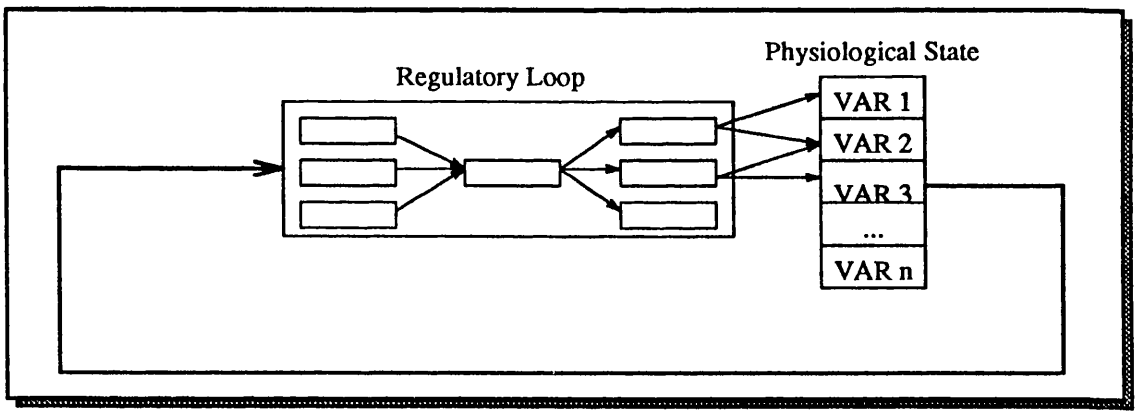

Figure 6.5: The Relationship between the Physiological State and A Regulatory Loop

The consideration of anatomy and physiology has allowed the identification of distinct tissue sites which participate in homeostasis and the stress response. These sites are grouped according to their function and communicate with other tissue sites. The construction of the generalised reflex loop forms the basis of an

individual representation of specific reflex loops.

6.8.3 Model Development — The Representation of Specific Loops

The description of the generalised reflex loop and its interaction with the physiological state emphasised that each loop could have several receptors, several effectors and a single intergrative centre. In the representation of a specific reflex loop, each tissue site of the model corresponds to an actual tissue site. Similarly, each communication link between tissue sites corresponds to a neuronal or hormonal pathway in the body. To represent these features in a model, each of the anatomical tissue sites (receptors, integrative centres and effectors) and the physiological state have been regarded as *objects.* The term objects is used to be consistent with the terms of object–oriented representation [148].

In object–oriented representation, objects are collections of data and functions. The data of an object are termed its *attributes* and the functions are termed its *operations.* In representing individual loops and the combination of loops involved in homeostasis and the stress response, the attributes of an object can be used to hold the structural (anatomical) information and the states of variables. The operations of the object can then be used to describe its functional (physiological) characteristics. Each tissue site within the physiological loop can then be represented as an object. The representation of receptor sites, integrative centres and effectors is described in the following sections.

The Representation of Receptor Sites

In physiology, receptor sites are described in terms of the quantity to which they are sensitive and their location. For instance, baroreceptors are sensitive to pressure and the carotid baroreceptors lie in the carotid arteries. It is therefore appropriate to include the name of the receptor group and the quantity to which it is sensitive

as attributes of the receptor object. Because the quantity to which a receptor is sensitive is a feature of the physiological state of the body, the quantity will be an attribute of the physiological state object (to be described later). Instead of containing the name of the quantity to which the receptor site is sensitive as an attribute, a receptor object contains the name of the appropriate attribute of the physiological state object. Each receptor site, or group of receptors, transmits information to an integrative centre in the body. Each integrative centre is also considered to be a specific anatomical site. Given that an integrative centre object will be defined, for the model, to represent the integrative centre site in the body, the receptor object can include the name of the appropriate integrative centre object of the model as an attribute.

Functionally, a receptor site monitors the quantity to which it is sensitive and transmits this value to the relevant integrative centre. The operations of the receptor object are therefore defined to be the measurement of its associated variable and the transmission of this value to the appropriate intergrative centre. The structure of the receptor object defined for the model is illustrated in Figure 6.6.

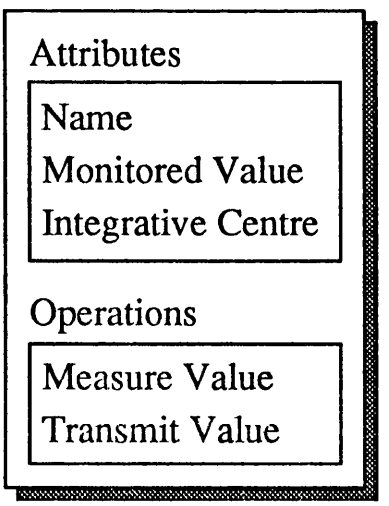

Figure 6.6: The Attributes and Operations of a Receptor Object

The Representation of Integrative Centres

Integrative centres are specific anatomical sites of the body. Integrative centres have physical links to receptor sites and to effector sites. As outlined in the description of the generalised loop, an integrative centre may receive input from several receptors and may modulate the activity of several effectors. Because it is possible for the values transmitted from each receptor site to be different, the integrative centre is required to arbitrate between potentially conflicting inputs. In the body, the most important imbalances take priority over those less important in the determination of compensation. While the precise mechanisms of this arbitration may be unknown, the characteristics are clear. As an approximation to the physiological reality, each integrative centre object has been defined to include a list of the receptor objects which correspond to the actual receptor sites to which the actual integrative centre is connected, and associated with each receptor object in the list is a priority. The priorities have been assigned to each receptor site in the list so as to enable the integrative centre to establish the most important value for which compensation is required.

Integrative centres in the body also influence the behaviour of effector sites. The integrative centre object therefore includes a list of effector objects to represent the neuronal or hormonal communication between the actual integrative centre site and effector sites.

In addition to the prioritised list of receptor objects and the list of effector objects, the integrative centre object also has an attribute containing the value of the highest priority imbalance recorded by one of its receptors, an attribute containing the current compensatory activity required by the integrative centre and an attribute containing the name of the integrative centre.

The functional characteristics of the integrative centre object include the determination of the highest priority imbalance from the receptors, the determination of the compensation for the imbalance and the transmission of the compensation

request to the effector objects. The operations of the integrative centre object therefore include these activities. The overall structure of an integrative centre object is shown in Figure 6.7.

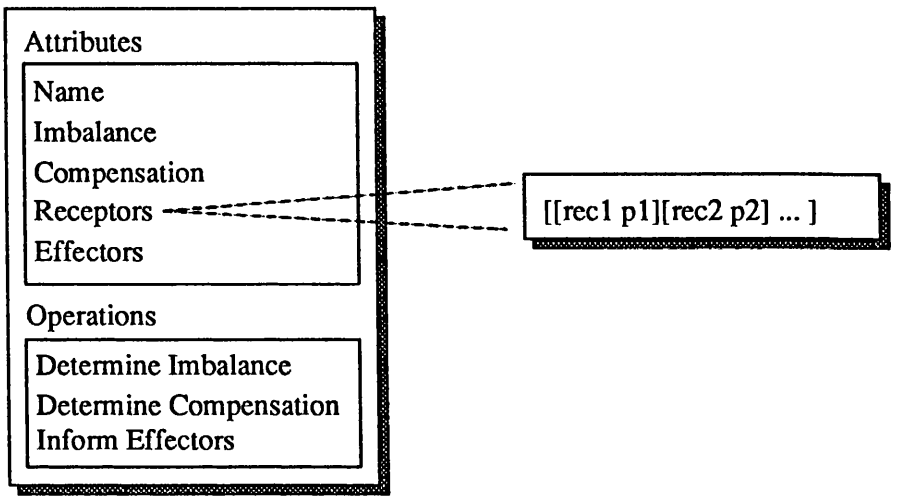

Figure 6.7: The Attributes and Operations of an Integrative Centre Object

The Representation of Effector Sites

Effector sites are responsible for enforcing changes in the physiological state of the body. The regulatory reflexes employ effectors to return a physiological quantity from an unacceptable value to a reasonable one. The stress response overrides the regulatory responses in the event of an extreme or unusual stress. In the body, the activity of the effector site may be influenced by nerve impulses from an integrative centre, by circulating hormones or both. It is generally the case that when hormones provide a communication link, the release of the hormone is controlled by an integrative centre. An effector object is intended to represent an effector site. Because the tissue site is anatomically distinct, the effector object has an attribute to contain the name of the effector site. Another attribute holds a value indicating the required activity of the effector. Because effectors can be required to produce increases or decreases in activity, two further attributes are included to specify the increase action and decrease action of the effector site respectively.

As described earlier, each effector site may be influenced by several integrative centres. In the body, the most important imbalances or the most extreme stimuli are given priority. As for the interaction between integrative centres and multiple receptors where the mechanisms of determining the most important stimulus are not precisely known, the effectors' mechanism for determining the most important compensation is not known. To represent the apparent priorities of several reflexes, each effector has an attribute containing a list of the integrative centre objects to which it has either neuronal or hormonal connections and each of the integrative centres in the list has a priority associated with it.

Each effector site is capable of altering one or more quantities within the physiological state e.g., the heart enforces changes in heart rate, blood pressures and cardiac output. Each effector object therefore has an attribute containing a list of the variable values in the physiological state object which it alters.

The operations of an effector object have been chosen so as to approximate the behaviour of effector sites. The effector object therefore contains operations to determine the most important integrative centre request and change its level of activity. The overall structure of an effector object shown in Figure 6.8.

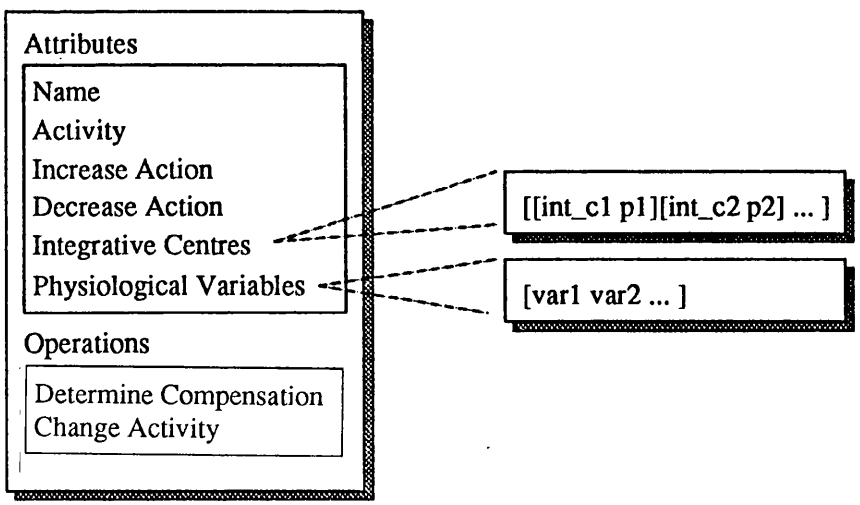

Figure 6.8: The Attributes and Operations of an Effector Object

The Representation of the Physiological State

The reflex loops monitor the physiological state of the body and make any necessary adjustment using effector sites. The physiological state is dependent upon changes in the internal and external environment and the actions of effector sites. The physiological state object has been defined to represent the physiological state of the patient. This object contains relevant physiological variables as attributes. These variables are modified as a result of effector actions and are monitored by receptors. In the model, the name of the variable will appear in the physiological variable list of each effector object and in the monitored value attribute of the each receptor object which is sensitive to its value and changes.

The physiological state object has an operation associated with it which allows the update of each of its variables. For this method to function, each of the variables must have a list of the effector objects which are associated with it. Each physiological variable has therefore been represented as a physiological variable object as described below. The overall structures of the physiological state object is shown in Figure 6.9.

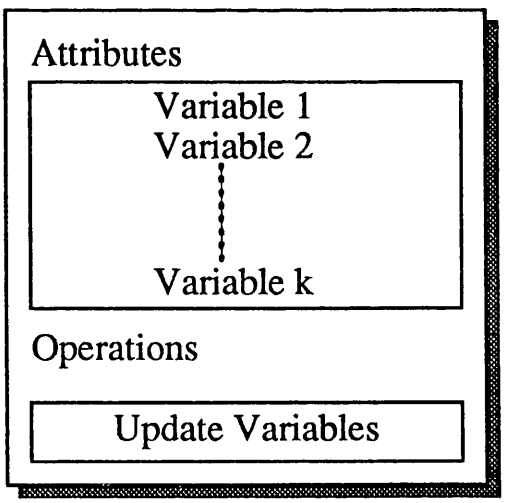

Figure 6.9: The Attributes and Operations of the Physiological State Object

The Representation of Physiological Variables

For completeness, a physiological variable object was defined to represent each physiological variable. Each physiological variable contains an attribute containing its name, an attribute containing its value, an attribute containing a list of receptor objects which are sensitive to its value and an attribute containing a list of effector objects which can change the value of the variable.

Each physiological variable object has an operation which allows the updating of the variable's value based upon the actions of its effectors. It also has an operation to inform receptor objects of a change in its value. The structure of a physiological variable object is shown in Figure 6.10.

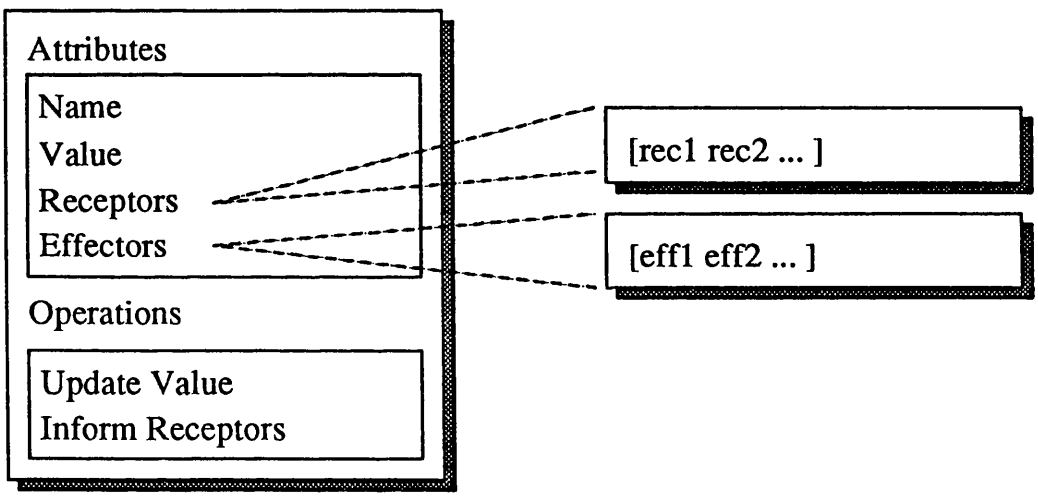

Figure 6.10: The Attributes and Operations of a Physiological Variable Object

Summary of the Representation of Loops

The previous sections have described the definitions for objects intended to represent the anatomical and physiological information of relevance to homeostasis and the stress response. The anatomical information has generally been incorporated within the attributes of objects and the physiological information within their operations. The current object definitions incorporate some redundancy within the representation of anatomical and physiological information. For instance, an

effector object contains a list of all the physiological variables which it can alter and each physiological variable object contains a list of all the effectors which can alter it. This obviously involves the duplication of information. In isolation, however, this representation is more expressive because each object has within it, details of all its interactions. A further useful feature is that, unlike the physiological reality, links in the model can be traversed in both forward and reverse directions. This feature will be demonstrated to be useful later.

6.8.4 A Prototype Implementation of the Model

The original specification for the model's performance was to produce a qualitative description of the changes in clinical signs arising from qualitative changes in physiological variables. Given that the values in the model are therefore qualitative, they can be represented symbolically. The value of a physiological variable can therefore be 'lowered', 'normal' or 'raised'. The value held by a receptor object can have the same values. An integrative centre may decide to 'raise' or 'lower' a variable or to make no changes. Effectors may 'increase', 'decrease' or make no change in their activity. These possible values and the tissue site, physiological state and physiological variable objects have been implemented using the MUSE AI Toolkit. The definitions of each of the objects were used to produce *classes* of objects (actually called schemas in MUSE). A class is a specific type of object which defines the structure and behaviour of all *instances* which are derived from it. An instance is a particular object and has unique values for its attributes. For this model, as an example, the receptor object is used to define a receptor class and instances of this class include the carotid baroreceptors. As described earlier, the object definitions include some redundancy. This implementation therefore makes use of a subset of the available attributes and operations.

Using the implementation of the model, the user is able to 'raise' or 'lower'

the values of variables within the physiological state object. Once this process is completed, the model is allowed to work towards the resulting compensation for the applied imbalances. The process of determining the compensation proceeds as follows:

1. The physiological state object is prompted to update the value of each of its variables using its 'update variables' operation.

2. Each of the variables is then prompted to inform its receptor objects of its current value using its 'inform receptors' operation. This process ensures that each receptor object has an up–to–date account of the variable which it monitors.

3. Each receptor object is then prompted to update its value to reflect that passed to it by its physiological variable.

4. Each integrative centre object then finds the most important imbalanced receptor value using its 'determine imbalance' operation. It then determines the compensation required for this imbalance using its 'determine compensation' operation.

5. Each effector object determines the most important of the requests for changes in its activity using its 'determine change' operation to investigate the compensation requests of each of its integrative centre objects and their priorities. The selected change in activity is then implemented using the 'change activity' operation.

6. The cycle returns to the first step so as to include effector activity in the determination of the next physiological state.

This process is schematically represented in Figure 6.11. In the prototype implementation, an object, the sequence object, has been defined to control

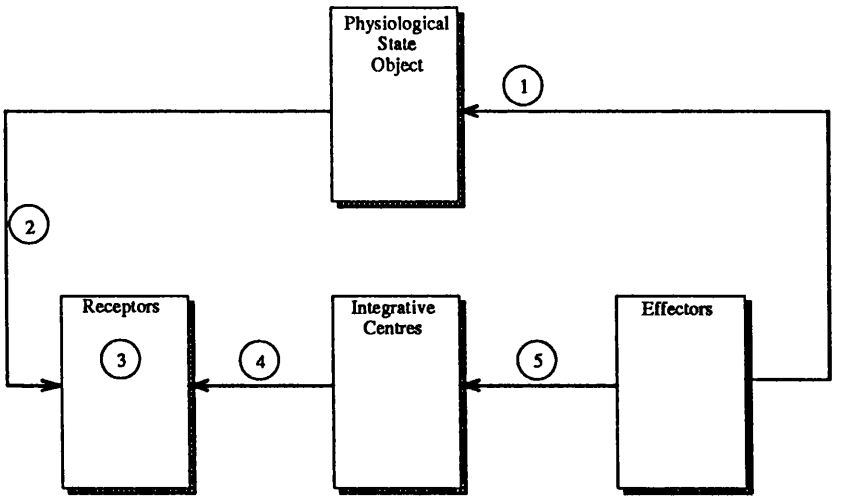

Figure 6.11: The Overall Operation of the Model

the performance of steps 1 to 5. The sequence object has no physiological or anatomical significance but ensures that the process of compensation in the model is easily understood and presented.

6.8.5 Illustration of Model Performance

The process described above allows realistic representation of the reflex loops and their interactions but it is not capable of producing a suitable representation of object activity. MUSE allows the creation of *indicators* and *fields* on a graphical display. An indicator is a box on the screen which can be shaded to different extents and a field is an area in which text can be printed.

To represent the model, an indicator was created for each physiological variable, receptor, integrative centre and effector and a field was provided for each physiological variable and effector. Indicators are shaded when a variable is not 'normal', the receptor receives a non 'normal' value or when an integrative centre or effector is effective. At other times indicators were clear. The fields were used to express the qualitative value of each physiological variable and the action being taken by effectors.

Figure 6.12 shows the MUSE screen display after initialisation of the model.

On startup, all indicators are clear, all values are normal and there are no effector changes from an assumed stable physiological state.

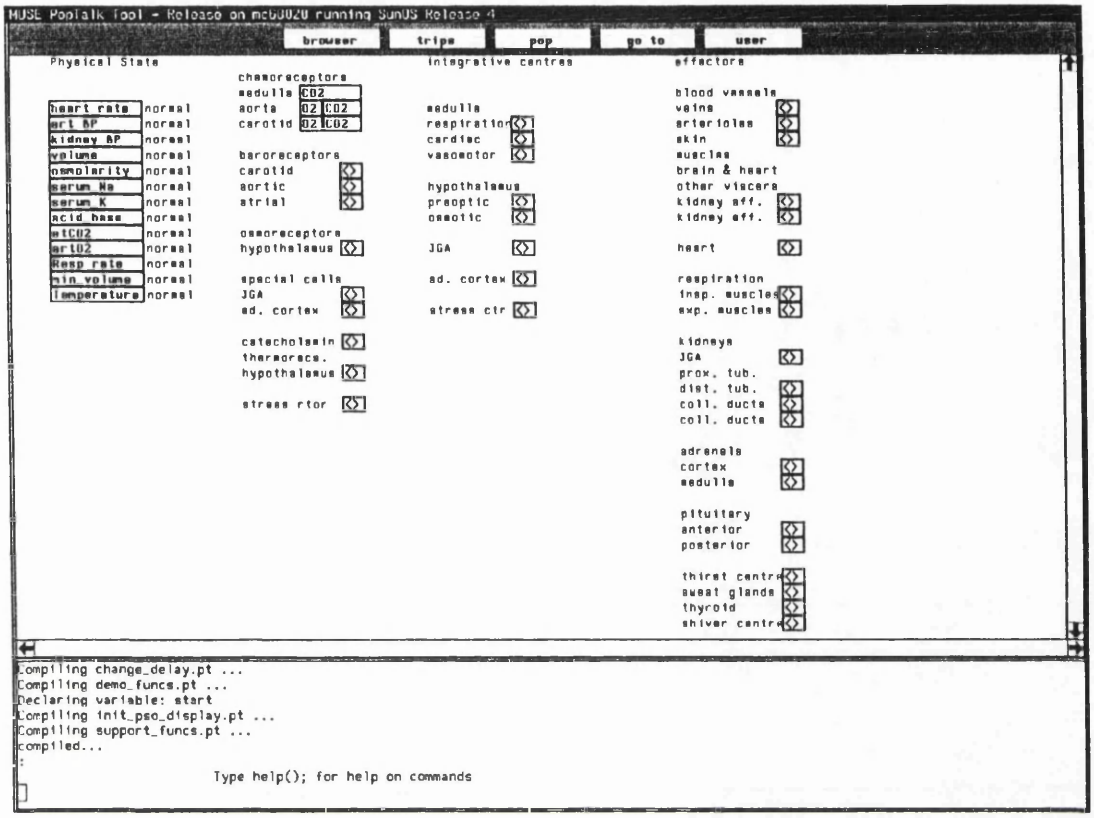

Figure 6.12: Screendump of the Model at Startup

Figure 6.13 is a screendump of the model during a run. In this test, the user has made changes in the physiological state of the model so as to raise the end-tidal carbon dioxide concentration (etCO2) from normal, and raise arterial blood pressure (art-bp) from normal. The indicators for these variables have therefore been shaded and their fields altered to reflect their new values.

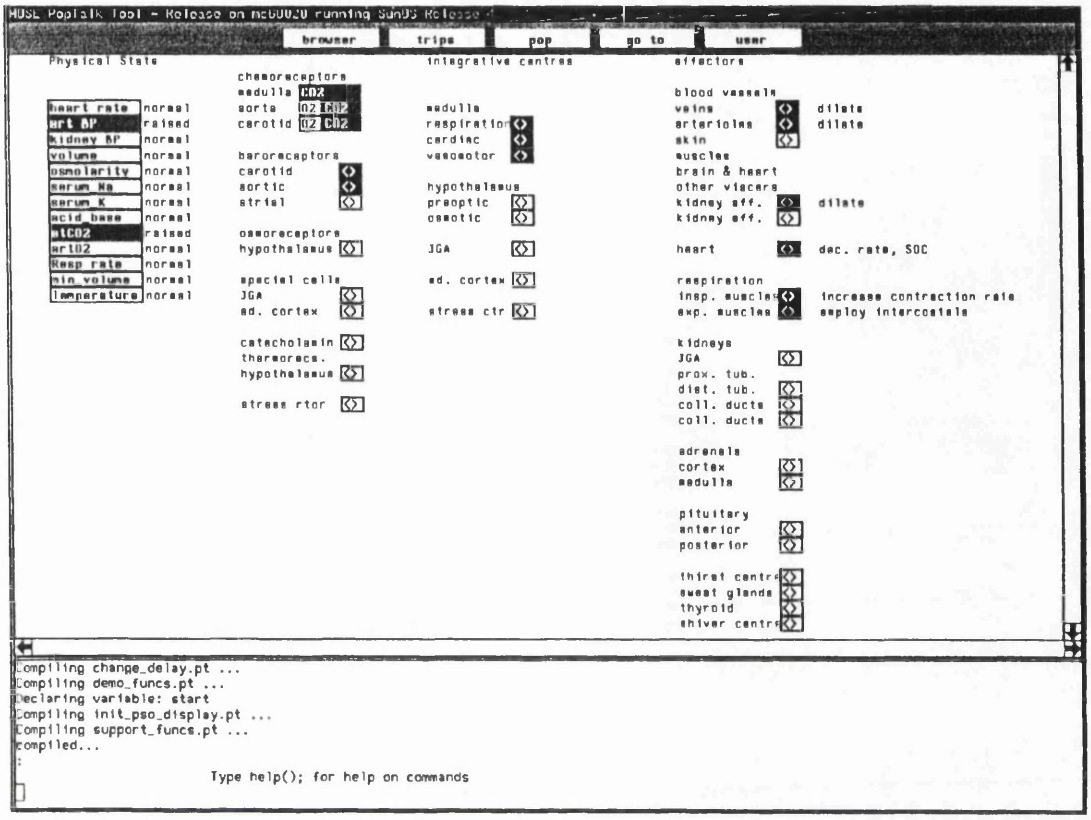

Figure 6.13: Screendump of the Model during Homeostasis Simulation

The changes in the physiological state have been processed by the receptors. The chemoreceptors[5] in the medulla (brainstem) and the aortic and carotid bodies have been stimulated in response to the change in carbon dioxide levels. The carotid and aortic baroreceptors[6] have been activated by the increased arterial pressure. The indicators for these receptors are shaded by the model to reflect their participation.

The respiration control centres in the medulla react in response to the changes detected by the chemoreceptors. The cardiac and vasomotor control centres respond to the changes detected by the baroreceptors. The participation of these integrative centres is reflected in the shading of their indicators.

In compensating for increased carbon dioxide, the respiration control centre has caused an increase in the respiration rate and the involvement of the intercostal

[5]receptors sensitive to chemical composition

[6]receptors sensitive to pressure

muscles in respiration. These changes are summarised in the fields associated with the inspiratory and expiratory muscle objects. The indicators of these sites are shaded to show their involvement. In response to the raised arterial pressure, the cardiac and vasomotor centres have caused the dilation of veins, arterioles and the kidney afferent arterioles and a decrease in heart rate and strength of contraction. The effectors involved in these changes have their indicators shaded. Their associated fields summarise the action taken.

Following the stage indicated by Figure 6.13, the changes in the effector activity rectify the original imbalances in the carbon dioxide and blood pressure variables. The compensatory effort has caused an increase in respiration rate and a decrease in heart rate. This in shown in the screendump of Figure 6.14.

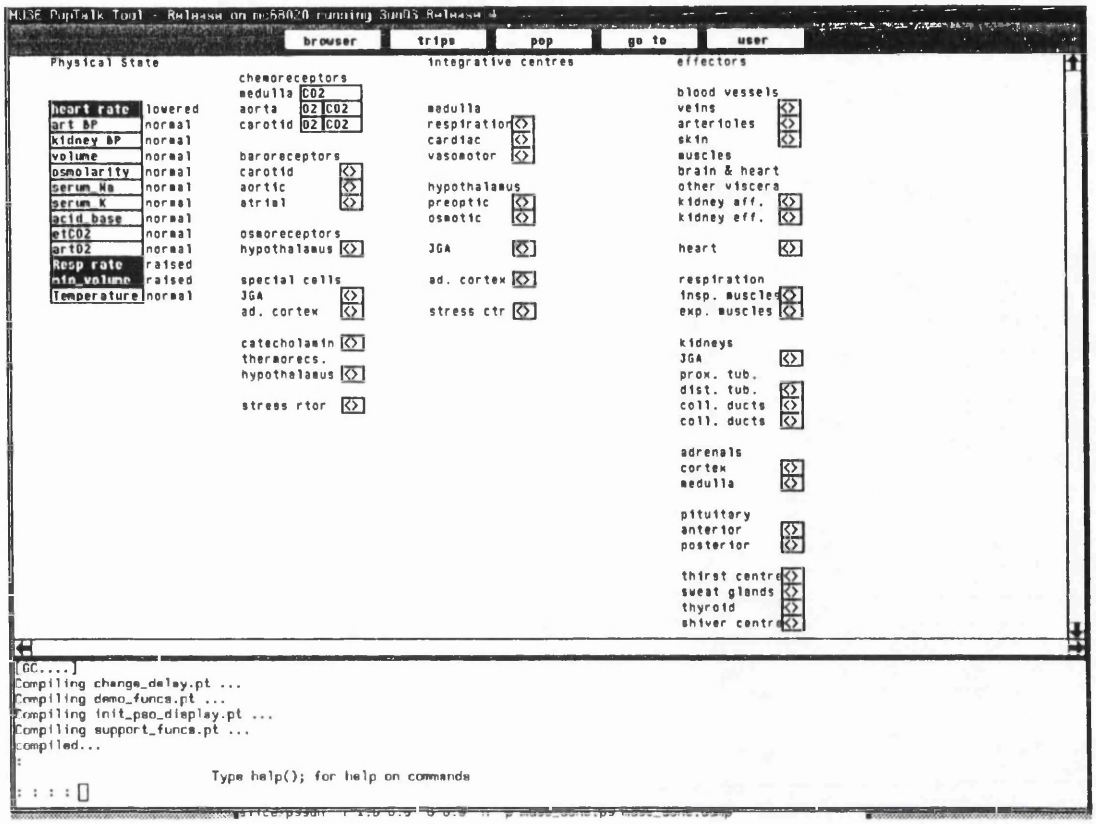

Figure 6.14: Screendump of the Model after Homeostasis Simulation

Figure 6.15 illustrates the model's response to an extreme or unusual stressor. Because the stress response can be elicited by any sufficiently extreme or unusual stimulus, a generalised stress receptor has been included in the model. For clarity, this receptor has been assumed to be connected to a stress centre (notionally the hypothalamus) which then coordinates the stress response. In Figure 6.15, the active sites have their indicators shaded as before and the effector fields indicate the changes effected. The model has predicted that a stress response will be characterised by the constriction of blood vessels, the increasing of heart rate and strength of contraction and the secretion of catecholamines (adrenaline and noradrenaline) by the adrenal medulla.

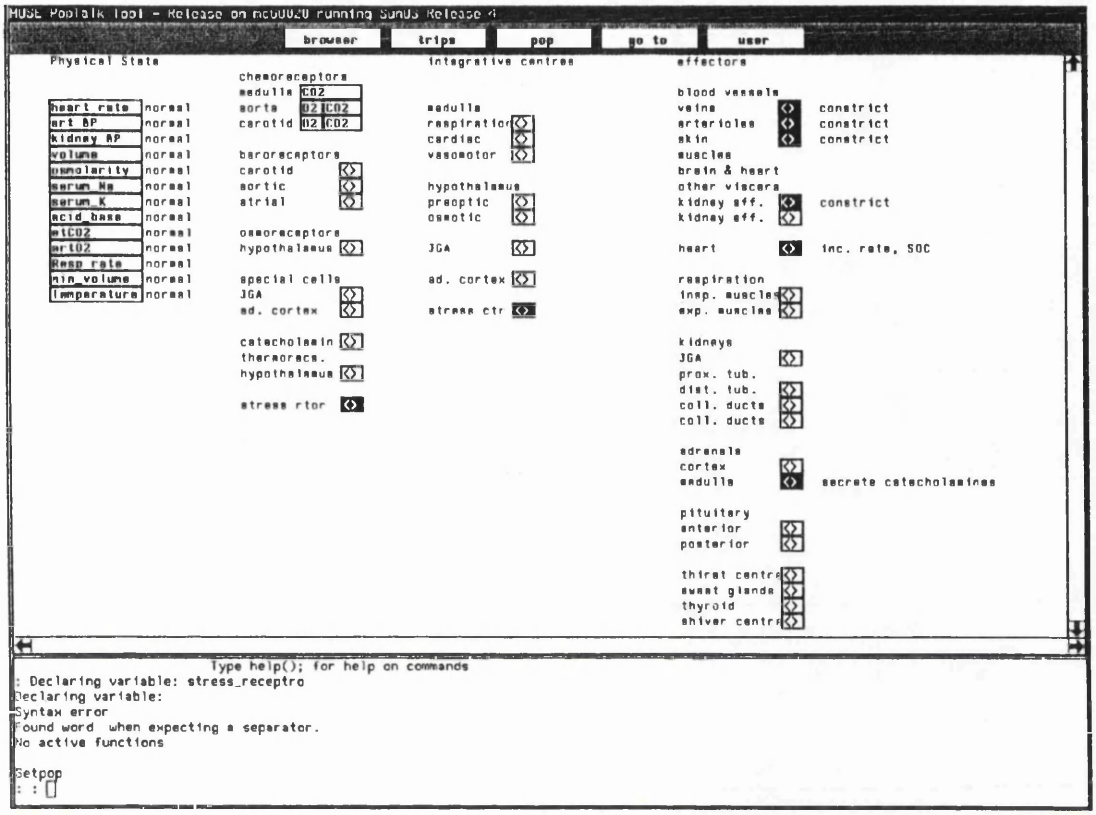

Figure 6.15: Screendump of the Model Stress Response

It should be noted that during the model's operation, the sequence object processes the physiological state object, then the receptors, then the integrative centres, the effectors and then starts again. To give an expressive demonstration, there is a user–defined time delay between the processing of each group. The default value is five seconds which allows sufficient time to see the recruitment of each centre. The appearance of the model at each individual stage in this process has not been illustrated because it would required too many screen dumps. This feature proves useful in the understanding of the model and the physiological processes.

6.9 Incorporating Drug Effects in the Model

Section 6.4 described the effects of anaesthetic drugs on the circulatory and respiratory systems. Many of these effects were explained in terms of the effects

of the anaesthetic drugs at specific sites. Halothane, for instance, caused changes in the circulatory system behaviour as a result of its direct effect on the heart. Isoflurane causes changes due to its dilating action on blood vessels.

The model of homeostasis and the stress response derived in this chapter explicitly represents the anatomical and physiological information relevant to tissue sites within the reflex loops and their connections. Given that the effects of anaesthetic drugs can be described in terms of their action at those sites, the effects of drugs on the reflex loops can be easily represented. This process involves the addition of pharmacological information to the existing anatomical and physiological information embodied in each tissue object.

The most straightforward implementation of this change is to add an attribute to each tissue site object for each drug which can alter its behaviour. Associated with these are operations which are used to modulate the activity of the site according to the drug level. A further operation may be added to produce an overall modulation of the sites activity in the event of multiple drug effects. The structure of the tissue site object will then be of the form shown in Figure 6.16.

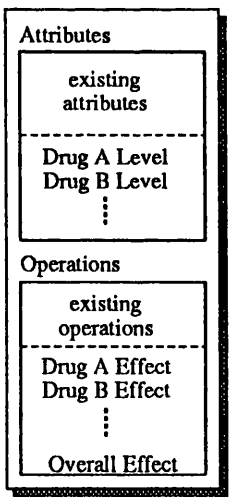

Figure 6.16: A Tissue Site Object Incorporating Pharmacological Information

To illustrate this approach, a possible incorporation of the effects of halothane can be considered. Halothane depresses the activity of the heart. This can be included in the effector object representing the heart. If the level of halothane

in the heart object is 'low' then no changes are made in the performance of the object. If the halothane level is 'normal' or 'high', the heart rate and strength of contraction can be 'lowered' from their present value for the heart object. The change in the activity of the heart then influences the physiological state object's variables. In this way, the physiological and pharmacological influences on the clinical signs of anaesthesia can be illustrated.

The representation of the effects of general anaesthetics are the most important in the representation of the physiological and pharmacological influences of the clinical signs. The incorporation of the effects of other drugs could however proceed in a similar way.

The model development process described in this chapter was not intended to produce a model incorporating the effects of drugs. This has been made particularly straightforward because of the explicit incorporation of anatomical and physiological information in the model. The explicit representation of anatomical sites supports the representation of pharmacological effects at those sites. An approximation to this approach is incorporated in Chapter 7 and future developments involving this structure are described in Chapter 8.

Chapter 7

Model–based Diagnosis of Anaesthetic State Imbalances

SUMMARY

This chapter describes the development and use of the Reversed Model of the regulatory and protective reflexes in the diagnosis of anaesthetic state imbalances. The use of automatic monitoring systems in anaesthesia is reviewed before introduction of the Reversed Model concepts. The prototype implementation of a Diagnoser is described and its off–line and on–line performances are presented.

7.1 Technological Assistance in the Monitoring of Anaesthesia

As described in Chapter 2, monitoring in anaesthesia consists of monitoring;

1. the anaesthesia machine and drug delivery,
2. the physiological condition of the patient and,
3. the depth of anaesthesia of the patient.

It is apparent that the vigilance of the anaesthetist is essential in the rapid detection of adverse conditions in any of these areas. A slow detection of an adverse condition delays the start of its management and in that time it is likely to become worse. Simple alarms were initially added to monitors and drug delivery equipment to generate audible or visual indications of an adverse condition. Sykes [149] suggests that there are two major problems with current alarms;

1. Alarms are generated by equipment which may be scattered around the operating room making their identification difficult.

2. Alarms may sound when there is no danger to the patient.

Sykes highlighted current incorporation of trend analysis to alarm systems and the integration of alarms from many sources in a single display according to their importance. Sykes referred to the work of Westenkow et al. [150] as an example of such integration.

Philip [151] suggested that an alarm system should indicate when the patient's state changes from a predetermined state. The anaesthetist then interprets the change to which he/she has been alerted and takes any action which may be appropriate.

Quinn [152] suggested that alarms should be centrally presented according to their importance and should clearly identify their source. He suggested that in response to audible alarms, the anaesthetist's response was to want to "stop–that–noise" and not to resolve the underlying problem.

Schreiber and Schreiber [153] also advocate central display of alarm information and suggest that an alarm can be either

1. a *warning* which requires immediate attention,

2. a *caution* which requires prompt attention, or

3. *advisory* which requires awareness.

They suggested that warning alarms are signalled by continuous sounds, caution alarms by intermittent sounds and advisory alarms by either single short sounds or without sounds. A further suggestion was that a screen display with three areas is used to identify current alarms.

Beneken and van der Aa [154] review many recent approaches to monitoring and alarm systems. They suggest the inclusion of alarm levels (emergency, caution, alert and information) and suggest that the values at which alarms are triggered may be determined by a number of methods including

1. forming the consensus opinion of experienced anaesthetists
2. using predictions of pharmacologic models
3. 'tuning-in' the alarms to the patient during a change
4. using statistical data from previous patients
5. using information derived from the combination of signals.

Beneken and van der Aa believe that future alarm systems will be based upon data stored from previous anaesthetics.

Fukui and Masuzawa [155] describe a knowledge-based approach to providing intelligent alarms. Their approach involves interpreting signals to detect an event in the signal, relating the events of different signals to each other, recognising the state transitions of the patient and activating appropriate alarms. This approach incorporates some monitoring activity in that it interprets signal information. The authors give an example of a system in which the physical condition of elderly people is monitored remotely and automatically. In one example, given in the paper, the system detects an 'abnormal heart rate' but establishes that this is due to movement.

Schecke et al. [156] describe a knowledge–based system which is intended to monitor the patient's physiological state during anaesthesia and eventually suggest

therapeutic action. The system has been developed for cardiac anaesthesia and identifies "state variables" relevant to the area. These state variables are to be maintained in a "normal" range. *If ... then ...* rules allow determination of the condition of the state variables from current measurement values. The system incorporates fuzzy logic to deal with uncertainty. This system operates on the current values of variables and the reasoning involves qualitative considerations e.g. "vascular tone is too high if systolic pressure is above normal and ...". The authors plan to incorporate the use of measurement trends in their future work.

7.2 An Automatic Monitor of the Patient's Anaesthetic State

The work of Fukui and Masuzawa [155], Schecke et al. [156] and Greenhow [77] involves interpretation of physiological variables so as to monitor the patient's state. each approach has involved the generation of rules to relate physiological, pharmacological and environmental events.

The remainder of this chapter describes the concepts and a prototype implementation of a model–based approach to the monitoring of the anaesthetic state of a patient. The approach has been developed to support;

1. monitoring of the physiological state of the patient,
2. monitoring of the depth of anaesthesia of the patient,
3. the incorporation of the effects due to anaesthetic drugs,
4. the incorporation of the effects due to non–anaesthetic drugs, and
5. the use of both value and trend information for each measurement.

7.3 The Anaesthetic State

Section 2.5.2 of Chapter 2 discussed the contention associated with the definition of terms related to anaesthesia. To clarify the use of some of these terms in the thesis, definitions were given of the terms to be used. Of particular interest to this chapter are the definitions of the anaesthetic state, anaesthetic state imbalances and an appropriate anaesthetic state.

The anaesthetic state was defined to consist of the physiological and pharmacological states of the patient. This definition was adopted so as to emphasise the mutual dependence of the physiological and pharmacological states. Following from this, the activities of the anaesthetist in managing the patient's anaesthetic state can also be seen to consist of both physiological and pharmacological manipulation.

The definition of anaesthetic state imbalance adopted a perspective which would support control development. An anaesthetic state imbalance was defined to be an inappropriate component of the patient's anaesthetic state which could be remedied by physiological or pharmacological changes. An appropriate anaesthetic state was then defined as an anaesthetic state of the patient which exhibited no anaesthetic state imbalances. This definition was intended to be consistent with the approach employed by anaesthetists but was also intended to be suitable for the development of an automatic controller for the anaesthetic state.

In providing anaesthesia for a patient, the anaesthetist does not approach each patient's anaesthetic with the intention of providing a predetermined set of values but tolerates values which have 'normal' ranges and which do not exhibit undesirable characteristics. To mirror this, an automatic controller, aiming to produce an appropriate anaesthetic state, would make changes so as to remove or remedy any anaesthetic state imbalances. To paraphrase, the controller's goal is to produce ananesthetic state with 'nothing wrong' which is in contrast to the

goals of most controllers which attempt to make 'everything right'.

This relaxation of the controller goal simplifies the development of a controller. Instead of having to identify and maintain a 'correct' anaesthetic state, the controller identifies anaesthetic state imbalances and corrects those. The most important step in this process is the identification of anaesthetic state imbalances.

7.4 Anaesthetic State Imbalances

The definition of an anaesthetic state imbalance was given in Section 2.5.2. Anaesthetic state imbalances have been subdivided into physiologic anaesthetic state imbalances and pharmacologic anaesthetic state imbalances according to the manipulation required to correct them. These are described in more detail below.

7.4.1 Physiological Anaesthetic State Imbalances

A physiologic anaesthetic state imbalance has been defined as an anaesthetic state imbalance which can be corrected by a change in the physiologic state of the patient. This definition has been used to assist in controller development: when a physiologic anaesthetic state imbalance is detected, its correction mechanism is apparent. The most common physiologic anaesthetic state imbalances will be rectified by changes in fluid delivery or ventilation. As examples, bleeding as a result of surgery, if significant, will reduce the circulating blood volume. In the short term, the blood volume deficit is compensated for by the baroreflexes as described in Chapter 6. The long term maintenance of homeostasis depends upon the restoration of the blood volume by the administration of blood or fluids. A related example occurs during automatic ventilation of a patient during muscle relaxation. The arterial carbon dioxide tension may rise above or fall below normal values. The patient's ability to compensate for this is impaired because their respiration reflex loops are not intact due to the paralysis of their respiratory

muscles. The correction of the carbon dioxide tension is achieved by alteration of ventilator settings or fresh gas mixture composition.

Pharmacologic Anaesthetic State Imbalances

A pharmacologic anaesthetic state imbalance may be corrected by a change in the pharmacologic state of the patient. The most obvious pharmacologic anaesthetic state imbalances are due to inadequate or excessive delivery of anaesthetic drugs. The correction of these imbalances requires an increase or decrease in the rate of administration of the anaesthetic.

7.5 The Diagnosis of Anaesthetic State Imbalances

While the definition of anaesthetic state imbalances supports correction of the imbalance, the unique and correct identification of imbalances is essential to the function of any controller. In order to diagnose an anaesthetic state imbalance, it is necessary for the imbalance to cause consistent and recognisable changes in the clinical signs of the patient. This is because the clinical signs are the source of information used in the assessment of the patient's anaesthetic state. The diagnosis of the imbalance then requires the interpretation of the clinical signs. This is the technique used to guide the manual administration of an anaesthetic by each anaesthetist except that, in this case, the intention is to automatically interpret the clinical signs.

A model of the homeostasis loops and stress response of the body was described in Chapter 6. This model predicts the effects of physiological anaesthetic state imbalances and the effects of the stress response on the clinical signs. The effects of the stress response generally become apparent if the anaesthetic is inadequate. The model therefore includes the effects of physiological anaesthetic state

imbalances and the likely effects of an inadequate anaesthetic (a pharmacological anaesthetic state imbalance).

To complement the representation of inadequate anaesthesia, excessive anaesthesia can be incorporated within the *existing* structure of the model described in Chapter 6. In representing the stress response, a 'stress receptor' passes information to the 'stress centre'. The stress centre then alters the activity of effector objects to produce the stress response. In all other integrative centres, the presentation of a 'lowered' value from receptors results in a 'raise' request being passed to the effectors. To enable the stress centre object to also exhibit this behaviour, an extreme or unusual stimulus was represented by the value 'lowered' held by the stress receptor object and presented to the stress centre object. Considering the effects of general anaesthetics to be the 'inverse' of the stress response[1] the effects of excessive general anaesthesia is therefore represented by applying the value 'raised' to the stress receptor object in the model causing the stress centre to 'lower' the activity of the appropriate effectors.

This inclusion allows the model to represent both physiological and pharmacological anaesthetic state imbalances and their effects upon the clinical signs of the patient as shown in Figure 7.1. This form of the model works *forward* from imbalances to compensations. In an earlier section, Section 6.8.3, it was emphasised that the object definitions included anatomical and physiological information and that there was redundancy within this representation. The Forward Model used some of the anatomical and physiological links within it to derive clinical signs patterns after imbalances. The Reversed Model uses some of the other links to derive imbalances from clinical sign patterns.

[1]This is a reasonable approximation since the stress response causes stimulation of the sympathetic nervous system whereas general anaesthetics cause its inhibition

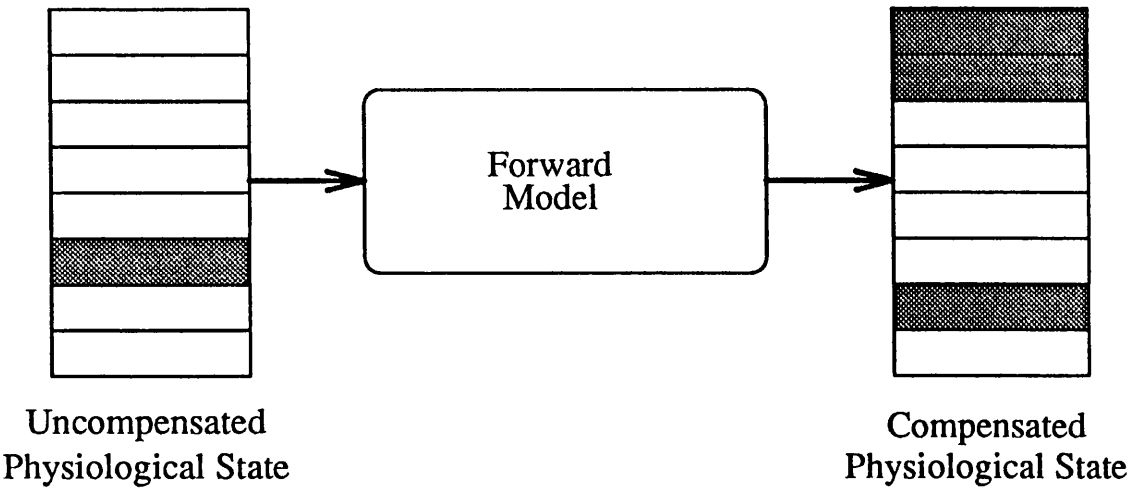

Figure 7.1: Forward Model Operation

7.5.1 The Reversed Model of Homeostasis and the Stress Response

The Forward Model interacted with a physiological state object which contained physiological variables. Each variable has associated with it a list of receptor objects which are sensitive to its value and a list of effector objects which can alter its value. Variables which have receptor sites associated with them are regulated by the body (e.g., arterial blood pressure). Variables without receptor sites reflect effector activity (e.g., heart rate). The physiological state object's variables therefore consist of both *regulated variables* and *effector actions.* The clinical signs used by the anaesthetist are a subset of the possible physiological variables because not all physiological variables can be, or need to be, measured. Within the clinical signs, some are regulated variables and some are effector actions. The clinical signs can therefore be used to provide information for the Reversed Model as shown in Figure 7.2. This information can be used to produce diagnoses of anaesthetic state imbalances.

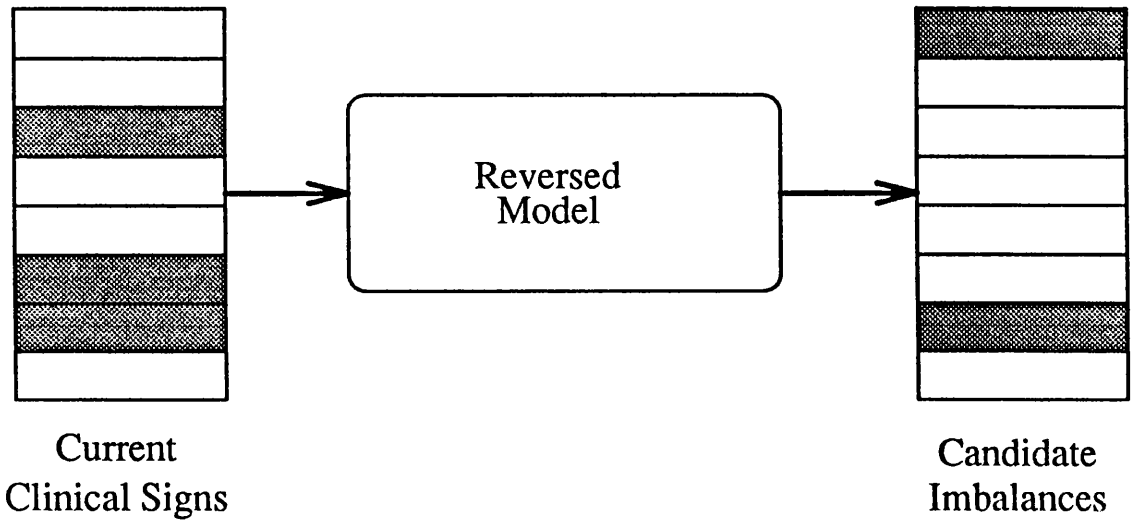

Figure 7.2: The Operation of the Reversed Model

7.5.2 Diagnosis of Anaesthetic State Imbalances using the Reversed Model

Figure 7.3 illustrates the diagnosis procedure which operates as follows. From a set of clinical sign measurements, those which are regulated variables are presented to the appropriate receptor objects of the model. Those which are effector actions are passed to the appropriate effector objects of the model. The diagnosis involves checking the consistency of the receptors and effectors associated with each integrative centre. This process is carried out for each integrative centre once for each of its effectors for which an effector action measurement is available. Each effector with a non-normal value passes its value, in turn, to its integrative centres. The integrative centres compare each effector value against their receptor values. The comparison yields outcomes as listed in Table 7.1.

'Conflict' Implies that the integrative centre could not have been responsible for the effector action. 'Compensated Imbalance' indicates that the integrative centre could have contributed to the effector activity in order to compensate for an

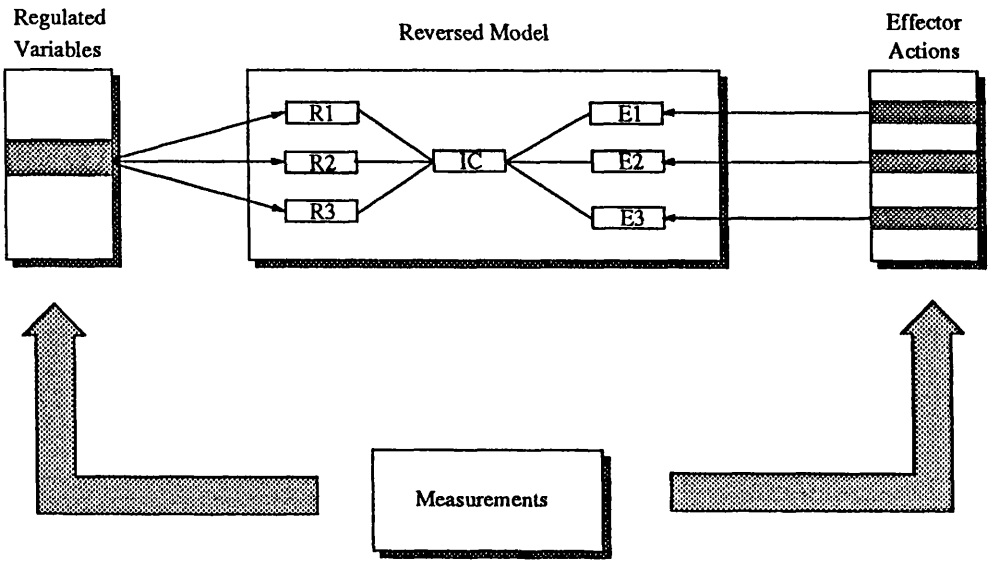

Figure 7.3: The Presentation of Clinical Sign Information to the Reversed Model

Effector	Receptor	Outcome
Lowered	Low	Conflict
Lowered	Normal	Compensated Imbalance
Lowered	High	Partially Compensated Imbalance
Normal	Low	Conflict
Normal	Normal	(never evaluated)
Normal	High	Conflict
Raised	Low	Partially Compensated Imbalance
Raised	Normal	Compensated Imbalance
Raised	High	Conflict

Table 7.1: Possible Outcomes in the Evaluation of Integrative Centre Involvement

imbalance and that compensation is now complete. 'Partially Compensated Imbalance' indicates that the integrative centre is likely to be involved in the partial compensation for an imbalance in the regulated value. The partial compensation may be due to the 'blunting' of the regulatory reflexes by anaesthetics or may reflect a large imbalance for which compensation cannot be complete without external intervention. As an integrative centre is evaluated, it totals the number of conflicts, compensated imbalances and partially compensated imbalances which occur. When each of the measured effector actions has been propagated to evaluate the appropriate integrative centres, the totals in each category within the integrative centre reflect the likelihood of its participation in the production of the current clinical sign pattern. In the current implementation of the reversed model, the presence of any conflicts excludes the integrative centre from consideration as a candidate, compensated imbalances support the existence of a hypothesis and partially compensated imbalances indicate the existence of a hypothesis, where the hypothesis is that the integrative centre has contributed to the pattern of clinical signs by compensating for its particular imbalance.

7.6 Prototype Implementation of the Diagnoser

The Forward Model of the regulatory and protective reflexes employed qualitative description of values: a physiological state value being either 'raised', 'normal' or 'lowered' and integrative centres deciding to 'raise' or 'lower' their activity. The Reversed model uses the same representation and therefore the same qualitative values. This is in contrast to the majority of measurements made by the anaesthetist which are presented as integer or decimal numbers e.g., pressures in mmHg, temperatures in celsius, gas fractions as percentages etc. The use of the reversed model, in its current form, therefore requires conversion of numerical values to the qualitative values used by the model. The most simple approach to

this is the generation of simple threshold values such that a value rising above an upper threshold becomes 'raised' and one falling below a lower threshold becomes 'lowered'. More sophisticated techniques such as those based upon Fuzzy Logic aim to smooth the transition between categories. In order to generate a fuller description of changes in physiological variables, the techniques described by Cheung and Stephanopoulos [157] [158] have been adopted.

7.6.1 The Representation of Process Trends

Cheung and Stephanopoulos [157] define a representation which allows the quantitative, semi–quantitative and the qualitative description of process trends. Full discussion of the representation formalism is not necessary here but the relevant aspects are summarised below.

The *qualitative state* of a variable x, at a time t, within a time interval $[a, b]$ is denoted $QS(x, t)$. $QS(x, t)$ is undefined if x is discontinuous at t but is otherwise defined to be

$$< [x(t)], [\delta x(t)], [\delta\delta x(t)] >$$

where

$$[x(t)] = \begin{cases} + \text{ if } x(t) > 0, \\ 0 \text{ if } x(t) = 0, \\ - \text{ if } x(t) < 0. \end{cases}$$

$$[\delta x(t)] = \begin{cases} + \text{ if } x'(t) > 0, \\ 0 \text{ if } x'(t) = 0, \\ - \text{ if } x'(t) < 0. \end{cases}$$

$$[\delta\delta x(t)] = \begin{cases} + \text{ if } x''(t) > 0, \\ 0 \text{ if } x''(t) = 0, \\ - \text{ if } x''(t) < 0. \end{cases}$$

The *qualitative trend* of a variable is represented by the continuous sequence of qualitative states over $[a, b]$. The qualitative trend is uniquely defined by a *concise qualitative history.* A concise qualitative history is composed of *maximal episodes.* A maximal episode over the interval $[t_i, t_j]$ is defined for the variable x as the pair.

$$< \text{temporal extent}, QS(x, t_i, t_j) >$$

where the temporal extent $= (t_i, t_j)$ and $QS(x, t_i, t_j) = QS(x, t)\ \forall t \in (t_i, t_j)$. A maximal episode is one for which there is no other episode with the same qualitative state and overlapping temporal extent. The qualitative trend therefore has the form:

$$QS(x, t_o), QS(x, t_o, t_1), QS(x, t_1), \cdots, QS(x, t_{n-1}, t_n), QS(x, t_n)$$

Discrete points within the qualitative trend are *geometric distinguished time points.* A geometric distinguished time point for a variable x over an interval $[a, b]$ exists at a and b together with the points where;

1. $x(t)$ has a discontinuity in its value or first derivative or,
2. $x(t) = 0$ or,
3. $x'(t) = 0$ or,
4. $x''(t) = 0$.

Episodes between geometric time points are always maximal.

An additional concept is that of the *domain distinguished time point.* A domain distinguished time point is a point at which either the value of the variable or its first derivative has an 'interesting' value in the context of the domain. The combination of geometric and domain distinguished time points produces an *essential point history.* The *descriptive state* of a variable, at a time point, is the combination of its qualitative state at the time point with its semi–qualitative

state. The semi–qualitative state consists of the value and first derivative of the variable or adjacent limits if the value of the variable is discontinuous at the time point. The combination of descriptive states generates the *descriptive trend* of the variable.

7.6.2 The Implementation of a Qualitising Filter

Of particular interest in the interpretation of clinical signs using the reversed model is the generation of the qualitative trend for each variable but also the generation of domain distinguished time points. A qualitising filter has therefore been implemented in C++ to achieve the following;

1. The production of a geometric qualitative description of a variable based upon numerical sample values.

2. The production of a domain–specific qualitative description using variable domain landmarks and the same numerical samples as the above.

The structure of the filter is illustrated in Figure 7.4.

The qualitiser is initialised with the sample interval used to generate the clinical sign samples. This value is used by the quantitative filter to calculate first and second derivatives of the input data value. The value, first and second derivatives are then processed by two additional filters. The qualitative filter generates a qualitative assessment of the current qualitative state. The domain filter produces domain specific assessment of the current quantitative state. If the value of the data value exceeds the domain–specific upper limit, its specific state (sx) becomes +. If it lies below the domain–specific lower limit, it becomes −, otherwise it is zero. The same procedure produces the specific state for the first derivative of the data value, sdx, and that of the second derivative, sddx. The outputs of the qualitative filter and the domain–specific filter are combined to give a descriptive state. The performance of the qualitising filter has been

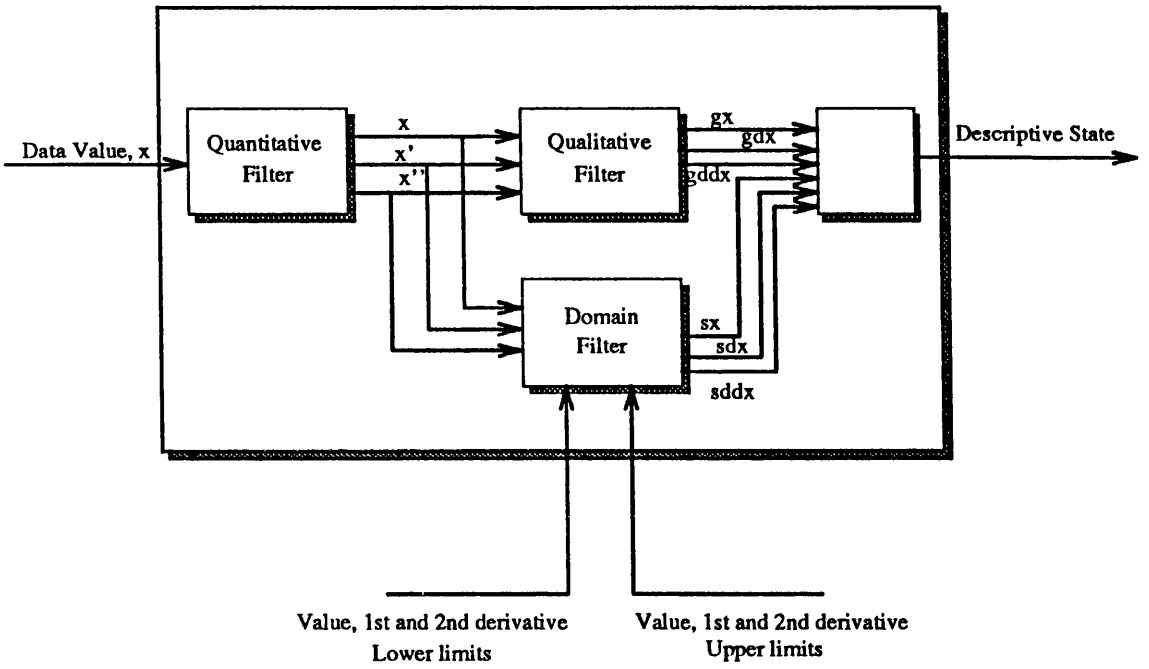

Figure 7.4: The Structure of the Qualitising Filter

tested by presenting a sine wave at the input and observing the descriptive state for varying domain–specific limits. In its current implementation, the qualitising filter can have the domain–specific upper and lower limits changed during filtering of the data. This supports the generation of qualitative information for input to a reversed model.

7.6.3 Implementation of the Reversed Model of Homeostasis and the Stress Response

Implementation of a comprehensive Reversed Model involves representation of many different loops. In order to present a more tractable task and investigate the performance of the Reversed Model concepts, a prototype has been implemented so as to provide the ability to automatically deduce the following anaesthetic state imbalances;

1. Reduced circulating blood volume,
2. Overload of fluids,
3. Inadequate anaesthesia,
4. Excessive anaesthesia,
5. Inadequate carbon dioxide elimination, and
6. Excessive carbon dioxide elimination.

The Reversed Model uses a qualitising filter for each of; respiratory rate, end–tidal carbon dioxide, heart rate and systolic arterial pressure. Of these, the domain–specific state of the respiratory rate is passed to the respiratory muscle site in the reversed model, the end–tidal carbon dioxide domain–specific state is passed to the chemoreceptor sites, the heart rate domain–specific state is passed to the heart effector site and the systolic arterial pressure domain–specific state is passed to the baroreceptor sites. In addition to this, if the systolic arterial pressure is 'raised', according to its domain–specific state, then 'lowered' is passed to the stress receptor.† Otherwise, 'raised' is passed to the stress receptor.

Following the update of each appropriate receptor and effector site in the model with the domain–specific qualitative state, the procedure for evaluating the contribution of each integrative centre described earlier is carried out.

7.7 Performance of the Reversed Model

Two versions of the Reversed Model have been implemented in order to test its capacity. The first version employs the diagnosis strategy described above to retrospectively assess the anaesthetic state imbalances using data logged from previous anaesthetics. In these logfiles, the actions of the anaesthetist have been entered at, or very close to, the time of their occurrence and explanations of

† to represent light anaesthesia.

the reasons for each action have been added. The hypotheses generated by the Reversed Model can therefore be compared with the actions taken by the anaesthetist. Some examples are given below.

In the second version, an interface has been added to the Reversed Model to allow the anaesthetist to dynamically set upper and lower limits for heart rate, respiration rate, end–tidal carbon dioxide tension and systolic arterial pressure. The implementation of this interface has employed a PC which is taken into the operating theatre and which automatically receives data from the anaesthesia monitors using the CLASS libraries (Section 2.7.2). The interface also includes display of the numerical values of each measurement, their domain–specific qualitative value (i.e. 'raised', 'lowered' or 'normal') and hypotheses about blood volume, elimination of carbon dioxide and depth of anaesthesia. Some examples of the on–line performance of the Reversed Model are also given.

7.7.1 The Off–line Performance of the Reversed Model

As an aid to understanding the performance of the anaesthetist, a logging program was developed to automatically gather data from the anaesthetic monitors and also accept keyboard input. The keyboard was used to log drug changes, fluid changes and ventilation changes along with the motivation for those. Other comments could also be added. The logging process therefore produced fully annotated data files which illustrated the practical monitoring and control of the anaesthetic state.

These logged data files have been used to test the Reversed Model. Data from the files has been passed into the Reversed Model and its hypotheses have been compared with the motivations for changes given by the anaesthetist during the procedure. The main advantage of using off–line data in this application is that the same anaesthetic can be reviewed by the Reversed Model several times using different limits for each variable.

This process is illustrated using data collected from an operation performed on

a 53 year–old female patient to create a vein loop for use in dialysis. The heart rate and blood pressure limits have been chosen within physiologically realistic ranges for the patient and are made less tolerant towards the end of the procedure so as to mimic the change in tolerance exhibited by the anaesthetist during a procedure.

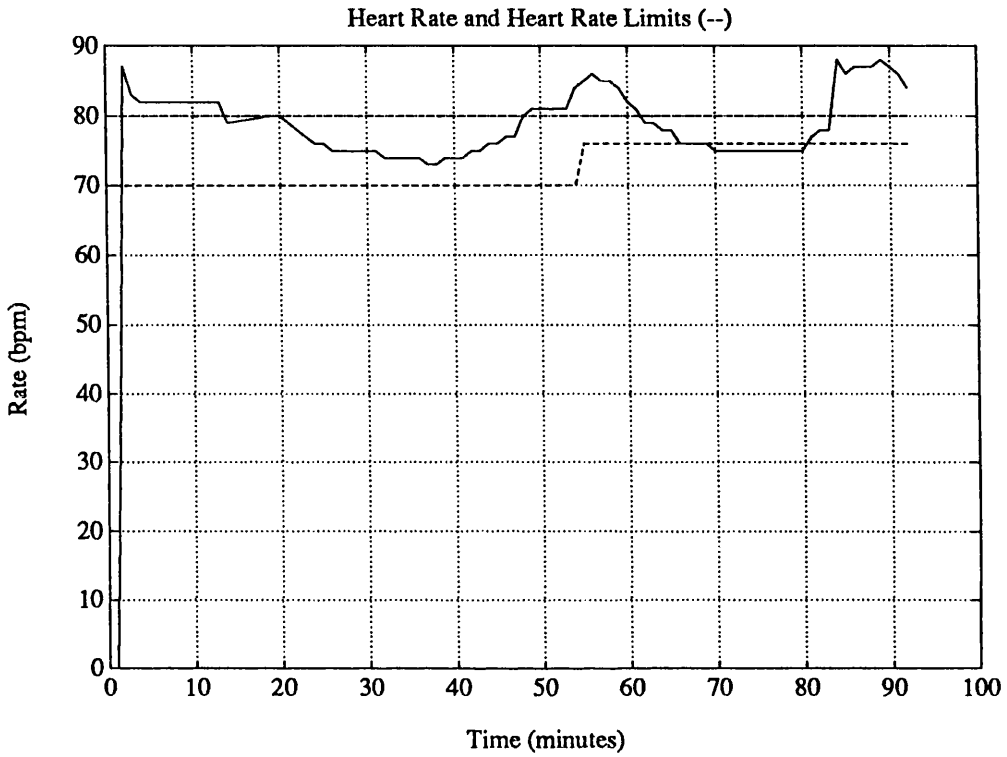

Figure 7.5: Heart Rate Measurements and Limits for the Offline Test

Figure 7.5 shows the measured heart rate along with the chosen upper and lower limits of the 'normal' range. Figure 7.6 shows the measured systolic arterial pressure along with the upper and lower limits for the 'normal' range used by the Reversed Model. Table 7.2 summarises the behaviour of the Reversed Model using the chosen limits. It is clear that during the early stages of the procedure (up to 13 minutes) the Reversed Model diagnosed a fluid problem. At this stage in the operation, the anaesthetist administered fluids. Between 55 and 59 minutes, the Reversed Model considered the anaesthetic 'light' but the anaesthetist made no changes during the actual procedure. Between 70 and 80 minutes, the Reversed Model considered the anaesthetic to be 'deep'. At 72 minutes, the anaesthetist

Time in minutes	Heart Rate	Systolic Pressure	Fluid	Depth	Anaesthetist's Action
0 to 12	high	low	low	normal	unable to achieve good fluid inflow
13	high	low	low	normal	rapid infusion given, vaporiser to 1%
14 to 44	normal	low	normal	normal	—
45 to 48	normal	normal	normal	normal	—
49 to 54	high	normal	normal	normal	—
55 to 59	high	high	normal	light	—
60 to 61	high	normal	normal	normal	—
62 to 65	normal	normal	normal	normal	—
66 to 69	normal	low	normal	normal	—
70 to 71	low	low	normal	deep	—
72	low	low	normal	deep	vaporiser to 0.5%
73 to 80	low	low	normal	deep	—
81 to 83	normal	low	normal	normal	—
84 to 86	high	low	low	normal	—
87 to 88	high	normal	normal	normal	—
89 to 92	high	high	normal	light	—
END					

Note: Fluid = fluid hypothesis; Depth = depth hypothesis

Table 7.2: A Summary of Reversed Model Hypotheses for the Off-line Test Example

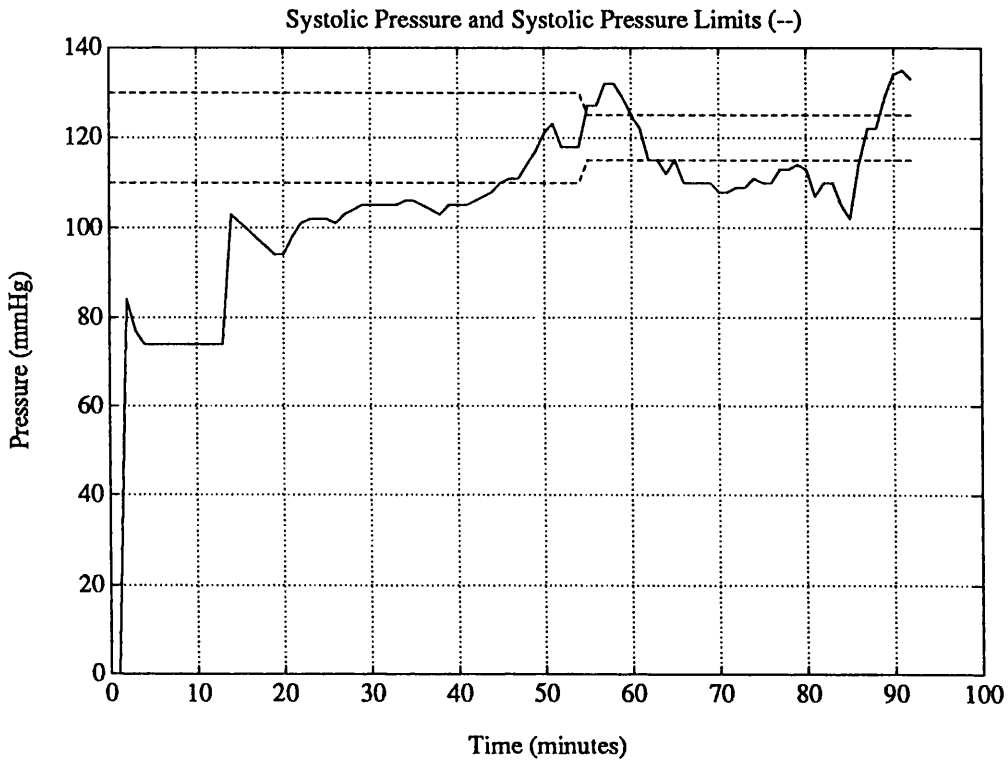

Figure 7.6: Systolic Arterial Pressure Measurements and Limits for the Offline Test

reduced the anaesthetic concentration. At the end of the operation (80 - 92 minutes) the Reversed Model considered the anaesthetic to be 'light'. The anaesthetist generally aims to 'lighten' anaesthesia at the end of the operation due to the decreased surgical stimulus and to speed the recovery of protective reflexes.

This case provided a useful test for the Reversed Model because a differential diagnosis between the fluid and anaesthetic problems was required. The Reversed Model has proved capable of this diagnosis.

7.7.2 The On–line Performance of the Reversed Model

The off–line tests carried out using the Reversed Model, as exemplified by the test described in the previous section, have indicated that the Reversed Model can be used to generate realistic diagnoses of anaesthetic state imbalances. An on–line

implementation was therefore developed so as to determine whether the technique can be useful during an actual procedure and operate in those conditions.

Structurally, no changes were made to the Reversed Model but an interface was developed to ease its use in theatre. The interface was designed to allow the following.

1. The display of current heart rate, systolic arterial pressure, respiration rate and end-tidal carbon dioxide values.

2. The setting and alteration of upper and lower limits of the 'normal' range for each variable.

3. The display of the qualitative assessment of each variable i.e., 'low', 'normal' or 'high'.

4. The display of hypotheses generated by the Reversed Model.

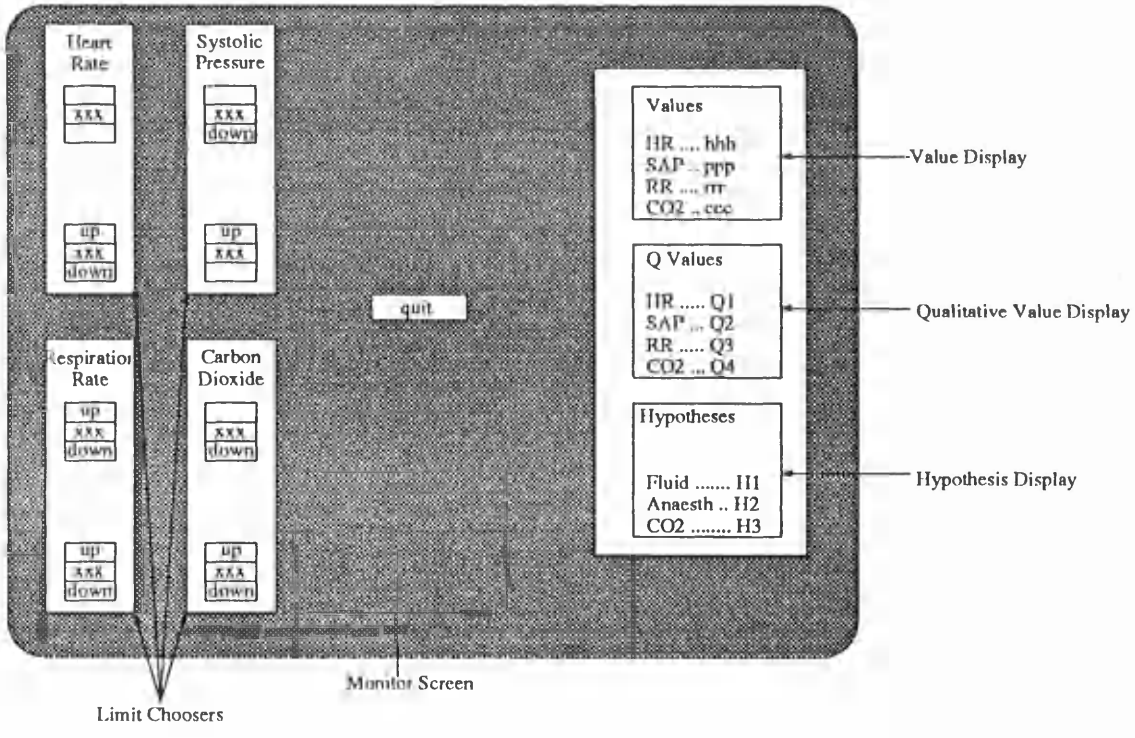

Figure 7.7: The Layout of the On-Line Reversed Model Interface

The interface was designed to use mouse input during a run. The layout of the interface is illustrated in Figure 7.7. Using this arrangement, the anaesthetist could set and change variable limits at any time during a run using only the mouse. Three separate tests using this arrangement are described in the following sections. In each test, thiopentone was used at induction and isoflurane and nitrous oxide were used during maintenance.

Test 1

This procedure was carried out on a 58 year–old male patient to repair an inguinal hernia. A statistically–based predictor for systolic arterial pressure uses the formulae

$$\text{SAP} = 108 + \frac{1}{2} \cdot \text{age}$$

for a male and

$$\text{SAP} = 98 + \frac{3}{4} \cdot \text{age}$$

for a female [61]. Using these formulae, the expected value for this patient was calculated as 137 mmHg. The initial lower and upper limits for the 'normal' range of systolic pressure for this patient were therefore set as 130 and 140 mmHg respectively. The initial heart rate lower and upper limits were set at 70 and 80 beats per minute respectively. Figure 7.8 shows the measured heart rate of the patient along with the heart rate limits used to define the 'normal' range for the Reversed Model. Figure 7.9 shows the measured systolic arterial pressure and the limits used to define the 'normal' range for the Reversed Model.

Table 7.3 summarises the hypotheses generated by the Reversed Model during the procedure. In the first 5 minutes, the Reversed Model considers the patient to be low on fluid. This coincides with the running of an infusion by the anaesthetist. Between 6 and 8 minutes and again between 10 and 12 minutes, the Reversed Model considers the anaesthetic 'light'. At 6 minutes, the anaesthetist increased the vaporiser setting to 3% and gave an increment of morphine. The anaesthetist returned the vaporiser to 2% at 15 minutes at which time the model considered the

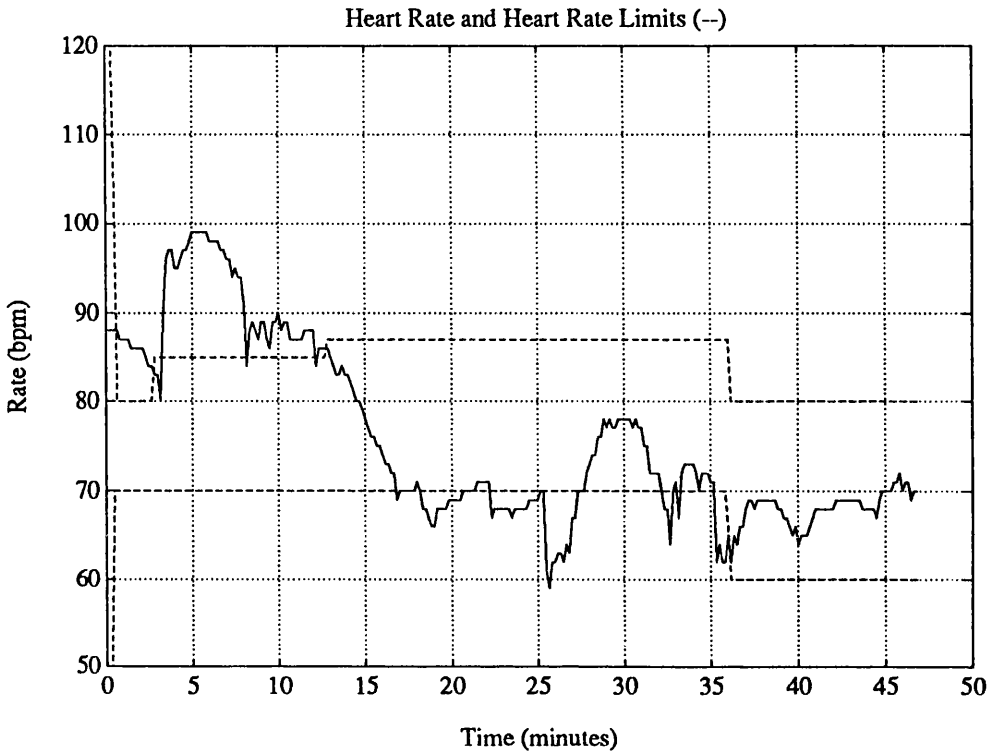

Figure 7.8: Heart Rate Measurements and Limits for Test 1

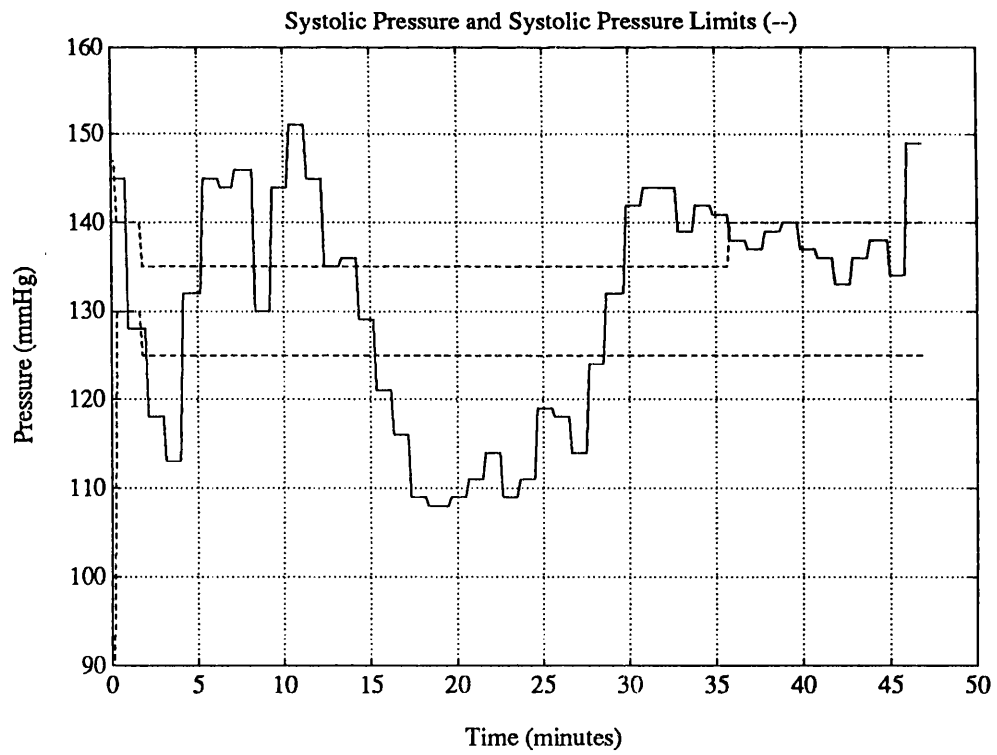

Figure 7.9: Systolic Arterial Pressure Measurements and Limits for Test 1

anaesthetic to be 'OK'. Between 18 and 20 minutes the Reversed Model indicated that the anaesthetic was 'deep'. At 19 minutes, the anaesthetist reduced the vaporiser setting to 1.5%. Between 22 and 27 minutes, the Reversed Model again reported that the anaesthetic was 'deep'. At 25 minutes the anaesthetist reduced the vaporiser setting to 1%. At 37 minutes, the variable limits were adjusted so as to make all variables 'normal' because the anaesthetist was satisfied with the patient's anaesthetic state at this time.

Time in minutes	Heart Rate	Systolic Pressure	Fluid	Depth	Anaesthetist's Action
0	high	low	low	normal	Vaporiser at 2%
1 to 5	high	high	normal	light	Infusion running
6	high	high	normal	light	Vaporiser to 3%, Morphine increment given
7 to 8	high	high	normal	light	—
8 to 9	high	normal	low	OK	—
10 to 12	high	high	normal	light	—
13 to 14	normal	high	normal	OK	—
14 to 15	normal	normal	normal	OK	—
15	normal	normal	normal	OK	Vaporiser to 2%
15 to 16	normal	low	normal	OK	—
17 to 18	normal	low	normal	OK	—
18 to 19	low	low	normal	deep	—
19	low	low	normal	deep	Vaporiser to 1.5%
19 to 20	low	low	normal	deep	—
21 to 22	normal	low	normal	normal	—
22 to 25	low	low	normal	deep	—
25	low	low	normal	deep	Vaporiser to 1%
25 to 27	low	low	normal	deep	—
27 to 28	normal	low	normal	OK	—
28 to 29	normal	normal	normal	OK	—
39 to 36	normal	high	normal	OK	—
37	—	—	—	—	Reset Limits
38 to 45 END	normal	normal	normal	OK	—

Note: Fluid = fluid hypothesis; Depth = depth hypothesis

Table 7.3: A Summary of Reversed Model Hypotheses for On-line Test 1

During this operation, the anaesthetist was asked to assess the validity of the hypotheses produced by the Reversed Model. When hypotheses seemed less realistic, variable limits were adjusted. At other times, the hypotheses were considered appropriate. Because of this, Table 7.3 cannot be interpreted as an indication that the Reversed Model is capable of achieving performance comparable to that of the anaesthetist because the anaesthetist is aware of the Model's hypotheses and was directly involved in the manipulation of the variable limits.

Test 2

This operation was carried out on a 63 year–old man to excise varicose veins. The target systolic arterial pressure predicted by the formula given previously is 139 mmHg but the anaesthetist recommended systolic arterial pressure limits of 125 and 135 mmHg. The heart rate limits were set at 70 and 90 beats per minute. During this procedure, a data collection fault occurred at around 40 minutes resulting in no new data being presented to the Reversed Model. This fault persisted until 51 minutes and the program was restarted at this time. The heart rate measurements for the procedure are shown in Figure 7.10 along with the limits of the 'normal' range chosen during the procedure. Figure 7.11 shows the limits and measured values of systolic arterial pressure during the procedure. The performance of the Reversed Model during this operation is summarised in Table 7.4.

In the first 6 minutes of the procedure, the Reversed Model concluded that the anaesthetic was 'deep'. After 3 minutes, the anaesthetist reduced the vaporiser setting from 3% to 1.5%. From 6 minutes to 19 minutes, the Reversed Model diagnosed no anaesthetic state imbalances. The anaesthetist reduced the vaporiser setting at 19 minutes to 1%. Between 20 and 24 minutes the Reversed Model considered the anaesthetic 'deep'. The Reversed Model produced no imbalance hypotheses from 24 minutes to 28 minutes when it again found the anaesthetic

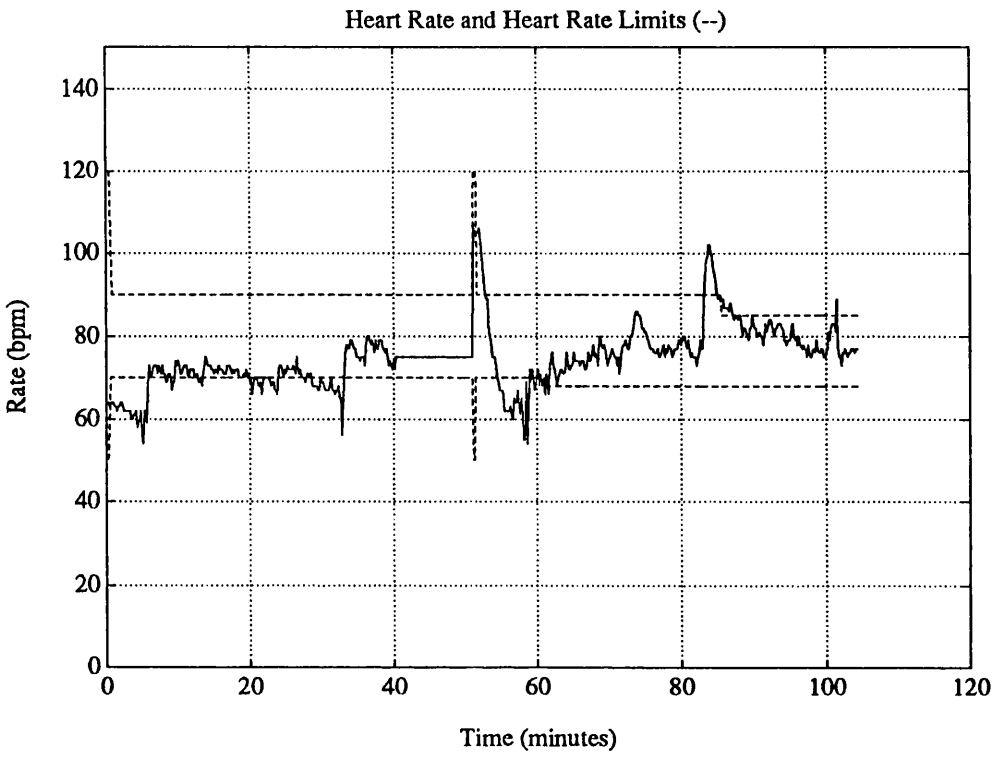

Figure 7.10: Heart Rate Measurements and Limits for Test 2

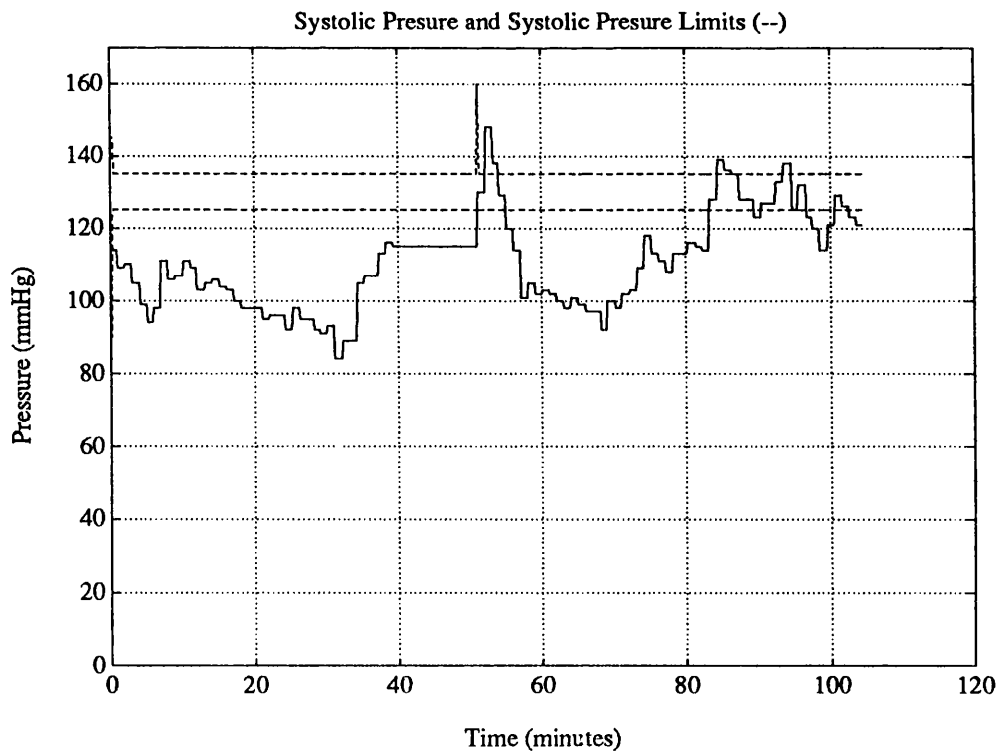

Figure 7.11: Systolic Arterial Pressure Measurements and Limits for Test 2

'deep'. This assessment was valid from 28 minutes until 33 minutes. The anaesthetist reduced the anaesthetic dose at 31 minutes to 0.5%. Between 33 and 40 minutes, no anaesthetic state imbalances were found. At 40 minutes the data collection fault occurred. The program was restarted at 51 minutes and the variable limits were restored to their previous values. At 52 minutes, the Reversed Model considered the anaesthetic 'light'. This coincided with the increase of both inhaled and injected anaesthetic drug delivery by the anaesthetist. Between 54 and 60 minutes, the Reversed Model concluded that the anaesthetic was 'deep'. At 56 minutes, the anaesthetist reduced the vaporiser setting to 2%. The anaesthetist reduced the vaporiser setting to 1% at 83 minutes. At this time, the Reversed Model considered the anaesthetic state appropriate. For short periods at 84 and 86 minutes, the Reversed Model considered the anaesthetic 'light'. The anaesthetist made no changes at this time. For the remainder of this procedure, the Reversed Model reported no imbalances in the anaesthetic state.

In this test, the diagnoses of anaesthetic state imbalances presented by the Reversed Model were realistic throughout the procedure. Limitations of the technique are illustrated by the change made by the anaesthetist at 19 minutes. The anaesthetist has realised that the patient's systolic arterial pressure is falling. The reduction of drug dose reverses this trend. In its present implementation, the Reversed Model only uses value information and the diagnosis of anaesthetic state imbalances is based upon this. The Qualitising Filters employed in the Reversed Model implementation do, however, provide rate information. This could be used within the Reversed Model to improve diagnostic performance.

Another aspect of note is that, during this procedure, the patient's systolic arterial pressure was consistently lower than the expected range. Towards the end of the procedure it was noted that the patient was being treated with antidepressant drugs which potentiate the effects of isoflurane. The arterial pressure can therefore be expected to be lower than expected for this patient

Time in minutes	Heart Rate	Systolic Pressure	Fluid	Depth	Anaesthetist's Action
0	—	—	—	—	Vaporiser at 3%
1 to 3	low	low	normal	deep	—
3	low	low	normal	deep	Vaporiser from 3% to 1.5%
3 to 6	low	low	normal	deep	—
6 to 8	normal	low	normal	OK	—
8 to 19	normal	low	normal	OK	—
19	normal	low	normal	OK	Vaporiser from 1.5% to 1%
20 to 24	low	low	normal	deep	—
24 to 28	normal	low	normal	OK	—
28 to 31	low	low	normal	deep	—
31	low	low	normal	deep	Vaporiser from 1% to 0.5%
32 to 33	low	low	normal	deep	—
33 to 40	normal	low	normal	OK	—
40 to 51	FAULT	FAULT	FAULT	FAULT	—
51	—	—	—	—	RESTART
52	high	high	normal	light	Vaporiser from 0.5% to 3%, Morphine increment
53 to 54	normal	high	normal	normal	—
54 to 56	low	low	normal	deep	—
56	low	low	normal	deep	Vaporiser from 3% to 2%
56 to 60	low	low	normal	deep	—
60 to 83	normal	low	normal	normal	—
83	normal	low	normal	normal	Vaporiser from 2% to 1%
84	high	high	normal	light	—
85	normal	high	normal	light	—
86	high	high	normal	light	—
87 to 102	normal	low	normal	normal	—
102	normal	low	normal	normal	Vaporiser OFF
102 to 104	normal	low	normal	normal	—
END					

Note: Fluid = fluid hypothesis; Depth = depth hypothesis

Table 7.4: A Summary of Reversed Model Hypotheses for On-line Test 2

during isoflurane anaesthesia. Because this effect was not noted at the start of the procedure and it would not have been practically possible to predict its magnitude, the arterial pressure limits were unnecessarily high. Nonetheless, the Reversed Model has generated satisfactory, realistic hypotheses.

Test 3

This operation was carried out on a 36 year–old female to repair a hernia. The target for systolic arterial pressure was calculated as 125 mmHg and the initial limits were therefore set as 120 and 130 mmHg. The heart rate limits were set at 70 and 85 beats per minute.

Figure 7.12 shows the measured heart rate along with the heart rate limits used during the procedure. Figure 7.13 shows the systolic arterial pressure measured values and the limits used by the Reversed Model. The diagnosis of the Reversed Model and the actions of the anaesthetist are summarised in Table 7.5.

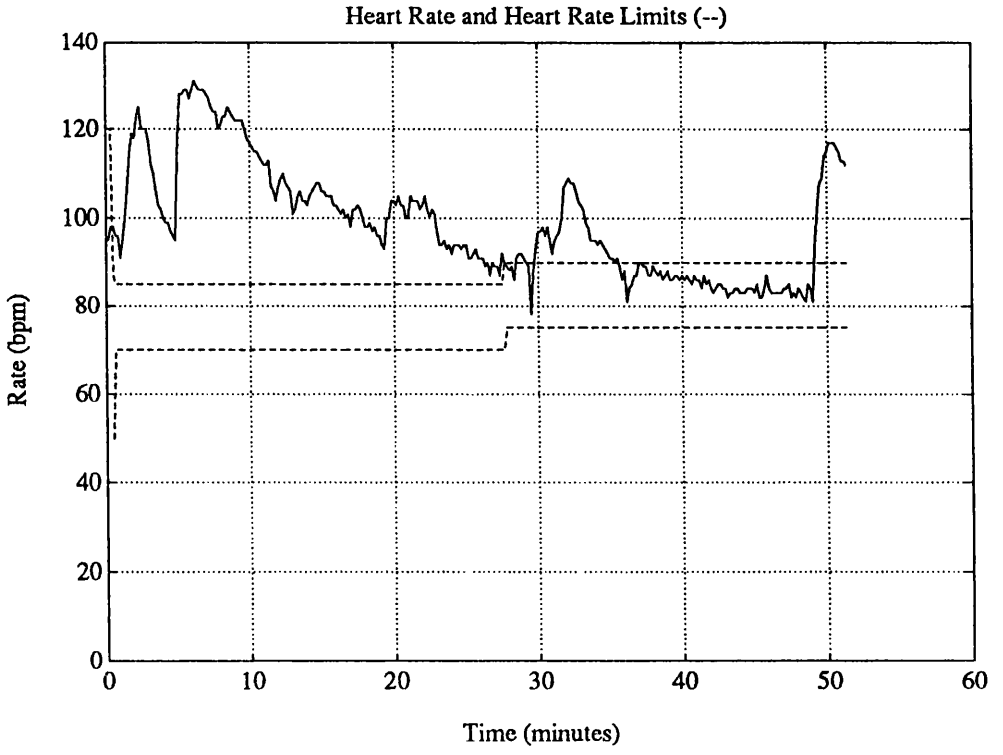

Figure 7.12: Heart Rate Measurements and Limits for Test 3

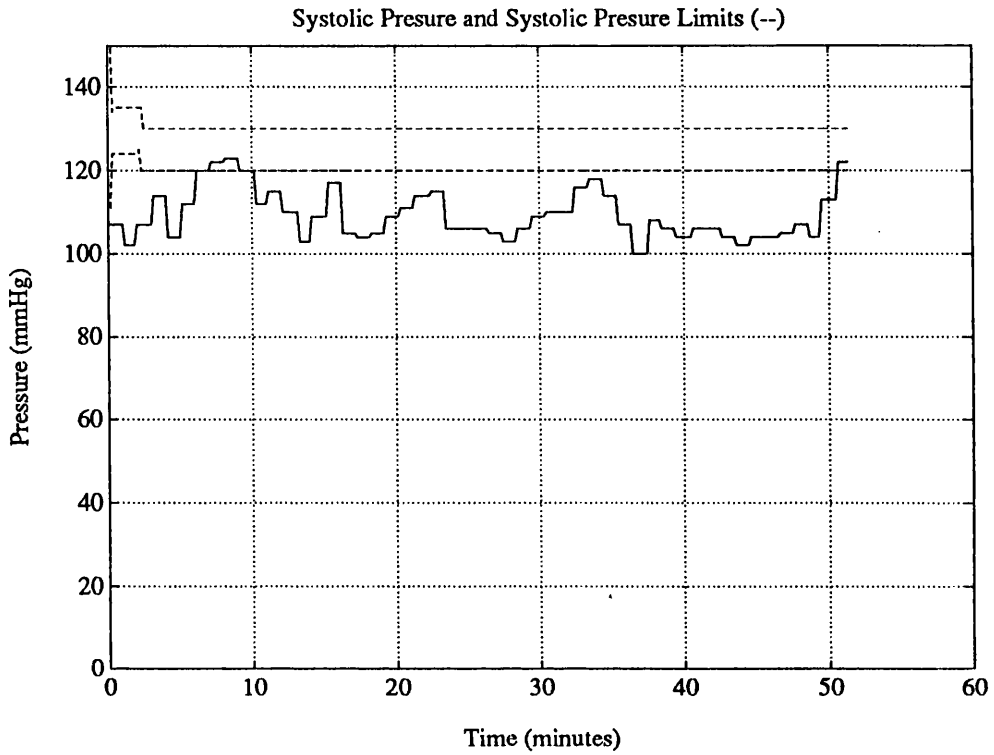

Figure 7.13: Systolic Arterial Pressure Measurements and Limits for Test 3

For the first 6 minutes, the Reversed Model diagnosed a fluid imbalance and indicated 'low' fluids. At this time, a 500ml infusion was started. The vaporiser was altered from 2% to 3% at 6 minutes and back to 2% at 8 minutes. Between 8 and 10 minutes the Reversed Model diagnosed no imbalances in the anaesthetic state but between 10 and 27 minutes, it diagnosed 'low' fluids. At 15 minutes a further 500ml fluid infusion was started. This diagnosis persisted until about 35 minutes and a further infusion was started at 32 minutes. The Reversed Model diagnosed no anaesthetic state imbalances between 35 minutes and 49 minutes.

During this procedure, the diagnoses of the Reversed Model were dominated by 'low' fluid status. These diagnoses were, at all stages, considered realistic by the anaesthetist. The provision of fluid reduced the heart rate to within the chosen 'normal' limits but the systolic arterial pressure stayed 'low' for the bulk of the procedure. It seems probable therefore that the 'normal' limits for this patient's arterial pressure should have been lower than those chosen although the

Time in minutes	Heart Rate	Systolic Pressure	Fluid	Depth	Anaesthetist's Action
0	—	—	—	—	Vaporiser at 2%
1 to 6	high	low	low	OK	Infusion started (500ml)
6	high	low	low	OK	Vaporiser to 3%
7 to 10	high	normal	low	OK	—
10 to 15	high	low	low	OK	—
15	high	low	low	OK	Second infusion started (500ml)
16 to 27	high	low	low	OK	—
28	normal	low	normal	OK	—
29	normal	low	normal	OK	—
30 to 32	high	low	low	OK	—
32	high	low	low	OK	Third infusion started (500ml)
32 to 35	high	low	low	OK	—
35 to 49	normal	low	normal	normal	—
49 to 51	high	low	low	OK	—
51	high	normal	low	OK	Infusion rate increased
END					

Note: Fluid = fluid hypothesis; Depth = depth hypothesis

Table 7.5: A Summary of Reversed Model Hypotheses for On-line Test 3

anaesthetist was content with the chosen values.

7.7.3 Discussion of Results

The Reversed Model has been demonstrated to present accurate, timely diagnoses of anaesthetic state imbalances. The mouse–controlled interface developed for the use of the Reversed Model in the operating theatre has supported its use on–line.

The Reversed Model is intended to produce diagnoses of anaesthetic state imbalances suitable for use in a controller of the anaesthetic state. Comparison of the Model's diagnosis with the actions of the anaesthetist in the off–line test and each of the three on–line tests reveals that the the Model has provided diagnoses which would have elicited the same action as that taken by the anaesthetist in practically all cases. Based upon this observation, it seems that, with some further refinements, such as the inclusion of rate information, the Reversed Model could provide the basis for a controller of the anaesthetic state.

A further point of note is that, in the same manner as the estimation scheme described in Chapter 5, the Reversed Model makes deductions with physiological and pharmacological concepts and values as intermediate stages in the process. The Reversed Model therefore generates hypotheses which are not only familiar to the anaesthetist but which are relevant to the management of the patient's anaesthetic state. This property ensures that if a controller based upon the Reversed Model is developed, the anaesthetist can be informed explicitly of the specific physiologic or pharmacologic anaesthetic state imbalances which are being manipulated. If the anaesthetist does not consider the hypothesis valid, the controller can be halted. The incorporation of intermediate stages with physiological or pharmacological meaning is very difficult in conventional controllers. Developments of the Reversed Model and uses for it are described in the next chapter.

Chapter 8

Conclusions and Further Work

SUMMARY

This chapter summarises the developments made in the work of the thesis and introduces the GAEL and MASIE software libraries. Further work in the refinement and application of the techniques described in the thesis is suggested with the intention of focussing future efforts.

8.1 Conclusions

The work described in this thesis has used engineering skills to support modelling, model representation and provide techniques suitable for use in the control of anaesthesia. Fundamental in each aspect of the work has been the preservation of the concepts which originate within anaesthesia, physiology or pharmacology. Specifically, this thesis has:

- Demonstrated the utility of bond graphs in the representation of physiologically–based models of inhaled and injected agent pharmacokinetics.
- Parameterised a physiologically–based model of isoflurane pharmacokinetics and used the bond graph representation of this model to analyse the

effects of inter–individual and intra–individual physiologic changes upon the pharmacokinetics.

- Introduced a scheme to allow the matching of a physiologically–based model of inhaled agent pharmacokinetics to an individual using only body mass and body fat measurements.

- Demonstrated the performance of an estimation scheme developed to estimate cardiac output and tissue anaesthetic tensions both in simulation and on–line in theatre.

- Described the development of a model of the homeostasis loops and the stress response of the body intended to represent compensation for physiological imbalances and demonstrated the performance of a prototype implementation of the model.

- Described the concepts of a Reversed Model of homeostasis and the stress response intended to infer physiological and pharmacological anaesthetic state imbalances from the clinical signs and demonstrated the performance of a prototype implementation using both off–line data and on–line data in theatre.

The implemented prototype of the estimation scheme has, following some refinement, proved capable of producing realistic and stable estimates of cardiac output indicating that the model matching scheme is successful and that the estimated tissue anaesthetic tensions are likely to be reliable. The specific use of the brain tension estimate from this scheme could be used within a controller of depth of anaesthesia.

As an aid to future developers wishing to use the estimation scheme the Glasgow Anaesthesia Estimation Libraries (GAEL) have been developed. These libraries include explicit representation of the patient, including the model

matching scheme, explicit representation of an inhaled drug incorporating its physicochemical parameters and a representation of the estimation scheme which uses the patient and drug representations to produce its internal model of pharmacokinetics for the patient and the drug.

The prototype implementation of the Reversed Model has shown that it can generate realistic diagnoses of anaesthetic state imbalances using clinical sign information gathered automatically during a procedure. The on–line tests performed using the Reversed Model indicate that it could form the basis of a controller for the anaesthetic state.

To support further developments using the Reversed Model, the Model–based Anaesthetic State Imbalance Evaluation libraries (MASIE) have been developed. The MASIE libraries include implementations of the qualitising filter, the Reversed Model and the mouse–driven screen interface used in the prototype implementation described in the thesis.

Overall, this thesis has described the development of techniques which preserve the anatomical, physiological and pharmacological information relevant to them. Because of this, an anaesthetist is able to understand and verify the techniques and their intermediate stages e.g., the estimation scheme includes a cardiac output estimate as an intermediate stage. The use of physiologically meaningful intermediate stages ensures that poor performance is immediately obvious due to unrealistic intermediate values e.g., cardiac output estimates outwith physiological ranges. The performance of the techniques has indicated that the explicit representation of anatomical, physiological and pharmacological information constitutes a valid and fruitful approach in the modelling and control of anaesthesia.

8.2 Further Work

This section describes straightforward extensions of the techniques developed in the thesis to provide controllers for anaesthesia. Minor changes to the estimation scheme are described and then three schemes are presented. These correspond to use of the estimation scheme, the use of the Reversed Model and the combination of the estimation scheme and the Reversed Model within controllers.

8.2.1 Refinement of the Estimation Scheme

The performance of the estimation scheme described in Chapter 5 was seen to be hampered by the characteristics of the measurements of end–tidal anaesthetic concentrations (Section 5.4.2). These characteristics led to the systematic underestimate of cardiac output at the start of an anaesthetic and its overestimate at the end. The error in cardiac output estimate produced further effects upon the tissue tension estimates. The exact source of the error in the end–tidal measurement has not become apparent. The development of a measuring system capable of accurately measuring inspired and end–tidal concentrations has been achieved by Morris et al. [159]. This system was demonstrated to produce end–tidal measurements comparable to those predicted theoretically. The modification of such a system to measure isoflurane concentrations would therefore avoid the errors described above.

Another area of improvement lies in the estimation of alveolar ventilation. In the present implementation, an estimate of the patient's alveolar ventilation is entered using a menu panel on the interface to the estimation scheme. If information such as respiration rate and tidal volume were available from a respiration monitor via a communication interface, the estimation of alveolar ventilation could be automatically produced and updated. This would make the estimation scheme much simpler to use.

One potential area of development concerns the generation of the cardiac output estimate. In the current implementation, this stage relies upon the accurate parameterisation of the patient model and measurement of inspired and end-tidal concentrations. The recent development of transtracheal and transoesophageal [160] doppler estimates of cardiac output would reduce the dependence upon these measurements. The transtracheal approach described by Abrams et al. [161] illustrates the incorporation of the ultrasound transducer within the endotracheal tube. This arrangement would be easy to apply during anaesthesia.

8.2.2 A Controller for Depth of Anaesthesia

Aside of the errors at the start and end of a procedure, which have been explained in terms of the current hardware setup, the estimation scheme has demonstrated satisfactory performance in the estimation of cardiac output and tissue tensions. The estimation scheme can therefore form the basis of a controller for brain tension. This is essentially the same arrangement as that described by Chilcoat, Lunn and Mapleson [79] and is represented in Figure 8.1.

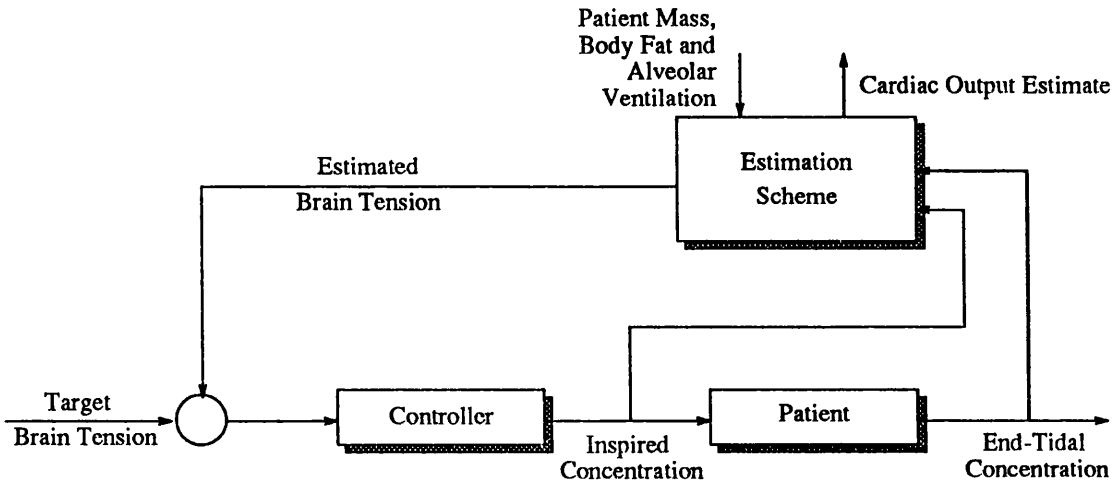

Figure 8.1: Control of Brain Tension using the Estimation Scheme

Using this scheme, the anaesthetist has access to the brain tension and cardiac output estimates produced by the estimator. The cardiac output estimate returned by the estimation scheme gives the anaesthetist an indication of the quality of the estimator performance and therefore of the likely overall controller performance. If the cardiac output estimate is physiologically realistic, the estimation scheme performance is likely to be reliable and the controller effective. This scheme could be easily implemented using the components within the GAEL libraries.

8.2.3 A Controller for the Anaesthetic State

The performance of the Reversed Model described in Chapter 7 has demonstrated that the approach can successfully differentiate between physiological and pharmacological anaesthetic state imbalances. Using the Reversed Model, the anaesthetist chooses the upper and lower limits of the 'normal' range for each clinical sign value. The Reversed Model then forms diagnoses when values move outwith their chosen 'normal' ranges. The use of the Reversed Model in a controller requires no changes in its operation and minimal extension. To form a controller, the diagnoses of anaesthetic state imbalances produced by the Reversed Model are used to initiate a control action. As examples, a 'light' anaesthetic indicates that the anaesthetic dose should be increased, a 'low' fluid status indicates that fluid should be infused. This scheme is illustrated in Figure 8.2.

Because the Reversed Model uses qualitative values generated by qualitising filters, a conversion from the qualitative expression of an imbalance to the quantitative change to be exerted is required. The most simple means of performing this conversion is to mimic the actions of the anaesthetist: When the anaesthetist makes a change during anaesthesia, the change is normally an increment or decrement of a setting e.g., a small change of vaporiser setting, the injection of an analgesic bolus or the delivery of a quantity of fluid. The controller

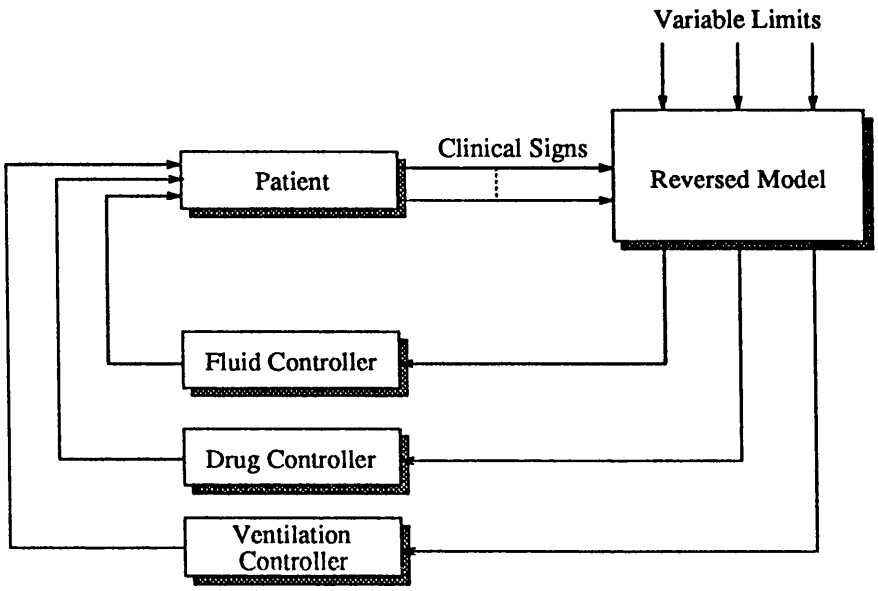

Figure 8.2: Control of the Anaesthetic State using the Reversed Model

for the anaesthetic state could then be configured to deliver these increments or decrements in response to a diagnosis. Simple limits could ensure safe operation e.g., by allowing no more than two vaporiser setting increments in 10 minutes. In Figure 8.2, each controller represents the generation of quantitative changes from the qualitative input given by the Reversed Model. This form of controller could be produced very easily with the Reversed Model components provided within MASIE.

8.2.4 The Combination of the Estimation Scheme and Reversed Model

The control of depth of anaesthesia is a task within the control of the anaesthetic state. The estimation scheme and the controller of brain tension based upon it can therefore be employed by the anaesthetic state controller based upon the Reversed Model. In this case, the diagnosis of 'light' or 'deep' anaesthesia by the Reversed Model will initiate a request for an increment or decrement of brain tension respectively. The increment will depend upon the potency of the agent used e.g., 0.5% may be appropriate for isoflurane. As a further advantage, because the

brain tension estimate is available to the Reversed Model, further changes in brain tension could be delayed until the previous change has exerted its effect. The brain tension controller may also call upon more simple, low–level controllers to effect the changes in inspired concentration which it requires. It may also be envisaged that comparable control schemes may be developed to handle fluid and ventilatory changes. The combination of the estimation scheme and the Reversed Model gives rise to the overall architecture for control of the anaesthetic state which has the form shown in Figure 8.3. This architecture depends mainly upon the estimation scheme and Reversed Model and can therefore be easily implemented using the GAEL and MASIE libraries.

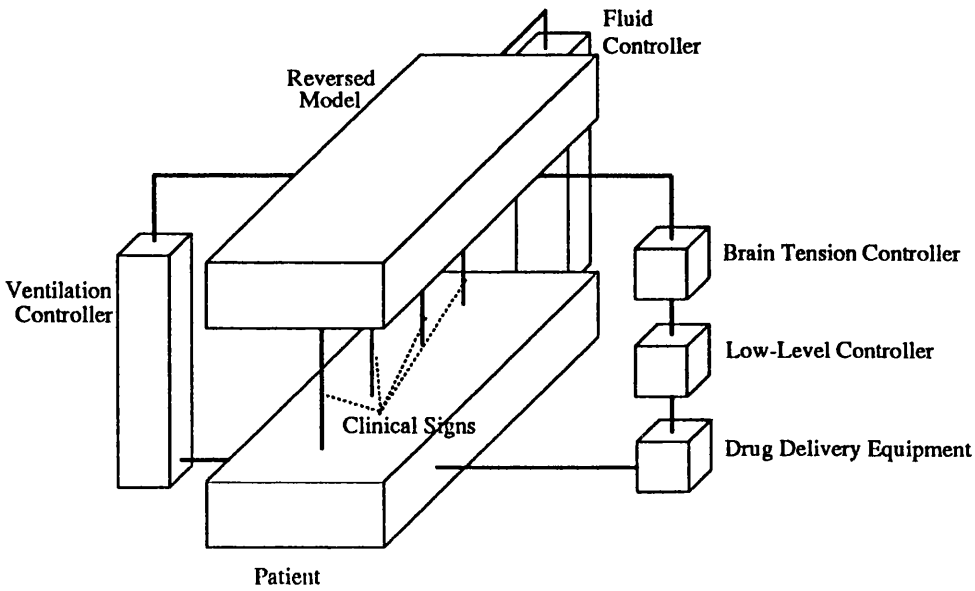

Figure 8.3: An Architecture combining the Estimation Scheme and Reversed Model

In summary, controllers for brain tension and the anaesthetic state can be readily derived from the techniques described in this thesis. The GAEL and MASIE software libraries reduce the implementation overhead of such developments significantly. In each of the suggested schemes, the physiological intermediate stages present within the schemes are available for appraisal by the anaesthetist. This enhances the anaesthetist's understanding of the approaches and appraisal of their performance. Sufficient support has been provided conceptually, theoretically and practically within this thesis to allow the development of anaesthesia controllers based upon physiological and pharmacological models by both engineers and anaesthetists.

Appendix A

The CLASS Library Report

A.1 Introduction

This report describes the design of the CLASS libraries and documents the programming interface to the equipment supported by CLASS version 1.0. The report consists of a description of the CLASS design concepts, documentation of the methods of CLASS objects, and listings of the C++ code used to generate the libraries.

A.2 The Motivation for CLASS

The CLASS libraries were developed in order to simplify the use of peripheral instruments and drug-delivery equipment in computer-controlled experiments. Examples of existing applications include data logging systems, muscle relaxant administration systems, the computer control of blood pressure and the control of anaesthesia.

Prior to the development of CLASS, each application requiring use of an instrument or drug-delivery device also required to code communication with the device in question. This stage was very time-consuming and detracted from the main tasks being pursued.

CLASS aims to produce a set of link-libraries so that in order to use an instrument or device, an application developer simply links application code with the CLASS libraries in order to provide safe and reliable communication with the devices.

A.3 CLASS Software Characteristics

The CLASS libraries have been written in Zortech C++ on an IBM PC AT compatible machine. They employ object-oriented design techniques to define interfaces to each item of equipment. Each type of equipment has associated with

it a standard set of methods which are available to an application developer as callable routines. These define the software interface to the hardware devices. In the future, development of new CLASS objects to add other items of equipment to the library requires only that routines specific to the equipment are developed, the interface will stay the same.

A.4 CLASS Hardware Support

The CLASS library currently contains support for the following hardware devices.

Device Type	Product	Description
Monitor	Datascope 3100	Anaesthesia monitor
	Datex Ultima	Anaesthesia gas analyser
Infusion pump	Braun Perfusor Secura	
Servo-vaporiser	CPBD SV100	Servo-controlled vaporiser

Table A.1: Currently supported hardware in CLASS

A.5 CLASS Objects and Services Overview

CLASS defines several classes of objects which are applicable to application development. Communication port handlers deal with low-level hardware communications and buffering, virtual devices are software interfaces to a real device. The objects are designed to be used together and an interface structure has been developed.The general structure of a CLASS device interface is shown in figure A.1.

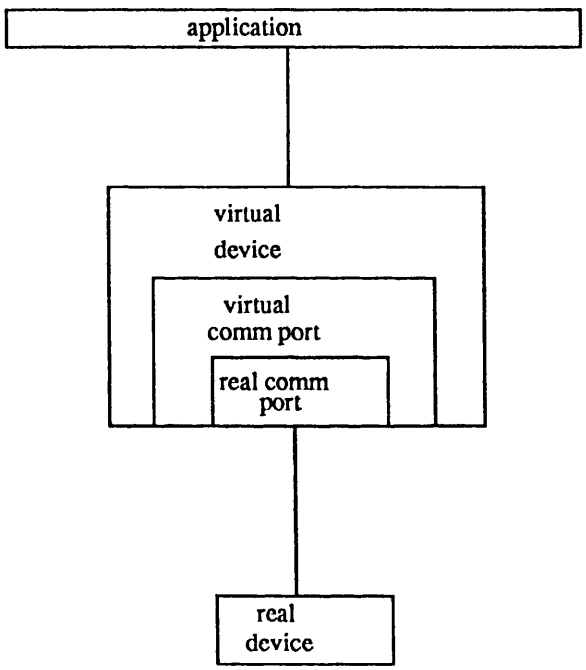

Figure A.1: CLASS device interface

Real devices are; existing monitors, infusion pumps or a servo-vaporiser. The real communication port can be either serial or parallel communication hardware in the computer being used. The virtual communication port provides a uniform interface to the virtual device and hides the implementation details of the real communication port. The virtual device provides a uniform interface to the application, allowing use of all of the features of each real device without requiring extensive knowledge of the communication parameters or protocols required to communicate with it. Because the virtual device uses a virtual communication

port, changes to the detail of the real communication port do not affect the virtual device or, indeed, the application. Assuming that a virtual communication port exists for a target machine, then an application and its virtual devices can then be moved onto another machine, relinked with the correct virtual communication port and then used. No other changes to source code will be needed. This offers considerable savings in time and resources.

The interfaces to the CLASS library communication port, monitor, infusion pump and servo-vaporiser objects which correspond to the virtual components of figure A.1 are defined by the services of those objects. The services deemed appropriate for the objects are described in the following sections.

A.5.1 Virtual Communication Port

A virtual communication port provides a software interface to a real communication port on a real machine. The interface to the virtual communication port is provided by its services. The services provided by each virtual communication port are independent of the hardware details of the port and of the machine. The model of a virtual communication port from the application developer's point of view is shown in figure A.2.

The programmer accesses both the transmit buffer and receive buffer of the virtual port. The virtual port manages the real port so that any characters arriving at the port are transferred to the recieve buffer preventing their loss. Similarly, when an opportunity for transmission exists, characters are read from the transmit buffer and sent to the device. The virtual comm. port is thus *event driven* so as to avoid lengthy delays in waiting for an entire message to be transmitted or received.

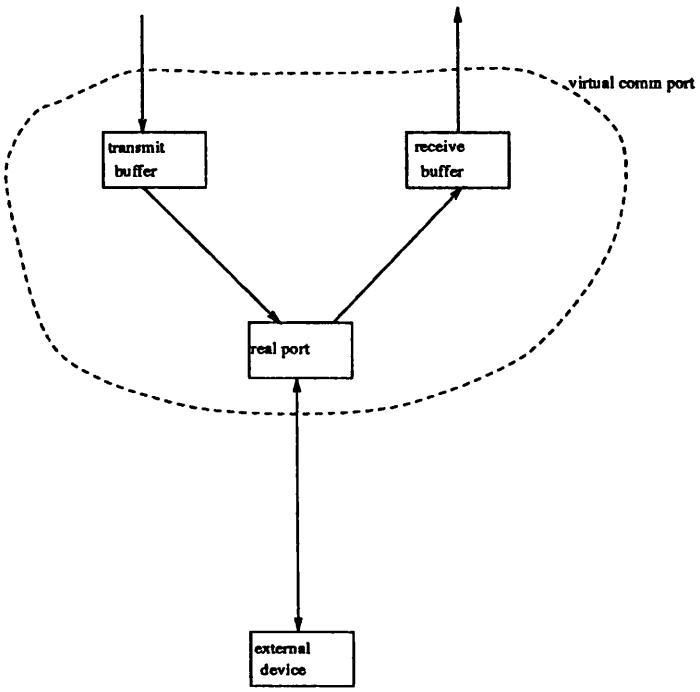

Figure A.2: Model of virtual communication port.

Services

In conjunction with the developers' model above (figure A.2) the following services are provided by the virtual communication port;

- write character

  This function should add a character to the transmit buffer to be transmitted when an opportunity arises.

- write

  This function adds a string to the transmit buffer for subsequent transmission.

- write buffer test

  This function tests whether the transmit buffer is empty. This allows determination of whether a message has been sent.

- read character

  This function removes a character from the receive buffer and returns it.

- read

  This function reads a string from the receive buffer.

- read buffer test

  This function checks whether the receive buffer is empty. This allows determination of whether a message has arrived.

A.5.2 Specific Communication Ports

The virtual communication port describes the interface and conceptual model of each communication port device. In reality, there must be an interface for each particular port type to take account of hardware differences between machines and also operating system differences. The CLASS library deals with this situation by making an abstract class called virtual comm port which defines the characteristics of all comm ports, and then specific comm port handlers become subclasses of the virtual comm port class and thus inherit its interface. This relationship is illustrated in figure A.3.

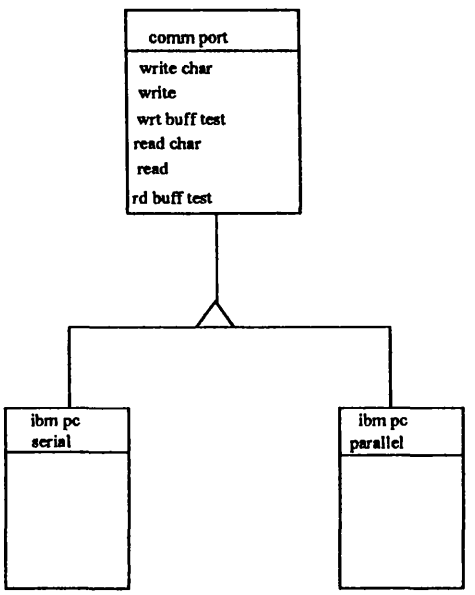

Figure A.3: Inheritance of interface from abstract class

A.5.3 Monitors

A virtual monitor creates an interface to a real monitor. Each monitor object uses a virtual comm port interface to provide communication with the real monitor. The virtual monitor ensures that the user or developer of an application does not need to be aware of the specific communication settings or protocols employed by the device. To the developer, the virtual monitor appears as shown in figure A.4.

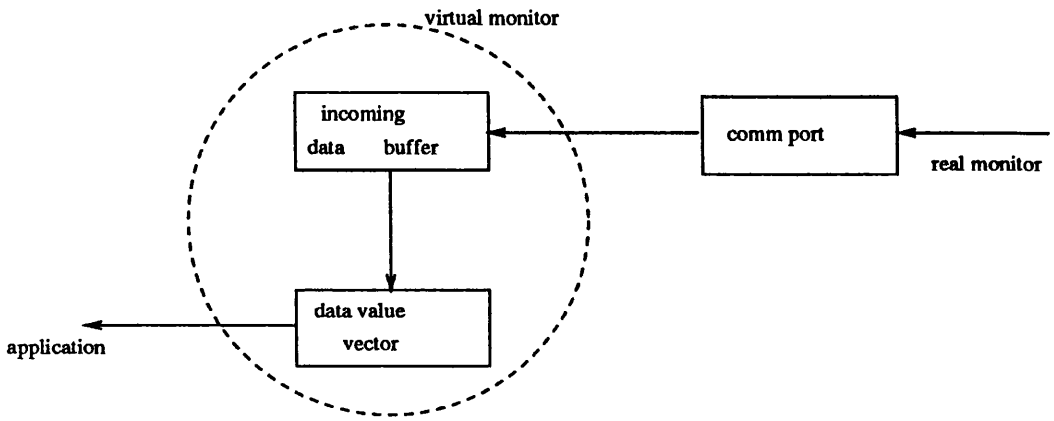

Figure A.4: Developers' model of a virtual monitor

Thus, data received from the real monitor via the communication port is placed in the data buffer of the virtual monitor. Data values from the buffer are then unpacked and stored in a data value vector.

Services

The services of the virtual monitor object are as follows;

- initialise

  Many monitors require an initialisation message to be sent to the monitor

from the computer before data communication can proceed. This service sends this message if appropriate.

- request data

  The computer sends a prompt to the monitor requesting that a new set of data values be returned.

- buffer input

  This function reads input characters from the buffer belonging to the virtual communication port and stores them in the buffer belonging to the virtual monitor.

- process input

  This function removes all complete strings from the virtual monitor's buffer, unpacks the values from the last string and places the values in a data structure inside the monitor object.

- return data

  This function returns the data structure if valid data is available.

- check errors

  This function returns an error code describing any errors in the monitor or the communication with the monitor.

- return monitor type

  This function returns the type of the monitor.

A.5.4 Specific Monitors

Specific monitors are handled in CLASS using inheritance. An abstract class called monitor is defined to have the interface described above, and all monitor handlers inherit characteristics from it. The use of a monitor handler is thus

independent of the particular monitor being used. This arrangement is shown in figure A.5

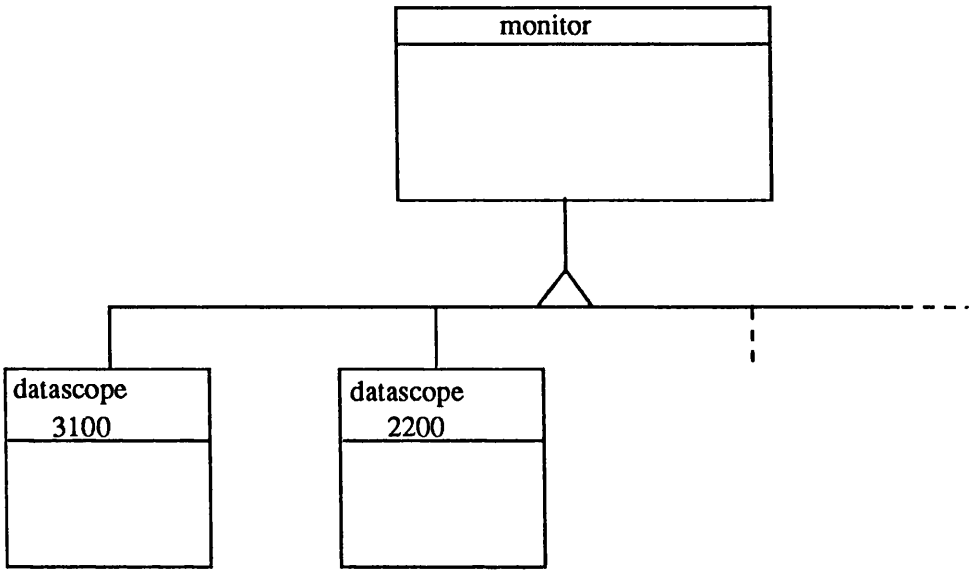

Figure A.5: Inheritance for monitor handlers

A.5.5 Infusion Pumps

The virtual infusion pump describes the interface provided by CLASS for any real infusion pump. The interface hides all implementation details and device specific information from the application developer. Each infusion pump handler uses a virtual communication port to manage the appropriate real communication port.

Services

The following services are provided by the virtual infusion pump;

- change rate

  This function queues a message which requests that the infusion rate be changed. The message is queued in the transmit buffer of the appropriate communication port handler. This service can be used to change infusions from their current value, or off, to the new value. If a non-attainable rate is requested, the function gives an appropriate return.

- stop infusion

  This function queues a message requesting that the infusion be stopped.

- restart

  This service constitutes a software reset of the infusion pump and is useful after an empty syringe is replaced, a line blockage cleared or other alarm condition is removed.

- check errors

  This function returns an error code describing errors in the infusion pump of communication with the pump.

- return pump type

  This returns the type of the pump.

- return drug

  This returns the drug employed in the syringe.

- return concentration

  This returns the concentration of drug in the syringe.

- return volume infused

  This returns the volume of drug solution infused thus far.

- return amount infused

  This returns the amount of drug administered thus far.

- return rate

  Thus returns the current infusion rate.

A.5.6 Specific Infusion Pumps

CLASS again employs inheritance to force the specific classes of infusion pump to adopt the interface of the virtual infusion pump. The virtual infusion pump is treated as a base class from which the specific classes inherit. This inheritance structure is shown in figure A.6.

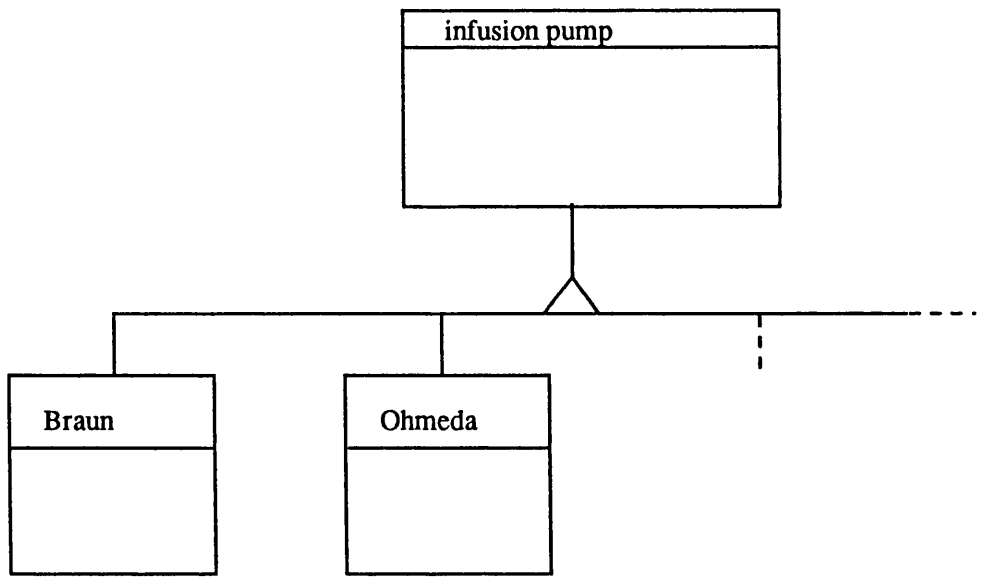

Figure A.6: Infusion pump inheritance strategy

A.5.7 The Servo-vaporiser

Although only one servo-vaporiser exists at the moment, it is still beneficial to define a virtual servo-vaporiser which exhibits 'idealised' interface characteristics. Thus the virtual servo-vaporiser defines behaviour which is independent of any hardware or communication details. A servo-vaporiser handler also uses a virtual communication port to manage the communication between the virtual servo-vaporiser and the real one. The definition of an 'idealised' interface for the servo-vaporiser has some essential characteristics in the context of this instrument. At the current time, the servo-vaporiser is still a prototype and does not employ any standard communication protocols. In the near future, the device may be improved to use RS–232 or some other 'standard' protocol. In such an event, applications already written for a previous version will not have to be changed. The code will simply be re-linked with the updated library object for the new servo-vaporiser. Any application is therefore protected from changes in hardware by the use of the 'idealised' interface.

Services

The servo-vaporiser interface is defined by the following services;

- change concentration

  This function changes the vaporiser concentration from the current setting, or off, to the new setting.

- stop vaporiser

  This function moves the vaporiser to the off position.

- estimate concentration

  This returns an estimate of the current concentration of the vaporiser.

- check errors

  This function returns an error code describing errors in the servo-vaporiser or in communication with the vaporiser.

A.5.8 Specific Servo–Vaporisers

Although only one type of servo–vaporiser actually exists, inheritance has been used to produce the CLASS servo-vaporiser objects. This allows easy addition of any other products which enter the market, and also changes to the existing product. The somewhat trivial inheritance structure is shown in figure A.7.

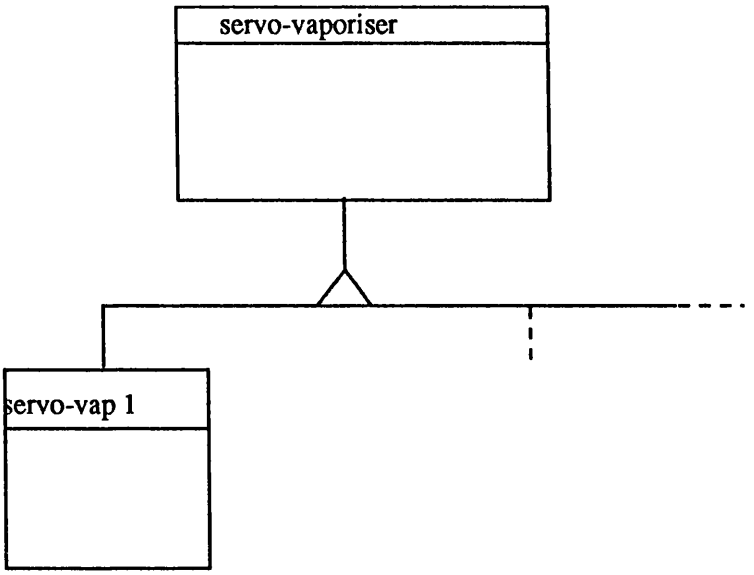

Figure A.7: Servo-vaporiser inheritance structure

A.6 CLASS Object Method Documentation

A.6.1 The Serial Port Handler

The CLASS library includes an object designed to handle interrupt driven serial communications via an RS-232 standard communications port. The use of a port for interrupt driven i/o requires the setting of several hardware registers associated with the 8250 UART device and also the registers of the 8259A programmable interrupt controller in a PC system.

Having enabled the generation of interrupts, an interrupt handler must be provided to take the appropriate action on receipt of an interrupt.

These procedures are intricate and time consuming. The serial port class of the CLASS library automatically performs these steps when an instance of the serial port class is created by an application.

Each serial port object has two ring buffers associated with it, one for transmitting and one for receiving. The managagement of these buffers is independent of the user.

Serial port interrupts

A serial port device can generate four different interrupts.

1. Receive data available
2. Transmit holding register empty
3. Receive line status
4. Modem Status

Interrupts (iii) and (iv) can be used to detect breaks in the line or failure of the modem and are not used in the CLASS serial port handler. Interrupt (i) signals that a new character has arrived at the port. The CLASS serial port interrupt handler for this interrupt reads the character from the buffer and stores it in the receive buffer associated with the port. Interrupt (ii) signals that there is no incoming data and that the transmit buffer is empty. The CLASS interrupt handler reads the port's transmit buffer on receipt of this interrupt and if a character is ready for transmission, it will be written to the transmit register.

Method Documentation

The interface to the serial port class is achieved using the methods of the class. These are as follows:

- s_port::s_port(int portnum, baud_var baud_rate, data_bits_var data_bits, stop_bits_var stop_bits, parity_var parity, struct port_control_regs * pcr)

  This method is the constructor for the serial port class and is called when an instance of the class is created. The arguments are as follows:

  - portnum

    The number of the port to be opened and used. Possible values are 1, 2 or 3 for COM1, COM2 and COM3 respectively.

- baud_rate

  The desired communication baud rate. The argument is of type baud_var.

- data_bits

  The number of data_bits per character. This argument is of type data_bits_var.

- stop_bits

  The number of stop bits per character. This argument is of type data_bits_var.

- parity

  None, even, or odd parity. This argument is of type parity_var.

- pcr

  This is a pointer to a structure containing the required set up for the 8250 interrupt enable register and modem control register. This accommodates the different requirements of each peripheral. The structure port_control_regs is defined in "s_port.hpp".

The constructor opens a serial port, attaches it to receive and transmit buffers, enables the required interrupts, sets up port lines and establishes an interrupt handler. From this stage onwards, interrupt driven i/o occurs in the port.

Note that the enumerated type baud_var, data_bits_var etc. are defined so as to only allow acceptable values for communication parameters to be set up. These types are defined in the file "s_port.hpp".

- s_port::~s_port(void)

This is the destructor for the serial port class. this method takes no arguments, restores the serial port devices to their state prior to use by this

application, and removes the installed interrupt handler. The destructor is called automatically when the serial port object is destroyed.

- int s_port::sendchar(char *c)

  This method accepts, as its argument, a pointer to a character. The character pointed at by c is loaded into the transmit queue to be sent from the port on receipt of a transmit register empty interrupt.

  This method always returns 1.

- char s_port::receivechar(char *c)

  This method takes a pointer to a character as its argument. If a character can be retrieved from the receive buffer, a 1 is returned from the method and the character is written into the location pointed at by c. If no character is available, 0 is returned.

- int s_port::receive(char * buffer)

  This method fills the space pointed at by *buffer* with the contents of the receive buffer. A trailing null is added to the buffer after the last character. If a string was received, the method returns 1. If no string was available, the method returns 0.

- int s_port::send(char * buffer)

  Thi method repeatedly calls sendchar until all of the characters in the array pointed at by *buffer* have been sent, or the queue is filled. The method returns 1.

- int s_port::is_transmit_buffer_empty(void)

  This method checks the status of the transmit buffer associated with the port. The method returns 1 for an empty buffer and 0 for a non-empty buffer.

- int s_port::is_receive_buffer_empty(void)

  This method checks the status of the receive buffer associated with the port. The method returns 1 for an empty buffer and 0 for a non-empty buffer.

A.6.2 The Infusion Pump Object

Routine use of an infusion pump under computer control is hindered by the time taken, and skills required, to develop code to communicate with the device. The CLASS libraries contain a generic infusion pump object. This object has a clearly defined set of methods and all hardware aspects of the real pump are invisible to the application developer. An infusion pump object employs a serial port object to perform interrupt driven serial communication with the actual pump.

Infusion Pump Object's Methods

The methods of the infusion pump object are as follows:

- infusion_pump::infusion_pump(int portnum)

  This method initialises general data items applicable to all infusion pumps. The constructor creates a circular buffer for use by the infusion_pump object in buffering incoming messages. The integer argument *portnum* is used only to set up an internal record of the port number for the infusion pump object.

- braun_infusion_pump::braun_infusion_pump(int portnum)

  This is the constructor for the braun infusion pump object and accepts the number of the serial port to which the pump will be attached as an argument. The constructor creates a serial port object to provide access to the infusion pump. Version 1.0 of CLASS allows portnum to have values 1, 2 or 3 for COM1, COM2 or COM3 respectively on a PC or compatible.

  This constructor also calls the infusion pump class constructor.

- infusion_pump::~infusion_pump(void)

  This is the destructor and deletes the circular buffer created by the constructor.

- braun_infusion_pump::~braun_infusion_pump(int portnum)

  This is the destructor for the braun infusion pump class and deletes the serial port handler created by the constructor. This desctructor also calls the infusion pump class destructor.

- int braun_infusion_pump::change_speed(int rate)

  The braun infusion pump can be configured to run infusions at between 0.1 ml/h and 99.9 ml/h for a 50ml syringe. The pump can however also accommodate a 25ml syringe, or two 50ml syringes giving an effective 100ml syringe. The possible infusion rates are therefore between 0.05ml/h and 1998 ml/h.

  The change speed method accepts one argument, *rate*, which is the desired infusion rate multiplied by 10 so that the argument for a desired rate of 45.6ml/h is 456. The method calculates the actual request to the actual infusion pump based upon the size of syringe used in the pump. The size of the syringe is set using the method *set_syringe_chars()*.

  The method returns -1 for an error in changing speed or a bad speed request and 0 for no errors.

- int braun_infusion_pump::stop_pump(void)

  This method stops the infusion. For each type of pump, the stop message will have a different form. The stop_pump method is therefore virtual to allow derived classes to redefine the method. The stop_pump method returns 1 for a successful issue of the command and 0 for a failure.

- int braun_infusion_pump::interpret_messages(void)

  This method is used to process the messages received from the infusion pump. Messages found are the switch-on message, rate change acknowledgements, pump life signals, empty/pressure alarm messages and device defective alarms. If error messages are received the error word stored within the infusion pump handler is updated.

  This method always returns 1.

- int braun_infusion_pump::check_errors(void)

  This method returns an error word which codes information relating to the status of both the infusion pump and communication with the pump. The errors coded in the error word are set up in the header file "inf_pump.hpp". Note that failure to buffer and process input from the pump can cause detection of a communication error because no message will have been correctly decoded for some time. The user of the infusion pump handler is therefore responsible for regular buffering and processing of incoming information.

- void braun_infusion_pump::update_amounts(void)

  This method updates the infusion pump handlers internal stored totals for the volume of drug infused and the amount of drug infused (in milligrammes or microgrammes). There are no returns from the method.

- float braun_infusion_pump::volume_total(void)

  This method returns the volume of solution infused at the current time and is the integral of the infusion rate–time curve at this time. This method merely returns the value of the volume_infused slot.

- float inf_pump::amount_total(void)

  This method is identical to volume_total except that the amount of drug

infused is returned. The amount infused is the volume infused multiplied by the concentration of drug in the syringe.

- int infusion_pump::set_syringe_chars(int size, int conc, char* name)
  This method takes three arguments, *size* the size of the syringe e.g. 75 for 75ml, *conc* the concentration in the syringe e.g. 2 for 2mg/ml if the amounts are desired in mg, and *name* the name of the drug in the syringe. These parameters are set up and then the method returns 1.

- int infusion_pump::give_pump_type(char * p)
  This method accepts a pointer to an array of characters as input argument. It copies the string holding the name of the infusion pump type to the array pointed at by p. The method returns 1.

- int infusion_pump::give_drug_name(char *p)
  This method copies the name of the drug currently held in the syringe to the character array pointed at by p. The routine always returns 1.

- int infusion_pump::give_drug_conc(int * n)
  This method writes the concentration in the syringe to the integer pointed at by n. The concentration is assumed to be an integer in either mg/ml or μg/ml. The method always returns 1.

- int infusion_pump::give_syringe_size(int * n)
  This method writes the size of the syringe in ml into the integer pointed at by n. The method always returns 1.

- int infusion_pump::give_infusion_rate(float * f)
  This method writes the infusion rate into the float pointed at by f. The method always returns 1.

A.6.3 The Monitor Object

The Monitor object provides a software interface to a real anaesthetic monitor. Real monitors are often capable of communicating with a computer using simple serial communications. Difficulty arises in this situation in establishing secure and reliable communication with the device and in decoding the strings received from the monitor. The CLASS monitor objects remove this burden from the application developer. Three main objects exist here; a virtual monitor object used to define the interface to all monitors and the methods common to all, a datascope 3100 object which defines the specific characteristics of the handler for a Datascope 3100 object and a datex object which defines the specific characteristics of the handler for a Datex Ultima gas analysis instrument.

Monitor Object's Methods

The methods of the monitor object and the derived classes for datascope 3100 and datex monitors are as follows.

- int monitor::initialise(void)

  This method is a prototype for every monitor and allows for initialisation of a monitor. The method returns 1.

- int monitor::buffer_input(void)

  This method transfers incoming data from the communication port handler associated with each monitor object to a circular buffer belonging to the monitor object. This prevents loss of data from the instrument and must be called periodically. This method always returns 1.

- int monitor::process_input(char *p)

  This method causes the last data string from the monitor to be removed from the monitor object's circular buffer and the data to be removed from the string and loaded into a data vector as defined in the header

file "monitor.hpp". This method calls *get_last_string()* and *unpack_string()* which are private routines specifically described for each monitor type. This method returns 1 if data has been converted from a string and 0 if no conversion has taken place. The single input argument *p* points to an array of characters which is used to store intermediate strings involved in decoding monitor messages.

- int monitor::get_last_string(char *p)

  This method is used to remove the last complete instrument string from the monitor circular buffer and store it in the array pointed at by *p*. All other data which preceeded the removed string are discarded. This method is redefined by other monitor objects. The method returns 1.

- int monitor::unpack_string(char *p)

  This method is used to remove the data and status information from the instrument string pointed at by *p* and load it into a datavector for later use. This method is also redefined for each type of monitor object because each monitor returns different string formats with different data elements in them.

- int monitor::return_data(DATAVECTOR * d)

  This method is applied to all monitor object subclasses. The datavector pointed at by d is loaded with the most recently decoded data values. This method returns 1. Note that return_data() is usually called directly after unpack_string().

- int monitor::check_errors(char * p)

  The monitors encountered so far give no indication of device error. The only errors which can be monitored are therefore communication errors between the computer and the instrument. This method checks whether a message has been received from the instrument within a specified maximum

time or whether a message to be transmitted to the instrument has been transmitted. These are implemented as simple time-outs based on the transmit and receive buffer statuses. The routine writes an error string to the character array pointed at by p and returns 1 for an error, but returns 0 if there is no error.

- int monitor::give_monitor_type(char * p)

  This method writes the name of the monitor into the character array pointed at by p and returns 1.

- datascope_3100::datascope_3100(int port_number)

  This method is the constructor for the datascope_3100 monitor object class. The constructor creates a serial port handler on the port specified by *port_number* for the monitor object to use and creates a circular buffer for storage of received strings. The constructor also initialises the parameters of the monitor and initialises the contents of the monitor's internally stored datavector to known values. The argument *port_number* can have value 1, 2 or 3 corresponding to COM1, COM2 or COM3.

- datascope_3100::~datascope_3100(int port_number)

  This is the destructor for the datascope_3100 class and deletes the circular buffer and serial port handler created by the constructor.

- int datascope_3100::initialise(void)

  This method redefines the initialise method for the datascope_3100 class. The method sends the correct initialisation string to the datascope. The methods always returns 1.

- int datascope_3100::request_data(void)

  This method is that of the virtual monitor object redefined for the datascope_3100. It returns 0 if the last request for data was unsuccessful and 0 if

the the last request was successful and a new request was started.

- int datascope_3100::get_last_string(char *p)

  This method is redefined to allow the last datascope formatted string to be removed from the monitor's circular buffer. The method accommodates the string format of the datascope instrument within it. If a complete string is found in the buffer, the method returns 1 otherwise it returns 0.

- int datascope_3100::unpack_string(char *p)

  This method redefines the unpack_string method of the virtual monitor object so as to unpack data from the datascope format string. As with the virtual method, the data is written into the monitor object's own datavector. This method returns 1.

- datex_ultima::datex_ultima(int port_number)

  This is the constructor for the datex_ultima class of monitor object. The constructor performs initialisation specific to the Datex Ultima such as establishing baud rate, and other communication parameters and then creates a serial port handler for the monitor object on the communication port specified by *port_number*. A circular buffer for the storage of received data is also created. The argument *port_number* can have value 1, 2 or 3 corresponding to COM1, COM2 or COM3.

- datex_ultima::~datex_ultima(int port_number)

  This is the destructor for the datex_ultima class of monitor object. The destructor deletes the serial port handler and the circular buffer which the constructor creates.

- int datex_ultima::initialise(void)

  This method redefines the virtual monitor object's initialise method to suit the datex_ultima handler. This methods returns 1.

- int datex_ultima::request_data(void)

  This method is redefined from the virtual monitor's method so as to perform actions associated with establishing data transfer between the Datex monitor and the application. If the last request for data was successful a new request is issued and 1 is returned otherwise 0 is returned.

- int datex_ultima::get_last_string(char *p)

  This method redefines that of the virtual monitor object so as to detect datex_ultima format strings. If no complete string is found, the method returns 0 and if a complete string is available, it is copied into the character array pointed at by p and a 1 is returned.

- int datex_ultima::unpack_string(char *p)

  This method redefines that of the virtual monitor object so as to unpack the data from the datex_ultima string pointed at by p. The data retrieved is stored in the internally held datavector of the monitor object. This method returns 1.

A.6.4 The Parallel Input/Output Board Handler

The servovaporiser used in the CLASS libraries requires to be interfaced using a PIO board. In our prototype development, the Amplicon PC 36 has proved adequate for the this job. The PC 36 is an 8255 based adapter and allows splitting of its 24 input/output lines into three groups of either inputs or outputs. For use with the servo–vaporiser, port A was configued as an input to read the results of the servo–vaporiser a/d conversion, port B was configured as an output to send the number of steps to the servo–vaporiser controller, port C upper was configured as outputs to allow setting of control lines for the vaporiser controller, and port C lower was configured as inputs to allow reading of status lines from the controller. The PIO handler makes these tasks simpler without adding too much specificity.

A.6.5 PIO Board Handler Methods

- pio::pio(void)

  This is the constructor for the pio handler and establishes the appropriate addresses of the board and the ports for use by the handler. These address are established as constants in the header file "pio.hpp".

- pio::~pio(void)

  This is the destructor for the pio handler and performs no operations.

- void pio::initialise(void)

  This method sets up the mode of the pio board for use as described above i.e. port A input etc.

- void pio::read_port_A(int *val)

  This method reads the input to port A and writes the integer value read into the integer pointed at by val.

- void pio::write_port_B(int val)

  This method writes the integer val to the port B of the pio board.

- void pio::set_c4(void)

  This method sets line 4 of port C to 1.

- void pio::set_c5(void)

  This method sets line 5 of port C to 1.

- void pio::set_c6(void)

  This method sets line 6 of port C to 1.

- void pio::set_c7(void)

  This method sets line 7 of port C to 1.

- void pio::reset_c4(void)

  This method sets line 4 of port C to 0.

- void pio::reset_c5(void)

  This method sets line 5 of port C to 0.

- void pio::reset_c6(void)

  This method sets line 6 of port C to 0.

- void pio::reset_c7(void)

  This method sets line7 of port C to 0.

- int pio::read_c0(void)

  This method returns the value on line 0 of port C.

- int pio::read_c1(void)

  This method returns the value on line 1 of port C.

- int pio::read_c2(void)

  This method returns the value on line 2 of port C.

- int pio::read_c3(void)

  This method returns the value on line 3 of port C.

A.6.6 The Servo–Vaporiser

The servo–vaporiser object is used to provide a software interface to the real servo–vaporiser. The real servo–vaporiser requires a pio board, another custom designed interface box and a controller box for the stepping motor which turns the vaporiser. The servo–vaporiser object makes the hardware complexity associated with this device invisible to the application developer.

A.6.7 Servo–Vaporiser Methods

The methods of the servo–vaporiser handler are as follows:

- servovap::servovap(void)

  This is the constructor for the servovap class. The constructor creates a pio board handler with which to handler communication with the real servo–vaporiser, and initialises it in the mode appropriate for its use. The constructor also performs initialisation of internally held data items.

- servovap::~servovap(void)

  The destructor for the servovap class deletes the pio board handler created by the constructor.

- int servovap::change_conc(float new_conc)

  This method accepts the floating point argument new_conc. Servo–vaporiser concentration settings are between 0 and 5 % and so a negative argument causes the actual vaporiser to be set to 0% and any argument over 5 causes the vaporiser to be set to 5%. Between 0% and 5% the vaporiser position is calculated by linear interpolation between calibrated points on the vaporiser scale. The calibration points are stored in arrays as detailed in the file "vapcalib.hpp".

  This method takes account of backlash in the servo–vaporiser gearbox and requests the correct number of pulses from the vaporiser interface box.

  This method returns 1.

- int servovap::vapour_off(void)

  This method sends appropriate signals to the vaporiser interface box to move the vaporiser to the OFF position. This method always returns 1.

- int servovap::check_position(void)

  This method estimates the position of the vaporiser from linear interpolation of an a/d converted potentiometer reading. This extimate is compared with the expected value of concentration stored at the last move. If the error

exceeds a reasonable tolerance -1 is returned otherwise 0.

- int servovap::check_errors(void)

  The check_errors() method employs check_position to find problems with the vaporiser moves. If problems are found, the error word is updated in internal storage. The error word is returned by this method.

- int servovap::restart(void)

  This method allows the servovap object to be reset to a known state. Instructions are sent to the vaporiser interface box to set the vaporiser to the OFF position, the error word is reset to 0 for no errors and subsequent use can continue.

  This method always returns 0.

- float servovap::estimate_concentration(void)

  This method uses linear interpolation to estimate the concentration at which the vaporiser is positioned based upon the converted potentiometer reading returned from the vaporiser. The estimate of concentration is returned by this method.

- int servovap::make_watchdog_pulse(void)

  The servo–vaporiser requires that a watchdog pulse be produced periodically during operation of the servo–vaporiser. This method generates this pulse and sends it to the vaporiser interface box for passing to the servo–vaporiser controller.

  This routine always returns 1.

A.7 Developing Applications using the CLASS Libraries

The CLASS libraries are provided as linkable object code. To an application developer, using CLASS library objects to perform communication and control of instruments and devices consists of two main steps;

1. Inserting the **class.hpp** header file in the application source code.
   This step allows the application to declare instances of communication port handlers, instrument handlers and drug-delivery device handlers. The file *class.hpp* actually includes all header files necessary in order to use the CLASS objects.

2. Linking the compiled application code with the CLASS library object code.
   This stage is extremely simple with the Zortech compiler and consists of specifying **"\class\class.lib"** in the command line argument for the Zortech Linker.

Both of these steps assume that the CLASS library code is installed in a directory called "class" which is positioned immediately below the root directory. The CLASS libraries have been compiled to produce 80286 code using the Large memory model within Zortech C++. The application should also be compiled to produce 80286 code using the Large memory model.

If necessary, a version of the CLASS libraries using 80386 code and the DOSX memory model will be compiled. At this stage, applications have not required this level of sophistication.

Appendix B

Physiology Knowledge Acquisition Diagrams

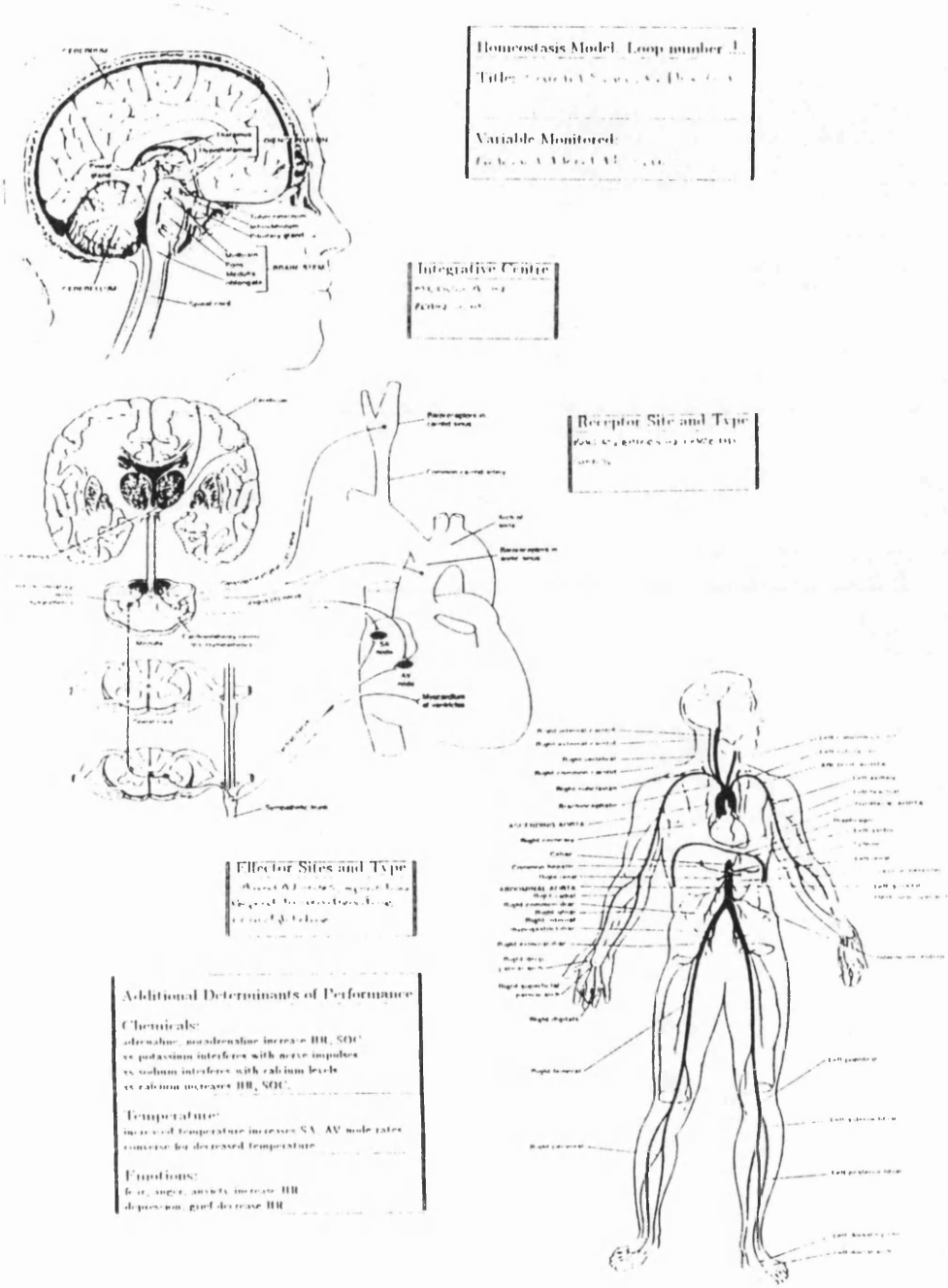
Homeostasis Model: Loop number
Variable Monitored:
Integrative Centre
Receptor Site and Type
Effector Sites and Type
Additional Determinants of Performance
Chemicals:
Temperature:
Emotions:

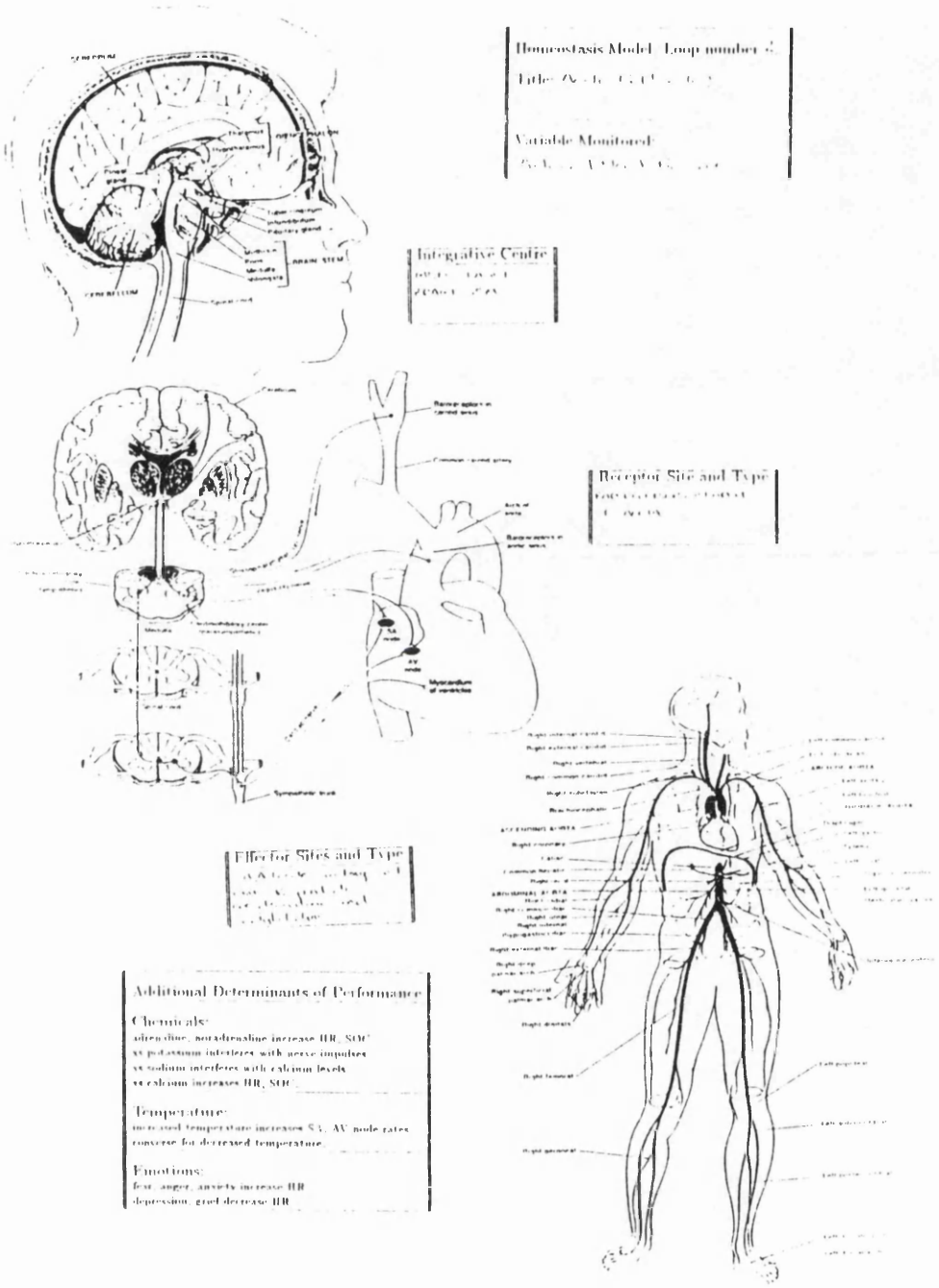
Homeostasis Model Loop number
Title
Variable Monitored
Integrative Centre
Receptor Site and Type
Effector Sites and Type
Additional Determinants of Performance
Chemicals:
adrenaline, noradrenaline increase HR, SOC
ss potassium interferes with nerve impulses
ss sodium interferes with calcium levels
ss calcium increases HR, SOC
Temperature:
increased temperature increases SA, AV node rates
converse for decreased temperature
Emotions:
fear, anger, anxiety increase HR
depression, grief decrease HR

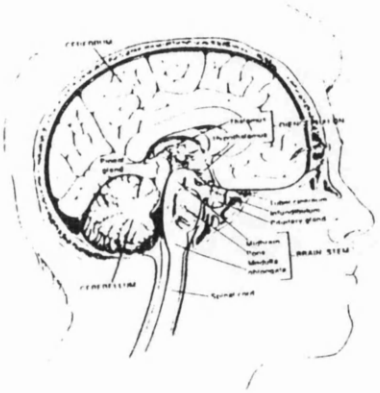

Homeostasis Model: Loop number

Title:

Variable Monitored:

Integrative Centre

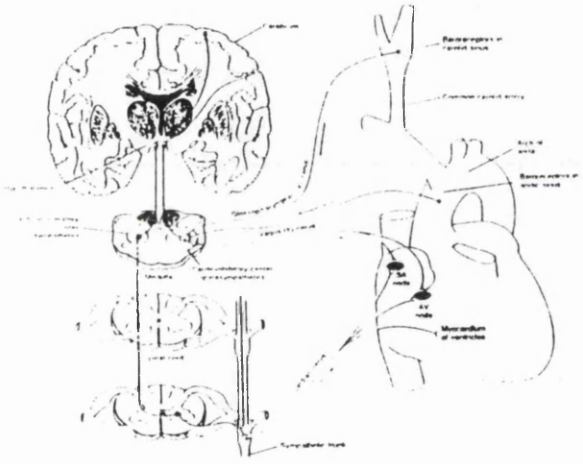

Receptor Site and Type

Effector Sites and Type

Additional Determinants of Performance

Chemicals:
adrenaline, noradrenaline increase HR, SOC
+ potassium interferes with nerve impulses
+ sodium interferes with calcium levels
+ calcium increases HR, SOC

Temperature:
increased temperature increases SA, AV node rates
converse for decreased temperature

Emotions:
fear, anger, anxiety increase HR
depression, grief decrease HR

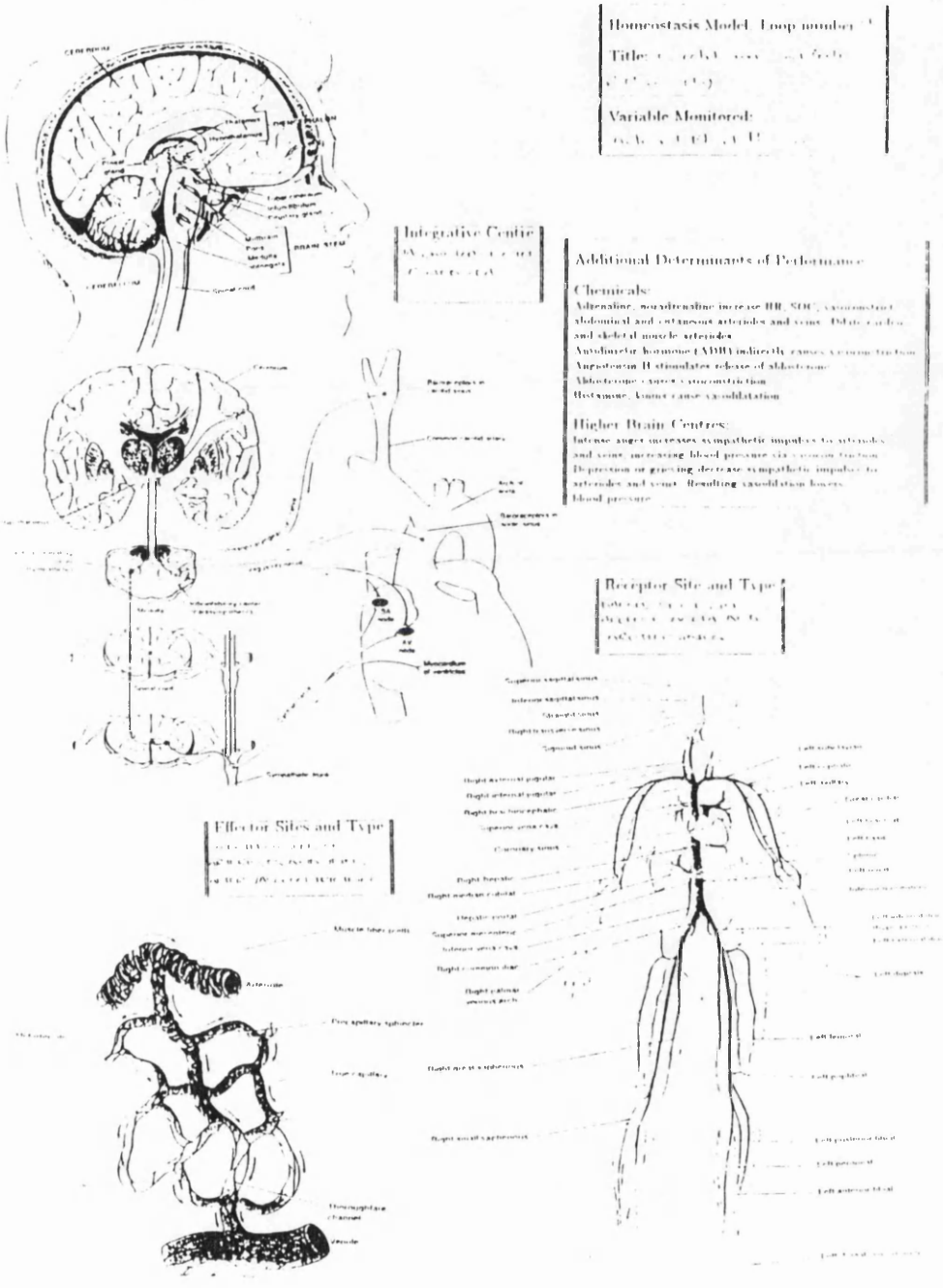
Homeostasis Model: Loop number
Title:
Variable Monitored:
Integrative Centre
Additional Determinants of Performance
Chemicals:
Higher Brain Centres:
Receptor Site and Type
Effector Sites and Type

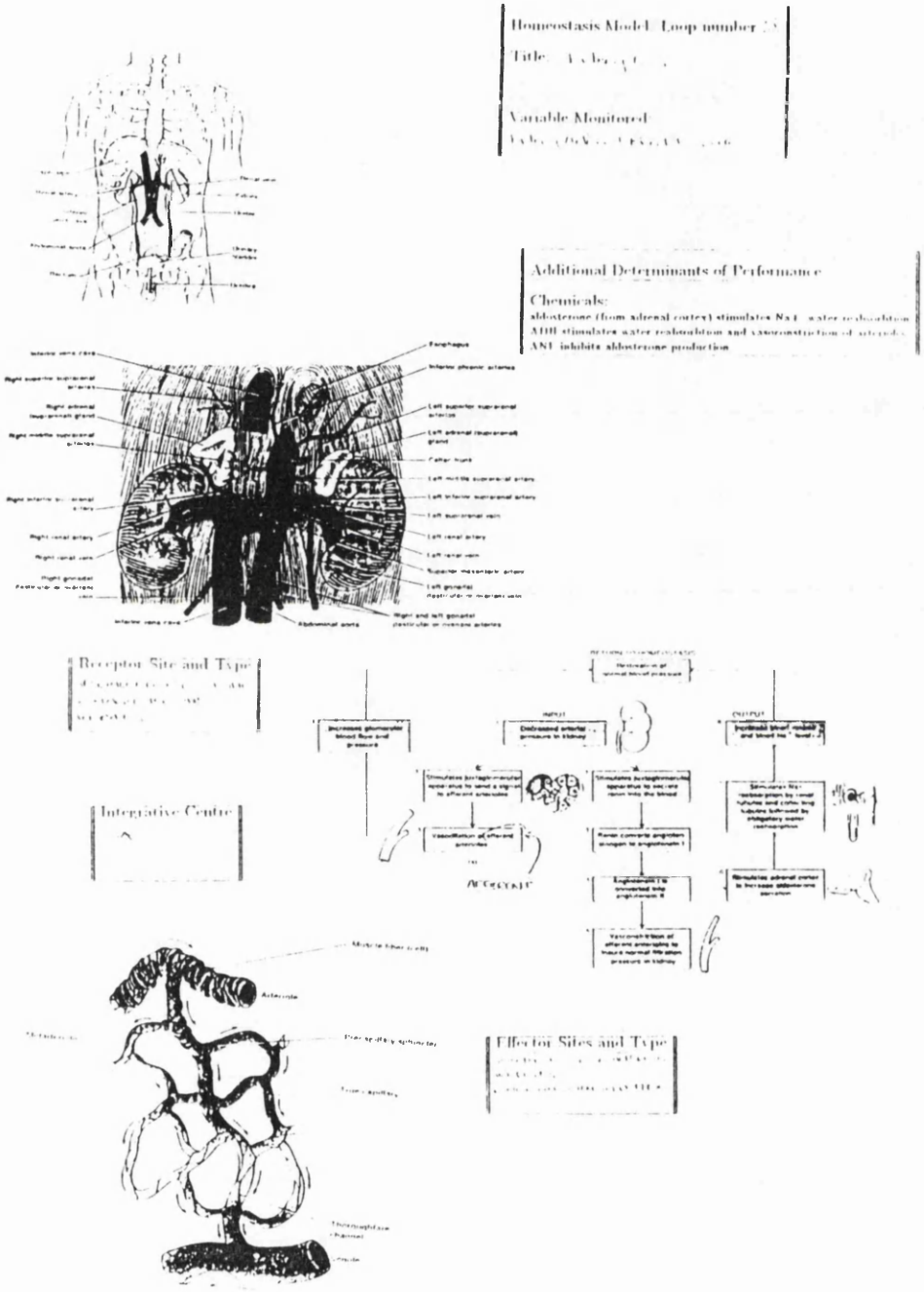
Homeostasis Model: Loop number
Title:
Variable Monitored:
Additional Determinants of Performance
Chemicals:
Receptor Site and Type:
Integrative Centre:
Effector Sites and Type:

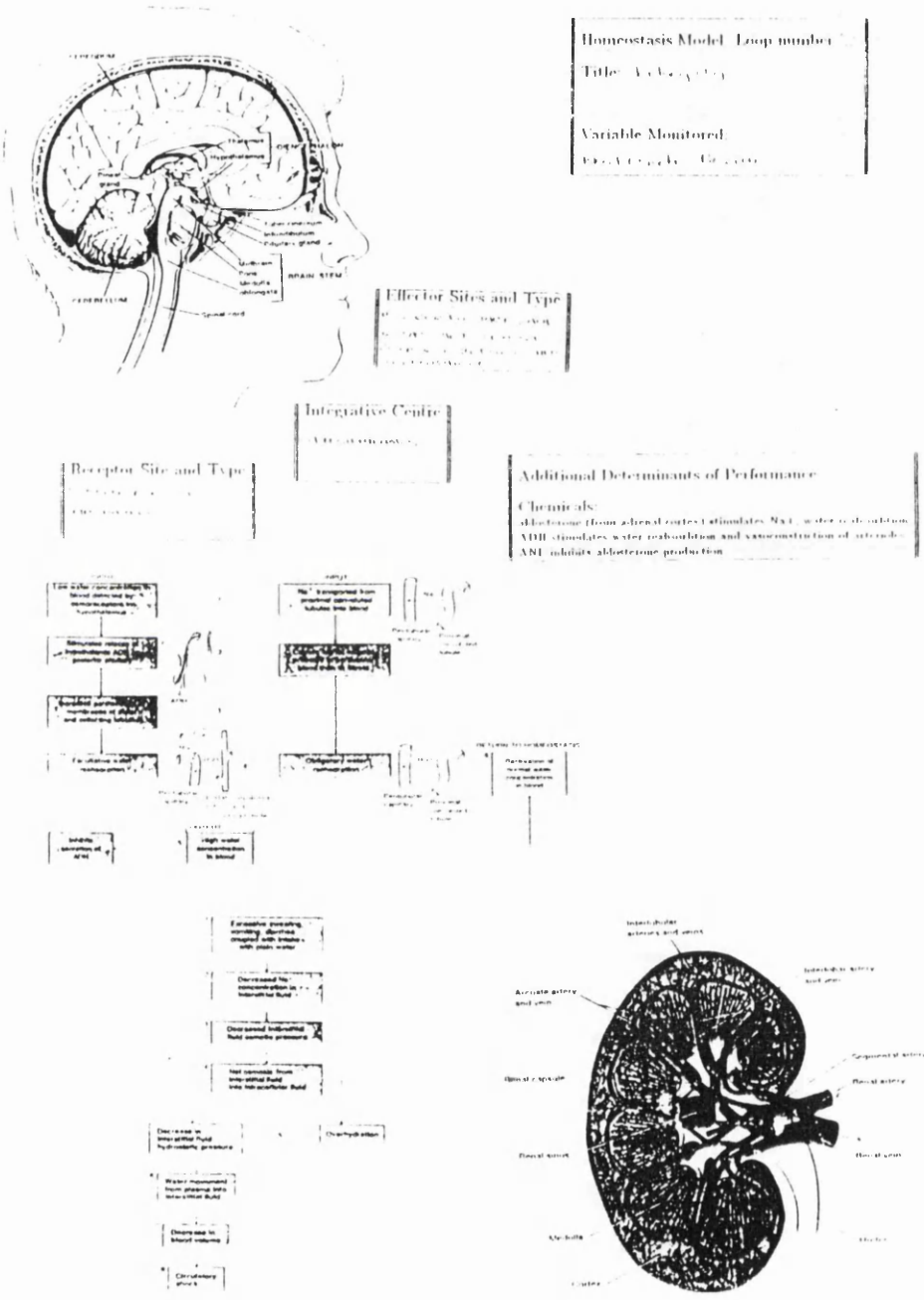
Homeostasis Model Loop number
Title
Variable Monitored
Effector Sites and Type
Integrative Centre
Receptor Site and Type
Additional Determinants of Performance
Chemicals:
ADH stimulates water reabsorption and vasoconstriction of arterioles
ANF inhibits aldosterone production

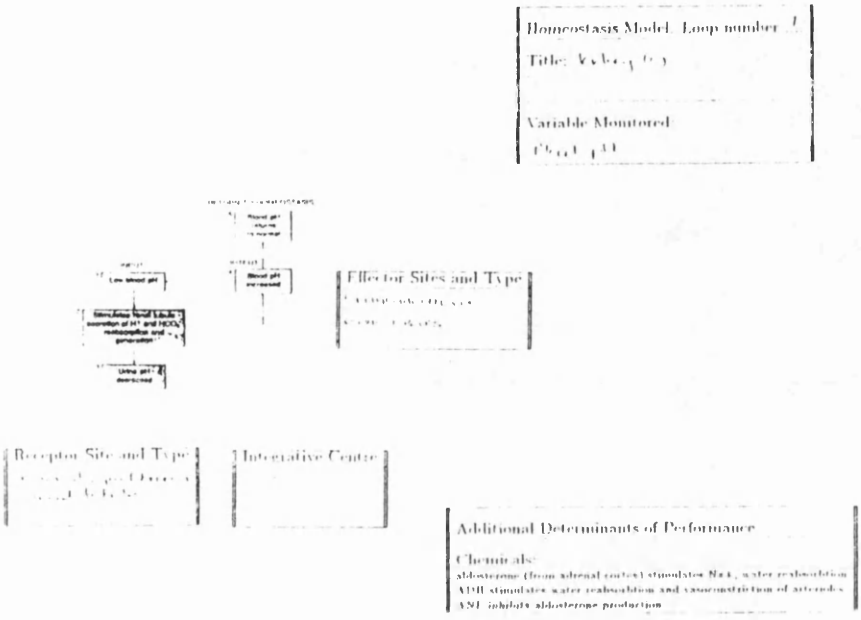
Homeostasis Model Loop number
Variable Monitored
Effector Sites and Type
Receptor Site and Type
Integrative Center
Additional Determinants of Performance
Chemicals:
aldosterone (from adrenal cortex) stimulates Na+, water reabsorption
ADH stimulates water reabsorption and vasoconstriction of arterioles
ANF inhibits aldosterone production

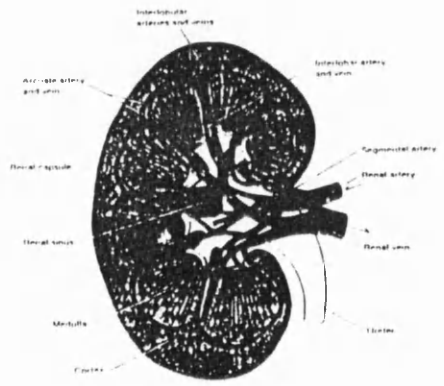
Interlobular arteries and veins
Arcuate artery and vein
Interlobar artery and vein
Renal capsule
Segmental artery
Renal artery
Renal vein
Renal sinus
Medulla
Cortex
Ureter

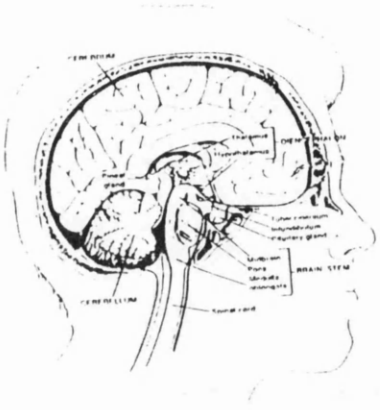

Homeostasis Model: Loop number

Title:

Variable Monitored:

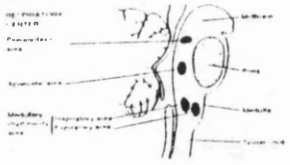

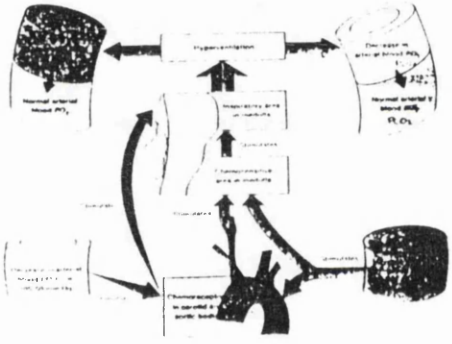

Integrative Centre

Receptor Site and Type

Effector Sites and Type

Additional Determinants of Performance

decrease in BP increases resp. rate
increase in BP decreases resp. rate
increase in temp. increases resp. rate
decrease in temp. decreases resp. rate
prolonged pain increases resp. rate
severe pain causes apnea
metabolic acidosis increases resp. rate
metabolic alkalosis decreases resp. rate

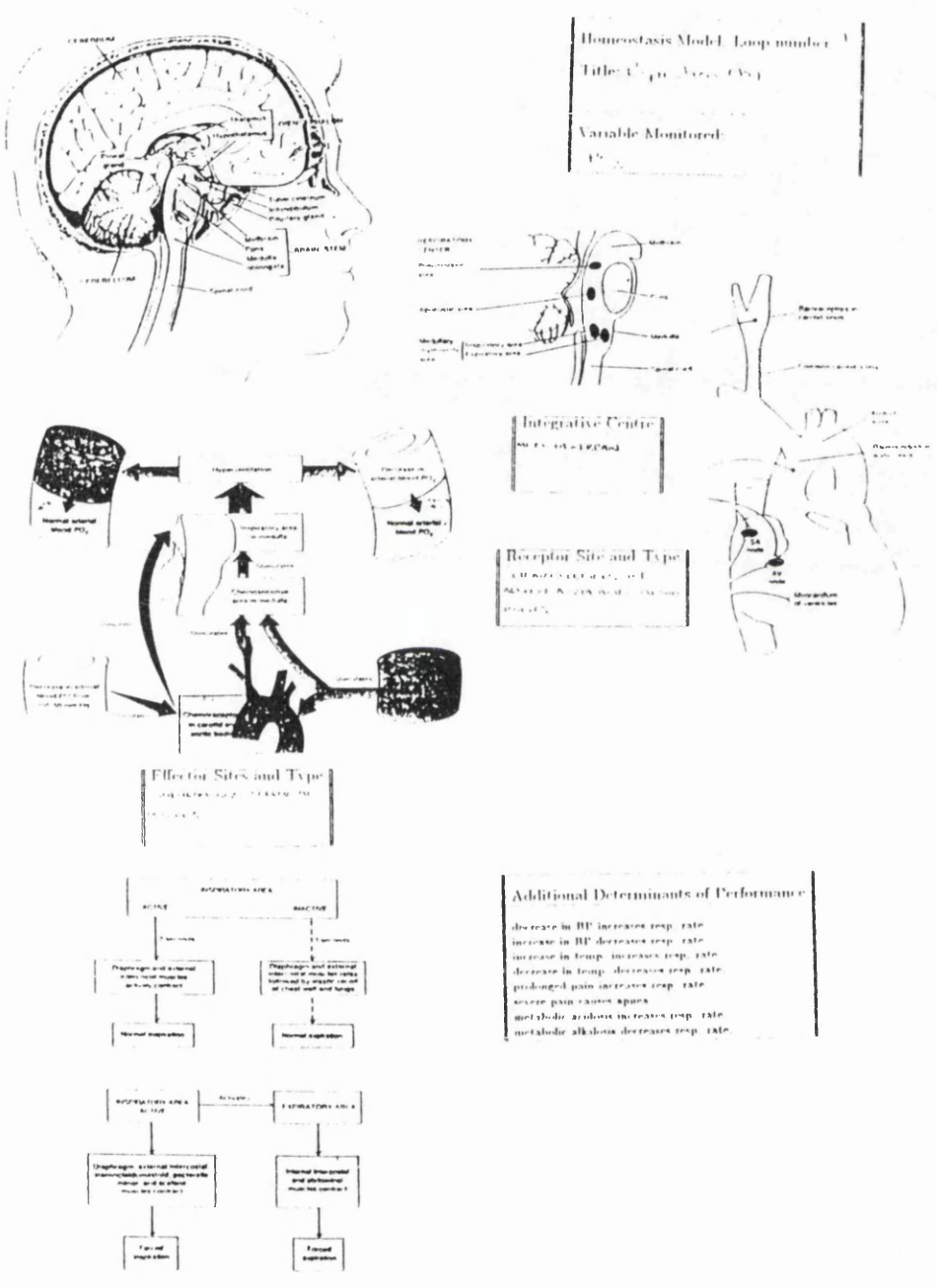
Homeostasis Model: Loop number
Variable Monitored:
Integrative Centre
Receptor Site and Type
Effector Sites and Type
Additional Determinants of Performance
decrease in BP increases resp. rate
increase in BP decreases resp. rate
increase in temp. increases resp. rate
decrease in temp. decreases resp. rate
prolonged pain increases resp. rate
severe pain causes apnea
metabolic acidosis increases resp. rate
metabolic alkalosis decreases resp. rate

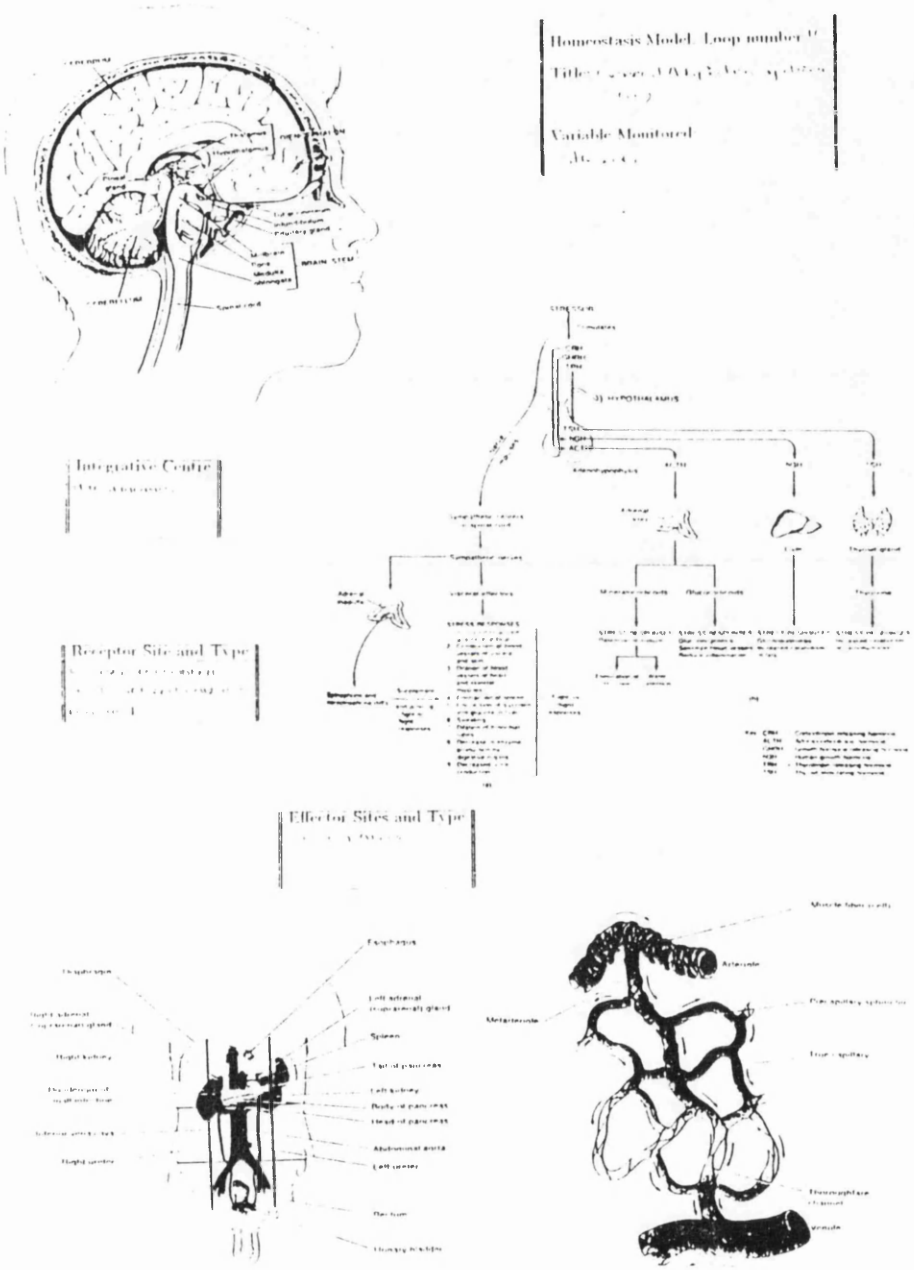
Homeostasis Model Loop number
Variable Monitored
Integrative Centre
Receptor Site and Type
Effector Sites and Type

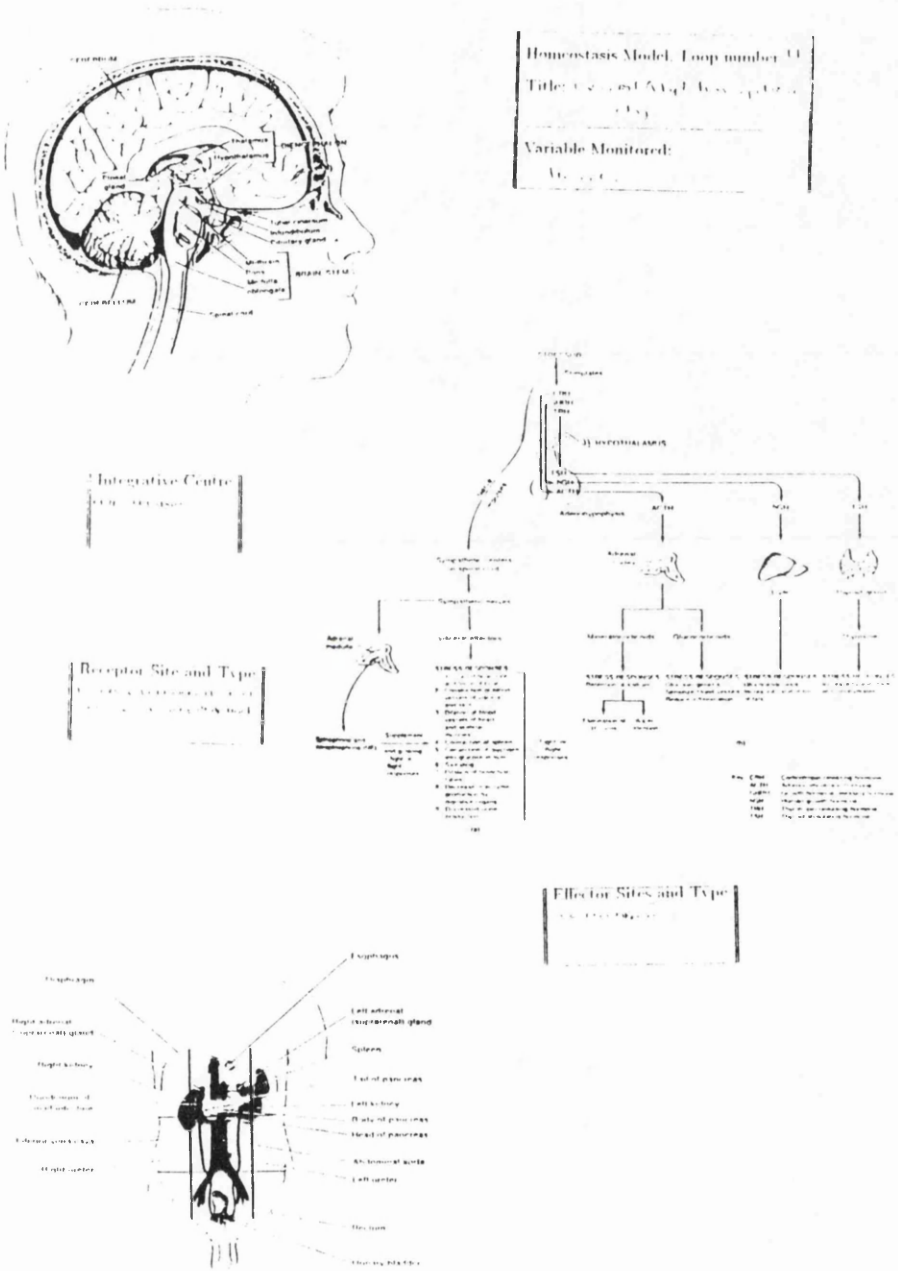
Homeostasis Model: Loop number 11
Variable Monitored:
Integrative Centre
Receptor Site and Type
Effector Sites and Type

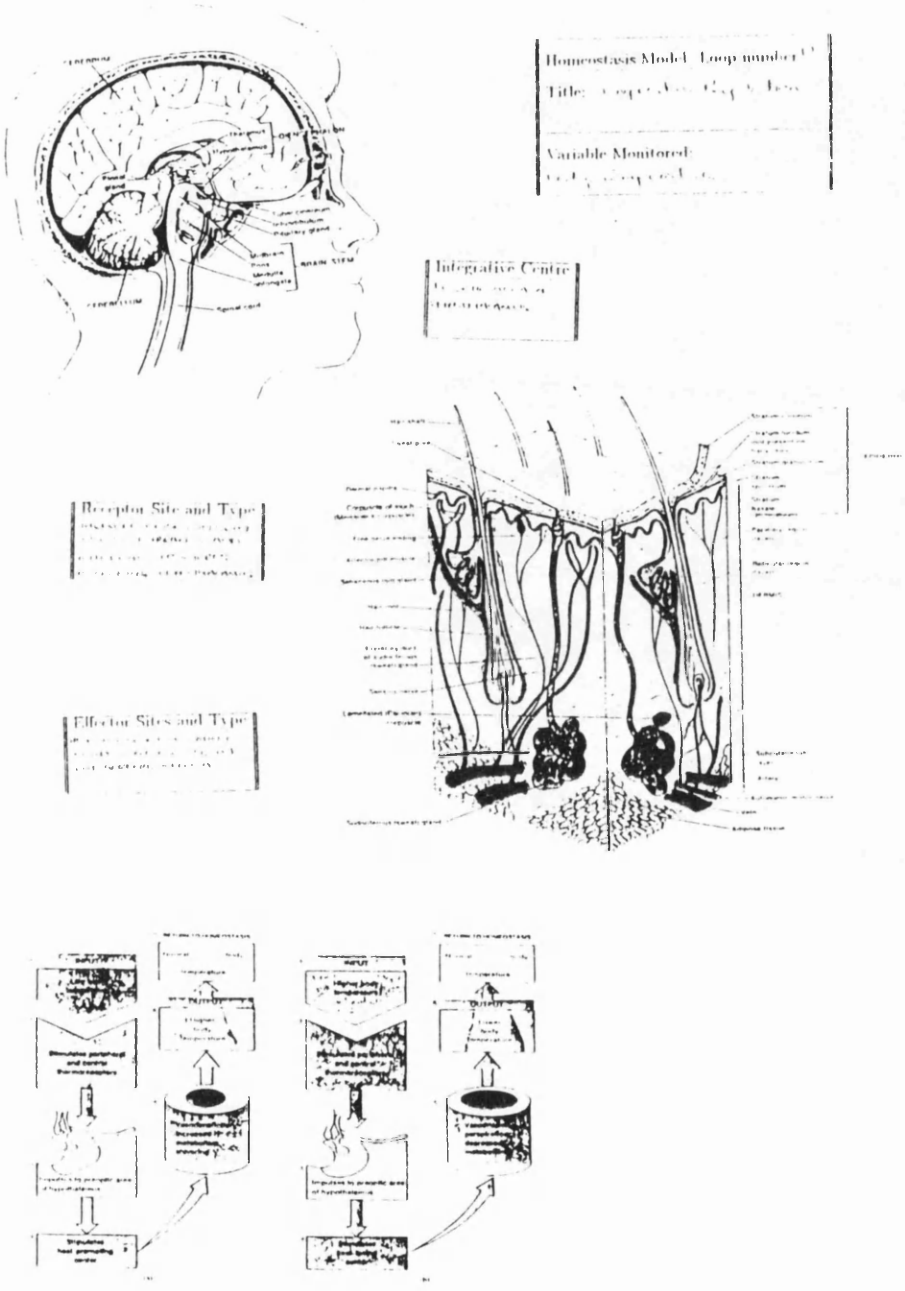
Homeostasis Model - Loop number
Title:
Variable Monitored:
Integrative Centre
Receptor Site and Type
Effector Sites and Type

Bibliography

[1] D. Linkens and S. Hacisalihzade, "Computer control systems and pharmacological drug administration: a survey," *Journal of Medical Engineering and Technology*, vol. 14, pp. 41–54, 1990.

[2] R. Summers, "Advances in intelligent instrumentation for the management of the critically ill patient," *Measurement and Control*, vol. 23, pp. 263–266, 1990.

[3] J. Packer, "Patient care using closed–loop control," *Computing and Control Engineering Journal*, vol. 1, pp. 23–28, 1990.

[4] E. Carson, "Measurement and control in medicine," *Measurement and Control*, vol. 23, pp. 260–262, 1990.

[5] D. Linkens, "Computer control for patient care," in *Computer control of real–time processes* (S. Bennett and G. Virk, eds.), Peter Peregrinus, 1990.

[6] R. Chilcoat, "A review of the control of depth of anaesthesia," *Transactions of the Institute of Measurement and Control*, vol. 2, pp. 38–45, 1980.

[7] M. Denai, D. Linkens, A. Asbury, A. MacLeod, and W. Gray, "Self–tuning pid control of atracurium–induced muscle relaxation in surgical patients," *IEE Proceeding Part D*, vol. 137, pp. 261–272, 1990.

[8] A. MacLeod, A. Asbury, W.M.Gray, and D. Linkens, "Automatic control of neuromuscular block with atracurium," *British Journal of Anaesthesia*, vol. 63, pp. 31–35, 1989.

[9] D. Linkens, A. Asbury, S. Rimmer, and M. Menad, "Identification and control of muscle–relaxant anaesthesia," *IEE Proceedings Part D*, vol. 129, pp. 136–141, 1982.

[10] D. Linkens, "Control of muscle relaxation during surgery," *Biomedical Measurements Informatics and Control*, vol. 1, pp. 31–39, 1986.

[11] R. Jaklitsch and D. Westenskow, "A model–based self–adjusting two–phase controller for vercuronium–induced muscle relaxation during anesthesia," *IEEE Transactions on Biomedical Engineering*, vol. 34, pp. 583–594, 1987.

[12] D. Linkens and M. Mahfouf, "Knowledge–based control for muscle relaxant anaesthesia," in *1st IEAC Symposium of Modelling and Control of Biomedical Systems*, 1988.

[13] T. Jannet and R. DeFalque, "Integrated instrumentation for closed–loop feedback control of muscle relaxation: Initial clinical trials," in *Proceedings of the IEEE Engineering in Medicine and Biology Society*, 1990.

[14] R. Millard, C. Monk, and C. Prys-Roberts, "Self–tuning control of hypotension during ent surgery using a volatile anaesthetic," *IEE Proceedings Part D*, vol. 135, pp. 95–105, 1988.

[15] L. Sheppard, "Computer control of the infusion of vasoactive drugs," *Annals of Biomedical Engineering*, vol. 8, pp. 431–444, 1980.

[16] J. Slate, L. Sheppard, V. Rideout, and E. Blackstone, "A model for design of a blood pressure controller for hypertensive patients," in *Proceedings of the*

1st Annual Conference of the IEEE Engineering in Medicine and Biology Society, 1979.

[17] J. Slate and L. Sheppard, "Automatic control of blood pressure by drug infusion," *IEE Proceedings Part D*, vol. 129, pp. 639–644, 1982.

[18] J. Arnsparger, B. McInnis, J. Glover, and N. Normann, "Adaptive control of blood pressure," *IEEE Transactions on Biomedical Engineering*, vol. 30, pp. 168–176, 1983.

[19] H. Kaufmann, R. Roy, and X. Xu, "Model reference adaptive control of drug infusion rate," *Automatica*, vol. 20, pp. 205–209, 1984.

[20] G. Voss, H. Chizeck, and P. Katona, "Self–tuning controller for drug delivery systems," *International Journal of Control*, vol. 47, pp. 1507–1520, 1988.

[21] J. Martin, A. Schneider, and N. Smith, "Multiple–model adaptive control of blood pressure using sodium nitroprusside," *IEEE Transactions on Biomedical Engineering*, vol. 34, pp. 603–610, 1987.

[22] K. Behbehani and R. Cross, "A controller for regulation of mean arterial blood pressure using optimal nitroprusside infusion rate," *IEEE Transactions on Biomedical Engineering*, vol. 38, pp. 513–521, 1991.

[23] J. Martin, A. Schneider, M. Quinn, and N. T. Smith, "Improved safety and efficacy in the control of arterial blood pressure through the use of a supervisor," *IEEE Transactions on Biomedical Engineering*, vol. 39, pp. 381–388, 1992.

[24] J. Martin, A. Schneider, M. Quinn, and N. T. Smith, "Supervisory adaptive control of arterial pressure during cardiac surgery," *IEEE Transactions on Biomedical Engineering*, vol. 39, pp. 389–393, 1992.

[25] G. Voss, "Closed loop drug delivery: An industry perspective," in *Proceedings of IEEE Engineering in Medicine and Biology Society*, 1990.

[26] S. Heijke and G. Smith, "Editorial ii. quest for the ideal inhalation anaesthetic agent," *British Journal of Anaesthesia*, vol. 64, pp. 3–5, 1990.

[27] R. Stoelting, *Pharmacology and Physiology in Anesthetic Practice.* Lippincott Press, 1990.

[28] C. Monk, R. Millard, P. Hutton, and C. Prys-Roberts, "Automatic arterial pressure regulation using isoflurane: comparison with manual control," *British Journal of Anaesthesia*, vol. 63, pp. 22–30, 1989.

[29] H. Rang and M. Dale, *Pharmacology.* Churchill–Livingstone, 1987.

[30] F. Roberts, J. Dixon, G. Lewis, R. Tackley, and C. Prys-Roberts, "Induction and maintenance of propofol anaesthesia: A manual infusion scheme," *Anaesthesia*, vol. 43, pp. 14–17, 1988.

[31] R. Tackley, G. Lewis, C. Prys-Roberts, R. Boaden, J. Dixon, and J. Harvey, "Computer controlled infusion of propofol," *British Journal of Anaesthesia*, vol. 62, pp. 46–53, 1989.

[32] J. Schuttler, S. Kloos, H. Schwilden, and H. Stoeckel, "Total intravenous anaesthesia with propofol and alfentanil by computer assisted infusion," *Anaesthesia*, vol. 43, pp. 2–7, 1988.

[33] H. Schwilden, "A general method for calculating the dosage scheme in linear pharmacokinetics," *European Journal of Clinical Pharmacology*, vol. 20, pp. 379–386, 1982.

[34] M. White and G. Kenny, "Intravenous propofol anaesthesia using a computerised infusion system," *Anaesthesia*, vol. 45, pp. 204–209, 1990.

[35] E. Gepts, K. Jonckheer, V. Maes, W. Sonck, and F. Camu, "Disposition kinetics of propofol during alfentanil anaesthesia," *Anaesthesia*, vol. 43, pp. 8–13, 1988.

[36] B. Marsh, M. White, N. Morton, and G. Kenny, "Pharmacokinetic model driven infusion of propofol in children," *British Journal of Anaesthesia*, vol. 67, pp. 41–48, 1991.

[37] W. W. Mapleson, "An electric analogue for uptake and exchange of inert gases and other agents," *Journal of Applied Physiology*, vol. 19, pp. 197–204, 1963.

[38] W. W. Mapleson, "Inert gas–exchange theory using an electric analogue," *Journal of Applied Physiology*, vol. 19, pp. 1193–1199, 1964.

[39] W. W. Mapleson, "Mathematical aspects of the uptake, distribution and elimination of inhaled gases and vapours," *British Journal of Anaesthesia*, vol. 36, p. 129, 1964.

[40] W. W. Mapleson, "Circulation-time models of the uptake of inhaled anaesthetics and data for quantifying them," *British Journal of Anaesthesia*, vol. 45, pp. 319–333, 1973.

[41] Y. Fukui and N. T. Smith, "Interactions among ventilation, the circulation and the uptake and distribution of halothane - use of a hybrid computer multiple model: I. the basic model," *Anesthesiology*, vol. 54, pp. 107–118, 1981.

[42] Y. Fukui and N. T. Smith, "Interactions among ventilation, the circulation and the uptake and distribution of halothane - use of a hybrid computer multiple model: Ii. spontaneous vs. controlled ventilation, and the effects of co_2," *Anesthesiology*, vol. 54, pp. 107–118, 1981.

[43] A. Zwart, N. Smith, and J. Beneken, "Multiple model approach to uptake and distribution of halothane: The use of an analog computer," *Computers and Biomedical Research*, vol. 5, pp. 228–238, 1972.

[44] J. Beneken and V. Rideout, "The use of multiple models in cardiovascular system studies: Transport and perturbation methods," *IEEE Transactions on Biomedical Engineering*, vol. 15, pp. 281–289, 1968.

[45] N. R. Davis and W. W. Mapleson, "Structure and quantification of a physiological model of the distribution of injected agents and inhaled anaesthetics," *British Journal of Anaesthesia*, vol. 53, pp. 399–405, 1981.

[46] N. Davis, *The Pharmacokinetics of Injected Analgesics.* Ph.d., University of Wales, 1987.

[47] W. Mapleson, P. Allott, and A. Steward, "A non–feedback technique for programmed anaesthesia," *British Journal of Anaesthesia*, vol. 46, p. 805, 1974.

[48] W. Mapleson, R. Chilcoat, J. Lunn, M. Blewett, M. Khatib, and B. Willis, "Computer assistance in the control of depth of anaesthesia," *British Journal of Anaesthesia*, vol. 52, p. 234, 1980.

[49] M. L. Tatnall, P. Morris, and F. Montgomery, "Controlled anaesthesia: an approach using patient characteristics identified during uptake," *British Journal of Anaesthesia*, vol. 53, pp. 1019–1026, 1983.

[50] P. Morris, M. L. Tatnall, and F. J. Montgomery, "Controlled anaesthesia: A clinical evaluation of an approach using patient characteristics identified during uptake," *British Journal of Anaesthesia*, vol. 55, p. 1065, 1983.

[51] M. L. Tatnall, "The development of a system for the control of inhalational anaesthesia," *Biomedical Measurement Informatics and control*, vol. 1, pp. 23–30, 1986.

[52] J. Ross, W. Wloch, D. White, and D. Hawes, "Servo–controlled closed circuit anaesthesia," *British Journal of Anaesthesia*, vol. 55, pp. 1053–1059, 1983.

[53] A. O'Callaghan, D. Hawes, J. Ross, D. White, and W. Wloch, "Uptake of isoflurane during clinical anaesthesia," *British Journal of Anaesthesia*, vol. 55, pp. 1061–1064, 1983.

[54] N. Smith, M. Quinn, Y. Fukui, R. Fleming, and J. Coles, "Automatic control in anaesthesia: a comparison in performance between the anesthetist and the machine," *Anesthesia and Analgesia Current Researches*, vol. 63, pp. 715–722, 1984.

[55] Y. Fukui, N. Smith, and R. Fleming, "Digital and sampled–data control of arterial blood pressure during halothane anaesthesia," *Anesthesia and Analgesia Current Researches*, vol. 61, pp. 1010–1015, 1982.

[56] R. Ritchie, E. Ernst, B. Pate, J. Pearson, and L. Sheppard, "Closed–loop control of an anaesthesia system: Development and animal testing," *IEEE Transactions on Biomedical Engineering*, vol. 34, pp. 437–443, 1987.

[57] R. Ritchie, J. Pearson, E. Ernst, and B. Pate, "Clinical experience with automatically controlled closed–circuit anesthesia delivery," in *Proceedings of the IEEE Engineering in Medicine and Biology Society*, 1990.

[58] R. Ritchie, E. Ernst, B. Pate, J. Pearson, and L. Sheppard, "Automatic control of anesthetic delivery and ventilation during surgery," *Medical Progress Through Technology*, vol. 16, pp. 61–67, 1990.

[59] J. Hayes, D. Westenkow, T. East, and W. Jordan, "Computer-controlled anaesthesia delivery system," *Medical Instrumentation*, vol. 18, pp. 224–229, 1984.

[60] R. Vishnoi and R. Roy, "Adaptive control of closed-circuit anesthesia," *IEEE Transactions on biomedical engineering*, vol. 38, pp. 39–47, 1991.

[61] H. M. Robb, "Towards the definition, measurement and assessment of the anesthestic state," M.Sc. Thesis, Glasgow University, 1989.

[62] C. H. Jr., "Lipid solubility, pharmacokinetics, and the eeg: Are you better off today that you were four years ago.," *Anesthesiology*, vol. 62, pp. 221–226, 1985.

[63] H. Schwilden and H. Stoeckel, "Quantitative eeg analysis during anaesthesia with isoflurane in nitrous oxide at 1.3 and 1.5 mac," *British Journal of Anaesthesia*, vol. 59, pp. 738–745, 1987.

[64] J. Scott, K. Ponganis, and D. Stanski, "Eeg quantification of the narcotic effect: The comparative pharmacodynamics of fentanyl and alfentanil," *Anesthesiology*, vol. 62, pp. 234–241, 1985.

[65] C. Thomsen, K. Christensen, and A. Rosenfalck, "Computerised monitoring of depth of anaesthesia with isoflurane," *British Journal of Anaesthesia*, vol. 63, pp. 36–43, 1989.

[66] C. Thomsen, A. Rosenfalck, and K. Christensen, "Assessment of anaesthetic depth by clustering analysis and autoregressive modelling of electroencephalograms," *Computer Methods and Programs in Biomedicine*, vol. 34, pp. 125–138, 1991.

[67] H. Schwilden, J. Schuttler, and H. Stoeckel, "Closed-loop feedback control of methohexital anaesthesia by quantitative eeg analysis in humans," *Anesthesiology*, vol. 67, pp. 341–347, 1987.

[68] H. Schwilden, H. Stoeckel, and J. Schuttler, "Closed-loop feedback control of propofol anaesthesia by quantitative eeg analysis in humans," *British Journal of Anaesthesia*, vol. 62, pp. 290–296, 1989.

[69] G. Schils, F. Sasse, and V. Rideout, "Automatic control of anesthesia using two feedback variables," *Annals of Biomedical Engineering*, vol. 15, pp. 19–34, 1987.

[70] T. Chang, W. Dworsky, and P. White, "Continuous electromyography for monitoring depth of anaesthesia," *Anesthesia and Analgesia Current Researches*, vol. 67, pp. 521–525, 1988.

[71] T. Savege, M. Dubois, M. Frank, and J. Holly, "Preliminary investigation into a new method of assessing the quality of anaesthesia: The cardiovascular response to a measured noxious stimulus," *British Journal of Anaesthesia*, vol. 50, pp. 481–487, 1978.

[72] P. Suppan, "Feedback monitoring in anaesthesia ii: Pulse rate control of halothane administration," *British Journal of Anaesthesia*, vol. 44, pp. 1263–1270, 1972.

[73] P. Suppan, "Feedback monitoring in anaesthesia iii: The control of halothane administration by respiratory patterns," *British Journal of Anaesthesia*, vol. 46, pp. 829–837, 1974.

[74] P. Suppan, "Feedback monitoring in anaesthesia iv: The indirect measurement of arterial pressure and ikts use for the control of halothane administration," *British Journal of Anaesthesia*, vol. 49, pp. 141–150, 1977.

[75] D. Lampard, J. Coles, and W. Brown, "Electronic digital computer control of ventilation and anaesthesia," *Anaesthesia and Intensive Care*, vol. 1, pp. 382–392, 1973.

[76] D. Linkens, S. Greenhow, and A. Asbury, "An expert system for the control of depth of anaesthesia," *Biomedical Measurement Informatics and Control*, vol. 1, pp. 223–228, 1986.

[77] S. Greenhow, *A Knowledge Based System for the Control of Depth of Anaesthesia.* Ph.d., University of Sheffield, 1990.

[78] P. Maitre, M. Ausems, S. Vozeh, and D. Stanski, "Evaluating the accuracy of using population pharmacokinetic data to predict plasma concentrations of alfentanil," *Anesthesiology*, vol. 68, pp. 59–67, 1973.

[79] R. Chilcoat, J. Lunn, and W. Mapleson, "Computer assistance in the control of depth of anaesthesia," *British Journal of Anaesthesia*, vol. 56, pp. 1417–1431, 1984.

[80] C. Prys-Roberts, "Anaesthesia: A practical or impractical construct – *editorial*," *British Journal of Anaesthesia*, vol. 59, pp. 1341–1345, 1987.

[81] M. Pinsker, "Anesthesia: A pragmatic construct," *Anesthesia and Analgesia Current Researches*, vol. 65, pp. 819–, 1986.

[82] P. Woodbridge, "Changing concepts concerning depth of anaesthesia," *Anesthesiology*, vol. 18, pp. 536–, 1957.

[83] J. Thornton and C. Levy, *Topics in Anaesthesia and Intensive Care.* London: Henry Kimpton, 1987.

[84] C. Ward, *Anaesthetic Equipment Physical Principles and Measurement.* London: Bailliere Tindall, 1975.

[85] J. Cooper, R. Newbower, C. Long, and B. McPeek, "Preventable anesthesia mishaps: a study of human factors," *Anesthesiology*, vol. 49, pp. 399–406, 1978.

[86] R. Loeb, J. Brunner, D. Westenkow, B. Feldman, and N. Pace, "The utah anesthesia workstation," *Anesthesiology*, vol. 70, pp. 999–1007, 1989.

[87] A. Greenburg and G. Peskin, "Monitoring in the recovery room and surgical intensive care unit," in *Monitoring in Anaesthesia* (L. Saidman and N. Smith, eds.), John Wiley, 1978.

[88] J. Benumof, "Monitoring respiratory function during anesthesia," in *Monitoring in Anaesthesia* (L. Saidman and N. Smith, eds.), John Wiley, 1978.

[89] C. Prys-Roberts, "Monitoring of the cardiovascular system," in *Monitoring in Anaesthesia* (L. Saidman and N. Smith, eds.), John Wiley, 1978.

[90] M. Lindop, "Monitoring of the cardiovascular system during anesthesia," in *Monitoring During Anaesthesia* (G. Gerson, ed.), Little, Brown and Company, 1981.

[91] E. Eger, "Monitoring the depth of anesthesia," in *Monitoring in Anaesthesia* (L. Saidman and N. Smith, eds.), John Wiley, 1978.

[92] D. Thomas and W. Runciman, "Monitoring depth of anaesthesia," *Anaesthesia and Intensive Care*, vol. 16, pp. 69–71, 1988.

[93] D. Cullen, E. Eger, W. Stevens, N. Smith, T. Cromwell, B. Cullen, G. Gregory, S. Bahlman, W. Dolan, R. Stoelting, and H. Fourcade, "Clinical signs of anesthesia," *Anesthesiology*, vol. 36, pp. 21–36, 1988.

[94] M. Nieman, W. Richardson, W. Gray, and A. Asbury, "A vaporizer controller for general anaesthesia," *Journal of Medical Engineering Technology*, vol. 11, pp. 1346–1355, 1987.

[95] C. Cobelli, "Identification of endocrine–metabolic and pharmacokinetic systems," in *IFAC Symposium on Identification and System Parameter Estimation, New York*, 1985.

[96] J. Jacquez, *Compartmental Analysis in Biology and Medicine.* Elsevier, 1972.

[97] K. R. Godfrey, *Compartmental Models and Their Application.* London: Academic Press, 1983.

[98] K. R. Godfrey and J. DiStefano, "Identifiability of model parameters," in *Identifiability of Parametric Models* (E. Walter, ed.), Pergamon Press, 1987.

[99] S. Vajda, J. DiStefano, K. R. Godfrey, and J. Fargarsan, "Parameter space boundaries for unidentifiable compartmental models," *Mathematical Biosciences*, vol. 97, pp. 27–60, 1989.

[100] N. Smith, A. Zwart, and J. Beneken, "Interaction between the circulatory effects and the uptake and distribution of halothane," *Anesthesiology*, vol. 37, pp. 47–58, 1972.

[101] H. Schwid, "A flight simulator for general anaesthesia training," *Computers and Biomedical Research*, vol. 20, pp. 64–, 1987.

[102] C. Larson, E. Eger, and J. Severinghaus, "The solubility of halothane in blood and tissue homogenates," *Anesthesiology*, vol. 23, no. 3, pp. 349–355, 1962.

[103] M. J. Higgins, "Clinical and theoretical studies with the opioid analgesic fentanyl," M.Sc. Thesis, Glasgow University, 1990.

[104] C. Hull, "How far can we go with compartmental models," *Anesthesiology*, vol. 72, pp. 399–402, 1990.

[105] H. M. Paynter, *Analysis and design of engineering systems.* Cambridge, Mass.: MIT Press, 1961.

[106] V. Gebben, "Bond graph bibliography," *Journal of the Franklin Institute*, vol. 308, pp. 361–369, 1978.

[107] D. C. Karnopp and R. C. Rosenberg, *System Dynamics: A Unified Approach.* John Wiley, 1975.

[108] R. Plant and J. Horowitz, "Energy conversion in biological systems–part i. chemical reactions and ion transport," *Journal of the Franklin Institute*, vol. 308, pp. 269–280, 1978.

[109] D. Karnopp and S. Azarbaijani, "Pseudo bond graphs for generalized compartmental models in engineering and physiology," *Journal of the Franklin Institute*, vol. 312, pp. 95–108, 1981.

[110] J. Lefevre and J. Barreto, "A mixed block diagram bond graph approach for biochemical models with mass action and rate law kinetics," *Journal of the Franklin Institute*, vol. 319, pp. 201–215, 1985.

[111] J. Thoma and H. Atlan, "Osmosis and hydraulics by network thermodynamics and bond graphs," *Journal of the Franklin Institute*, vol. 319, pp. 217–226, 1985.

[112] J. Thoma, "Bond graphs and biology," *Computer Methods and Programs in Biomedicine*, vol. 8, p. 145, 1978.

[113] R. C. Rosenberg and D. C. Karnopp, *Introduction to Physical System Dynamics.* McGraw-Hill, 1983.

[114] C. Hull, "Editorial: Symbols for compartmental models," *British Journal of Anaesthesia*, vol. 51, p. 815, 1979.

[115] P. J. Gawthrop, N. A. Marrison, and L. Smith, "MTT: A bond graph toolbox," in *Proceedings of the 5th IFAC/IMACS Symposium on Computer-aided Design of Control Systems:CADCS91, Swansea, Wales*, pp. 274–279, 1991.

[116] J. Lerou, R. Dirksen, H. B. Kolmer, L. Booji, and G. Borm, "A system model for closed–circuit inhalation anesthesia i. computer study," *Anesthesiology*, vol. 75, pp. 345–355, 1991.

[117] J. Lerou, R. Dirksen, H. B. Kolmer, L. Booji, and G. Borm, "A system model for closed–circuit inhalation anesthesia ii. clinical validation," *Anesthesiology*, vol. 75, pp. 230–237, 1991.

[118] A. Steward, P. Allot, A. Cowles, and W. Mapleson, "Solubility coefficients for inhaled anaesthetics for water, oil and biological media," *British Journal of Anaesthesia*, vol. 45, pp. 282–293, 1973.

[119] J. Lerman, B. Schmitt-Bantel, G. Gregory, M. Willis, and E. Eger, "Effect of age on the solubility of volatile anesthetics in human tissues," *Anesthesiology*, vol. 65, pp. 307–311, 1986.

[120] N. Yasuda, A. Targ, and E. Eger, "Solubility of i-653, sevoflurane, isoflurane and halothane in human tissues," *Anesthesia and Analgesia Current Researches*, vol. 69, pp. 370–373, 1989.

[121] V. Fiserova-Bergerova, M. Tichy, and F. D. Carlo, "Effects of biosolubility on pulmonary uptake and disposition of gases and vapors of lipophilic chemicals," *Drug Metabolism Reviews*, vol. 15, pp. 1033–1070, 1984.

[122] A. Steward, W. Mapleson, and P. Allott, "A comparison of in-vivo and in-vitro partition coefficients for halothane in the rabbit," *British Journal of Anaesthesia*, vol. 44, pp. 650–655, 1972.

[123] P. Allott, A. Steward, and W. Mapleson, "Pharmacokinetics of halothane in the dog," *British Journal of Anaesthesia*, vol. 48, pp. 279–294, 1976.

[124] A. Steward, P. Allott, and W. Mapleson, "The solubility of halothane in canine blood and tissues," *British Journal of Anaesthesia*, vol. 47, pp. 423–433, 1975.

[125] F. Frei, D. Thomson, and A. Zbinden, "Influence of ventilatory and circulatory changes on the pharmacokinetics of halothane and isoflurane," *Experientia*, vol. 44, pp. 178–181, 1988.

[126] J. Durnin and J. Womersley, "Body fat assessed from total body density and its estimation from skinfold thickness: measurements on 481 men and women aged from 16 to 72 years," *British Journal of Nutrition*, vol. 32, pp. 77–97, 1974.

[127] J. Durnin and M. Rahaman, "The assessment of the amount of fat in the human body from measurements of skinfold thickness," *British Journal of Nutrition*, vol. 21, pp. 681–689, 1967.

[128] J. Brozek, F. Grande, J. Anderson, and A. Keys, "Densitometric analysis of body composition: Revision of some quantitative assumptions," *Annals of the New York academy of Sciences*, vol. 110, pp. 113–140, 1963.

[129] G. Tortora and N. Anagnosstakos, *Principles of Anatomy and Physiology.* Harper and Row, 1990.

[130] C. Prys-Roberts, "Regulation of the circulation," in *The Circulation in Anaesthesia* (C. Prys-Roberts, ed.), Blackwell Scientific Publications, 1980.

[131] N. Smith, "Myocardial function and anaesthesia," in *The Circulation in Anaesthesia* (C. Prys-Roberts, ed.), Blackwell Scientific Publications, 1980.

[132] J. Marty and J. Reves, "Cardiovascular control mechanisms during anesthesia," *Anesthesia and Analgesia Current Researches*, vol. 69, pp. 273–275, 1989.

[133] K. Kortly, T. Ebert, E. Vucins, F. Igler, J. Barney, and J. Kampine, "Baroreceptor reflex control of heart rate during isoflurane anesthesia in humans," *Anesthesiology*, vol. 60, pp. 173–175, 1984.

[134] R. Takeshima and S. Dohi, "Comparison of arterial baroreflex function in humans anesthetized with enflurane or isoflurane," *Anesthesia and Analgesia Current Researches*, vol. 69, pp. 284–290, 1989.

[135] H. Schwid and D. O'Donnell, "The anesthesia simulator–recorder: A device to train and evaluate anesthesiologists' responses to critical incidients," *Computers and Biomedical Research*, vol. 72, pp. 191–197, 1990.

[136] M. Leaning, H. Pullen, E. Carson, and L. Finkelstein, "Modelling a complex biological system: The human cardiovascular system – 1. methodology and model description," *Transactions of the Institute of Measurement and Control*, vol. 5, pp. 70–86, 1983.

[137] M. Leaning, H. Pullen, E. Carson, M. Al-Dahan, N. Rajkumar, and L. Finkelstein, "Modelling a complex biological system: The human cardiovascular system – 1.model validation, reduction and development," *Transactions of the Institute of Measurement and Control*, vol. 5, pp. 87–98, 1983.

[138] I. Bratko, I. Mozetic, and N. Lavrac, *Kardio: A Study in Deep and Qualitative Knowledge for Expert Systems.* MIT Press, 1989.

[139] J. Hunter, N. Gotts, I. Hamlet, and I. Kirby, "Qualitative spacial and temporal reasoning in cardiac electrophysiology," Tech. Rep. AUCS/TR8904, University of Aberdeen Department of Computing Science, 1989.

[140] P. Toal and J. Hunter, "A qualitative model of cardiac haemodynamics," Tech. Rep. AUCS/TR9001, University of Aberdeen Department of Computing Science, 1990.

[141] J. Hunter, I. Kirby, and N. Gotts, "Using quantitative and qualitative constraints in models of cardiac electrophysiology," Tech. Rep. AUCS/TR9005, University of Aberdeen Department of Computing Science, 1990.

[142] C. Slymon, G. Strube, J. Hunter, and R. Vincent, "A qualitative model of heart failure," Tech. Rep. AUCS/TR9010, University of Aberdeen Department of Computing Science, 1990.

[143] S. Jennet, *Human Physiology.* Churchill Livingstone, 1989.

[144] S. Mikal, *Homeostasis in Man.* Churchill Press, 1967.

[145] R. Hardy, *Homeostasis.* Edward Arnold, 1976.

[146] B. Brenner and J. Stein, *Sodium and Water Homeostasis.* Churchill Livingstone, 1978.

[147] B. Brenner and J. Stein, *Acid-base and Potassium Homeostasis.* Churchill Livingstone, 1978.

[148] J. Rumbaugh, M. Blaha, W. Premerlani, F. Eddy, and W. Lorensen, *Object-Oriented Modeling and Design.* Prentice-Hall, 1991.

[149] M. Sykes, "Panel on practical alarms: Fifth international symposium on computing in anesthesia and intensive care," *Journal of Clinical Monitoring*, vol. 5, pp. 192–193, 1989.

[150] D. Westenkow, R. Loeb, J. Brunner, and N. Pace, "Expert alarms and autopilot in an anesthesia workstation," *Anesthesiology*, vol. 69, p. A731, 1988.

[151] J. Philip, "Overview: Creating practical alarms for the future," *Journal of Clinical Monitoring*, vol. 5, pp. 194–195, 1989.

[152] M. Quinn, "Semipractical alarms: A parable," *Journal of Clinical Monitoring*, vol. 5, pp. 196–200, 1989.

[153] P. Schreiber and J. Schreiber, "Structured alarm systems for the operating room," *Journal of Clinical Monitoring*, vol. 5, pp. 201–204, 1989.

[154] J. Beneken and J. van der Aa, "Alarms and their limits in monitoring," *Journal of Clinical Monitoring*, vol. 5, pp. 205–210, 1989.

[155] Y. Fukui and T. Masuzawa, "Alarms and their limits in monitoring," *Journal of Clinical Monitoring*, vol. 5, pp. 211–216, 1989.

[156] T. Schecke, G. Rau, H. Popp, H. Kasmacher, G. Kalff, and H. Zimmermann, "A knowledge–based approach to intelligent alarms in anesthesia," *IEEE Engineering in Medicine and Biology Magazine – December*, vol. 10, pp. 38–44, 1991.

[157] J. Cheung and G. Stephanopoulos, "Representation of process trends – part i. a formal representation framework," *Computers and Chemical Engineering*, vol. 14, pp. 495–510, 1990.

[158] J. Cheung and G. Stephanopoulos, "Representation of process trends – part ii. the problem of scale and qualitative scaling," *Computers and Chemical Engineering*, vol. 14, pp. 511–539, 1990.

[159] P. Morris, M. L. Tatnall, and P. West, "Breath–by–breath halothane monitoring during anaesthesia," *British Journal of Anaesthesia*, vol. 51, pp. 979–982, 1979.

[160] A. Perrino, J. Fleming, and K. LaMantia, "Transesophageal doppler ultrasonography: Evidence for improved cardiac output monitoring," *Anesthesia and Analgesia Current Researches*, vol. 71, pp. 651–657, 1990.

[161] J. Abrams, R. Weber, and K. Holmen, "Transtracheal doppler:a new procedure for cardiac output measurement," *Anesthesiology*, vol. 70, pp. 134–138, 1989.